



## Durham E-Theses

---

### *Some experimental and theoretical aspects of structure and bonding as studied by ESCA*

Adams, David Brinley

#### How to cite:

---

Adams, David Brinley (1973) *Some experimental and theoretical aspects of structure and bonding as studied by ESCA*, Durham theses, Durham University. Available at Durham E-Theses Online: <http://etheses.dur.ac.uk/8802/>

#### Use policy

---

The full-text may be used and/or reproduced, and given to third parties in any format or medium, without prior permission or charge, for personal research or study, educational, or not-for-profit purposes provided that:

- a full bibliographic reference is made to the original source
- a [link](#) is made to the metadata record in Durham E-Theses
- the full-text is not changed in any way

The full-text must not be sold in any format or medium without the formal permission of the copyright holders.

Please consult the [full Durham E-Theses policy](#) for further details.

UNIVERSITY OF DURHAM

A Thesis Entitled

SOME EXPERIMENTAL and THEORETICAL ASPECTS of  
STRUCTURE and BONDING as STUDIED by ESCA

Submitted by

David Brinley Adams, B.Sc.

(Van Mildert College)



A Candidate for the Degree of Doctor of Philosophy  
1973.

### ACKNOWLEDGEMENTS

The work described in this thesis was carried out under the supervision of Dr D.T. Clark, and I wish to express my sincere thanks for his unfailing help and enthusiasm. I would also like to express thanks to my colleagues Dr D. Kilcast and Mr I.W. Scanlan for many valuable discussions, and to Dr's. R.D. Chambers, W.J. Feast, M.Y. Gribble and W.E. Preston of the University of Durham for supplying several of the fluorocarbon compounds studied in this work.

Thanks are also due to the staff of the University of Durham Computer Unit and the Atlas Computer Laboratory (especially Dr V.R. Saunders and Mr D. Rowley) for their invaluable assistance and help in the implementation of the ab initio molecular orbital programs employed in this work.

Finally I would like to thank the Science Research Council for the provision of a research studentship.

D.B. Adams  
Durham, 1973

## MEMORANDUM

The work described in this thesis was carried out at the University of Durham between October 1970 and September 1973. It has not been submitted for any other degree and is the original work of the author except where acknowledged by reference.

Part of the work in this thesis has formed the subject matter of the whole, or part, of the following publications:

1. Halogenated Methanes. Equivalent Core and Charge Potential Models for Interpreting Core Binding Shifts, D.T. Clark and D.B. Adams, *Nature (Phys. Sci.)* 1971, 234, 95.
2. Charge Distributions in Aromatic Hydrocarbons and their Perfluoro Analogues as Determined by ESCA, D.T. Clark, D.B. Adams and D. Kilcast, *Chem. Phys. Lett.*, 1972, 13, 439.
3. Interpretation of ESCA Chemical Shifts Using Minimal Basis Set Calculations. D.T. Clark and D.B. Adams, *J. Electron Spectrosc.*, 1972/3, 1, 302.
4. Ab Initio Molecular Orbital Calculations of ESCA Chemical Shifts Using the Equivalent Cores Method. D.T. Clark and D.B. Adams, *J. Chem. Soc. Faraday Trans. II*, 1972, 68, 1819.
5. Charge Distributions in Dodecafluorotricyclo[5.2.2.0<sup>2,6</sup>] undeca-2,5,8-triene and Tetradecafluorotricyclo[6.2.2.0<sup>2,7</sup>] dodeca-2,6,9-triene as determined by ESCA. D.T. Clark, W.J. Feast, D. Kilcast, D.B. Adams and W.E. Preston, *J. Fluorine Chem.*, 1972/3, 2, 199.

6. Orientation of Nucleophilic Substitution in Perfluoroindene by ESCA., D.B. Adams, D.T. Clark, W.J. Feast, D. Kilcast, W.K.R. Musgrave and W.E. Preston, Nature (Phys. Sci.), 1972, 239, 47.
7. On the Core and Valence Energy Levels of Fluorobenzene, D.T. Clark, D. Kilcast, D.B. Adams and I.W. Scanlan, J. Electron. Spectrosc. 1972/3, 1, 153.
8. Structure and Bonding in Halogenated Organic Molecules as Revealed by ESCA. D.T. Clark, D. Kilcast and D.B. Adams, Faraday Discussions of the Chem. Soc. 1972, No. 54, 182.
9. An ESCA Study of the Molecular Core Binding Energies of the Fluorobenzenes. D.T. Clark, D. Kilcast, D.B. Adams, and W.K.R. Musgrave, J. Electron. Spectrosc. 1972/3, 1, 227.
10. Estimation of Core Electron Binding Energies for Free Atoms: A Test of the Validity of the Equivalent Cores Approximation. D.B. Adams and D.T. Clark, J. Electron Spectrosc. In press.
11. Ab Initio Calculations of Core Electron Binding Energies and Shifts in Halomethanes. D.B. Adams and D.T. Clark, Theor. Chim. Acta., Accepted for publication.

## SUMMARY

Shifts in core electron binding energies, as measured by ESCA, are shown to be adequately accounted for by non-empirical molecular orbital calculations within the Hartree-Fock formalism. A detailed comparison is made of the basis set dependencies of the shifts predicted using Koopmans' theorem, differences in energy between the molecule and the core hole state, and shifts predicted by the equivalent cores approximation. The equivalent cores approximation yields shifts which are quite insensitive to the basis set employed and for the  $C_{1s}$  levels the calculations indicate that the weak, but probably not the strong, form of the approximation is valid. However, an analysis of the equivalent cores approximation, for free atoms, in terms of experimental ionization energies shows that even the weak form of the approximation fails for the 2s levels of second row elements but this may be qualitatively understood in terms of shielding constants.

The charge potential model for the interpretation of core binding energy shifts may be inverted to yield experimental charge distributions in quite complex molecules from ESCA data. These charge distributions are in good agreement with those predicted by semi-empirical CNDO/2 SCF MO calculations and do not require detailed assignments of binding energy shifts.

Used in conjunction with CNDO/2 charges the charge potential model may be used to simulate the  $C_{1s}$  spectra of the component

compounds of nucleophilic substitution in perfluoroindene and combined with other known experimental data the major site of substitution is identified as the 3-position. The  $C_{1s}$  spectrum of the product of fluoride ion initiated trimerization of perfluorocyclobutene may be used to determine which of several postulated isomers is formed, either by comparison with  $C_{1s}$  binding energy data of fluorocarbons of known structure or by simulation of the  $C_{1s}$  spectra using the charge potential model.

## ABBREVIATIONS

AO	Atomic Orbital
BE	Binding Energy
ESCA	Electron Spectroscopy for Chemical Analysis (also known as X-ray Photoelectron Spectroscopy, XPS)
eV	Electron volt
h	Planck's constant
$\hbar$	Planck's constant divided by $2\pi$
KE	Kinetic Energy
LCAO	Linear Combination of Atomic Orbitals
n.m.r	Nuclear magnetic resonance
n.q.r.	Nuclear quadrupole resonance
MO	Molecular Orbital
PES	Photoelectron Spectroscopy (usually ultraviolet)
SCF	Self Consistent Field
UPS	Ultraviolet Photoelectron Spectroscopy

$$\langle \dots | \dots \rangle \equiv \int \dots \dots \dots d\tau$$

$$\langle \dots | \mathcal{H} | \dots \rangle \equiv \int \dots \mathcal{H} \dots d\tau \text{ where } \mathcal{H} \text{ is an operator}$$

## CONTENTS

	<u>page</u>
<b><u>CHAPTER I:</u> ESCA (Electron Spectroscopy for Chemical Analysis) - a General Introduction</b>	<b>1</b>
1. The Early Development of ESCA	1
2. Processes Involved in ESCA and Related Spectroscopies	4
a) Photoionization	4
b) Shake-up and Shake-off Processes	5
c) X-ray Spectroscopies	8
d) Auger Spectroscopy	10
3. Instrumentation	13
a) X-ray Generator	13
b) Sample Region	13
c) Energy Analyzer	16
d) The Detector and Data Acquisition	19
4. Reference Levels and the Relationship between Binding Energies in Solid and Gaseous Samples.	20
5. Sample Handling.	25
a) Involatile Solids (non-metallic)	25
b) Liquids	27
c) Volatile Solids	28
d) Gases	28
6. Important Features of ESCA Spectra	29
a) Binding Energies	29
b) Chemical Shifts	30
c) Spin-Orbit Splitting	31
d) Multiplet Splitting	33
e) Electrostatic Splitting	34
f) Satellite Peaks	35

6.	g) Line Widths	36
	h) Escape Depths	37
	i) Deconvolution of Partially Resolved Spectra	39
7.	A Brief Survey of the Applications of ESCA in Chemistry.	39

<b><u>CHAPTER II</u></b>	<b>Molecular Orbital Theory.</b>	<b>42</b>
	Introduction	42
1.	A Brief Summary of Quantum Mechanics	43
2.	Hartree-Fock Self Consistent Field Theory	53
3.	Basis Functions and Basis Sets	60
	a) Single Exponential functions	61
	b) Gaussian Type Functions	61
	c) Minimal Basis Sets	64
	d) Split Valence Basis Sets	65
	e) Double Zeta and Extended Basis sets	65
	f) Gaussian Basis Sets	66
	g) Polarization Functions	68
4.	Mulliken Population Analysis	68
5.	Limitations of Hartree-Fock Calculations	70
6.	Improvements on the Hartree-Fock Method	72
7.	Computer Programs for ab-initio Calculations	73
	a) Programming Philosophies	76
	b) A Brief Description of the Programs Used in this work	78
	c) Open Shell SCF Calculations using ATMOL 2	84

	page
8. Semi-Empirical LCAO SCF MO Calculations	86
a) Semi-Empirical All-Valence Electron Neglect of Diatomic Overlap Method (NDDO)	87
b) All Valence Electron, Complete Neglect of Differential Overlap Method (CNDO)	88
<b><u>CHAPTER III</u></b> <b>The Theoretical Interpretation of ESCA Chemical Shifts.</b>	<b>97</b>
1. Introduction	97
a) Equivalent Cores Method	98
b) Charge Potential Model	102
c) Koopmans' Theorem	107
d) Hole State Calculations	114
e) Quantum Mechanical Potential at the Nucleus Model	118
2. Equivalent Cores Shifts from CNDO calculations	124
3. A Comparison of Equivalent Cores, Koopmans' Theorem and Charge Potential Shifts from Minimal Slater Basis Set Calculations.	127
4. A Comparison of Koopmans' theorem, Equivalent Cores Calculations and Hole State Calculations as a Function of Basis Set.	136
a) Koopmans' Theorem Calculations	138
b) Hole State Calculations	142
c) Equivalent Cores Calculations	145
d) Reorganization Effects	150
5. Equivalent Core Estimates of Core Electron Binding Energies in Atoms from Ionization Potential Data.	153
6. A Comparison of Assignments of $C_{1s}$ Binding Energies Based on Koopmans' Theorem and the Charge Potential Model.	159

	page
<b><u>CHAPTER IV</u></b> The Charge Potential Model and Molecular Charge Distributions.	162
1.    Background and Development	162
2.    Uses of the Charge Potential Model	173
3.    Charge Distributions - the Inversion of the Charge Potential Model	177
a)    Charge Distributions in Aromatic Hydrocarbons and their Perfluoro-Analogues	178
b)    Use of Experimental Charge Distributions for Detecting Sample Charging Effects.	187
c)    Charge Distributions in Large Molecules	189
d)    Experimental Charge Distributions in the Fluorobenzenes	195
e)    Experimental Charge Distributions in the Chlorobenzenes	202
4.    A Note on the Use of CNDO/2 Calculations on Molecules containing Second Row Elements for the Assignment of Shifts in Molecular Core Binding Energies.	209
5.    Discussion	211
<b><u>CHAPTER V</u></b> The Application of ESCA to Some Problems in Fluorocarbon Chemistry.	213
1.    Orientation of Nucleophilic Substitution in Perfluoroindene	213
a)    Background	213
b)    Simulation of the C <sub>1s</sub> Spectra of Mono-substituted Perfluoroindenes and Identification of the Major Component	216
2.    Determination of the Product of the Fluoride Ion Initiated Trimerization of Perfluorocyclobutene	222
a)    Background	222
b)    Experimentally Based Identification	224
c)    Theoretical Determination of the Structure of C <sub>12</sub> F <sub>18</sub>	235
d)    Discussion	240

**APPENDIX I**    **Orbital Exponents and Contraction Coefficients**

**APPENDIX II**    **Coordinates used in Molecular Orbital and Experimental  
Charge Distribution Calculations.**

**APPENDIX III**    **Computer Programs Used for the Analysis of ESCA  
data.**

**REFERENCES**

**CHAPTER I**

**ESCA**

**(Electron Spectroscopy for Chemical Analysis)**

**A General Introduction**

## 1) The Early Development of ESCA

Since the introduction of the first commercial ESCA spectrometers in 1970 there has been a rapid increase in the use of ESCA by chemists. This is hardly surprising since ESCA is a technique which, being independent of nuclear spin properties, can be used to study any element. (Hydrogen and helium are exceptions since they are the only elements for which the core levels are simultaneously valence levels). The sample being studied may be a solid, liquid, or gas and the requirement is low, (in favourable cases  $\sim 1$  mg of a solid,  $0.1\mu\text{l}$  of a liquid or  $0.5$  cc of a gas at STP). The information obtained, which may relate to both core and valence electrons, is directly related to the electronic structure of the molecule and the theoretical interpretation of the spectra is straightforward but may, if required, be taken to a high degree of sophistication.

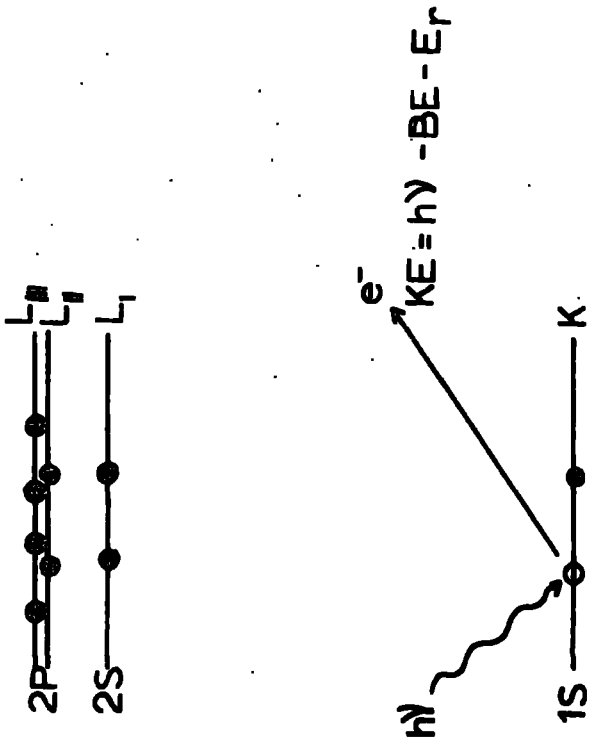
The technique of ESCA, as used today, was developed and named by Siegbahn and co-workers in Uppsala.<sup>1</sup> However, some earlier investigations into the energies of photoelectrons emitted from samples irradiated by X-rays had previously been carried out in England (by H. Robinson)<sup>2,3,4</sup> and in France (by M. de Broglie).<sup>5</sup> These early investigations used a homogeneous magnetic field for the energy analysis of the electrons and the spectra were recorded photographically (a magnetic spectrograph). The anode material in an X-ray tube emits strong characteristic X-rays of a particular energy superimposed on a continuous background radiation (Bremsstrahlung). If X-rays impinge on a sample (e.g. a metal foil) photoelectrons are emitted and these were recorded on a photographic plate in the magnetic spectrograph. Electron energy distributions were obtained which had long tails with edges at the high



energy end and, by measuring the positions of the edges, the energies of the photoelectrons ejected from the different atomic shells in the element were obtained. Using the known energies of the X-ray lines in the primary X-ray beam the binding energies of the electrons in the different shells were calculated. The results were not very accurate since the edge positions were not well defined because of the energy absorption from the electrons emerging from the foil. More accurate data on atomic energy levels could then be obtained from X-ray absorption and X-ray emission spectroscopies, and the few further attempts<sup>6,7,8,9</sup> to extend the early work of Robinson and de Broglie met with comparatively little success.

In 1951 K. Siegbahn initiated a research programme aimed at the very high resolution study of the energy spectrum of electrons expelled by X-rays. The instrument developed was an iron-free double focussing magnetic spectrometer which was initially used for studying  $\beta$ -rays from radioactive sources.<sup>10,11</sup> In 1954 the instrument was ready for use with X-ray excitation of photons. It was observed that, at high resolution, a sharp strong line could be resolved from the edge of each electron veil<sup>1</sup> (Fig.1.1). This line arises from electrons which do not undergo any energy loss and corresponds to the binding energy of the relevant inner shell. An intensity minimum separates this line from the approximately continuous energy distribution of electrons emitted with lower kinetic energy. This minimum occurs because electrons passing through the sample can only lose energy in certain discrete amounts (plasmon excitations, ionizations and excitations in interband transitions).<sup>12</sup> The line widths of the photoelectrons emitted without energy loss depend on:<sup>1</sup>

PHOTOIONIZATION of a CORE ELECTRON



ELECTRON SPECTRUM of MgO with Cu K $\alpha$  X-RAYS

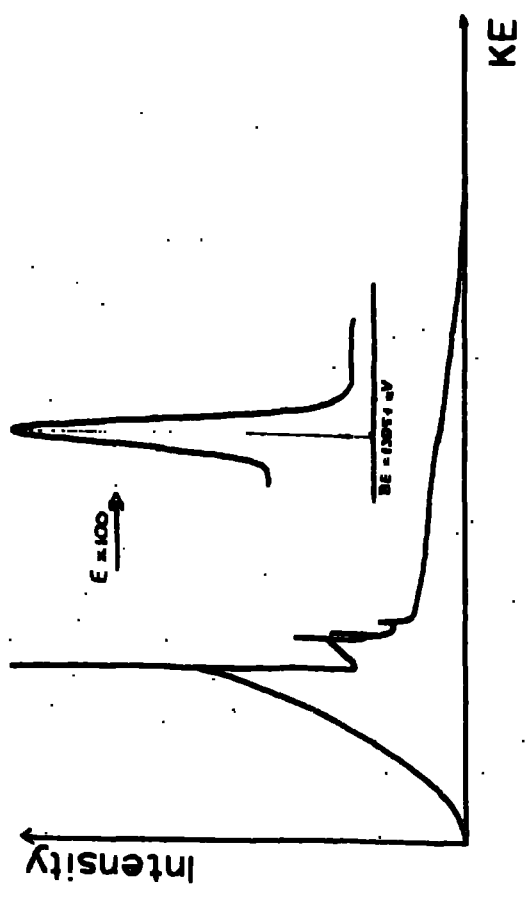


Figure (1.1)

Figure (1.2)

- i. the natural width of the incident X-ray line
- ii. the width of the atomic level from which the electrons are ejected
- iii. the aberration of the spectrometer
- iv. the width of the source and detector slits of the spectrometer.

Although chemical shifts of inner electronic levels in copper and its oxides were reported as early as 1958<sup>13</sup> the observation of great importance, made in 1964, was the appearance of two 1s peaks from the distinct oxidation states of sulphur in sodium thiosulphate.<sup>14</sup> It was the observation of such chemical shifts that lead to the realization of the potential uses of ESCA in chemistry. (Chemical shifts in X-ray spectroscopic data had previously been observed<sup>15,16</sup> but in emission spectra they were small and difficult to interpret and in absorption spectra they were difficult to study because of complicated edge structures). Early E.S.C.A. studies were carried out on solids, or condensed vapours, but with the provision of differential pumping gaseous samples may also be studied.<sup>17</sup>

## 2) Processes Involved in ESCA and Related Spectroscopies

### a) Photoionization

The sample being studied is irradiated with X-rays of known energy, typically  $MgK_{\alpha 1,2}$  (1253.7 eV) or  $AlK_{\alpha 1,2}$  (1486.6 eV). Electrons which have a binding energy less than the energy of the exciting radiation may be ejected allowing the study of both core and valence electrons. Consider the emission of a 1s electron from a gaseous sample Fig.1.2. The kinetic energy of the photoelectron, KE, is given by

$$KE = h\nu - BE - E_r$$

where  $h\nu$  is the energy of the photon ( $h$  is Planck's constant and  $\nu$  is the frequency of the radiation),  $BE$  is the binding energy of the electrons and  $E_r$  is the recoil energy of the sample. The recoil energy is usually negligible except where high energy X-rays are used with light atoms (e.g. for Li using  $AlK_{\alpha}$  (1486.6 eV) and  $AgK_{\alpha}$  (22,000 eV) the recoil energies are 0.1 and 2 eV respectively. Since this work considers molecules containing atoms higher in the periodic table than lithium and uses low energy X-rays,  $AlK_{\alpha 1,2}$  or  $MgK_{\alpha 1,2}$ , then the recoil energy is negligible. The binding energy of the electrons ( $BE$ ) in a gaseous sample is therefore simply the difference in energy between the X-ray energy ( $h\nu$ ) and the kinetic energy of the photoelectron ( $KE$ )

$$KE = h\nu - BE$$

(The relationship between binding energies in solids and gases will be discussed later (Chapter I.4)).

The complementary technique of ultraviolet photoelectron spectroscopy<sup>18</sup> (U.P.S. or P.E.S.) is based on the same principles and normally employs He(I) radiation (21.22 eV) although other radiation, mainly HeII (40.8 eV),<sup>19</sup> has been used. Only valence electrons can be studied but total line widths in PES (typically 0.015 eV) are much less than those in ESCA (typically 1-2 eV) and vibrational fine structure can often be resolved. (The ion formed by photoionization is generally in a vibrationally excited state since the equilibrium bond distances are usually not equal in the ground states of the molecule and ion. A high degree of vibrational structure is associated with ionization from a strongly bonding, or antibonding, orbital). The cross sections for photoionizations of particular electrons vary with photon energy<sup>1,17,18</sup>

and valence electron spectra of molecules studied by PES and ESCA show considerably different intensity ratios, Fig.1.3. A knowledge of the change in cross sections for photoionizations as a function of photon energy of, for example, the 2s and 2p electrons would allow an estimate of the contributions of the atomic orbitals to the molecular orbital. Studies of the angular distribution of the intensities may also yield information on the symmetries of orbitals.<sup>20</sup> The Mg radiations of yttrium (132 eV) and some other second transition series elements can be used to probe further into the valence region than is possible with He radiation.<sup>21,22</sup>

#### b) Shake up and Shake off Processes

When ionization of a core electron occurs the sudden perturbation of the valence cloud may lead to the simultaneous excitation (shake-up) or emission (shake-off) of an outer electron<sup>17,23,24</sup> (Fig.1.4). These processes give rise to satellite peaks with lower kinetic energy than the main photoionization peak,

$$KE = h\nu - BE - \bar{E}$$

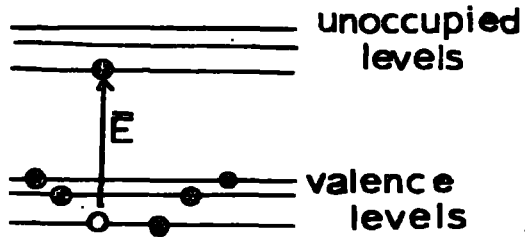
where  $\bar{E}$  is the energy of the shake up or shake off process.

The probability of exciting an electron from the orbital denoted by  $nlj$  of the neutral atom to the orbital  $n'lj$  of the ion is given by,<sup>24</sup>

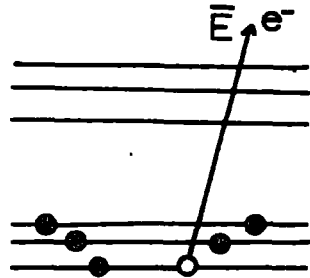
$$P_{n'lj \leftarrow nlj} = N \left| \int \Psi_{nlj}^* \Psi'_{n'lj} d\tau \right|^2$$

Where  $N$  is the number of electrons in orbital  $nlj$  and  $\Psi_{nlj}$  and  $\Psi'_{n'lj}$  are the wave functions of orbitals  $nlj$  in the atom and  $n'lj$  in the ion. Since the probability of shake up involves the overlap of the two orbitals

SHAKE-UP



SHAKE-OFF



$$KE = h\nu - BE - \bar{E}$$

Figure(1.4)

Differential Changes in Cross Section  
with photon Energy

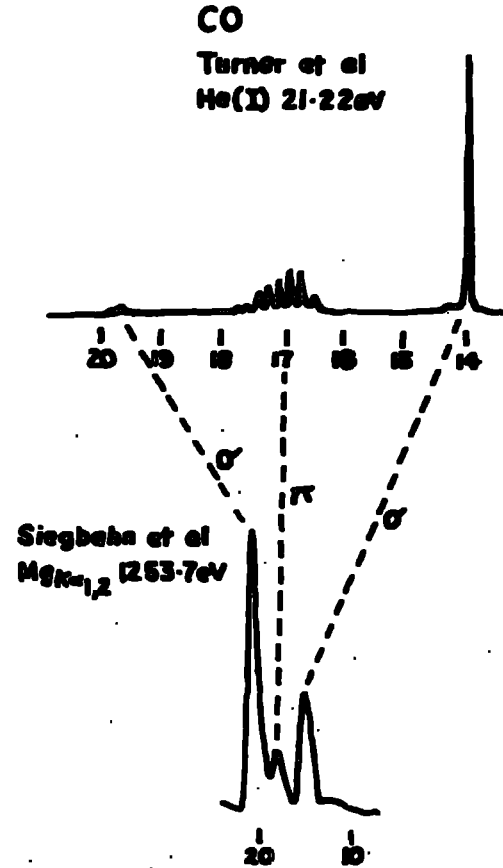


Figure (1.3)

		<u>CNDO</u>	
		C	O
		% 2s	2p
σ		36.5	42.5
π		29.5	70.5
σ		30	52.6

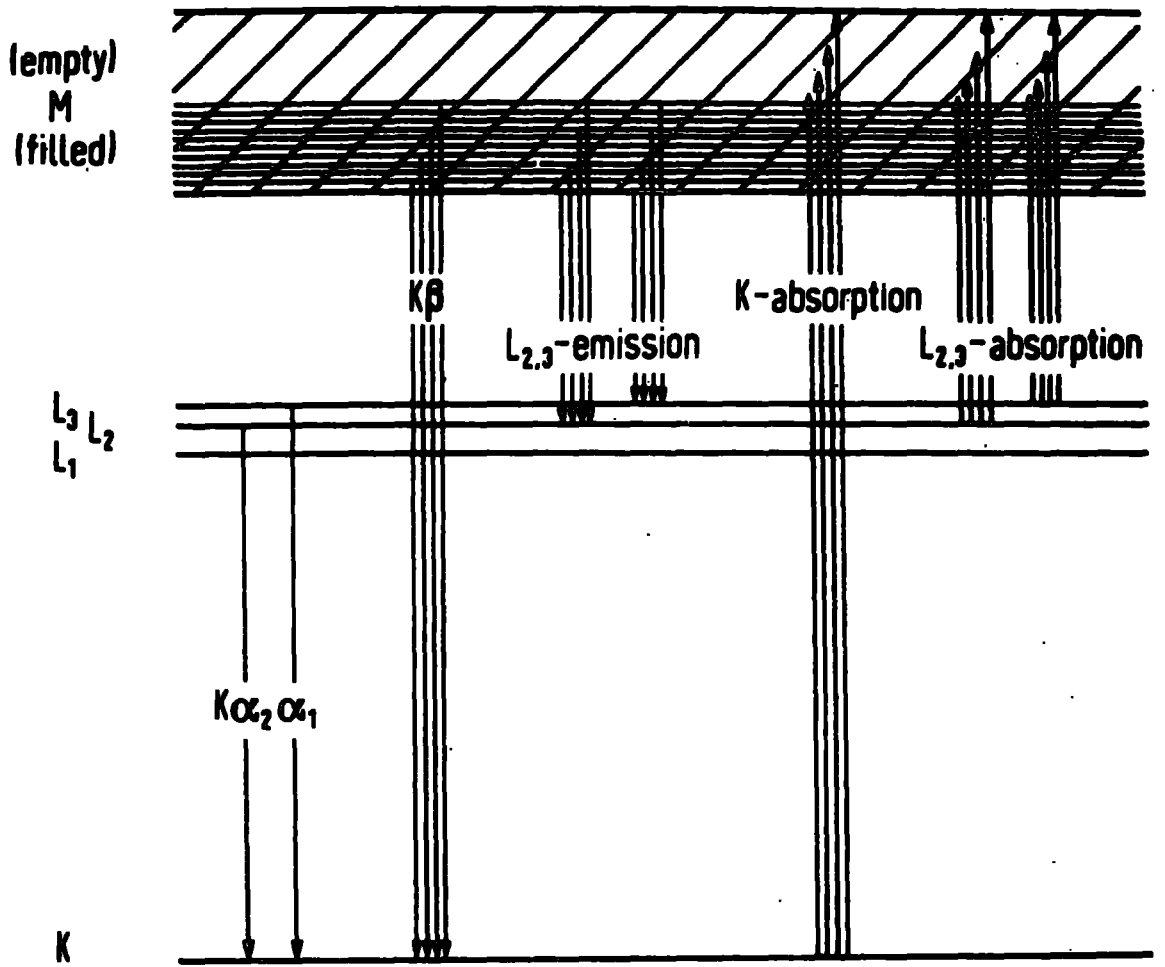
involved the selection rules governing the shake up excitation are of the monopole type

$$\Delta J = \Delta L = \Delta S = \Delta M_J = \Delta M_L = \Delta M_S = 0$$

This analysis has been extended to molecules<sup>25</sup> and satellite peaks arising from shake up processes have been observed in inert gases<sup>17</sup> and molecules<sup>26</sup> in both vapour and condensed phases.

### c) X-ray Spectroscopies

The removal of a core electron from an atom leaves the atom in a highly excited state. The core vacancy is filled by an electron from an outer orbital and energy may be released in the form of an X-ray and it is this process which gives rise to X-ray emission spectroscopies<sup>1,27,28</sup> (Fig.1.5). For the production of X-rays in X-ray guns the core vacancy is produced by bombardment of the metal anode with a high energy beam of electrons. However, this is not suitable for the study of compounds since chemical decomposition often occurs. Therefore in X-ray emission studies secondary X-rays are excited by means of a primary X-ray beam (as in ESCA) and the energies of the emitted X-rays give information on the differences in energy levels in the sample. (The observed emissions are those permitted by the atomic selection rules  $\Delta l = \pm 1$ ,  $\Delta j = \pm 1, 0$ ). Siegbahn<sup>29</sup> has recently carried out some ultra soft X-ray emission studies of the  $CK_{\alpha}$  X-ray emission line (285 eV) and has succeeded in resolving components from the  $3\sigma$  and  $1\pi$  valence orbitals in gaseous carbon monoxide using electrons to create the core vacancies. With further improvements in resolution and intensity it may be possible to resolve the vibrational fine structure.



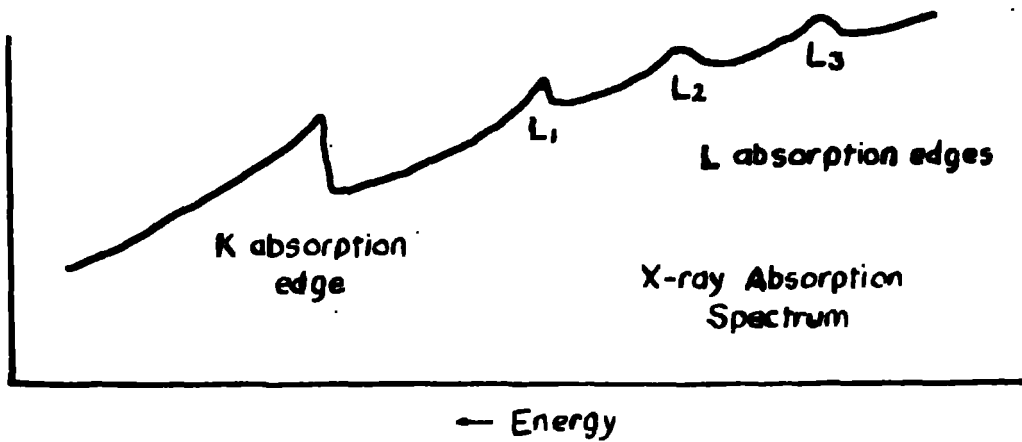
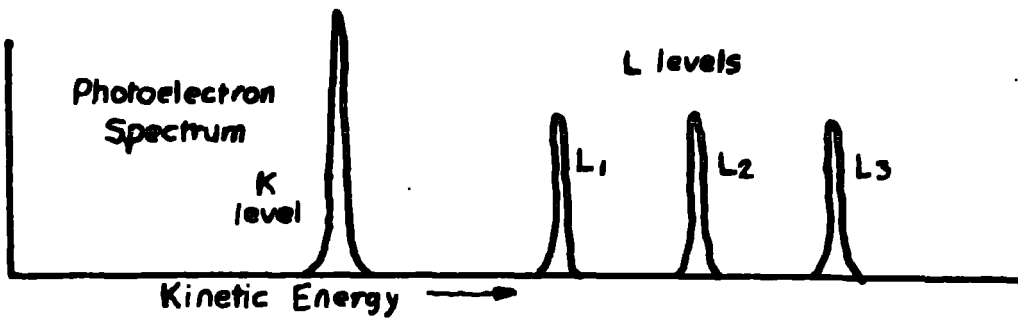
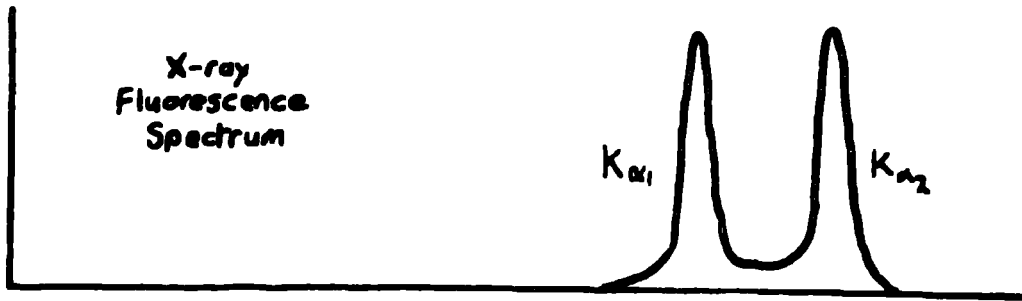
Simplified level diagram with the possible X-ray transitions for elements of the 3rd period. The horizontal shading denotes the occupied part of the valence band.

Figure(1.5)<sup>28</sup>

X-ray absorption spectroscopy involves passing the X-ray beam through the sample and measuring the intensity of the radiation passing through the sample as a function of wavelength.<sup>28</sup> This gives rise to absorption edges which correspond to the energy required to excite an electron from one of the inner shells to the lowest unoccupied level (Fig.1.5). The relationship between electron spectroscopy, X-ray emission spectroscopy and X-ray absorption spectroscopy is illustrated in Fig.1.6.

#### d) Auger Electron Spectroscopy

The alternative mode of relaxation after photoionization of a core electron is Auger electron emission.<sup>30,31,32,33</sup> An electron from an outer shell fills the vacancy, but instead of photon emission the energy is transferred to another electron which is also emitted to give a doubly ionized species Fig.1.7. If one of the final vacancies is in the same shell as the primary vacancy the process is known as a Coster-Kronig transition<sup>34,35</sup> and the primary hole state has a short lifetime and this produces line broadening of the photoelectron peak.<sup>17</sup> Auger electron emission is more probable than X-ray emission for elements of low atomic number (Fig.1.8). These electrons are also recorded in ESCA spectra, but since their energies are independent of the exciting radiation (provided it is great enough to create the primary vacancy), they may readily be distinguished from photoelectrons by changing the energy of the exciting radiation. Chemical shifts have also been observed in Auger spectra.<sup>17</sup> Excitation of Auger spectra normally uses electrons since it is relatively easy to generate and focus a high intensity beam. Because of the relatively small mean free path of electrons in solids (as compared with photons for example) Auger spectroscopy is particularly suited for surface work.



Simulated X-ray fluorescence, X-ray absorption, and photoelectron spectra for same elements

Figure (1.6)

# AUGER ELECTRON EMISSION

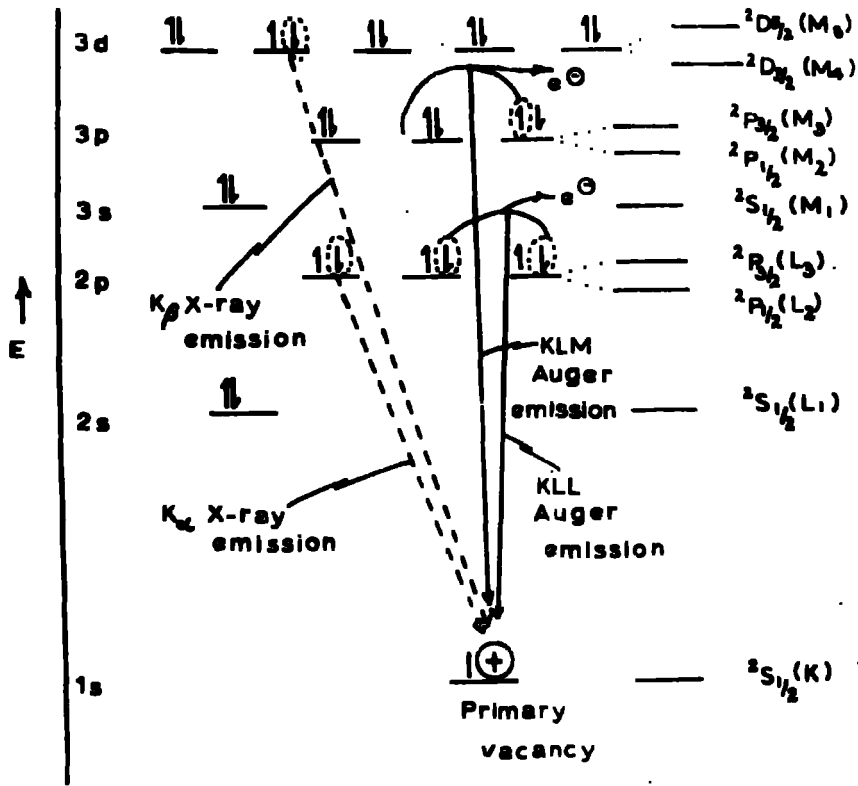


Figure (1.7)

## PROBABILITY of AUGER ELECTRON EMISSION and X-RAY FLUORESCENCE

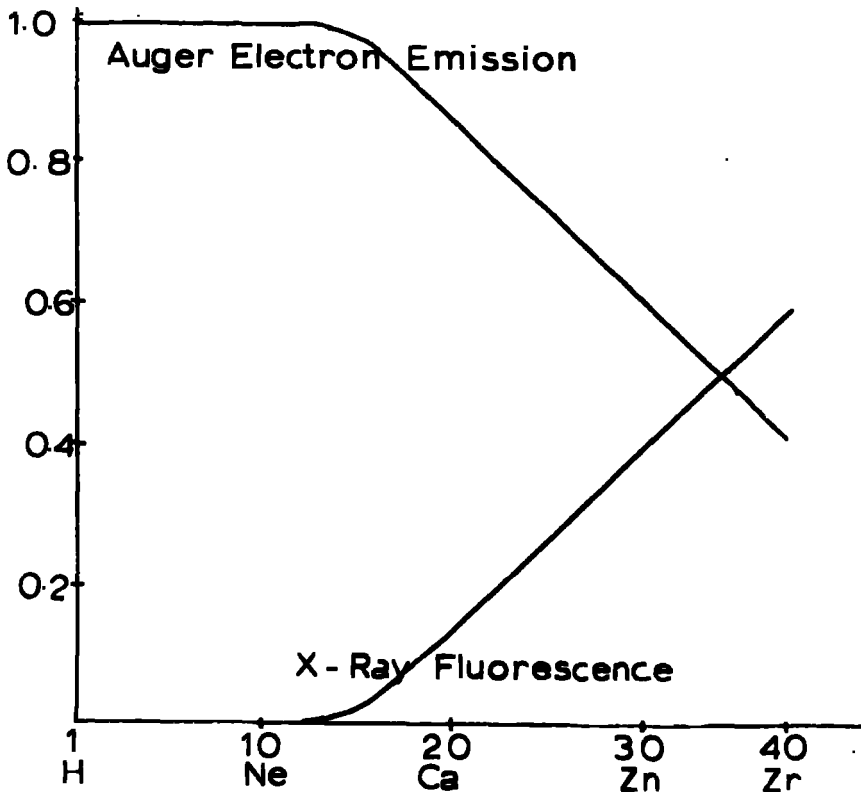


Figure (1.8)

### 3) Instrumentation

Fig.1.9 shows a schematic diagram of the AEI ES100 spectrometer employed in this work. The essential components of this, and other electron spectrometers are:

#### a) X-ray Generator

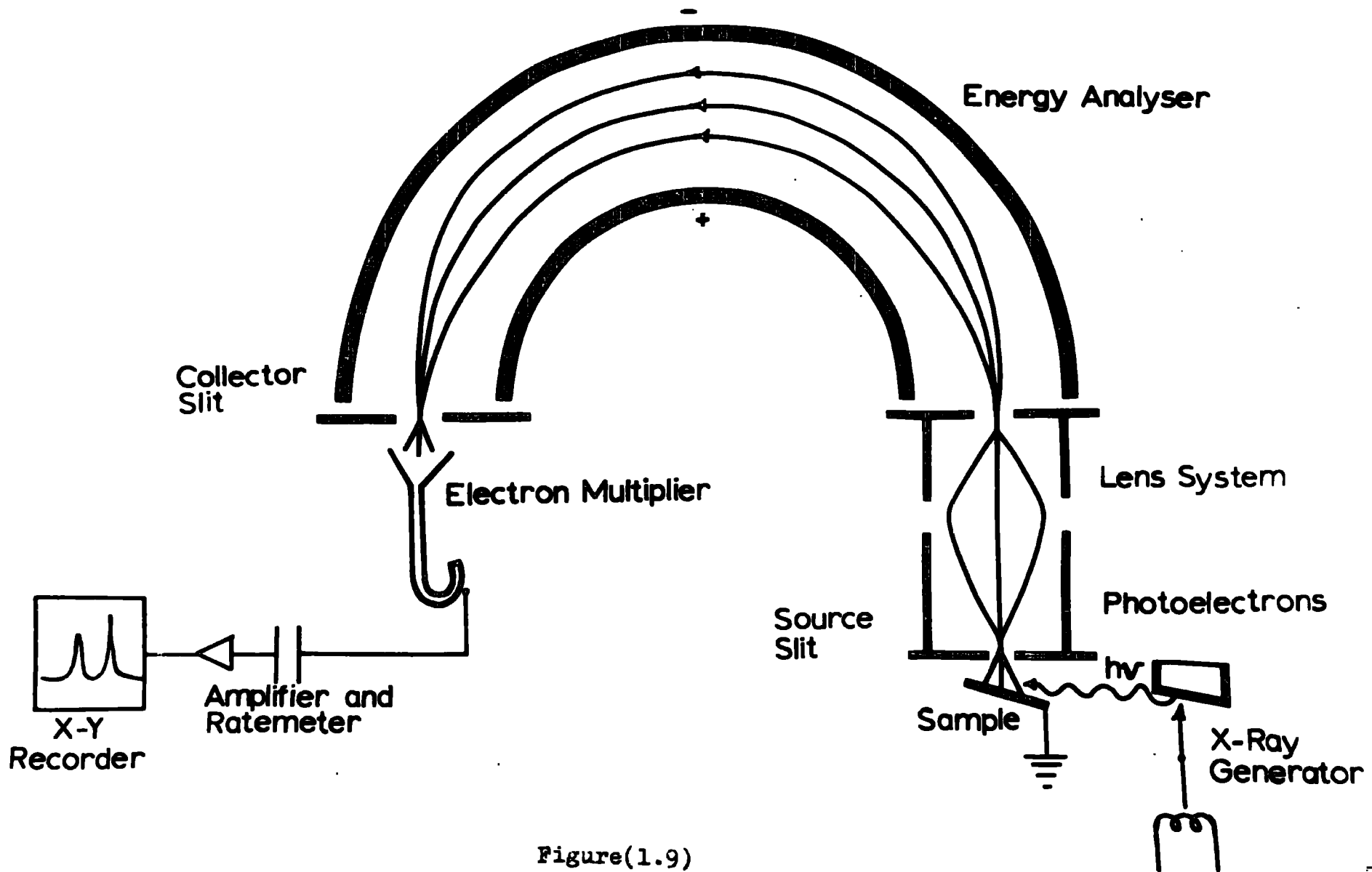
The most commonly used X-ray sources are  $MgK\alpha_{1,2}$  and  $AlK\alpha_{1,2}$  radiation with photon energies (and line widths) of 1253.7 eV ( $\sim 0.7$  eV) and 1486.6 eV ( $\sim 0.9$  eV) respectively. Typical operating conditions for the X-ray generator would be a pressure of less than  $4 \times 10^{-6}$  torr and 12KV, 20 mA for a magnesium target. Line widths may be reduced by monochromatization techniques<sup>1,17</sup> and this improves resolution and eliminates unwanted background radiation and X-ray satellites. The wavelength of  $AlK\alpha$  radiation ( $\lambda$ ) is  $8.34 \text{ \AA}$ ,<sup>36</sup> and by diffraction from the 100 plane of quartz at an incident angle  $\theta$  of  $78.5^\circ$  the required conditions for the Bragg equation are satisfied<sup>17</sup>

$$n\lambda = 2d \sin\theta \quad \begin{array}{l} n \text{ is an integer} \\ d \text{ is the interatomic spacing.} \end{array}$$

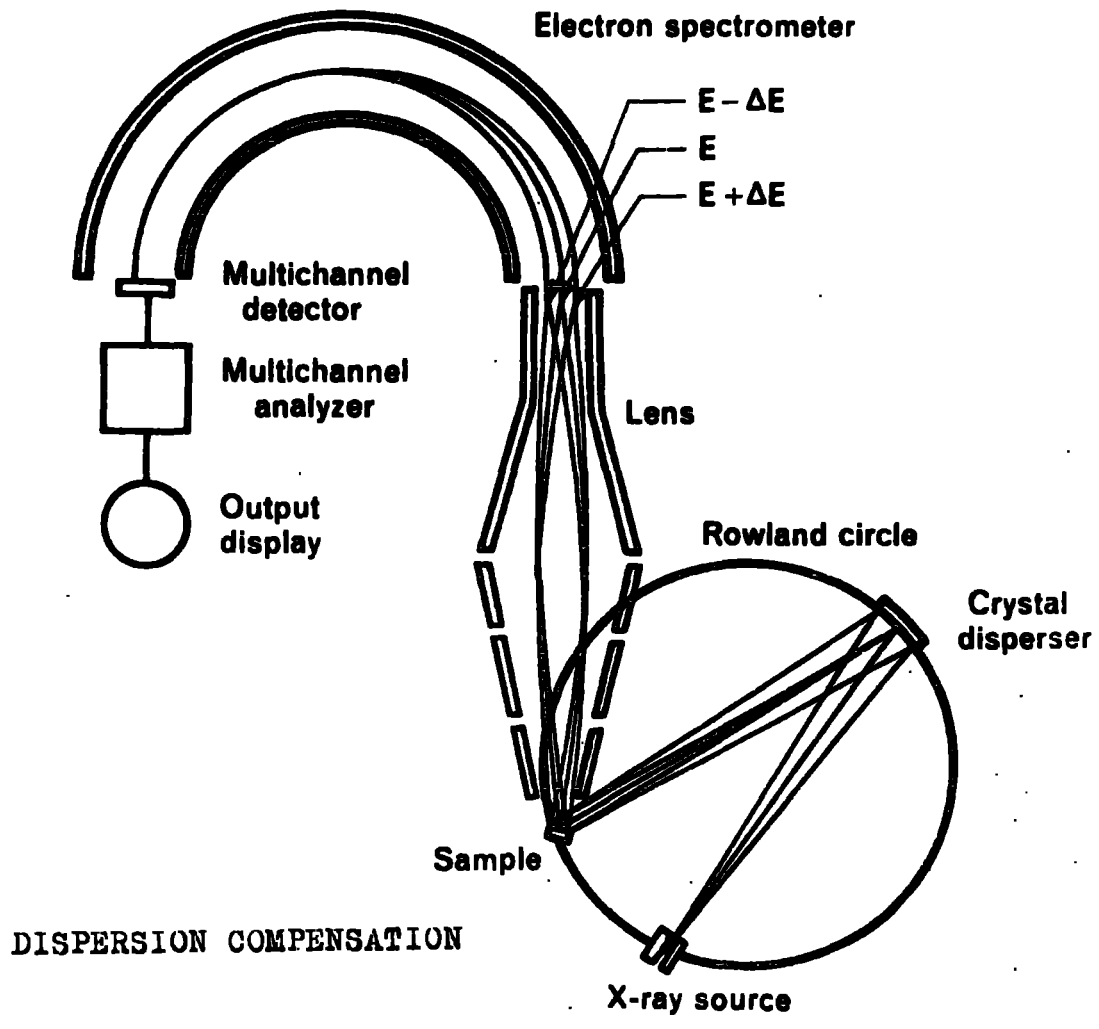
(Similar conditions cannot be satisfied in the case of magnesium  $K\alpha$  radiation. After separating the  $AlK\alpha$  radiation from the background it may be passed through a slit to reduce the line width prior to impinging on the sample (slit filtering) or the photoelectrons may be passed through a lens system to allow for the peak shape of the  $K\alpha$  radiation (dispersion compensations).<sup>37,38</sup> The principles of these methods are shown in Fig.1.10.

#### b) Sample Region

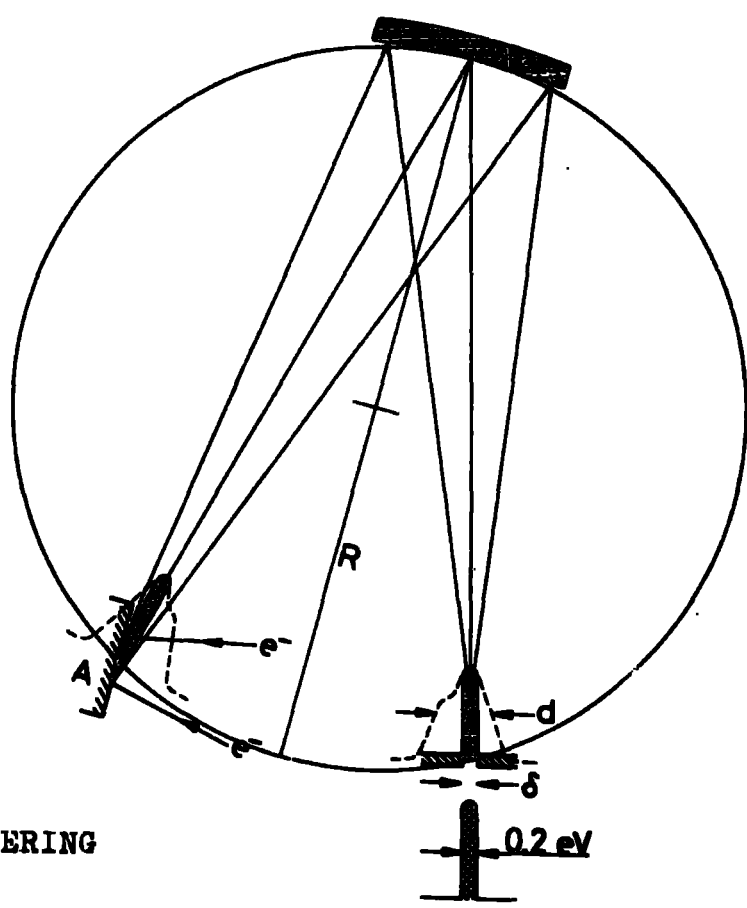
The sample region of the spectrometer is separated from the X-ray generator by a thin (0.3 thou) aluminium window which ensures that electrons



Figure(1.9)



DISPERSION COMPENSATION



SLIT FILTERING

Figure(1.10)

from the electron gun do not enter the sample region. Samples are studied on the tip of a probe which may be inserted into the sample region (via an insertion lock) without letting the sample region up to atmospheric pressure. The tip of the probe may be heated to over 250°C or cooled to liquid nitrogen temperatures as required and the probe can be oriented in the X-ray beam to obtain maximum signal intensity. Typical operating pressures are  $5 \times 10^{-6}$  torr or better but some spectrometers are suitable for ultra high vacuum work (better than  $10^{-9}$  torr). Sample handling techniques will be discussed in more detail later (Chapter I.5).

c) Energy Analyzer

The electron energy analyzer should have a resolution in the region of one part in  $10^4$ . The analyzer on the ES100, and most other commercial ESCA spectrometers, is a hemispherical double focussing analyzer based essentially on the principles described by Purcell.<sup>39</sup> The resolution of the analyzer,  $\Delta E/E$ , where E is the energy of the electrons depends on the mean radius of the hemispheres R and the combined widths of the entrance and exit slits W

$$\frac{\Delta E}{E} = \frac{R}{W} \quad (1)$$

The resolution can be improved by reducing the slit widths (which reduces the signal intensity), increasing the radius of the hemispheres (which greatly increases engineering difficulties), or by retarding the electrons before they enter the analyzer. A compromise must be made in terms of the analyzer size based on cost and ease of construction since difficulties which arise include accurate machining and support of the hemispheres without mechanical distortion. A large analyzer section would also require

a very efficient pumping system due to its size. Before entering the energy analyzer the electrons, in the ES100, pass through a retarding lens system. This has a twofold purpose:

- i) By removing the sample region away from the analyzer more flexible sample handling facilities are possible.
- ii) By employing a retarding potential the stringency on the resolution requirements of the analyzer may be reduced as outlined by Helmer and Weichert;<sup>40</sup>

The transmitted electron current,  $I$ , of the relevant monoenergetic electrons is given by

$$I = BA\Omega \quad (2)$$

where  $B$  is the brightness of the electron illumination of the entrance slit, in units of current per unit area per unit solid angle,  $A$  is the area of the entrance slit, and  $\Omega$  is the solid angle of the aperture of the spectrometer as viewed from the entrance slit ( $A\Omega$  is the luminosity of the spectrometer). The brightness  $B$  is determined by the strength of the X radiation at the sample and since it is low a high luminosity,  $A\Omega$ , is required. The luminosity is given by

$$A\Omega = CR^2 \left( \frac{\Delta E}{E} \right)^2 \quad (3)$$

If  $E$  is reduced by applying a retarding potential to the electrons before they enter the entrance slit of the spectrometer the luminosity may be increased, without affecting  $\Delta E$ , by increasing the slit dimensions and acceptance angles (3). Furthermore the dimensional precision of the instrument is relaxed by the larger overall value of  $\Delta E/E$  (1). The brightness of the electron beam is proportional to its kinetic energy and

is therefore reduced in a retarding field. If  $B_0$  is the electron brightness at the sample, where the photoelectrons have energy  $E_0$ , and  $E$  is the kinetic energy of the electron as it passes through the entrance slit to the analyzer the brightness is given by

$$B = \left( \frac{B_0}{E_0} \right) E \quad (4)$$

and combining (2) and (3) gives

$$I = B_0 CR^2 \left( \frac{(\Delta E)^2}{E \cdot E_0} \right) \quad (5)$$

and hence an increase in intensity of the transmitted current  $I$  is also obtained. Thus, for example, if the electrons are retarded from 1000 eV to 100 eV then an increase in the luminosity of up to a factor of 100 may be obtained by increasing the slit dimensions and acceptance angle and an increase in the transmitted current of a factor of 10 occurs (5) despite the factor of ten reduction in brightness at the analyzer entrance slit (4).

Electrons of the required kinetic energy may be focussed at the collector slit by either

- a) Scanning the retarding potential while keeping a constant potential between the analyzer hemispheres
- or b) Scanning the retarding potential and the potential between the analyzer hemispheres simultaneously keeping a constant ratio between the two. This is the method used in the ES100.

The overall resolution  $\Delta E_m/E$  depends also on contributions other than from the analyzer

$$(\Delta E_m)^2 = (\Delta E_x)^2 + (\Delta E_1)^2 + (\Delta E_s)^2$$

where  $\Delta E_x$  is the width of the X-ray line inducing the emission

$\Delta E_1$  is the width of the natural energy distribution of the electron energy level

$\Delta E_s$  is the width of the broadening due to spectrometer aberration and depends on the emission energy E and the slit width.

The width of the collector slit is variable (0.2, 0.1 or 0.03 inches), the choice being a compromise between resolution and sensitivity. Typical operating pressures for the analyzer are better than  $10^{-8}$  torr.

Magnetic double focussing analyzers have also been used<sup>1</sup> but while these are simpler to construct they are more bulky than electrostatic analyzers since they require Helmholtz coils to eliminate stray magnetic fields. The types of energy analyzers used in both high and low energy electron spectroscopy have been briefly reviewed.<sup>41</sup>

#### d) The Detector and Data Acquisition

The electrons passing through the collector slit are detected by a channel electron multiplier and the pulses obtained are amplified and fed into counting electronics. (With most designs of double focussing analyzers their focal plane properties may be exploited by incorporating multichannel detectors which can give spectacular increases in the rate of data acquisition; this system is now being implemented on some commercial spectrometers). Spectra may be generated either by continuous or step scans. In the continuous mode of operation the field (either

electronic or magnetic) is increased continuously while the detector signal is monitored by a rate meter. If the signal is sufficiently strong and the signal to background sufficiently high then the spectrum (a graph of counts per second versus kinetic energy of the electrons) is plotted out directly on an X-Y recorder. Alternatively the energy may be incremented in small steps (typically 0.1eV) and at each setting either a fixed number of counts may be timed (useful if the cross sections for the process are not known) or a count can be made for a fixed length of time. By storing this data in a multichannel analyzer several scans of the region of interest can be made thus averaging any random fluctuations in background and many spectrometers have facilities for varying degrees of computer control. The presence of both wide and narrow scan facilities permits both preliminary searches and detailed study of specific regions.

#### 4) Reference Levels and the Relationship between Binding Energies in Solid and Gaseous Samples.

The natural definition of the binding energy of an electron in a free atom or molecule is the energy required to remove the electron from a given level to infinity (vacuum level). In a solid, however, the outer electronic levels are broadened into bands and a potential barrier exists at the surface; it is therefore more convenient to refer the binding energies of solids to the Fermi level.<sup>1</sup> The Fermi level

$E_f$  is defined by

$$\int_0^{E_f} N(E) dE = N \text{ where } N(E) = Z(E), F(E)$$

(functions of energy).  $Z(E)$  is the density of states for electrons

i.e. the number of states (energy levels) between  $E$  and  $E + \Delta E$ ,  $F(E)$  is the Fermi probability distributions:- the probability that a Fermi particle in a system in thermal equilibrium at temperature  $T$  will be in a state with energy  $E$ .

$$F(E) = \left( e^{\frac{(E-E_f)/kT}{+1}} + 1 \right)^{-1} \quad (kT \ll E_f)$$

$N$  is the total number of electrons in the system and the electrons fill the available states up to the Fermi level. Consider photoionization from a core level in a sample which is in electrical contact with the spectrometer fig (1.11). Since the sample and spectrometer are in electrical contact their Fermi levels are the same and any difference between the work functions of the sample and spectrometer gives a difference in macro potential<sup>42,43</sup> and an electric field arises in the space between the sample and spectrometer chamber. The kinetic energy,  $KE$ , of the electron when it enters the sample chamber is thus slightly different from the energy,  $KE'$ , which it had on emerging from the sample. It is the energy  $KE$  which is measured and taking zero binding energy to be at the Fermi level gives the relationship

$$BE = h\nu - kE - \phi_{sp}$$

The binding energy referred to the Fermi level does not depend on the work function of the sample but on that of the spectrometer,  $\phi_{sp}$ ,

### BINDING ENERGY REFERENCE LEVEL in SOLIDS

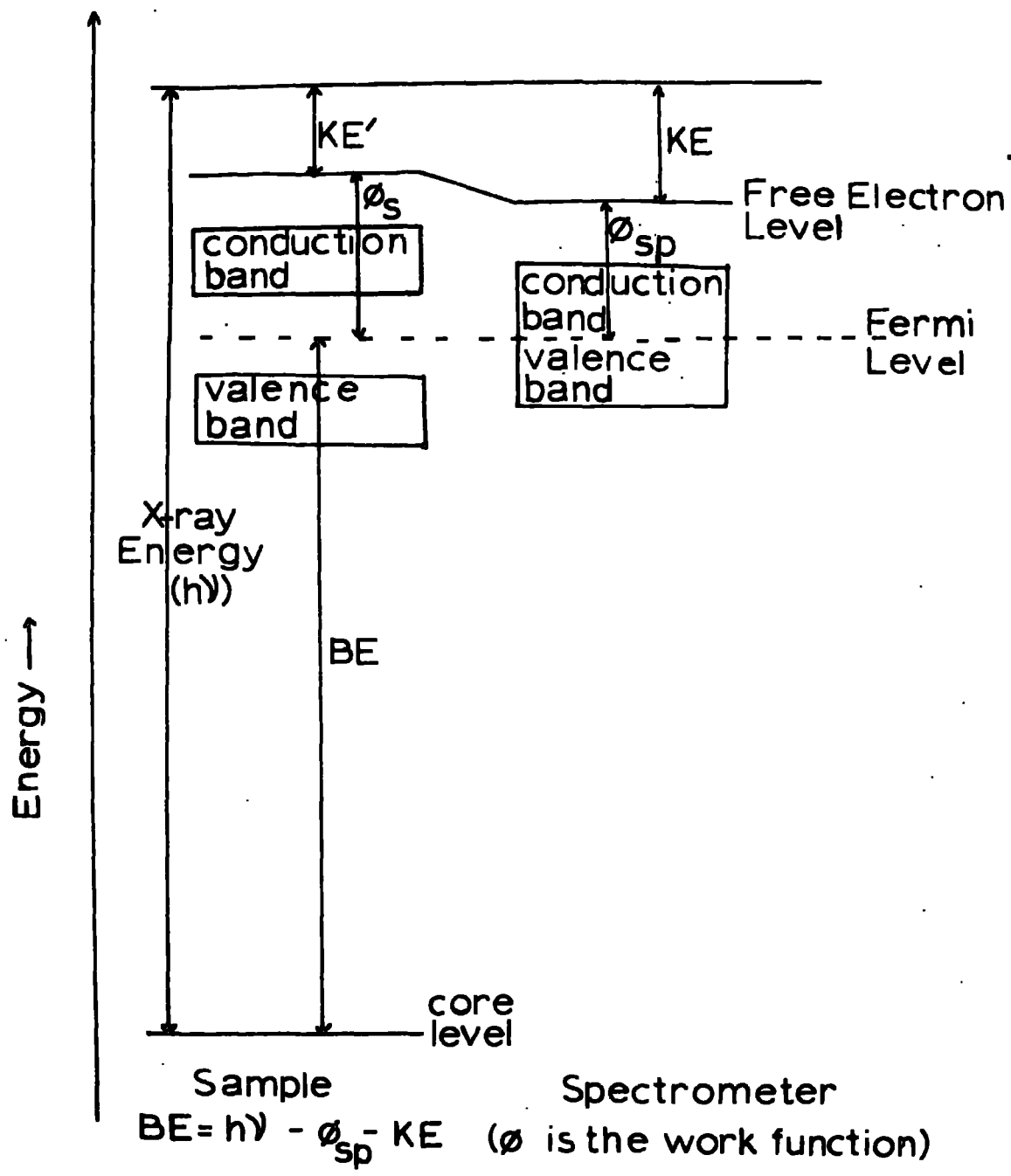
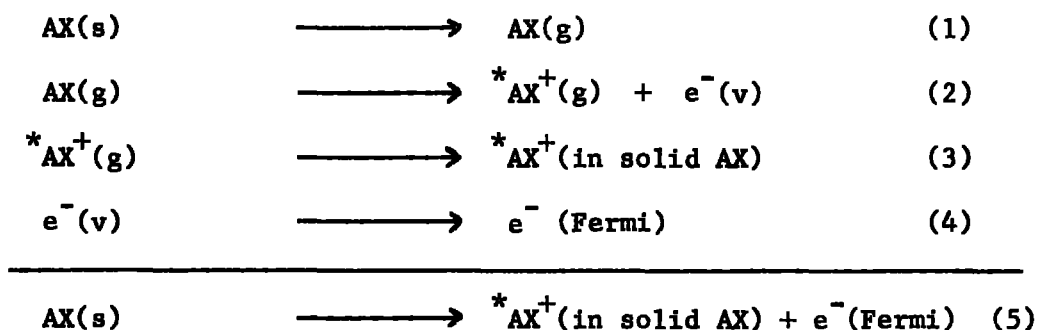


Figure (111)

and this represents a constant correction to all binding energies. For this relationship to hold for non metallic samples a sufficient number of free charge carriers must be present so that the Fermi levels can adjust to a thermodynamic equilibrium state. Electrically insulating samples may be studied by ESCA since a sufficient number of free charge carriers is formed during X-ray irradiation.<sup>1</sup> However, in the case of insulating samples a build up of charge on the surface may occur and this sample charging can shift the energies of all the emitted electrons by a significant amount (typically up to one or two eV with the ES100 used in this work).

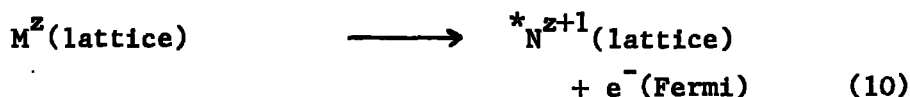
For core ionization from atom A in molecule AX the binding energies in the solid (5) and vapour phase (2) may be related by the processes



(where \* indicates a vacancy in a core level)

The binding energy difference between solid and vapour therefore depends not only on the work functions of the sample (4) but also on the energy required to remove a molecule of AX from the solid (1) and the energy of placing the core ionized species  ${}^* \text{AX}^+$  back into the solid. However, for molecules in the absence of strong interactions

(e.g. Hydrogen bonding) in the solid phase the shifts in binding energy are similar in gases and solids, but the actual binding energies are higher in gases due to the difference in reference level. For ionic solids ionization from a gaseous ion (7) is analogous to reaction (2). Consider an atom M with charge  $z$  in an ionic lattice<sup>39</sup>



Processes (6) and (8) are similar to lattice energies and the energy of process (6) is the actual lattice energy for a lattice in which interchange of the cations and anions yields an indistinguishable lattice (this is a characteristic of most MX lattices).<sup>44</sup> These 'lattice energies' are not simply related to  $z$  and it is unlikely that the combined energy of processes (6) and (8) will be the same for a common ion in different lattices. Thus, while the core electron binding energies in gaseous ions are a smooth function of  $z$ ,<sup>45</sup> there is no reason to expect more than a rough correlation between the binding energies in the lattice and the charge  $z$ . The observation of shifts in binding energies in ionic compounds caused by expansion of the lattice (and consequent change in lattice energy) on heating

has been made<sup>46</sup> and although the shifts are very small they agree well with the expected values.

#### 5) Sample Handling.

The following discussion refers in particular to the AEI ES100 although where relevant mention will be made of additional facilities available on other spectrometers.

##### a) Involatile Solids (non metallic)

The simplest method of sample preparation for an involatile solid is to mount the sample on the spectrometer probe by means of double sided adhesive tape. This has the disadvantage that the sample is not in electrical contact with the spectrometer and sample charging may occur. However, the binding energies do not change with time and the  $C_{1s}$  binding energy from the adhesive tape may be used for calibration purposes. An improvement on this method is mounting a small amount of sample on electrically conducting adhesive tape.<sup>47</sup> The layer of pump oil which forms on the sample surfaces is often used as a reference.<sup>1,47</sup> Where possible a more satisfactory method of sample preparation is to deposit a thin layer of the sample onto a conducting backing (e.g. gold) by evaporation from a solution in a suitable volatile solvent. If a sufficiently thin layer of the sample is deposited such that, for example, the core levels from the conducting backing are observable the photoconductivity induced throughout the sample ensures that the sample takes up the same potential as the sample plate and eliminates

sample charging effects, and the  $4f_{7/2}$  signal from the gold backing (binding energy 84.0 eV) may be used as reference. If, however, a thick layer of sample is deposited the signal from the gold is not observable and some sample charging may occur. Another method of reducing sample charging effects, which has been incorporated in some spectrometers, is to direct a beam of low energy electrons onto the sample (an electron flood gun).<sup>48</sup>

Other methods of sample handling include

- i) Pressing a disc of a powder sample and mounting this on the probe. This generally improves count rates compared with powder samples and the slight deposit of hydrocarbon on the surface may be used as reference.
- ii) A powder sample may be pressed into a wire gauze on the probe.
- iii) Samples in the form of foils or sheets can be clipped directly onto the probe.

Other method of calibrating for charging effects include

- i) Making an intimate mixture of a powder sample with a reference powder (this may be pressed into a disc).
- ii) An internal element may sometimes be used as reference if its chemical environment is known not to change from sample to sample.
- iii) A conducting surface may be deposited on the sample and will take up the same potential as the sample surface and may be used as reference (e.g. the gold decoration technique).

b) Liquids

Liquid samples are introduced by injection through a septum plug into a heatable (25 to 150°C) evacuated reservoir shaft. The vapour diffuses through a metrosil leak and is condensed onto a cooled gold plate on the tip of the sample probe (typical temperatures would be in the range -80 to -150°C). This method ensures that the surface of the sample is continually being renewed and prevents surface contamination by the residual atmosphere in the spectrometer and also obviates difficulties which may arise from X-ray damage. (However, a very low temperature, < 130°C, sometimes leads to the condensation of some water vapour). While the layer of condensed sample is thin, and the Au4f<sub>7/2</sub> peak is observable, no sample charging occurs. However, with a high rate of condensation over an extended period sample charging may occur and this results not only in a change in binding energy but also an increase in peak width.<sup>49</sup> Sample charging effects of this type may readily be monitored by measuring the binding energy of a particular core level when the sample layer is thin and repeating this measurement at regular intervals throughout the experiment.<sup>49</sup>

On some spectrometers liquids may be vaporized and studied directly in the gas phase<sup>17</sup> (This is now routine in several laboratories and is standard in u.v. photoelectron spectroscopy). Work is also being carried out by Siegbahn et al.<sup>21</sup> on the study of liquid beams and they have found that very thin, even submillimeter, well behaved beams of liquid can be formed in a vacuum. When applied to ESCA the beam would pass parallel to the spectrometer slit and could be pumped back to the liquid reservoir for continuous circulation.

c) Volatile solids.

Volatile solids are generally studied by sublimation of the sample from a capillary tube, which may be heated, and subsequent condensation onto a cooled probe. The same considerations of sample charging apply as with condensed liquids. Solids which are very volatile may be injected into the reservoir shaft, using a solid syringe, to reduce the rate of condensation. Solids which are only slightly volatile may be treated similarly to involatile solids but with cooling of the sample probe to prevent sublimation.

d) Gases

Gases may be studied by condensation onto a cooled probe, but several electron spectrometers have facilities for studying samples in the gas phase and gas phase studies have the following advantages:-<sup>38</sup>

- i) No inherent broadening of the levels due to solid state effects.
- ii) Problems of sample charging removed.
- iii) Increased signal to background ratio.
- iv) Radiation damage, if it occurs, is of no importance provided that the sample is not recirculated.
- v) Easy calibration by mixing with standard gases.
- vi) Possibility of distinguishing between inelastic losses and shake up processes by varying the sample pressure.
- vii) Direct comparison with theoretical results simplified.

6) Important Features of ESCA Spectraa) Binding Energies.

The binding energies of core electrons, which are essentially localized and do not take part in bonding, are characteristic of a particular element. Typical examples of approximate core electron binding energies for some elements are shown in Table (1.1).

Table (1.1)

	Li	Be	B	C	N	O	F	Ne	
1s	55	111	188	284	399	532	686	867	eV
	Na	Mg	Al	Si	P	S	Cl	A	
1s	1072	1305	1560	1839	2149	2472	2823	3203	
2s	63	89	118	149	189	229	270	320	
2p <sub>1/2</sub>	31	52	74	100	136	165	202	247	
2p <sub>3/2</sub>	31	52	73	99	135	164	200	245	

Knowledge of binding energies permits the detection or identification of elements in a sample.<sup>1</sup> Although some core levels are too tightly bound to be studied with Mg or Al Xrays there are always less tightly bound core electrons which can be studied. When choosing the core level to study the following considerations are required:

- i) The core level should give a high intensity spectrum (i.e. have a high cross section for photoionization) and in solids the escape depth should also be considered (Chap I.6.h).
- ii) There should be no interference from other peaks in the same kinetic energy region.
- iii) The line width should be narrow e.g. for second row elements such as sulphur and chlorine although the cross sections are similar it is usual to study the 2p levels since the line

- widths of the 2s electrons are broadened by the short lifetime of the hole states due to the highly efficient Coster-Kronig relaxation process.<sup>35</sup>
- iv) The peak should have a high signal to background ratio. (High backgrounds may be caused by inelastic scattering of the electrons from strong peaks of higher kinetic energy).
- v) The information content may vary from peak to peak. e.g. In the study of multiplet effects it is often convenient to study photoionization from s levels since the interpretation of the data is relatively straightforward (Chap. I.6.f). Thus for first row transition elements the 3s level is often studied even though the signal to background ratio is unfavourable compared with other core levels.

#### b) Chemical Shifts

Variations of binding energy within a core level depend on the electronic environment of the atom.<sup>1,14,17</sup> The classic illustration of chemical shifts is the C<sub>1s</sub> spectrum of ethyl trifluoroacetate Fig (1.12). Shifts in binding energy of over 10eV have been observed<sup>1,17</sup> for a given level and thus even smaller shifts in core electron binding energies are of a similar magnitude to energies of chemical reactions (1eV = 23.1 kcal/mole) and relationships between chemical shifts and thermodynamic data have been derived.<sup>44,50,51.</sup> Models for the interpretation of chemical shifts will be discussed in more detail later (Chapter III). For a particular core level (with due allowance made

for any shake up or shake off processes) the peak intensities are proportional to the number of atoms in a particular environment. For example the  $C_{1s}$  spectrum of acetone<sup>17</sup> shows two carbon peaks with area ratio 1:2 corresponding to the C=O (higher binding energy) and  $CH_3$  carbon atoms respectively Fig. (1.12).

c) Spin-Orbit Splitting.

If photoionization occurs from an orbital which has an orbital quantum number ( $l$ ) greater than 1 (i.e. p, d and f orbitals) then a doublet structure is observed.<sup>1</sup> This arises from coupling between spin and orbital angular momenta which gives rise to two possible values of the total quantum number ( $J$ ) for the hole state formed. The intensities of the peaks in the doublet are proportional to the ratio of the degeneracies of the states ( $2J + 1$ ). The relevant intensity ratios are shown in Table (1.2) and the  $4f_{5/2,7/2}$  doublet of gold is shown in Fig. (1.13).

Table (1.2)

	<u>Orbital quantum no.</u>	<u>Total quantum no.</u>		<u>Intensity ratio</u>
	1	J	$(l \pm s)$	$(2J + 1) / (2J + 1)$
s	0		$\frac{1}{2}$	No splitting
p	1	$\frac{1}{2}$	$\frac{3}{2}$	1:2
d	2	$\frac{3}{2}$	$\frac{5}{2}$	2:3
f	3	$\frac{5}{2}$	$\frac{7}{2}$	3:4

MULTIPLY SPLITTING in O<sub>2</sub> and NO

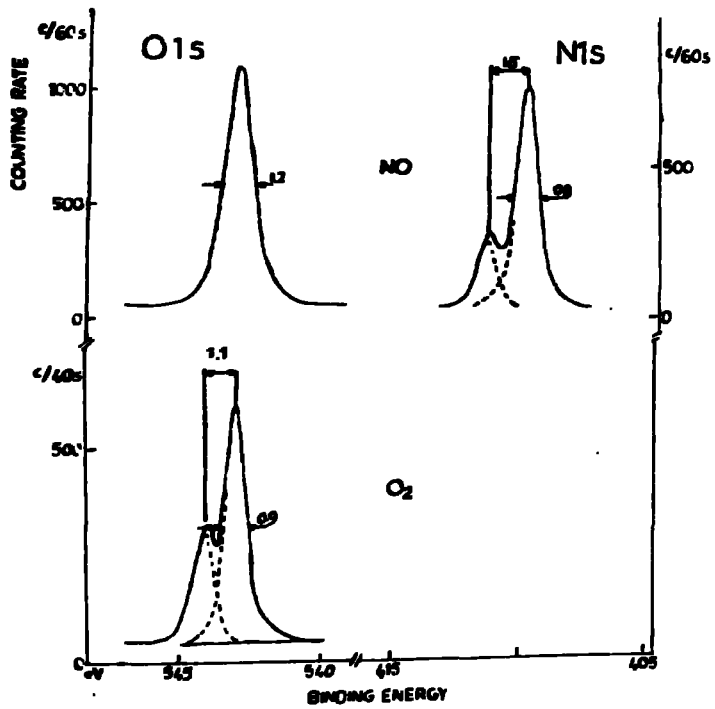


Figure (1.14)

SPIN-ORBIT SPLITTING Au 4f

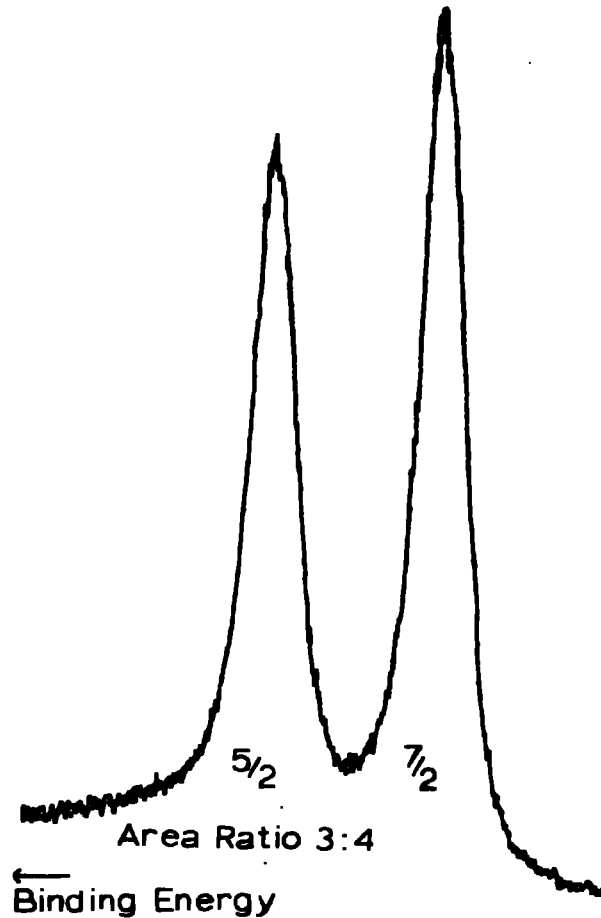
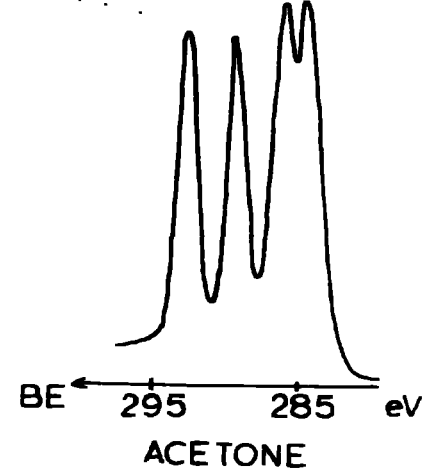
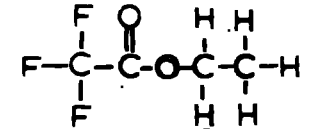


Figure (1.13)

CARBON 1s SPECTRA

Chemical Shifts



ACETONE

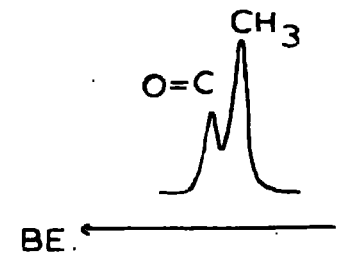


Figure (1.12)

#### d) Multiplet Splittings

Multiplet splittings in ESCA spectra were predicted by Watson and Freeman<sup>52</sup> and occur if the system being studied contains unpaired electrons since exchange interaction affects core electrons with  $\alpha$  and  $\beta$  spins differently. Such effects were first observed in the solid state by Fadley et al.<sup>53</sup> for the 3s level in some fluorides and oxides of manganese and iron which contain unpaired 3d electrons, and in the vapour phase ( $O_2$  and NO) by Siegbahn et al.<sup>17</sup> Fig. (1.14). The interpretation is relatively straightforward only for s-hole states. The following discussion considers s-hole states and is based on van Vleck's vector coupling model<sup>54</sup> which was originally conceived for atoms. This gives the following results for s-hole states where S is the total spin of the  $l^n$  configuration in the ground state. The two possible final states have a total spin of  $S \pm 1/2$ . The splitting  $\Delta E$  (i.e. the energy difference between the states  $S + 1/2$  and  $S - 1/2$ ) is proportional to the multiplicity of the ground state

$$\Delta E = (2S + 1)K$$

where K is the exchange integral between the core (c) and valence (v) electrons under consideration and is defined by

$$K = \langle \phi_v(1) \phi_c(2) | \frac{1}{r_{12}} | \phi_v(2) \phi_c(1) \rangle$$

The intensities of the peaks are proportional to the degeneracies of the final spin states

$$\text{i.e. } (2(S + 1/2) + 1) : (2(S - 1/2) + 1) = (2S + 2) : 2S$$

Unlike intermolecular shifts the magnitudes of multiplet splittings are independent of sample charging effects and reference level.

Multiplet splittings in photoelectron spectra have recently been discussed in some detail by Fadley.<sup>55</sup> The magnitude of the splitting for a given ion (or atom) can give valuable information concerning the localization or delocalization of the unpaired valence electrons in compounds<sup>17,56,57</sup> since the greater the spin density on an atom the greater the splitting. If the total population of unpaired electrons can be assigned among the atoms with a fraction  $f_i$  assigned to the  $i^{\text{th}}$  atom, then the multiplet splitting on the  $i^{\text{th}}$  atom  $\Delta E^i$  is approximated by<sup>56</sup>

$$\Delta E \approx f_i (2S + 1) K_i.$$

#### e) Electrostatic Splitting

Splittings in the  $5p_{3/2}$  levels of uranium and thorium metals and compounds, and in some compounds of gold<sup>58,59</sup> have been observed. These were interpreted as arising from the differential interaction of the internal electrostatic field with the  $M = \pm 1/2$  and  $M = \pm 3/2$  substates of the  $5p_{3/2}$  electrons, and a definite correlation was found between this type of splitting obtained by photoelectron spectroscopy, and the quadrupole splittings obtained from Mossbauer spectroscopy<sup>60</sup> which arise from the interaction of the nuclear quadrupole moment with an inhomogeneous electric field. Novakov<sup>61</sup> has also observed the known 2eV crystal field splitting of the valence 3d levels in  $\text{CoSO}_4$  in ESCA spectra and crystal field splittings should be observable in other systems.<sup>62</sup>

f) Satellite Peaks

Satellite peaks arising from shake up and shake off processes occur on the low kinetic energy side of the main peak and have been discussed earlier (Chap. I. 2.b). Also configuration interaction satellite peaks in photoelectron spectra may be observed whenever there are other final states with the same symmetry and which have energies close to, but greater than, the single-hole state energy.<sup>63</sup> These satellite peaks may be considered as arising from doubly excited states of the hole state, (as opposed to the shake up and shake off processes which may be thought of in terms of singly excited states), occurring on emission of an inner electron. They have been observed in some alkali metal halides.<sup>63,64</sup> In solids discrete peaks can arise from surface and bulk plasmon losses and interband transitions.<sup>1</sup> Satellite peaks in gases may also be caused by energy loss from the photoelectron after emission if it undergoes a secondary collision with an atom or molecule causing excitation of that atom or molecule. The intensity of these energy loss peaks is pressure dependant and they are therefore readily identifiable.<sup>17</sup>

The Xray source may itself be a cause of satellite peaks. These peaks have a higher kinetic energy than the main photoelectron peak and are formed by the small percentage of higher energy  $K_{\alpha_{3,4}}$  and  $K_{\alpha_{5,6}}$  radiation<sup>17</sup> which arises from KL double hole states and KLL triple hole states of the emitting atom<sup>65</sup> but they are eliminated if a monochromatized Xray source is used. When employing Mg  $K_{\alpha_{1,2}}$  radiation and passing it through an aluminium window to remove scattered electrons some Al  $K_{\alpha_{1,2}}$  radiation is also produced and gives rise to a satellite

photoelectron spectrum displaced by 232.9eV to higher kinetic energy. This is useful since it may be used to identify Auger peaks which, being independent of the energy of the exciting radiation, do not show these satellites.

### g) Line Widths

The effects contributing to the total line widths  $\Delta E_M$  have previously been mentioned (Chapter I.3.c). The natural line width at half maximum height of the core level under investigation  $\Delta E_S$  and that of the incident radiation  $\Delta E_X$  (unless monochromatization is employed) depend on the uncertainty principle,  $\Delta E \Delta t \approx h/2\pi$ ,<sup>66</sup> where  $\Delta t$  is the lifetime of the state. The line widths of some X-ray atomic energy levels are given in table (1.3). (A line width of 1eV corresponds to a lifetime of approximately  $6.6 \times 10^{-16}$  sec.<sup>66</sup>).

Table 1.3

#### Full Width at Half Maximum of X-ray Atomic Levels (eV)

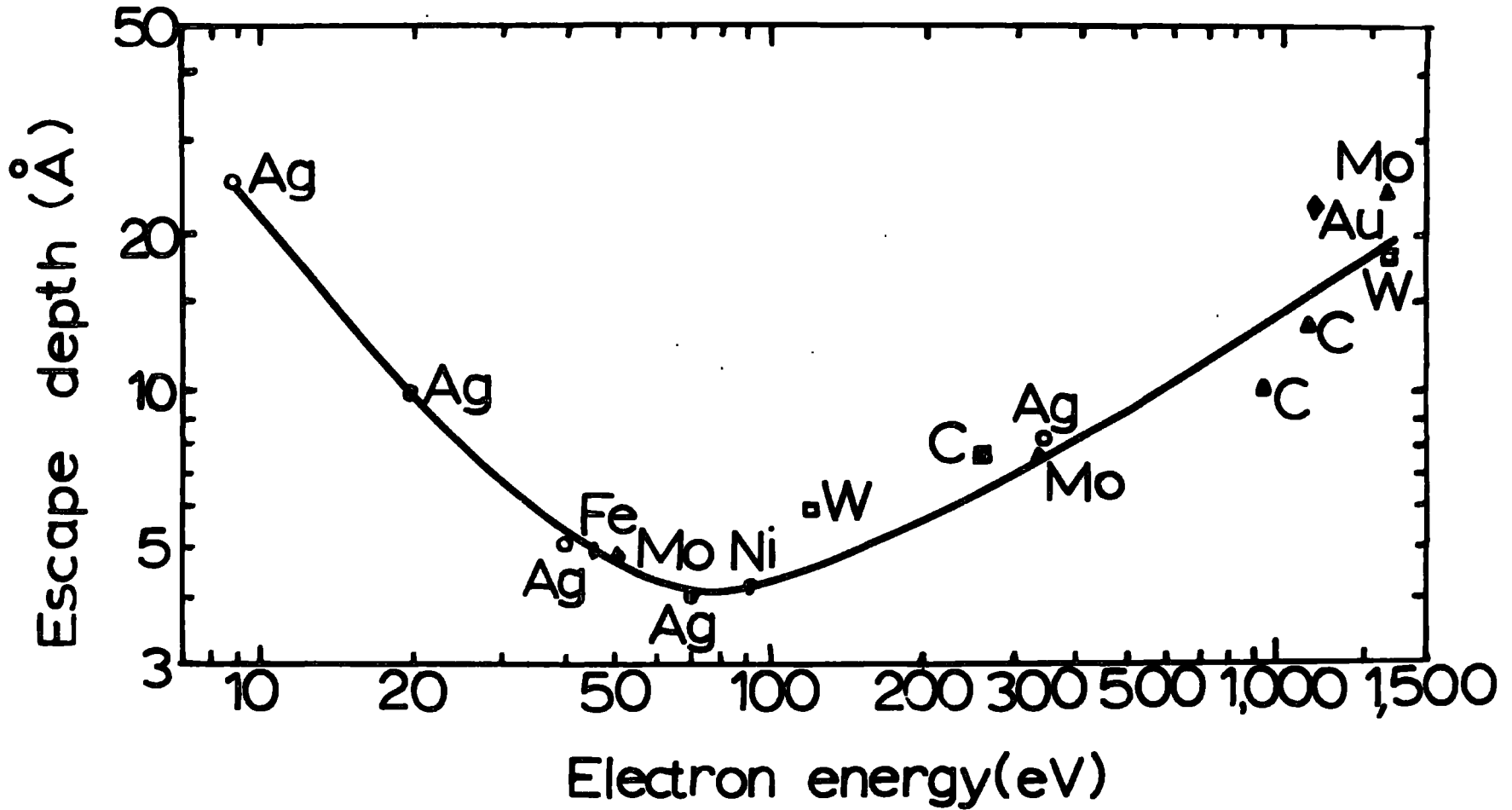
Level	Atom						
	S	Ar	Ti	Mn	Cu	Mo	Ag
1s	0.35	0.5	0.8	1.05	1.5	5.0	7.5
2p <sub>3/2</sub>	0.1	-	0.25	0.35	0.5	1.7	2.2

The photoelectric process is believed to occur in a time interval of the order of  $10^{-18}$  sec.<sup>66</sup> where as nuclear relaxation times are of the order of  $10^{-13}$  sec.<sup>45</sup> and the hole created in the core will have a lifetime of approximately  $10^{-16}$  sec.<sup>66</sup> Thus the process may be regarded as sudden compared with nuclear (but not electronic) motion. The line widths also illustrate that, in general, there is no advantage in studying the most tightly bound core electrons since

these levels are broad and this may obscure chemical shifts. Some small changes in line widths ( $\sim 0.1\text{eV}$ ) have been observed to be caused by chemical effects which have a small effect on the lifetime of the core hole state.<sup>67,68</sup> (This emphasises that peak intensities should be measured by area and not by height).

#### h) Escape Depths

Depending on the core level studied and on the Xray source used the escape depths of photoelectrons contributing to the elastic peaks are typically 0-100 $\text{\AA}$ . This was first demonstrated by Siegbahn and co-workers by depositing successive layers of  $\alpha$ -iodosteric acid on the probe and monitoring the intensity of the  $I_{3d_{5/2}}$  core level.<sup>1</sup> Spectra could also be obtained from less than a monolayer illustrating both the sensitivity of the technique and its potential in catalysis work since it is possible to monitor both the surface and the adsorbed species simultaneously. The penetration of the Xray beam into the sample under typical conditions is  $> 10^3 \text{\AA}$  so that it is the mean free paths of the electrons which determine the escape depths. In studies of Auger electrons and photoelectrons in gold and aluminium oxide the escape depth was found to be proportional to the square root of the electron energy.<sup>69</sup> A collection of measured escape depths as a function of kinetic energy has been made by Tracy<sup>70</sup> and is shown in figure (1.15). It is evident, therefore, that ESCA measurements on solids may monitor the bulk, semi-surface or surface depending on the core level involved.



Escape depth dependence on kinetic energy for electrons.

Figure(1.15)

### i) Deconvolution of Partially Resolved Spectra

Partially resolved peaks may be resolved into their individual components by use of a Du Pont 310 curve resolver (an analogue computer). For detailed deconvolutions a prior knowledge of line shapes (usually approximately gaussian) and peak widths for a particular level is required. This is obtained from a study of similar compounds, with well resolved peaks, which have been studied under the same experimental conditions. Since the peak areas for a given level are proportional to the number of atoms in a particular environment and if the total number of atoms of the element is known, then setting peak widths and areas and varying the peak positions to obtain a fit to the experimental spectrum allows the individual binding energies to be determined. In complex cases theoretical calculations, usually employing the charge potential model,<sup>17</sup> may be required to assign the binding energies to particular atoms.<sup>71,72</sup> The integration facility on the curve resolver also permits the areas of peaks to be determined and thus, for example, in fluorocarbon compounds the ratios of the C, CF, CF<sub>2</sub> and CF<sub>3</sub> carbon atoms are readily determined.

### 7) A Brief Survey of the Applications of ESCA to Chemistry.

The following survey is intended to give a few examples of a wide range of some of the more important, interesting and unusual applications of ESCA in the field of chemistry. A more comprehensive review of the literature is given in reference 73.

Since ESCA chemical shifts depend directly on the electronic structure of the molecule<sup>17</sup> (Chapter III) attempts have been made to correlate ESCA chemical shifts with shifts obtained from spectroscopies such as n.m.r., n.q.r. and Mossbauer which are also affected by the electronic environment of the atom. Correlations with n.q.r. data<sup>74</sup> and Mossbauer chemical shifts<sup>75,76</sup> have been observed for series of closely related compounds. However, there is little correlation between the <sup>13</sup>C n.m.r. shifts in the halomethanes, especially the bromomethanes, and the C<sub>1s</sub> ESCA chemical shifts<sup>38</sup> and previous direct correlations of this nature should<sup>77a,b,c.</sup> not be extrapolated. The close relationship between ESCA chemical shifts and atomic charge distributions permits detailed charge distributions in molecules to be determined experimentally (Chapter IV). Besides the use of ESCA in catalysis studies<sup>78,79</sup> the surface nature of the technique has been used to study systems ranging from the surface oxidation of metals such as aluminium<sup>80</sup> and tungsten,<sup>81</sup> to the adsorption of sulphur compounds on smoke particles<sup>82</sup> and the surface oxidation of wool fibres.<sup>83,84</sup>

Applications in the field of organic chemistry include the study of substituent effects in aliphatic,<sup>77c</sup> and more importantly, in aromatic compounds,<sup>72,85,86,87</sup> the study of carbonium ions in order to gain information about charge localization or delocalization and hence to obtain information of the classical or non-classical structure of the ions,<sup>88,89,90</sup> and studies of problems in fluorocarbon (Chapter V) and chlorocarbon systems<sup>91</sup> which were not readily amenable to solution by other techniques. Much useful information, e.g. the proportion

of comonomers incorporated in copolymers can be obtained from ESCA studies of polymer systems.<sup>92,93</sup>

ESCA can be used for both qualitative and quantitative analysis. Thus  $\mu\text{g}$  quantities of Pd, Cd and Bi deposited on a mercury coated platinum electrode may be detected by ESCA<sup>94</sup> and after the preparation of calibration curves the bulk ratio  $\text{MoO}_2$  to  $\text{MoO}_3$  in a mixture of the two oxides can be determined within a few percent.<sup>95</sup> ESCA has also been used in the study of rock samples obtained from the moon.<sup>96,97</sup> An application of biological importance is the analysis of the quality and quantity of grain protein,<sup>98</sup> where the N1s peak from lysine and arginine may be distinguished from the amide nitrogen and the sulphur content estimated from the S2p peaks (comparisons with compounds of known elemental composition permits quantitative estimates and no elaborate sample preparation is required). Other compounds of biological interest which have been studied include insulin,<sup>1</sup> vitamin B<sub>12</sub><sup>1</sup> and nucleic acid bases and t-RNA.<sup>99,100,101</sup> A further ingenuous use of ESCA, in combination with some thermodynamic data, is the estimate proton affinities of several compounds.<sup>44</sup>

CHAPTER II

MOLECULAR ORBITAL THEORY

## Introduction

Sufficient background theory is presented in this chapter to form a basis for the discussion presented in subsequent chapters. A brief summary is therefore given of both non-empirical and semi-empirical molecular orbital treatments together with a brief discussion of the programs employed in this work for the molecular Hartree-Fock calculations. The discussion is restricted to computations within the Hartree-Fock formalism although, where appropriate, reference will be made to correlation and relativistic corrections. The reasons for limiting the discussion to the Hartree-Fock formalism are threefold:-

- i) As will become apparent many features of ESCA data can be quantitatively understood within the Hartree-Fock model.
- ii) With currently available computing power both semi-empirical and non-empirical Hartree-Fock molecular orbital calculations may be carried out routinely.
- iii) The Hartree-Fock concept, namely the hypothesis of one electron orbitals, is about the last chance to retain an intuitive representation of the electronic structures of atoms, ions and molecules. This is a very important consideration for a model on which experimental data are interpreted and has great intuitive appeal to chemists.

1) A BRIEF SUMMARY OF QUANTUM MECHANICS

The electronic structure of an atom, ion or molecule is described by a mathematical function,  $\psi$ , of all the coordinates of the system, including time, and is known as the wave function. It is this function which contains all the information about the properties of the system. If the system is conservative i.e. a system in which the total energy does not vary with time, then separation of the time coordinate can be carried out

$$\Psi(x,y,z,t) = \psi(x,y,z)\phi(t) \quad (1)$$

and this leads to the time independent Schroedinger equation

$$\mathcal{H}\psi = E\psi \quad (2)$$

which is the starting point for the application of quantum mechanics to chemical systems.  $\mathcal{H}$  is the hamiltonian (total energy operator) of the system and  $E$  is the eigenvalue corresponding to the total energy of the system. Such a system is known as a stationary state and only time independent calculations will be considered. (Although in theory this may not be justified a priori<sup>103</sup> for the discussion of photoionization phenomena it will become clear both from this work and the work of others that to a good approximation a quantitative discussion based on stationary states is entirely adequate). In order to obtain  $\psi$  it is necessary to solve equation (2). For a system of nuclei

( $\mu, \nu \dots$ ) with coordinates  $X$  and electrons ( $i, j \dots$ ) with coordinates  $x$  the total spin free, (i.e. non relativistic)

Hamiltonian operator is given by

$$\mathcal{H}(x, X) = - \sum_{\mu} \frac{\hbar^2}{2M_{\mu}} \nabla_{\mu}^2 - \sum_i \frac{\hbar^2}{2m} \nabla_i^2 + V_{ne}(x, X) + V_{ee}(x) + V_{nn}(X) \quad (3)$$

where the first two summation terms account for the kinetic energies of the nuclei and the electrons and the terms  $V_{ne}(x, X)$ ,  $V_{ee}(x)$  and  $V_{nn}$  represent the nuclear-electron attraction, electron-electron repulsion and nuclear-nuclear repulsion respectively

$$V_{ne}(x, X) = - \sum_{\mu} \sum_i \frac{Z_{\mu} e^2}{r_{\mu i}}, \quad V_{ee}(x) = \sum_{i < j} \frac{e^2}{r_{ij}}, \quad V_{nn} = \sum_{\mu < \nu} \frac{Z_{\mu} Z_{\nu} e^2}{r_{\mu \nu}} \quad (4)$$

In order to obtain the electronic Shroedinger equations the Born-Oppenheimer approximation is invoked. Separating the nuclear kinetic energy terms

$$\mathcal{H}_n(X) = - \sum_{\mu} \frac{\hbar^2}{2M_{\mu}} \nabla_{\mu}^2 \quad (5)$$

then

$$\mathcal{H}(x, X) - \mathcal{H}_n(X) = \mathcal{H}_e(x, X) \quad (6)$$

is the Hamiltonian which describes the motion of the electrons for fixed positions of the nuclei and  $\mathcal{H}_e$  depends on the position but not the momentum of the nuclei.

The total wave function is assumed to be separable into an electronic and a nuclear part

$$\psi = \psi_e(x, X) \chi_{ne}(X) \quad (7)$$

the electronic wave function is defined by

$$\mathcal{H}_e(x, X) \psi_e(x, X) = E_e(X) \psi_e(x, X) \quad (8)$$

and the nuclear wave function by

$$[\mathcal{H}_n(X) + E_e(X)] \chi_{ne} = E \chi_{ne}(X) \quad (9)$$

( $\chi_{ne}$  can be further separated into vibrational, rotational and translational components).

The electronic wave function is solved for fixed positions of the nuclei by solving (8) to give the electronic energy  $E$ , which is the potential energy determining the motion of the nuclei so that the Shroedinger equation for the nuclei has the form (9).

The total energy is the sum of the electronic energy (evaluated at the equilibrium configuration) plus the nuclear energy

$$E = E_e(X_0) + E_n \quad (10)$$

The conditions under which the Born-Oppenheimer approximation is valid are examined below. The total Schrodinger equation may be written:

$$[\mathcal{K}_e(x, X) + \mathcal{K}_h(X)] \psi_e(x, X) \chi_{ne}(X) = E \psi_e(x, X) \chi_{ne}(X) \quad (11)$$

Since the only differential terms in  $\mathcal{K}_e$  are functions of  $x$  then from (8)

$$\begin{aligned} \mathcal{K}_e(x, X) \psi_e(x, X) \chi_{ne}(X) &= \chi_{ne}(X) \mathcal{K}_e(x, X) \psi_e(x, X) \\ &= \chi_{ne}(X) E_e(X) \psi_e(x, X) \end{aligned} \quad (12)$$

But  $\mathcal{K}_h$  is a differential function of  $X$  and both  $\psi_e$  and  $\chi_{ne}$  are functions of  $X$ , hence using (5)

$$\begin{aligned} \mathcal{K}_h(X) \psi_e(x, X) \chi(X) &= - \sum_{\mu} \frac{\hbar^2}{2M_{\mu}} [\psi_e(x, X) \nabla_{\mu}^2 \chi_{ne}(x) \\ &+ 2 \nabla_{\mu} \psi_e(x, X) \nabla_{\mu} \chi_{ne}(X) + \chi(X) \nabla_{\mu}^2 \psi_e(x, X)] \end{aligned} \quad (13)$$

Substitution of (12) and (13) into (11) gives (9) provided that the terms in  $\nabla_{\mu} \psi_e$  and  $\nabla_{\mu}^2 \psi_e$  in (13) can be neglected. Thus the Born-Oppenheimer approximation is valid provided that the electronic wave function  $\psi_e$  is a slowly varying function of the nuclear coordinates.

In dealing with the equations of quantum mechanics it is convenient to introduce atomic units which lead to a considerable simplification in the form of the Schroedinger equation viz:-

Length:- the atomic unit of length is the Bohr radius  $a_0$

$$\begin{aligned} a_0 &= \frac{\hbar^2}{4\pi^2 m_e e^2} = 0.529167 \times 10^{-8} \text{ cm} \\ &= 0.529167 \text{ \AA} \end{aligned}$$

Energy - the atomic unit of energy (the Hartree) is the energy of interaction of two unit charges separated by one Bohr radius

$$\epsilon_0 = \frac{e^2}{a_0} = 4.35942 \times 10^{-11} \text{ erg} = 27.21 \text{ eV}$$

Mass - the atomic unit of mass is the electron mass

$$m = 9.0191 \times 10^{-28} \text{ gm.}$$

The electronic Hamiltonian operator  $\mathcal{H}_e$  is therefore given by

$$\mathcal{H}_e = - \sum_i \frac{1}{2} \nabla_i^2 - \sum_{\mu} \sum_i \frac{Z_{\mu}}{r_{\mu i}} + \sum_{i < j} \frac{1}{r_{ij}} \quad (15)$$

For many electron systems terms representing the interelectronic repulsion,  $\sum_{i < j} \frac{1}{r_{ij}}$ , are included as part of the potential energy in the Schroedinger equation. However, if inter-electronic repulsions could be neglected then the wave function could be expressed in terms of a summation of products of one electron function

$$\Psi = \psi_a(1) \psi_b(2) \dots \psi_k(n)$$

and

$$\mathcal{H} = \mathcal{H}_1 + \mathcal{H}_2 \dots \mathcal{H}_k$$

In this form the wave function would be separable into a set of equations each involving the coordinates of only one electron and the solution of these equations would give the  $\psi$ 's. Although interelectronic repulsion cannot be completely neglected, it cannot be taken properly into account since the many-body problem is not exactly soluble in quantum, or classical, mechanics. However, the idea of a one electron function (the orbital approximation) is conceptually simple and it is therefore very useful to consider products of one electron functions and to determine how close it is possible to approach the exact functions. Within the orbital approximation it is possible to describe adequately the average repulsion experienced by an electron due to the other electrons in the system. However, it is relatively difficult to incorporate the instantaneous correlations of electronic motions.

Associated with each electron is a spin ( $m_s = \pm \frac{1}{2}$ ) and the two possible spin functions are written as  $\alpha(m_s = \frac{1}{2})$  and  $\beta(m_s = -\frac{1}{2})$ . The product of a spatial orbital defined above and a spin function is known as a spin orbital  $\phi$ .

$$\phi_i(1) = \psi_i(1)\alpha \quad \text{or} \quad \psi_i(1)\beta$$

where  $\psi_i$  is a function which depends only on the space coordinates of the electron and also  $\alpha$  and  $\beta$  are orthogonal

$$\int \alpha \beta \, d\tau = 0$$

(This separation into spin and space coordinates is possible only because the non-relativistic (i.e. spin free) Hamiltonian was used).

The total wave function must be in accord with the Pauli antisymmetry principle which allows for the fact that electrons are indistinguishable from each other. Thus all acceptable wave functions for particles of half-integral spin (Fermions) must be antisymmetric upon interchange of any two particles. The single product wave function

$$\Psi(1,2, \dots, 2n) = \psi_1(1)\alpha \psi_1(2)\beta \psi_2(3)\alpha \dots \psi_n(2n)\beta \quad (16)$$

is not antisymmetric but can be made so by writing it in determinantal form

$$\Psi(1,2, \dots, 2n) = \sqrt{\frac{1}{(2n)!}} \begin{vmatrix} \psi_1(1)\alpha & \psi_1(1)\beta & \psi_2(1)\alpha & \dots & \psi_n(1)\beta \\ \psi_1(2)\alpha & \psi_1(2)\beta & \psi_2(2)\alpha & \dots & \psi_n(2)\beta \\ \vdots & \vdots & \vdots & \ddots & \vdots \\ \psi_1(2n)\alpha & \psi_1(2n)\beta & \psi_2(2n)\alpha & \dots & \psi_n(2n)\beta \end{vmatrix} \quad (17)$$

where  $\sqrt{\frac{1}{(2n)!}}$  is a normalizing constant. This is known as a Slater determinant and is often abbreviated by writing only the diagonal elements, the normalization factor being understood

$$\begin{aligned} \Psi(1,2 \dots, 2n) &= \begin{vmatrix} \psi_1\alpha & \psi_1\beta & \psi_2\alpha & \psi_2\beta & \dots & \psi_n\alpha & \psi_n\beta \\ \psi_1\bar{\alpha} & \psi_1\bar{\beta} & \psi_2\bar{\alpha} & \psi_2\bar{\beta} & \dots & \psi_n\bar{\alpha} & \psi_n\bar{\beta} \end{vmatrix} \\ &= \begin{vmatrix} \psi_1 & \bar{\psi}_1 & \psi_2 & \bar{\psi}_2 & \dots & \psi_n & \bar{\psi}_n \end{vmatrix} \end{aligned}$$

Exchange of any two electrons interchanges two rows of the determinant and therefore reverses the sign of the wave function ensuring the required antisymmetry. Also if two electrons are placed in the same spin orbital the value of the determinant is zero since two rows of the determinant would be identical and this accounts for the Pauli exclusion principle.

The wave function must be continuous and single valued and have an integrable square (i.e. be capable of being normalized).

$$\int \psi_i^2 d\tau = 1$$

Also it can be shown that<sup>102a</sup> different eigenfunctions of the same Hamiltonian corresponding to different eigenvalues are mutually orthogonal. Hence

$$\int \psi_i \psi_j d\tau = \delta_{ij} \quad \begin{array}{l} \delta = 1 \text{ for } i = j \\ \delta = 0 \text{ for } i \neq j \end{array}$$

The perfect single determinantal wavefunction (for the ground state of the system) gives an expectation value for the energy corresponding to the Hartree-Fock limit.

From the discussion given above it is obvious that expressing the wave function in terms of a Slater determinant is an approximation and hence a yardstick is required for gauging how close to physical reality is the description of the system provided by the wave function.

Such a criterion is provided by the variation theorem.

The variation principle states that:-

Given any approximate wavefunction satisfying the boundary conditions of the problem, the expectation value of the energy calculated from this function will always be higher than the true ground state energy.<sup>102</sup>

Therefore if  $\psi$  is an approximation to the exact wavefunction,

$$\int \psi^* \mathcal{H} \psi d\tau = E \geq E^0$$

where  $E^0$  is the true energy. The variation method is used by starting with a trial wave function containing one or more variational parameters and then minimizing the expectation value of the energy with respect to these parameters. The method generally used to obtain suitable trial functions for molecular orbitals is to take a linear combination of basis functions, known as the basis set, and, as the number of functions tends to infinity, the perfect wave function (within the Hartree-Fock formalism) is approached. The simplest approach of this type is to take a linear combination of atomic orbitals (LCAO method), the basis of which is the reasonable assumption that the electronic distribution in a molecule can be represented as a sum of atomic distributions. Consider a molecular orbital  $\psi$  which is a linear combination of appropriate atomic orbitals  $\chi_i$

$$\psi = \sum_{i=1}^n c_i \chi_i \quad (18)$$

and the coefficients  $c_i$  are used as the variational parameters.

(However, variational parameters could equally well be incorporated in the basis functions themselves)

$$\begin{aligned}
 E &= \frac{\int \psi^* \mathcal{H} \psi \, d\tau}{\int \psi^* \psi \, d\tau} & (19) \\
 &= \frac{\sum_{i,j} c_i^* c_j \int \chi_i^* \mathcal{H} \chi_j \, d\tau}{\sum_{i,j} c_i^* c_j \int \chi_i^* \chi_j \, d\tau} \\
 &= \frac{\sum_{i,j} c_i^* c_j H_{ij}}{\sum_{i,j} S_{ij}}
 \end{aligned}$$

$$\text{where } H_{ij} = \int \chi_i^* \mathcal{H} \chi_j \, d\tau$$

$$S_{ij} = \int \chi_i^* \chi_j \, d\tau$$

$$\therefore \sum_{i,j} c_i^* c_j (H_{ij} - E S_{ij}) = 0$$

Differentiating with respect to  $c_k$

$$\sum_{i=1}^n c_i^* (H_{ik} - E S_{ik}) - \sum_{i,j} c_i c_j S_{ij} \frac{\partial E}{\partial c_k} = 0$$

For the minimum value of  $E$ ,  $\frac{\partial E}{\partial c_k} = 0$  for all  $k$

$$\therefore \sum_{i=1}^n c_i^* (H_{ik} - E S_{ik}) = 0 \quad \text{for } k = 1 \text{ to } n \quad (20)$$

These sets of  $n$  simultaneous equations are known as secular equations and for a non-trivial, solution the  $n$  by  $n$  secular determinant must equal zero

$$|H_{ik} - E S_{ik}| = 0 \quad (21)$$

Hence the roots of the equations  $E_1, E_2, \dots, E_n$  may be obtained and by substitution back into (20) the coefficients  $c$ , and hence the molecular orbitals  $\psi$ , may be determined.

## 2) HARTREE-FOCK SELF CONSISTENT FIELD THEORY

The basis of the Hartree-Fock self consistent field treatment of molecules lies in the extension of the treatment of atomic systems by Hartree<sup>104</sup> which was modified by Fock<sup>105</sup> and Slater<sup>106</sup> to include the antisymmetry of the wave functions. The method consists of minimizing the energy resulting from the single determinant wave function (17) to derive a set of integrodifferential equations, the Hartree-Fock equations. The Hartree-Fock wave function is the best wave function which can be constructed by assigning each electron to a separate orbital, or function, depending only on the coordinates of that electron. Only for one electron systems e.g. the hydrogen atom can the Hartree-Fock equation be solved in closed form, however for atoms the equations may be solved to a high degree of accuracy by numerical integration.<sup>107</sup> It is not possible to use a mathematically

complete set of functions in molecular orbital calculations and only an approximate solution to the Hartree-Fock equations can be obtained. The best (lowest energy) single determinantal function constructed within a finite basis set is the self consistent field function.

Suppose the wave function for a system of  $n$  electrons is written as a single product of  $n$  spin orbitals

$$\Psi = \psi_a(1) \psi_b(2) \dots \psi_k(n) \quad (22)$$

The energy of this wave function is evaluated by

$$E = \int \Psi \mathcal{K} \Psi d\tau \quad (23)$$

where  $\mathcal{K}$  is the electronic Hamiltonian.  $\mathcal{K}$  may be written in the form

$$\mathcal{K} = \sum_i H^c(i) + \sum_{ij} \left( \frac{1}{r_{ij}} \right) + V_{nn} \quad (24)$$

where  $H^c(i)$  is the core Hamiltonian which consists of the kinetic energy operator and the electron-nuclear attraction terms for electron  $i$  and  $V_{nn}$  is the nuclear repulsion energy.

Substituting (22) and (24) into (23) gives

$$E = \sum_{r=a}^k H_{rr}^c + \sum_{\substack{\text{pairs} \\ rs}} J_{rs} + V_{nn} \quad (26)$$

$$\text{where } H_{rr}^c = \int \psi_r H^c \psi_r d\tau \quad (27)$$

$$\text{and } J_{rs} = \iint \psi_r(i) \psi_s(j) \left( \frac{1}{r_{ij}} \right) \psi_r(i) \psi_s(j) d\tau_i d\tau_j \quad (28)$$

Expression (26) consists of two parts: the first involving  $H^c$  is the sum of the energies that each electron would have if all other electrons were absent, the second is the total of all electron-electron repulsion energies. However wave function (22) does not satisfy the antisymmetry requirement, but this is corrected by converting the single product to a Slater determinant of spin orbitals

$$\Psi = |\psi_a \psi_b \dots \psi_k \dots \psi_n| \quad (29)$$

Provided the spin orbitals are mutually orthogonal by substituting (29) into (23), (30) is obtained

$$E = \sum_{r=a}^k H_{rr}^c + \sum_{\substack{\text{pairs} \\ rs}} (J_{rs} - K_{rs}) + V_{nn} \quad (30)$$

This differs from (26) by the terms  $K_{rs}$

$$K_{rs} = \iint \psi_r(i) \psi_s(j) \left( \frac{1}{r_{ij}} \right) \psi_s(i) \psi_r(j) d\tau_i d\tau_j \quad (31)$$

$J_{rs}$  is called a coulomb integral and  $K_{rs}$  an exchange integral. If  $\psi_r$  and  $\psi_s$  have different associated spin functions (i.e. one  $\alpha$  and the other  $\beta$ ) then from integration over the spin coordinates it follows that  $K_{rs}$  is zero.

Applying the variation principle to wave functions (22) or (29) and requiring that the respective energies (26) and (30) be minimized is sufficient to define the orbitals  $\psi$  and orbitals evaluated in this way are known as SCF (self consistent field) orbitals. The orbitals defined with respect to (22) are Hartree orbitals while those defined with respect to the antisymmetrized product (29) are the Hartree-Fock orbitals. The conditions which define the Hartree-Fock orbitals are now examined.

Suppose that the function (29) does not give the lowest energy of the state. Then there is some other functions say

$$\Psi' = | \psi'_a \psi_b \dots \psi_k | \quad (32)$$

which has a lower energy. Assuming  $\psi'_a$  differs only slightly from  $\psi_a$  and can be written

$$\psi'_a = \psi_a + c_t \psi_t \quad (33)$$

where  $\psi_t$  is a spin orbital which is orthogonal to the set

$\psi_a \dots \psi_k$ . Providing  $c_t$  is small  $\psi'_a$  will still be normalized since renormalization only involves a term in  $c_t^2$ . From (33), (32) may be written in the form

$$\begin{aligned} \Psi' &= | \psi_a \psi_b \dots \psi_k | + c_t | \psi_t \psi_b \dots \psi_k | \\ &= \Psi + c_t \Psi_a^t \end{aligned} \quad (34)$$

(i.e.  $\Psi'$  is formed by adding to  $\Psi$  a small amount of the state  $\Psi_a^t$  which arises from the excitation of an electron from  $\psi_a$  to  $\psi_t$ ).

For  $\Psi$  to be the best wave function of its type  $c_t$  must be zero and this further requires that the Hamiltonian integral between  $\Psi$  and  $\Psi_a^t$ ,  $F_{at}$ , be zero.

$$F_{at} = \int \Psi \mathcal{H} \Psi_a^t d\tau = 0 \quad (35)$$

Expressing this integral in terms of the spin orbitals gives

$$F_{at} = H_{at}^c + \sum_{s=a}^k \left[ \iint \psi_a(i) \psi_s(j) \left( \frac{1}{r_{ij}} \right) \psi_t(i) \psi_s(j) d\tau_i d\tau_j \right. \\ \left. - \iint \psi_a(i) \psi_s(j) \left( \frac{1}{r_{ij}} \right) \psi_s(i) \psi_t(j) d\tau_i d\tau_j \right] \quad (37)$$

For this to be zero for any spin orbital, not just  $\psi_a$ , it is necessary that the  $\psi$  be eigenfunctions of the operator  $F$  which has the property of depending on its own eigenfunctions.

$$F = H^c + \sum_{s=a}^k (J_s - K_s) \quad (38)$$

where  $J_s$  and  $K_s$  are coulomb and exchange operators which are defined by their integrals

$$(J_s)_{at} = \iint \psi_a(i) \psi_s(j) \left( \frac{1}{r_{ij}} \right) \psi_t(i) \psi_s(j) d\tau_i d\tau_j \\ (K_s)_{at} = \iint \psi_a(i) \psi_s(j) \left( \frac{1}{r_{ij}} \right) \psi_s(i) \psi_t(j) d\tau_i d\tau_j \quad (39)$$

( $(J_s)_{rr}$  and  $(K_s)_{rr}$  are the integrals  $J_{rs}$  and  $K_{rs}$  defined by (28) and (31) and  $(J_a)_{at} = (K_a)_{at}$ ).

The potential governing the SCF orbitals therefore consists of the core potential, the coulomb potential of all the electrons, and an exchange potential for each electron. Since the coulomb and exchange potentials depend on the orbitals themselves an iterative method has to be adopted to calculate the SCF orbitals and the condition of self consistency is reached when the orbitals are consistent with the potential from which they were determined. The eigenvalues of  $F$  (the Fock operator,  $F\psi = \epsilon\psi$ ) are the orbital energies  $\epsilon$ . Thus from (37)

$$\epsilon_r \equiv F_{rr} = H_{rr}^c + \sum_{s=a}^k (J_{rs} - K_{rs}) \quad (40)$$

The sum of the energies of all occupied spin orbitals is

$$\sum_{r=a}^k \epsilon_r = \sum_{r=a}^k H_{rr}^c + \sum_{r=a}^k \sum_{s=a}^k (J_{rs} - K_{rs}) \quad (41)$$

Comparing this with (30) and noting that  $J_{rr} = K_{rr}$

$$\sum_{r=a}^k \sum_{s=a}^k (J_{rs} - K_{rs}) = 2 \sum_{\substack{\text{pairs} \\ rs}} (J_{rs} - K_{rs}) \quad (42)$$

gives

$$E = \sum_{r=a}^k \epsilon_r - \sum_{\substack{\text{pairs} \\ rs}} (J_{rs} - K_{rs}) + V_{nn} \quad (43)$$

Thus for SCF orbitals the total electronic energy is not just the sum of the orbital energies plus the nuclear repulsions energy.

In the case of SCF orbitals for a closed-shell configuration each orbital is occupied by two electrons with  $\alpha$  and  $\beta$  spins and expressions (30), (37) and (40) become

$$\text{Total energy, } E = 2 \sum_r H_{rr}^c + 2 \sum_{\substack{\text{pairs} \\ rs}} (2J_{rs} - K_{rs}) + \sum_r J_{rr} + V_{nn} \quad (44)$$

$$F_{at} = H_{at}^c + \sum_{s=a}^k \left[ 2 \iint \psi_a(i) \psi_s(j) \left( \frac{1}{r_{ij}} \right) \psi_t(i) \psi_s(j) d\tau_i d\tau_j \right. \\ \left. - \iint \psi_a(i) \psi_s(j) \left( \frac{1}{r_{ij}} \right) \psi_s(i) \psi_t(j) d\tau_i d\tau_j \right] \quad (45)$$

$$\text{Orbital energy } e_r = H_{rr}^c + \sum_{s=a}^k (2J_{rs} - K_{rs}) = F_{rr} \quad (46)$$

where the summations are now over all occupied orbitals and not spin orbitals.

If the SCF orbitals are represented by a linear combination of basis functions

$$\psi = \sum_v c_v \phi_v \quad (47)$$

then by substituting (47) into (45) and picking out terms in  $c_{\mu} c_{\nu}$

it is found that

$$F_{\mu\nu} = H_{\mu\nu}^c + \sum_{s=a}^k \sum_{\rho} \sum_{\sigma} c_{\rho} c_{\sigma} \left[ 2 \iint \phi_{\mu}(i) \phi_{\rho}(j) \left( \frac{1}{r_{ij}} \right) \phi_{\nu}(i) \phi_{\sigma}(j) d\tau_i d\tau_j \right. \\ \left. - \iint \phi_{\mu}(i) \phi_{\rho}(j) \left( \frac{1}{r_{ij}} \right) \phi_{\sigma}(i) \phi_{\nu}(j) d\tau_i d\tau_j \right] \quad (48)$$

The SCF orbitals for a closed shell system in this form are then determined by solving the secular equations

$$\sum_{\nu} c_{\nu} (F_{\mu\nu} - ES_{\mu\nu}) = 0 \quad (49)$$

through the determinant

$$| F_{\mu\nu} - ES_{\mu\nu} | = 0 \quad (50)$$

These are known as Roothaan's equations<sup>108</sup> and an iterative procedure starting with an initial estimate of the values of the c's is necessary for their solution since  $F_{\mu\nu}$  itself depends on the coefficients c. The values of c (eigenvectors) are then used as input for the next iteration and the process is repeated until input and output vectors agree within a given accuracy. i.e. they are self consistent.

### 3) BASIS FUNCTIONS AND BASIS SETS

The molecular orbitals used to describe a system of nuclei and electrons are generally expanded in terms of a linear combination of atomic orbitals (LCAO) and the atomic orbitals are further described as a linear combination of functions,  $\chi_i$  known as the basis functions. Thus

$$\psi_{MO} = \sum c_i \psi_i \quad (51)$$

$$\psi_i = \sum a_{\mu i} \chi_{\mu} \quad (52)$$

The types of basis function  $\chi$  used in Hartree-Fock calculations fall into two distinct classes depending on whether the radial portion of the function is a single exponential Slater type function ( $e^{-zr}$ ) or a gaussian type function ( $e^{-\alpha r^2}$ )

a) Single Exponential Functions

The use of exponential functions was first suggested by Slater<sup>109</sup> and the functions are of the type

$$\chi(r, \theta, \phi) = N r^{n-1} e^{-zr} \cdot Y_{lm}(\theta, \phi) \quad (53)$$

Where  $N$  is a normalization factor,  $n$  is the principal quantum number and  $z$  is the orbital exponent, the value of which determines the radial maximum of the orbital from the nucleus. The angular dependence is given by the spherical harmonic terms  $Y_{lm}(\theta, \phi)$ . In their simple analytical form Slater functions are not orthogonal but they can be made so by taking appropriate linear combinations.

b) Gaussian Type Functions

The use of gaussian functions was first suggested by Boys<sup>110</sup> and they have the form

$$N r^n e^{-\alpha r^2}$$

where  $n$  is the analogue of the principle quantum number in the Slater

function case and can take the values 1, 1 + 2, 1 + 4 etc. Angular dependence may be introduced by multiplication by the spherical harmonics  $Y_{lm}(\theta, \phi)$  or may be introduced in the form

$$N x^p y^q z^s e^{-\alpha r^2}$$

where p, q and s are integers and these are known as cartesian gaussians. The use of gaussian functions considerably simplifies multicentre integral evaluation since it can be proved that the product of two gaussian functions on different centres is another gaussian function positioned on the line joining the two original centres. Thus, for example, integrals of the type

$$\int \phi(g)_a \phi(g)_b \frac{1}{r_{12}} \phi(g)_c \phi(g)_d d\tau \quad (54)$$

(where  $\phi(g)_a$  etc. are gaussian type functions) are simplified to the form

$$\int \phi(g)_e \frac{1}{r_{12}} \phi(g)_f d\tau \quad (55)$$

Shavitt<sup>111</sup> has given a general discussion on the properties and uses of gaussian functions and integrals involving gaussian functions. However, for the s type function the form of a single gaussian does not resemble the form of a true atomic orbital particularly in the nuclear region where the cusp is lacking (Fig. 2.1). In the case of the neon atoms, for example, a basis set of ten s

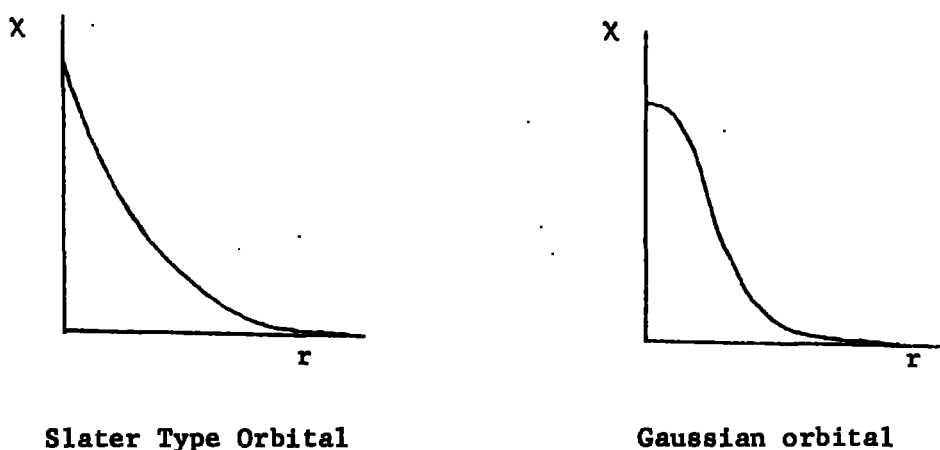


Fig. 2.1

and six p gaussian functions is required to improve on a SCF energy given by a basis of four s and two p Slater functions.<sup>112</sup> Therefore, while the use of gaussian functions greatly facilitates the evaluation of multicentre integrals in molecular calculations, a much larger basis set is required to obtain the accuracy given by Slater functions.

Another method of using gaussian functions was developed independantly by Preuss<sup>113</sup> and Whitten.<sup>114</sup> This is the gaussian lobe method and uses only 1s type gaussians ( $e^{-\alpha r^2}$ ) but the functions are not required to be atom-centred and linear combinations of these lobe functions are used to simulate s, p, d etc. orbitals. One of the simplest ab initio methods possible is the floating spherical gaussian orbital (FSGO) method introduced by Frost.<sup>115</sup> For closed-shell molecules,  $n/2$  1s type gaussian functions are used to construct a single determinantal wave function. However, these spherical gaussians are allowed complete flexibility and the energy of the n-electron wave function is minimized with respect to both their positions and orbital exponents ( $\alpha_i$ ).

c) Minimal Basis Sets

A minimal basis set is one which includes only one function for each occupied atomic orbital with distinct  $n$  and  $l$  quantum numbers for the component atoms of the molecule. The functions used in minimal basis sets are usually Slater functions. When using minimal Slater basis sets the question arises of what value of the orbital exponent  $z$  should be used. Slater<sup>116</sup> proposed a set of rules to determine

$$z = \frac{(Z-s)}{n^*} \quad (56)$$

in which  $Z$  is the charge on the nucleus,  $s$  is a screening constant depending on the other electrons in the atom and  $n^*$  is an effective quantum number. However, Clementi and co-workers<sup>117,118</sup> have approached the problem more directly by optimizing  $z$  values in repeated atomic SCF calculations, on the ground states of atoms, until sets of orbital exponents yielding the lowest possible (minimal basis set) SCF energies were obtained. These atom optimized minimum basis sets may be used directly in molecular Hartree-Fock LCAO SCF MO calculations. Further lowering of the total energy of the molecule may be obtained by re-optimizing the exponents  $z$  by repeated molecular SCF calculations. However, this can become a computationally expensive procedure and it is generally better to extend the size of basis set.

One of the main advantages of minimal basis set calculations is their conceptual simplicity and most semi-empirical methods e.g. CNDO<sup>119</sup> are in principle based on a minimal Slater basis set. To avoid the difficulties which arise in the calculation of two-electron integrals in polyatomic molecules when using Slater functions each Slater function may be expanded in terms of a linear combination of gaussian functions.<sup>120,121</sup> Such an expansion is known as an STO-nG function where n is the number of gaussian type functions used in the least squares fit to the Slater function. This circumvents the difficulties of calculating multicentre integrals over Slater orbitals while retaining the conceptual simplicity of minimal basis set calculations.

#### d) Split Valence Basis Sets

As a variant of the STO-nG orbitals Pople and co-workers have made extensive use of the STO-4,31G<sup>122</sup> basis set in which the core (1s) orbital is described by a least squares fit of four gaussian orbitals, while the valence orbitals are also described by four gaussian orbitals but an extra degree of freedom is allowed by splitting off the outer gaussian function of the valence orbital and allowing this to vary independently. This more flexible description of the valence orbitals allows for their distortion on bond formation in molecules.

#### e) Double Zeta and Extended Basis Sets

A double zeta basis set has twice as many functions as a minimal basis set (i.e. two Slater functions with different exponents for each atomic orbital). These have again been optimized from atomic ground state SCF calculations.<sup>123,124,125</sup> To obtain SCF energies very close

to Hartree-Fock energies a larger than double zeta basis set is required and this is known as an extended basis set.<sup>126,127</sup> Table(2.1) shows the ground state SCF energies obtained from minimal, double zeta and extended basis set calculations for the first row atoms.

Table 2.1

Ground State SCF Energies Using Slater Basis Sets (a.u.)

	<u>Minimum</u> <sup>117</sup>	<u>Double Zeta</u> <sup>125</sup>	<u>Extended</u> <sup>126</sup>
Li	-7.4185	-7.4327	-7.4327
Be	-14.5567	-14.5724	-14.5730
B	-24.4984	-24.5279	-24.5291
C	-37.6224	-37.6868	-37.6886
N	-54.2689	-54.3980	-54.4009
O	-74.5404	-74.8043	-74.8094
F	-98.9421	-99.4013	-99.4093
Ne	-127.8122	-128.5351	-128.5471

f) Gaussian Basis Sets

Gaussian basis sets of various sizes have been optimized for the ground states of atoms by varying the exponents and minimizing the SCF energy. However, as mentioned previously, a larger number of gaussian functions is required compared with Slaters in order to obtain the same accuracy. The numbers of integrals to be computed depends approximately on the fourth power of number of basis functions used as given by the formulae

$$\begin{aligned} \text{Number of one electron integrals (p)} &= \frac{n(n+1)}{2} \\ \text{Number of two electron integrals} &= \frac{p(p+1)}{2} \end{aligned} \quad (57)$$

Thus for molecules using basis sets of a quality equal to those of Slater functions the storage space required for the integrals can become excessive. The other time consuming step in the calculation is the solution of the SCF equations using the Roothaan procedure<sup>108,128</sup> (time approximately proportional to the fourth power of the number of basis functions). Also the procedure is iterative and large basis sets generally need more iterations in order to attain convergence. These problems may be overcome by reducing the degree of variational freedom

$$\psi_{MO} = \sum_i c_i \psi_i$$

$$\psi_i = \sum_{\mu} a_{\mu i} \chi_{\mu}$$

The coefficients of the atomic orbitals  $c_i$  in the LCAO approximations are always allowed complete variation freedom. However, the number of basis functions describing the atomic orbitals may be reduced by fixing some of the coefficients  $a_{\mu i}$  relative to each other and manipulating the linear combinations of gaussians as one function<sup>114,129</sup> thus saving considerable time per iteration as well as greatly reducing the number of integrals to be stored. These are known as contracted basis sets and the coefficients  $a_{\mu i}$  are known as contraction (or expansion) coefficients. Dunning<sup>130</sup> has outlined the important points in

devising contraction schemes and these are i) to retain maximum flexibility in the valence region and ii) to allow a function to vary freely if it contributes strongly to more than one atomic orbital in the atom. A double zeta gaussian basis set is one in which two contracted gaussian functions contribute to each atomic orbital.

#### g) Polarization Functions

In principle to reach the Hartree-Fock limit a complete (and necessarily infinite) basis set is required. This is obviously impracticable but as Nesbet has emphasized<sup>131,132</sup> the inclusion of functions with higher  $l$  values (e.g. p or d functions on hydrogen, d or f functions on nitrogen etc.) than occur in the atom can improve the energy and also give more reliable values of other properties of chemical interest. Such functions are known as polarization functions.

#### 4) MULLIKEN POPULATION ANALYSIS

Although the electron density distribution within a molecule is continuous it is a useful concept to assign a charge to each atom in a molecule. Such populations are given by a Mulliken population analysis<sup>133</sup> and are known as gross atomic populations. For a diatomic molecule the net atomic population of an atom arising from the  $i^{\text{th}}$  MO of the normalized form  $c_{Ai}\psi_A + c_{Bi}\psi_B$  is given by  $n_i c_{Ai}^2$  for atom A and  $n_i c_{Bi}^2$  for atom B where  $n_i$  is the number of electrons in the  $i^{\text{th}}$  molecular orbital. Thus  $n_i c_{Ai}^2$  is the number of electrons associated with atom A in the  $i^{\text{th}}$  molecular orbital. The electron density between the two nuclei arising from the  $i^{\text{th}}$  molecular orbital is given by the

overlap population  $2n_i c_{Ai} c_{Bi} S_{AB}$  where  $S_{AB}$  is the overlap integral

$$\int \psi_A \psi_B d\tau \equiv \langle \psi_A | \psi_B \rangle.$$

The gross atomic population is then found by assuming that the overlap population can be divided equally between the two nuclei and then added to the net atomic population.

Thus,  $n_i (c_{Ai}^2 + c_{Ai} c_{Bi} S_{AB})$  is the gross atomic population

of electrons on atom A in the  $i^{\text{th}}$  molecular orbital. This may

readily be extended to polyatomic systems in which the molecular

orbitals  $\psi_i$  are expressed in terms of basis functions  $\chi_\mu$ . If there

are two electrons per molecular orbital the total electron density  $\rho$

is defined by

$$\rho = 2 \sum_i^{\text{occupied}} \psi_i^2 = \sum_\mu \sum_\nu P_{\mu\nu} \chi_\mu \chi_\nu$$

where  $P_{\mu\nu}$  is the density matrix defined by

$$P_{\mu\nu} = 2 \sum_i^{\text{occupied}} c_{\mu i} c_{\nu i}$$

The diagonal element  $P_{\mu\mu}$  is the coefficient of the distribution  $\chi_\mu^2$  and measures the net electron population for this orbital. The off

diagonal elements  $P_{\mu\nu}$  are overlap populations related to the charge

density associated with the overlap  $\chi_\mu \chi_\nu$ . The gross population for

$\chi_\mu$  is then defined by  $q_\mu$

$$q_\mu = P_{\mu\mu} + \sum_{\nu \neq \mu} P_{\mu\nu} S_{\mu\nu}$$

where  $S_{\mu\nu}$  is the overlap integral  $\int \chi_{\mu} \chi_{\nu} d\tau$ . The charge assigned to atom A is then given by

$$\text{Charge} = Z_A - \sum_{\mu}^A q_{\mu}$$

where  $Z_A$  is the atomic number and the sum is taken over all atomic orbitals on atom A.

However, ascribing the electron population to a given atom just because an orbital is centred on that atom is a simplification, especially if the orbital concerned is diffuse, and it is also rather arbitrary to divide the overlap populations equally between the centres concerned. A Mulliken population analysis therefore only gives a rough idea of the electron distribution in a molecule and the calculated values of the charges at atoms depend quite markedly on the basis set used. But, in spite of the limitations, a population analysis is conceptually close to qualitative ideas about charge distributions in molecules.

#### 5) LIMITATIONS OF HARTREE FOCK CALCULATIONS

While, given a large enough basis set and sufficient computer power, it is possible to approach the Hartree-Fock limit there are still certain limitations on the wave functions obtained.

i) From the virial theorem ( $V = -2T$  where  $V$  is the potential energy and  $T$  the kinetic energy) it is obvious that an electron in a region of high potential will have a correspondingly high kinetic energy. Thus for core electrons, which are in a region of high potential, relativistic effects, neglected in the Hartree-Fock model, may become

important and this may have some significance with regard to calculations on core electron photoionization. However, as will become apparent in chapter III relativistic corrections to shifts in core electron binding energies are small.

ii) The Hartree-Fock approximation takes into account the average interaction between an electron and all the other electrons in the molecule. It does not, however, take into account the instantaneous correlation of electronic motion which occurs since two electrons are unlikely to get very close to each other due to interelectronic repulsion. The major correlation effect occurs between pairs of electrons in the same spatial orbital.

$$E_{\text{Total experimental}} = E_{\text{Hartree Fock}} + E_{\text{relativistic}} + E_{\text{correlation}}$$

For diatomic molecules the molecular Hartree-Fock wave functions do not correlate with the Hartree-Fock wave functions describing the correct states of the separated atoms and the  $F_2$  molecule is predicted to have a negative dissociation energy.<sup>134</sup> In general, the most serious drawback of the Hartree-Fock approximation is its inability to describe molecule formation and dissociation correctly. However for chemical reactions involving only closed shell species Snyder and Basch<sup>135</sup> have shown that double zeta calculations give good agreement with experimental heats of reaction. Also the work of Ditchfield, Hehre et al<sup>136,137</sup> on bond separation energies has shown that for isodesmic reactions

even minimal basis set STO3G calculations give good values for heats of reaction. (Isodesmic reactions are reactions in which there is a retention of the number of bonds of a given formal type (i.e. single, double etc.) but with a change in their relation to one another<sup>137</sup>). For reactions of this type changes in correlation energies are small. The effect of correlation energies on photoionization calculations will be discussed in chapter III.

#### 6) IMPROVEMENTS ON THE HARTREE FOCK METHOD

i) Correlated wave functions have been used. However, this necessitates dispensing with the orbital approximation, and hence the conceptual simplicity is lost. These functions include interelectronic distance and although very accurate results may be obtained they are only feasible for small systems such as He<sup>138,139</sup> and H<sub>2</sub><sup>140</sup>.

ii) The method generally used for approaching the correlation energy problem is configuration interaction (C.I.),<sup>141</sup> that is to allow the calculated Hartree Fock ground state to interact with other doubly excited states of the same symmetry. (For closed shell states of molecules singly excited states do not interact directly with the ground state. However, since singly excited states can interact with doubly excited states there can be an indirect effect.) Thus the improved wave function  $\Psi$  is given by

$$\Psi = a \Psi_0 + b \Psi_1 + c \Psi_2 \dots\dots$$

where  $\Psi_0$  is the ground state Hartree-Fock wave function and from the virtual orbitals which resulted from its computation excited states  $\Psi_1$ ,  $\Psi_2$  etc. of the appropriate symmetry are constructed. The function is then optimized, by the variational method, to determine the best values of the mixing coefficients a, b, etc.

iii) A further improvement on the Hartree-Fock method is the multiconfigurational SCF method<sup>142</sup> which uses a wave function expressed as a linear combination of Slater determinants of the form

$$\Psi = a \Psi_0 + b \Psi_1 + c \Psi_2 + \dots$$

but not only are the best coefficients a, b etc found but also simultaneously the best forms of the constituent wave functions are determined. However, this method is difficult to implement for complex systems.

## 7) COMPUTER PROGRAMS FOR AB INITIO CALCULATIONS

Several standard packages are now available for performing non empirical molecular calculations. The writing and development of these programs has required many man-years of labour to produce efficient programs and they tend to have been written by teams of people. Once programs have been written they tend to be generally available through organizations such as the Quantum Chemistry Program Exchange. Initially efficient programming techniques and

optimum use of computer resources, such as core store, drum and disc store and magnetic tape, often took second place to the implementation of a working program. Most modern programs are derived from two approaches which differ in their basic design philosophies, which will be discussed later.

The essential stages in ab initio molecular orbital calculations are:

- i) The computation of integrals over the basis functions.
- ii) The transformation of these integrals over the contracted functions.
- iii) Assembly of the Fock matrix.
- iv) Diagonalization of the Fock matrix.

Steps (iii) and (iv) are repeated until the required degree of self consistency is obtained. The relative timing within the SCF section may be divided approximately

70% Assembly of Fock matrix  
30% Diagonalization of Fock matrix

Hence, for efficient running of the SCF section of the program the integrals should be stored on a fast random access facility (i.e. magnetic disc rather than tape).

The large number of integrals involved (approximately proportional to the fourth power of the number of basis functions) requires that the integral evaluation procedure be as efficient as possible and may

also raise problems about the most efficient methods of integral storage and retrieval. The core requirements of the program are also important especially if the program is to be run in a multiprogramming environment. However, since the programs are generally written largely in FORTRAN it is difficult to introduce dynamic arrays efficiently and so the same amount of core storage is required for a small molecule as for the largest systems which can be studied with that program.

Other desirable features, as far as practical use of the program is concerned, include:

- i) General applicability to all molecular systems (size being the only limiting factor).
- ii) They should be largely machine independent so that they may be implemented on different types of computer.
- iii) The system should require minimal input i.e. it should be possible to create and store prior data files of standard exponents and contraction coefficients to avoid the necessity of punching and inputting large decks of cards thereby increasing the possibility of mechanical or human error. Also, the input should be in as flexible a format as possible.
- iv) Since the calculations require large amounts of computer time the program should include restart facilities in both the integrals and SCF sections. This allows long calculations to be run in steps and in the SCF section also allows monitoring of the output to ensure that correct convergence is occurring.

- v) Facilities to check data input without actually performing any calculations are useful to check for human error and may prevent wastage of machine time.
- vi) The program should have facilities for adding, removing or changing basis functions and/or atoms and also facilities for moving atoms without having to recalculate those two electron integrals which are not affected by such changes to the system. Such facilities greatly reduce the amount of computer time required for many studies of chemical interest.

#### a) Programming Philosophies

The ab initio molecular orbital programs currently in use have generally followed one of two basic programming philosophies which are based on the POLYATOM and IBMOL programs which employ gaussian basis functions.

##### i) POLYATOM<sup>207</sup>

The requirements of the POLYATOM system were, in order of importance:-

- 1) The system should be general in the sense that it should not be restricted to, for example, diatomic or linear triatomic molecules.
- 2) The system should be largely machine independent, that is it should be workable on an IBM, a CDC or an ICL machine with the minimum of change.
- 3) The system should be heavily segmented with the segments having a standard type of interface.

The aim of these requirements was entire generality, and in any conflicts, efficiency was sacrificed to this aim. In order to minimize integration time the symmetry characteristics of the basis functions under the operations that constitute the point group of the molecule were used to generate a list of integral labels for integrals that were zero by symmetry and to group together those integrals that were equal to within a sign so that only one member of the group needed be evaluated. A list of integral labels in a standard order was produced and used as input to the integrals section of the program where a file of labels and values was produced. This is then used as input to the next section of the program which assembles and diagonalizes the Fock matrix. When this section of the program is complete a file containing the matrix of coefficients is produced and this provides the prime input for the PROPERTIES program. This segmentation of the program into several sections reduces the amount of core storage required and it is therefore suited for implementation in a multiprogramming environment.

ii) IBMOL

The IBMOL programs, developed in IBM laboratories, are oriented towards dedicated use with large core requirements (~ 500K) since the various stages are not segmented. Much of the program is written in FORTRAN but many of the subroutines are written in even faster, lower level machine dependent language (ASSEMBLER). Thus the IBMOL programs

are not suitable for implementation in a multiprogramming environment and are not readily implemented on other than IBM machines. The integral evaluation also differs in that all the integrals are evaluated and stored sequentially. (Any symmetry present in the molecule is defined explicitly in the contraction data). Since labels are not stored with the integrals the storage required for the integrals is reduced. Also for molecules of low symmetry time is not spent in searching for integrals which could be equal or zero by symmetry (the time taken to generate such a list and labels is proportion to approximately the third or fourth power of the number of basis functions whether or not zero or equal integrals occur in the molecule).

b) A Brief Description of the Programs Used in this Work.

Three program packages for non empirical LCAO SCF MO calculations have been employed in this work. They are ALCHEMY,<sup>208</sup> IBMOL 5<sup>187</sup> and ATMOL 2.<sup>188</sup> and were implemented on the Rutherford High Energy Physics Laboratory IBM 360/195 computer.

1) ALCHEMY

This program performs calculations with Slater basis sets but is, at present, limited to calculations on linear molecules and also requires a large amount of core (about 500 K bytes) and is therefore not suited to a multiprogramming environment. The program is written

in FORTRAN in order to be largely machine independent. The input required is relatively simple and flexible in format since FORTRAN NAMELIST input has been employed throughout. The input requirements for the integrals section are essentially the geometry of the molecule in atomic units (Z-coordinates only), and for each basis function the N, L and M (positive only) quantum numbers, and the orbital exponent of each basis function. The one centre integrals are calculated analytically and the others numerically. The integrals are ordered and stored on disc for use in the SCF section. This section requires an initial estimate of the eigenvalues (i.e. the coefficients of the basis functions) which are generally obtained from CNDO/2 calculations for the valence orbitals and by inspection for the core orbitals. The output from the program includes a population analysis and provision for the computation of several expectation values as well as the total energy and the final eigen values and eigenvectors. Punched card output of the final vectors may be obtained and these may be used as starting vectors for calculations on similar molecules or in configuration interaction calculations on the same molecule. However, since no configuration interaction studies were carried out in this work this will not be discussed further.

A typical breakdown of the c.p.u. time required for integral evaluation and SCF time is given below for  $C_3O_2$  which was a minimal Slater basis set calculation and consisted of 20 Slater type functions ( $p_x$  and  $p_y$  are equivalent).

<u>Calculation</u>	<u>Time (sec.)</u>
2-electron integrals	835
1-electron integrals	126
SCF	8
	<hr/>
Total	939
	<hr/>

IBMOL 5

IBMOL 5, like ALCHEMY, was developed at the IBM research laboratory in San Jose and, like ALCHEMY, is not segmented and requires a large amount of core storage. The input deck is large since the program uses gaussian functions and there are no built in library facilities for the storage of standard contraction coefficients and exponents. The data required for the integrals section of the program include the nuclear coordinates and charges and for each centre the exponents of the gaussian functions and their symmetry (e.g. S,  $P_x$ ,  $P_y$  etc.). This is followed by contraction coefficient data. Three contractions are possible. The first contraction is used to contract functions of the same type on the same centre. The second contraction may be used to contract functions (defined by the first contraction) of different types on the same centre and thus may be used to construct hybrid orbitals. The third contraction defines the third contracted basis set in terms of the functions defined in the previous contraction and may be used to construct symmetry adapted functions (e.g. a planar molecule may be factored into  $\sigma$  and  $\pi$  components).

The SCF input is in NAMELIST format and an initial estimate of the eigenvectors for each occupied molecular orbital in each symmetry grouping is required. For the valence orbitals these are usually obtained from CNDO calculations while for core orbitals they may readily be obtained by inspection.

Facilities exist for deleting, (but not adding), basis functions and also for the recalculation of those two electron integrals which are changed when an atom is moved or the basis functions on an atom changed while retaining the two electron integrals not concerned with that centre. Restart facilities are available in both the integral evaluation and SCF sections. The output does not include a population analysis and this has to be obtained from a separate program using the punched card output of the final vectors.

A typical breakdown of the c.p.u. times required for the various sections of the program is illustrated by a calculation on  $\text{CHF}_3$ . This consisted of 100 gaussian type basis functions contracted to 59 and was further symmetry factored into blocks of 39 and 20 depending on the symmetry of the orbitals under reflection through the plane of symmetry.

<u>Calculation</u>	<u>Time (sec.)</u>
2-electron integrals	3,487
1-electron integrals	2
SCF	220
Total	<u>3,707</u>

### iii) ATMOL 2

ATMOL 2 consists of a group of programs rather than just one large program (e.g. separate integral and SCF programs). The core

storage required for each of the programs (typically 220K bytes) is therefore not as large as that required for ALCHEMY or IBMOL and ATMOL is therefore suited to a multiprogramming environment. Restart facilities are available in both the integral and SCF programs and a library file is available for the storage of standard contractions thus reducing the amount of input required. The integral program uses gaussian functions although a program, compatible with the ATMOL group of programs, for use with Slater basis functions has recently been introduced.<sup>209</sup> Extensive integral file handling facilities are provided by the service program and are useful for carrying out move calculations, the addition or removal of basis functions and for staging integrals from tape to disc to obtain more efficient running of the SCF programs. The integrals are stored in blocks which also carry information concerning the labelling of integrals. (e.g. if the integral contains the basis functions  $\chi_i$ ,  $\chi_j$ ,  $\chi_k$  and  $\chi_l$  where  $\chi_i$  denotes the  $i^{\text{th}}$  basis function then information on the values of  $i, j, k$  and  $l$  is also stored).

The symmetry properties of the molecule may be used to improve the efficiency of the 2-electron integrals calculation since in a highly symmetric molecule many integrals will be zero or equal to within a sign and these need not be recalculated. Centres of symmetry are declared in the integrals input and these may include local symmetry as well as symmetry centres for the molecule as a whole. The efficiency of the integrals calculation is also improved

by orienting the molecule within the coordinate system so as to maximize the number of 2-electron integrals which are zero by symmetry. The ATMOL programs therefore follow much of the programming philosophy of the POLYATOM system.

Symmetry adapted functions may be introduced in the SCF section if required and in general the input for the SCF programs of ATMOL is more flexible than that for IBMOL. Beside the input of trial vectors an initial set of trial molecular orbitals may be obtained by use of the START directive when the trial molecular orbitals are formed by diagonalization of the 'unscreened' one electron Hamiltonian operator matrix. Trial molecular orbitals may also be formed by input of the expected value of the negative of the diagonal elements of the Fock matrix at self consistency (these values depend on the basis set used but are approximately invariant under change in molecular environment). The open shell SCF programs contain a LOCK directive which, if used, causes the iterated molecular orbitals to be selected on the principle of maximum overlap with the trial molecular orbitals. This directive is used in this work for the open shell calculations on core hole states using the closed shell eigenvectors as input for the trial molecular orbitals.

The output from the SCF programs includes eigenvalues and eigenvectors for both occupied and virtual orbitals. (Punched card output of these vectors may also be obtained and used as input for trial vectors in other SCF calculations or in population analyses). A

Mulliken population analysis and the dipole moment are also included in the output although a separate, and more versatile, Mulliken population analysis program is also available.

A STO 4.31G calculation on  $\text{CF}_4$ , which consists of 100 gaussian type orbital contracted to 45 required the following times

<u>Calculation</u>	<u>Time (sec.)</u>
2-electron integrals	558
1-electron integrals	2
SCF	71
Total	<u>631</u>

This calculation, however, was performed before the incorporation of the symmetry routine into the integrals evaluation program. The effect of the use of symmetry in the calculations is clearly illustrated in the case of a STO 4.31G calculation on methane (26 gaussian functions contracted to 17) where the integral evaluation time was 18 second without the symmetry routine but only 3.7 seconds when the symmetry of the molecule was taken into account.

### c) Open Shell SCF Calculations using ATMOL 2

The open shell SCF calculations reported in this work were carried out by the ATMOL 2 Restricted Hartree-Fock SCF program which minimizes the energy of a single determinantal wavefunction constructed from doubly occupied and singly occupied molecular orbitals. (The singly occupied molecular orbitals have a common spin factor). The aims of this program and those of Roothaan<sup>210</sup> are identical in cases

where the state studied is not orbitally degenerate. In the case where states are orbitally (spatially) degenerate the ATMOL 2 RHF program yields molecular orbitals which optimally describe only one component of the degenerate manifold, whilst Roothaan's procedures yield molecular orbitals which are used to construct the set of degenerate wavefunctions. Thus, the ATMOL 2 RHF-SCF programs always minimize a one component energy expression of the form

$$\langle \psi | \mathcal{H} | \psi \rangle / \langle \psi | \psi \rangle$$

whereas Roothaan's procedures minimize

$$\left( \sum_{i=1}^g \langle \psi_i | \mathcal{H} | \psi_i \rangle / \langle \psi_i | \psi_i \rangle \right) / g$$

where each wavefunction  $\psi_i$  is constructed from a common set of molecular orbitals and  $g$  denotes the degeneracy. In general, the energy of a degenerate state produced by ATMOL 2 will be lower than that given by Roothaan's procedure. Also, the discontinuities in the energy surface which are observed with Roothaan's 'symmetry equivalenced' procedures when Jahn Teller distortions of molecular geometry are studied do not occur using the spatially unrestricted methods of ATMOL 2. However, the total wave function produced by ATMOL 2 may not be an eigenfunction of all the symmetry operators which commute with the total Hamiltonian whilst that produced by the methods of Roothaan will.

In the RHF procedures the doubly occupied spatial orbitals are degenerate regardless of whether the spin of the electron is parallel or antiparallel to that of the unpaired electron(s). However, this restriction may be removed to yield the spin unrestricted Hartree-Fock wave function,<sup>211</sup> (i.e. one electron per spin orbital rather than two electrons per doubly occupied and one electron per singly occupied spatial orbital). Thus for each doubly occupied spatial orbital in the RHF procedure two orbitals, corresponding to  $\alpha$  and  $\beta$  spins are calculated with consequent increase in computing time. This procedure yields energies slightly lower than the RHF procedure.<sup>212</sup> The main objection to the UHF method<sup>213</sup> is that the resulting single determinant wave function is not an exact eigenfunction of the spin operator  $S^2$ . i.e. it does not satisfy the condition

$$S^2 \psi_e = S(S + 1) \psi_e$$

although this equation is nearly satisfied.<sup>214</sup> No UHF calculations were performed in this work.

## 8) SEMI-EMPIRICAL LCAO SCF MO CALCULATIONS

Even minimal basis set calculations of the non-empirical type become computationally very expensive for molecules of a moderate size. One of the main obstacles in ab initio calculations is the large number of three and four centre two electron integrals which require calculation. A number of semi-empirical methods based essentially

on a minimal basis set of Slater functions have therefore been devised in which the number of integrals requiring calculation is reduced either by approximating them to zero or by estimating them from empirical data. This can greatly reduce the computational time required and allow larger systems to be studied.

a) Semi-empirical All-valence Electron, Neglect of Diatomic Overlap Method (NDDO)

The approximations involved in this method are:-

- i) Only the valence electrons are specifically accounted for, the inner shells being regarded as an unpolarizable core.
- ii) Only atomic orbitals of the same principle quantum number as that of the highest occupied orbitals in the isolated atoms are included in the basis set.
- iii) Diatomic differential overlap is neglected

$$\text{i.e. } S_{ij} = \int \chi_i(\mu) \chi_j(\mu) d\tau = 0$$

if the orbitals  $\chi_i$  and  $\chi_j$  are not on the same atom, and

$$\iint \chi_i(\mu) \chi_k(\nu) \frac{1}{r_{\mu\nu}} \chi_j(\mu) \chi_l(\nu) d\tau_\mu d\tau_\nu = 0$$

unless  $\chi_i$  and  $\chi_j$  are atomic orbitals belonging to the same atoms A and  $\chi_k$  and  $\chi_l$  are atomic orbitals belonging to the same atoms A or B.

Inner electrons are therefore neglected by treating them as part of a core whose charge will be approximately equal to that of the nucleus minus one unit charge per core electron. Also by only considering valence electrons the initial number of integrals to be calculated is greatly reduced. All three and four centre integrals also are set to zero as are some two centre integrals. Little work has been carried out within the NDDO approximations, however, since with modern computers comparable non empirical minimal basis set calculations are only about an order of magnitude slower.

b) All Valence Electron Complete Neglect of Differential Overlap (CNDO) Method

Even using the above approximations the number of integrals requiring to be calculated is still large and further simplifications are necessary. However, the approximations must be made such that the results are independent of the choice of coordinate systems.<sup>143</sup> In the complete neglect of differential overlap method both one and two centre integrals involving differential overlap are also set to zero.<sup>143,144,145.</sup> Writing the electronic interactions integrals

$$\iint \chi_A^2(\mu) \frac{1}{r_{\mu\nu}} \chi_B^2(\nu) d\tau_\mu d\tau_\nu \quad (58)$$

as  $\Gamma_{AB}$  the Fock matrix elements  $F_{ij}$  become

$$F_{ii} = H_{ii} + (P_{AA} - \frac{1}{2} P_{ii}) \Gamma_{AA} + \sum_{B \neq A} P_{BB} \Gamma_{AB} \quad (59)$$

$$F_{ij} = H_{ij} - \frac{1}{2} P_{ij} \Gamma_{AB} \quad (i \neq j) \quad (60)$$

where atomic orbital  $\chi_i$  is centred on atom A and  $\chi_j$  on atom B and  $P_{ij}$  are the components of the charge density and bond order matrix.

$$P_{ij} = 2 \sum_m^{\text{occ.}} a_{mi} a_{mj} \quad (61)$$

and  $P_{AA}$  is the total charge density on atom A

$$P_{AA} = \sum_i^A P_{ii} \quad (62)$$

The core matrix elements  $H_{ii}$  may be separated into two components, the diagonal matrix elements of  $\chi_i$  with respect to the one-electron Hamiltonian containing only the core of its own atom ( $U_{ii}$ ), and the interaction of an electron in  $\chi_i$  on atom A with the cores of the other atoms B.

$$H_{ii} = U_{ii} - \sum_{B \neq A} V_{AB} \quad (63)$$

and therefore equation (59) may be written as

$$F_{ii} = U_{ii} + (P_{AA} - \frac{1}{2}P_{ii})\Gamma_{AA} + \sum_{B \neq A} (P_{BB}\Gamma_{AB} - V_{AB}) \quad (64)$$

and the total energy may be expressed as the sum of one and two atom terms

$$E = \sum_A E_A + \sum_{A < B} E_{AB} \quad (65)$$

where

$$E_A = \sum_i^A P_{ii} U_{ii} + \frac{1}{2} \sum_i^A \sum_j^A (P_{ii} P_{jj} - \frac{1}{2} P_{ij}^2) \Gamma_{AA} \quad (66)$$

and

$$E_{AB} = \sum_i^A \sum_j^B (2 P_{ij} H_{ij} - \frac{1}{2} P_{ij}^2 \Gamma_{AB}) + (Z_A Z_B \frac{1}{R_{AB}} - P_{AA} V_{AB} - P_{BB} V_{BB} + P_{AA} \Gamma_{AB}) \quad (67)$$

where  $R$  is the distance between nuclei  $A$  and  $B$ .

The neglect of the one centre interactions involving differential overlap between two orbitals result in some one-centre exchange integrals such as  $(2s2p_x 2s2p_x)$  being omitted. This renders the method incapable of introducing quantitatively Hund's rule effects i.e. that two electrons in different atomic orbitals on the same atom have a lower repulsion energy if their spins are parallel. However this omission is not serious for calculations on ground states of closed shell molecules.

The integrals are estimated by the following methods:

i) One electron integrals  $U_{ii}$ . An estimate of this integral is obtained from spectroscopic data

$$U_{ii} = -I_i - (Z_A - 1)\Gamma_{AA} \quad (68)$$

where  $I_i$  is the ionization potential of an electron from the orbital  $\chi_i$  belonging to atom  $A$  (referred to appropriate average atomic states).<sup>145</sup>

An alternative procedure would have been to use atomic electron affinities  $A_i$  and

$$-A_i = U_{ii} + Z_A \Gamma_{AA} \quad (69)$$

However in order to account for the tendency of an atomic orbital to both acquire and loose electrons the relationship used in CNDO/2 calculations is

$$-\frac{1}{2} (I_i + A_i) = U_{ii} + (Z_A - \frac{1}{2}) \Gamma_{AA} \quad (70)$$

$$\therefore U_{ii} = -\frac{1}{2} (I_i + A_i) - (Z_A - \frac{1}{2}) \Gamma_{AA} \quad (71)$$

ii) One centre two electron integrals  $\Gamma_{AA}$ . These are calculated as the electrostatic repulsion energy of two electrons in a Slater s orbital irrespective of the fact that the orbitals concerned may be p or d orbitals. Thus

$$\Gamma_{AA} = \iint \chi_{S_A}^2(\mu) \frac{1}{r_{\mu\nu}} \chi_{S_A}^2(\nu) d\tau_\mu d\tau_\nu \quad (72)$$

iii) Two-centre two-electron integrals  $\Gamma_{AB}$ . These are calculated as

$$\Gamma_{AB} = \iint \chi_{S_A}^2(\mu) \chi_{S_B}^2(\nu) d\tau_\mu d\tau_\nu \quad (73)$$

where  $\chi_{S_A}$  and  $\chi_{S_B}$  are the Slater s-type orbitals for atoms A and B. These integrals represent the interaction between electrons in valence atomic orbitals on atoms A and B. (This is the two-centre coulomb integral involving valence s functions and is close to an average of all such integrals involving atoms A and B).<sup>144</sup> Formulae for these integrals have been listed by Roothaan.<sup>146</sup>

iv) Two-centre One-Electron Integrals  $H_{ij}$  (Resonance integrals).

This integral is taken as being directly proportional to the overlap integral  $S_{ij}$  between the orbitals  $\chi_i$  and  $\chi_j$  centred on A and B respectively.

$$H_{ij} = \beta_{AB}^0 S_{ij} \quad (74)$$

where Slater atomic orbitals are used to calculate  $S_{ij}$ . To preserve rotational invariance  $\beta_{AB}^0$  should be characteristic of  $\chi_i$  and  $\chi_j$  but independent of their coordinates. The parameter  $\beta_{AB}^0$  is therefore taken as an average of a  $\beta^0$  parameter for each atom

$$\beta_{AB}^0 = \frac{1}{2} (\beta_A^0 + \beta_B^0) \quad (75)$$

where the parameters  $\beta_A^0$  etc. are chosen experimentally to reproduce results obtained from experiment or ab initio calculations.<sup>144, 145, 147.</sup>

v) Coulomb Penetration Integrals  $V_{AB}$

In the CNDO/1<sup>144</sup> method the penetration terms ( $Z_B \Gamma_{AB} - V_{AB}$ ) were evaluated by approximating the coulomb penetration integrals as

$$V_{AB} = \int \chi_{S_A}^2 \frac{Z_B}{r_{\mu B}} d\tau_{\mu} \quad (76)$$

where  $Z_B$  is the core charge on atom B,  $\chi_{S_A}$  is the Slater 2s orbital of atom A and  $r_{\mu B}$  is the distance of the electron  $\mu$  from B. Formulae for these integrals have also been listed by Roothaan.<sup>146</sup> A major failure of the CNDO/1 method was its inability to give reasonable values for bond lengths (these were too short) and bond energies (too large) for diatomic molecules. This was compensated for in the CNDO/2 method<sup>145</sup> by neglecting the penetration terms by setting

$$V_{AB} = Z_B \Gamma_{AB} \quad (77)$$

The final form of the Fock matrix in the CNDO/2 method is then given by<sup>145</sup>

$$F_{ii} = -\frac{1}{2} (I_i + A_i) + [(P_{AA} - Z_A) - \frac{1}{2}(P_{ii} - 1)] \Gamma_{AA} + \sum_{B \neq A} (P_{BB} - Z_B) \Gamma_{AB}$$

$$F_{ij} = \beta_{AB}^0 S_{ij} - \frac{1}{2} P_{ij} \Gamma_{AB} \quad (78)$$

Initial estimates of the LCAO coefficients are obtained from a Huckel-type theory using matrix elements<sup>145</sup>

$$F_{ii}^0 = -\frac{1}{2} (I_i + A_i)$$

$$F_{ij}^0 = \beta_{AB}^0 S_{ij} \quad (79)$$

and the final solution approached by an iterative scheme<sup>144,145</sup> until the desired amount of self consistency is obtained in the values of the coefficients.

When the molecular orbitals  $\psi_m$  have been determined the charge density may be analyzed in terms of the basis functions  $\chi_1$ . For two electrons in each occupied molecular orbital the total charge density  $P$  is given by

$$P = 2 \sum_m^{\text{occ.}} \psi_m = \sum_k \sum_l P_{kl} \chi_k \chi_l \quad (80)$$

where  $P_{kl}$  is the density matrix defined in equation (61). The diagonal element  $P_{kk}$  is the coefficient of the distribution  $\chi_k^2$  and measures the electron population of that orbital. The off diagonal elements  $P_{kl}$  are overlap populations related to the overlap region of atomic orbitals  $k$  and  $l$ . In order to assign a specific charge to each atom a Mulliken population analysis is used. The total population for an orbital  $k$  is given by

$$q_k = P_{kk} + \sum_{k \neq l} P_{kl} S_{kl} \quad (81)$$

where  $S_{kl}$  is the overlap integral. However, since overlap is ignored in the CNDO approximation the second terms of equation (81) drop out to give

$$q_k = P_{kk} \quad (82)$$

and the total charge density on atom A is then given by the sum over all the atomic orbitals centred on A

$$P_{AA} = \sum_k^A P_{kk} \quad (83)$$

and the net charge on atom A is given by

$$\text{Charge} = P_{AA} - Z_A$$

where  $Z_A$  is the effective atomic number (i.e. the atomic number minus the number of core electrons).

In CNDO/2 calculations the Hartree-Fock equations are solved after most of the integrals have been eliminated, set equal to zero, or calculated from empirical data. Table (2.2) shows the number of two electron integrals which require evaluation in a calculation on propane at various levels of sophistication.

Table 2.2

Two electron integrals required to be evaluated for a calculation on propane

<u>Integrals</u>	<u>Hartree-Fock (minimal basis)</u>	<u>NDDO</u>	<u>CNDO</u>
1 centre	368	173	11
2 centre	6652	568	55
3 and 4 centre	31206	0	0
Total	38226	741	66

The CNDO calculations reported in this work were carried out using the standard program CNINDO<sup>148</sup> written in FORTRAN IV. This program can perform CNDO/2 calculations on molecules containing the elements hydrogen to chlorine and iterations are performed until consecutive values of the total energy agree to within  $10^{-6}$  a.u. The program was, however, modified slightly so that the convergence limit could be changed if required and it was also redimensioned so that calculations on molecules containing up to 120 basis functions, (rather than the previous maximum of 80), could be performed. A further modification was also introduced so that 3d orbitals could be excluded from calculations on second row elements if required.

CHAPTER III

THE THEORETICAL INTERPRETATION

OF ESCA CHEMICAL SHIFTS.

## 1) INTRODUCTION

Besides the use of empirical parameters characteristic of directly bonded groups,<sup>51</sup> there have been five distinct, but interrelated, approaches to the quantitative interpretation of chemical shift data and these are:-

- i) The equivalent cores approach
- ii) The charge potential model
- iii) Koopmans' theorem calculations
- iv) Core hole state calculations
- v) The quantum mechanical potential at the nucleus model

It is convenient to discuss the theoretical background and uses of each of these models separately and to indicate the relationships between the models where they occur. The main aims of the work presented in this chapter are:-

- i) To test the use of the equivalent cores approximation using heats of reaction obtained from molecular orbital calculations.
- ii) To compare the equivalent cores approach, Koopmans' theorem calculations and core hole state calculations from the point of view of the basis set dependence and the accuracy of the calculated shifts. No such detailed comparisons have previously been reported.

iii) To obtain information about relaxation effects which occur on photoionization of a core electron.

iv) To obtain information on the validity of both the weak and strong forms of the equivalent cores approximation.

In this study molecular orbital calculations have been carried out on two series of molecules:-

i) A series of small molecules containing hydrogen, carbon, nitrogen, oxygen, fluorine and sulphur.

ii) The closely related series of the fluoro and chloromethanes in which regular trends are expected to facilitate interpretation.

For the majority of the molecules in (i) and all the molecules in (ii) gas phase values of binding energies and shifts have been reported and this allows a direct comparison with the theoretical calculations.

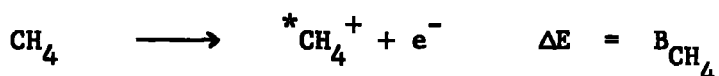
a) Equivalent Cores Method.

The equivalent cores approximation was developed by Jolly and Hendrickson<sup>44</sup> to calculate shifts in core electron binding energies from ground state thermodynamic data and states that

'When a core electron is removed from an atom in a molecule or ion, the valence electrons relax as if the nuclear charge on the atom had increased by one unit'.

Thus atomic cores that have the same charge are considered to be chemically equivalent. The following example illustrates how this principle may be used to estimate the gas phase shift in  $C_{1s}$  binding energy between the carbon atoms in methane and fluoromethane.

- i) The carbon  $1s$  electron binding energy in methane  $B_{CH_4}$  is given by the energy of the process

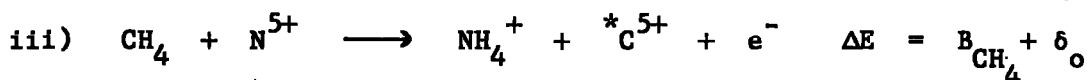


where  $*$  indicates a vacancy in a core level ( $C_{1s}$  in this case)

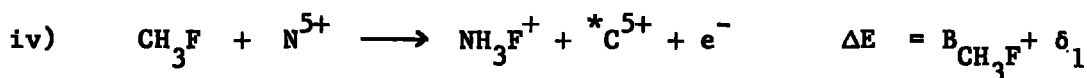


This reaction is the exchange of the  ${}^*C^{5+}$  core and the equivalent  $N^{5+}$  core. According to the principle of equivalent cores the energy of this reaction,  $\delta_0$ , is zero.

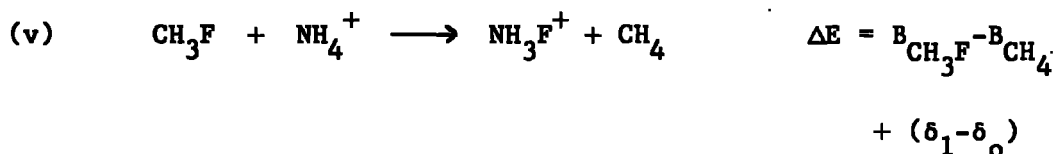
Summing reactions (i) and (ii) gives



A similar reaction may be written for  $CH_3F$ , or any other compound containing a carbon atom.



The difference of reactions (iii) and (iv) gives



The strong form of the equivalent cores approximation given above states that  $\delta_1 = \delta_0 = 0$  and hence the difference in  $C_{1s}$  binding energies between methane and fluoromethane is given by the energy of reaction (v). However, reaction (v) still gives the shifts in binding energy if  $\delta_1 = \delta_0$  i.e. if the energy of core exchange is independent of the molecular environment (this is known as the weak form of the equivalent cores approximation). Some typical gas phase data are shown in table (3.1)<sup>50</sup> and in general indicate good agreement between experimental and thermodynamic shifts. Extension to solid samples requires the estimation of the energies of the processes outlined in Chapter I.4.<sup>44,149</sup> The main restriction to the use of the equivalent cores method is the lack of and/or inaccuracy of thermodynamic data especially with regard to the positive ions involved in the reactions.

However, the heats of reaction may be obtained from SCF calculations on the molecules and ions in their ground states.<sup>121,122</sup> Pople and co-workers have shown that for reactions involving closed shell species even minimal basis set (STO 3.G) calculations, which are computationally relatively inexpensive, can reliably reproduce heats of reaction. Particularly accurate results are obtained in the case of reactions in which the number and type (i.e. single, double etc.) of bonds are the same in both reactants and products since correlation energy changes are very small. Such processes have been designated isodesmic reactions and it is exactly this type of reaction which is involved in the equivalent cores method of calculating shifts. Since heats of reaction are involved there is also the possibility that semi-empirical calculations, which are computationally inexpensive,

Table 3.1

Experimental and Thermodynamic Binding Energy Shifts<sup>50</sup>

<u>Atomic level</u>	<u>Compound</u>	<u>Experimental Shift</u>	<u>Chemical Reaction Energy</u>
N <sub>1s</sub>	NH <sub>3</sub>	0	0
N <sub>1s</sub>	(CH <sub>3</sub> ) <sub>2</sub> NH	- 0.7	-0.7
N <sub>1s</sub>	(CH <sub>3</sub> )NH <sub>2</sub>	- 0.3	-0.4
N <sub>1s</sub>	HCN	1.2	0.95
N <sub>1s</sub>	<u>NNO</u>	3.2	2.6
N <sub>1s</sub>	N <sub>2</sub>	4.35	3.5
N <sub>1s</sub>	NO	5.5	4.4
N <sub>1s</sub>	N <sub>2</sub> F <sub>2</sub>	6.8	6.3
N <sub>1s</sub>	NO <sub>2</sub>	7.3	6.8
C <sub>1s</sub>	CH <sub>4</sub>	0	0
C <sub>1s</sub>	CO	5.4	4.1
C <sub>1s</sub>	CO <sub>2</sub>	6.8	6.9
C <sub>1s</sub>	CF <sub>4</sub>	11.0	12.3
Xe 3d <sub>5/2</sub>	Xe	0	0
Xe 3d <sub>5/2</sub>	XeF <sub>2</sub>	2.95	2.7
Xe 3d <sub>5/2</sub>	XeF <sub>4</sub>	5.5	5.4
Xe 3d <sub>5/2</sub>	XeOF <sub>4</sub>	7.0	6.3
Xe 3d <sub>5/2</sub>	XeF <sub>6</sub>	7.9	7.85



may be used to predict, at least qualitatively, the required shifts. (However, this may be expected to be strongly dependant on the parameterization used and some recently reported calculations<sup>150</sup> using MINDO/1 give better results than the CNDO/2 calculations reported in this work). Thermodynamic data refer to the isoelectronic cations with their nuclei in the equilibrium positions but since photoionization is a rapid process compared with nuclear motion<sup>66,151</sup> it is more realistic to consider the cations to have the same geometry as the parent molecule. This condition may be imposed in molecular orbital calculations. Also by using the same geometry for the molecules and isoelectronic cations in ab initio LCAO MO SCF calculations many of the two electron integrals may be retained and this greatly reduces the amount of computing time required. By the very nature of the equivalent cores approximation if the element being studied has more than one core level then identical shifts in binding energy are predicted for all core levels.

#### b) Charge Potential Model

The charge potential model relates core electron binding energies with the charge on the atom from which core ionization takes place and the potential from the charges in the remainder of the molecule<sup>17</sup>

$$E = E^0 + kq_i + \sum_{j \neq i} \frac{q_j}{r_{ij}}$$

where

$E$  is the binding energy

$E^{\circ}$  is a reference level

$q_i$  is the charge on atom  $i$

$k$  is a constant (approximately the one-centre repulsion integral between a core and valence electron on atom  $i$ ).

The summation term is an intra-molecular Madelung type potential but in an ionic compound the summation should be taken over the complete lattice.

$E^{\circ}$  and  $k$  depend on the definition of atomic charge and in an LCAO MO SCF treatment on the basis set used.

A non-rigorous derivation of the charge potential model may be made from Koopmans' theorem<sup>152</sup> (Figures 3:1a,b,c). The crucial feature in the derivation of the charge potential equation is the constancy with varying electronic environments of many of the terms which arise.

Since the charge potential model may be derived from Koopmans' theorem it also potentially suffers from the same deficiencies as Koopmans' theorem. Thus any large differences in, or non systematic variations of, relaxation energies between atoms in different chemical environments will be noticeable in both Koopmans' theorem and charge potential calculations. (This difficulty may, however, be overcome by regarding  $k$  and  $E^{\circ}$  as empirical parameters derived from a series of similar molecules).

The use of semi-empirical calculations (CNDO/2) to obtain molecular charge distributions allows the charge potential model to be used on large organic systems and Chapter IV will contain a more detailed

## Charge Potential Model

### (i) Koopmans' Theorem

$$\begin{aligned} \epsilon_r &= \langle \psi_r | -\frac{1}{2} \nabla_i^2 - \sum_n \frac{Z_n}{r_{ni}} | \psi_r \rangle + \sum_{s=0}^k (2J_{rs} - K_{rs}) \\ &= \langle \psi_r | -\frac{1}{2} \nabla_i^2 - \frac{Z_m}{r_{mi}} | \psi_r \rangle + J_{rr} + \langle \psi_r | - \sum_{n \neq m} \frac{Z_n}{r_{ni}} | \psi_r \rangle + \sum_{s \neq r}^k 2J_{rs} - K_{rs} \end{aligned}$$

$\psi_r$  core orbital on atom m

$$\langle \psi_r | -\frac{1}{2} \nabla_i^2 - \frac{Z_m}{r_{mi}} | \psi_r \rangle$$

$J_{rr}$

constants essentially independent of  
valence electron distribution

### C<sub>1s</sub> levels

<u>Molecule</u>	<u>Atom</u>	$q$	$\langle \psi_r   -\frac{1}{2} \nabla_i^2   \psi_r \rangle$ a.u.	$\langle \frac{1}{R} \rangle$	Koopmans' shift
H-C≡C-F	H-C	-0.061	16.0168	5.6559	0.33 e.v.
	F-C	+0.112	16.0181	5.6563	2.96 e.v.
H-C≡C-Cl	H-C	-0.136	16.0189	5.6515	0.24 e.v.
	Cl-C	-0.078	16.0175	5.6515	1.60 e.v.

Krs exchange integrals

$\psi$ s orbitals on other atoms  
in molecule

$\approx 0$

$$\epsilon_r = E_0 + \langle \psi_r | - \sum \frac{Z_n}{r_{ni}} | \psi_r \rangle + \sum_{s \neq r}^k 2J_{rs}$$

$\psi_r$  localized on atom m

$$\epsilon_r \approx E_0 + \sum_{n \neq m} \frac{-Z_n}{r_{nm}} + \sum_{s \neq r}^k 2J_{rs}$$

Terms in summation  $\psi_j$  core orbital on atom n

$$J_{rj} = \langle \psi_r(1) \psi_j(2) | \frac{1}{r_{12}} | \psi_r(1) \psi_j(2) \rangle \frac{1}{r_{nm}}$$

$\psi_i$  valence MO

$$J_{ri} = \sum_p C_{ip}^2 \langle \psi_r(1) \phi_p(2) | \frac{1}{r_{12}} | \psi_r(1) \phi_p(2) \rangle$$

Two types

(i)  $\phi_p$  valence AO on M

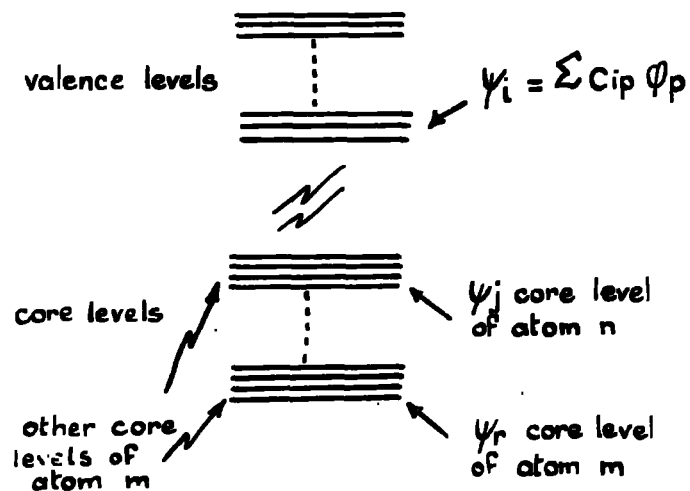
(ii)  $\phi_p$  " AO on atom n

$$J_{ri} = \sum C_{ip}^2 \langle \psi_r(1) \phi_p(2) | \frac{1}{r_n} | \psi_r(1) \phi_p(2) \rangle$$

sum over all  $\phi_p$  on atom m

$$\sum C_{ip}^2 + \frac{1}{r_{nm}}$$

Figure(3.1b)



$$\epsilon_r = E_0 + \sum \frac{-Z_n}{r_{nm}} + \sum \frac{z}{r_{nm}} + \sum \sum \frac{2C_{ip}^2}{r_{nm}} + \sum C_{ip}^2 \langle \psi_r(1) \phi_p(2) | \frac{1}{r_{12}} | \psi_r(1) \phi_p(2) \rangle$$

collecting terms common to each atom

valence orbitals  $\phi_p$  on  $m$

$$\epsilon_r = E_0 + \sum \left( \frac{-Z_n}{r_{nm}} + \frac{z}{r_{nm}} \right) + \sum \frac{2C_{ip}^2}{r_{nm}} + \sum C_{ip}^2 \langle \psi_r(1) \phi_p(2) | \frac{1}{r_{12}} | \psi_r(1) \phi_p(2) \rangle$$

$-Z_n + \sum z + \sum 2 C_{ip}^2$  is charge  $q_n$  on atom  $n$

$$\therefore \epsilon_r = E_0 + \sum_{n \neq m} \frac{q_n}{r_{mn}} + \sum 2 C_{ip}^2 \langle \psi_r(1) \phi_p(2) | \frac{1}{r_{12}} | \psi_r(1) \phi_p(2) \rangle$$

$2 C_{ip}^2$  valence electron population on  $m \propto$  charge on  $m$

$$\therefore \epsilon_r = E_0 + k q_m + \sum_{n \neq m} \frac{q_n}{r_{nm}}$$

discussion of the qualitative development of the charge potential model and a detailed examination of its use in the field of organo-halogen chemistry for predicting ground state charge distributions in molecules.

c) Koopmans' Theorem

Koopmans' theorem<sup>153</sup> equates the binding energy of an electron with the negative of the orbital energy and is derived below.

For a closed shell molecule  $E_M$  described by the Slater determinant of spin orbitals

$$\Psi_M = | \psi_a \psi_b \dots \psi_k |$$

the total energy is written as

$$E_M = \sum_{r=a}^k E_r - \sum_{\substack{\text{pairs} \\ rs}} (J_{rs} - K_{rs}) + V_{nn}$$

where the orbital energies  $E_r$  are expressed as

$$E_r = H_{rr}^c + \sum_{s=a}^k (J_{rs} - K_{rs}) \quad (1)$$

If an electron is removed from spin orbital  $\psi_a$  but the wave functions of the other electrons are left unchanged, then the

energy of the positive ion  $E_M^+$  having the wave function

$$|\psi_b \dots \dots \psi_k|$$

is given by

$$E_M^+ = \sum_{r=b}^k H_{rr}^C + \sum_{\substack{\text{pairs} \\ rs \\ r \neq a, s \neq a}} (J_{rs} - K_{rs}) + V_{nn}$$

and from (1)

$$\begin{aligned} E_M^+ &= E_M - H_{aa}^C + \sum_{s=a}^k (J_{as} - K_{as}) \\ &= E_M - E_a \end{aligned}$$

Therefore  $-E_a$  can be equated to the ionization potential ( $E^+ - E$ ) which is the energy required to ionize the molecule, providing that the ionization process is adequately represented by the removal of an electron from an orbital without change in the wave functions of the other electrons.

Not only does Koopmans' theorem neglect relativistic and correlation energy contributions to the binding energy but also the relaxation energy associated with the reorganization of electrons which occurs on photoionization. Hartman and Clementi<sup>154</sup> have shown in calculations on argon, that most of the relativistic correction is associated with the core electrons and that for argon the 1s contribution

in its ions is essentially the same as in the atom. (In the extreme case of  $\text{Ar}^{10+}$  the correction changes by only 0.72eV compared with the atom). These data<sup>154</sup> verify the assumption of Scherr et al.<sup>155</sup> that the relativistic contribution of any subshell is independent of the number of electrons in the outer shells. Thus differences in relativistic corrections to shifts in core electron binding energies between a particular core level for atoms in different chemical environments are small.<sup>151</sup> Some typical estimates of the total relativistic energies and correlation energies for first row atoms are shown in table 3.2. From an analysis of atomic data for first row atoms it is also known that the magnitudes of the correlation energies of the 1s electrons are very similar and intra shell correlation energies are small<sup>135</sup> (Table 3.3).

Table 3.2

Estimates of Relativistic Energies and Correlation Energies for First

Row Atoms<sup>156</sup>

	$E_{\text{rel}}$	$E_{\text{corr}}$	(eV)
Li	-0.015	-1.423	
Be	-0.060	-2.092	
B	-0.164	-2.803	
C	-0.376	-3.833	
N	-0.755	-5.162	
O	-1.344	-6.694	
F	-2.255	-8.612	
Ne	-3.570	-10.827	

Table 3.3

Atomic Orbital Pair Correlation Energies  $\epsilon_{ij}$  (eV)<sup>135</sup>

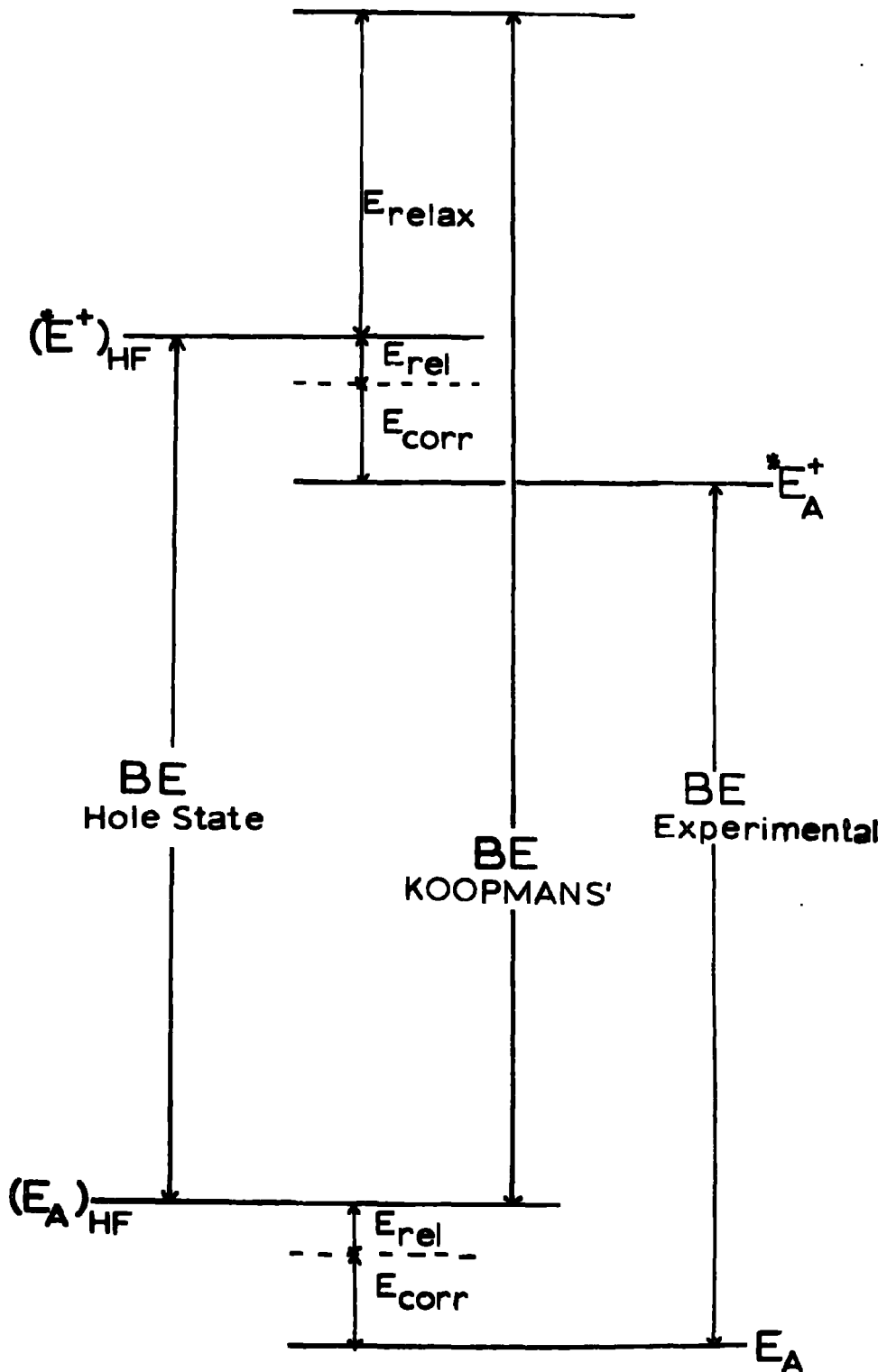
Pair ij	C	N	O	F	Ne	H
1s1s	-1.11	-1.11	-1.09	-1.08	-1.09	-1.11
1s2s	-0.04	-0.04	-0.04	-0.04	-0.04	
1s2p	-0.04	-0.04	-0.03	-0.04	-0.04	
2s2s	-0.77	-0.37	-0.35	-0.32	-0.29	
2s2p	-0.38	-0.38	-0.32	-0.23	-0.19	
2p2p	-0.70	-0.70	-0.70	-0.70	-0.70	
2p2p'	-0.33	-0.33	-0.33	-0.33	-0.33	

$$E_{\text{corr}} = \sum_i \epsilon_{ii} \frac{1}{2} \rho_i + \sum_{i > j} \epsilon_{ij} \rho_i \rho_j$$

where  $\rho_i$  is the atomic orbital electron density for orbital  $i$ .

Thus to a good approximation correlation energy corrections will remain reasonably constant for core levels (which are essentially localized and atomic in nature) and play little or no part in shifts in core electron binding energies. In a detailed study of the ionized states of the  $\text{CH}_4$  molecule with a basis set approaching the Hartree-Fock limit Clementi and Popkie<sup>157</sup> have demonstrated that for the 1s hole state the correlation energy is the same as for the neutral molecule. The differences between the experimental binding energies

## Relationship between Experimental and Calculated Binding Energies for Atom A



Figure(3.2)

and those measured by Koopmans' theorem are illustrated in figure 3.2. From the above discussion the relativistic and correlation energy corrections to the binding energies are relatively small and almost complete cancellation of these effects will occur when calculating shifts in core electron binding energies between molecules. For core levels the major difference between the Koopmans' theorem binding energy and the experimental binding energy is the neglect of the relaxation energy. Most of the electronic reorganization which occurs on core ionization is associated with the valence electrons as is illustrated by the radial expectation values of various electrons obtained from Hartree-Fock calculations on neon and its hole states<sup>158</sup> (Table 3.4).

Table 3.4

Radial Expectation Values for Electrons in Neon and its Hole States<sup>158</sup> (a.u.).

	<u>Ne</u> Atom	2p hole	<u>Ne</u> <sup>+</sup> 2s hole	1s hole
$\langle r \rangle_{1s}$	0.1576	0.1576	0.1578	0.1545
$\langle r \rangle_{2s}$	0.8921	0.8603	0.8536	0.8171
$\langle r \rangle_{2p}$	0.9652	0.8759	0.8841	0.7993

Removal of a 1s electron has very little effect on the radius of the remaining 1s electron but the outer electrons contract markedly.

Since relaxation is associated largely with the valence electrons the relaxation energy is expected to vary somewhat with the electronic environment of the atom. Koopmans' theorem calculations overestimate the binding energy by the relaxation energy and relative shifts are affected by differences in relaxation energies. Table 3.5 illustrates some experimental and Koopmans' theorem binding energy shifts for the  $C_{1s}$  level in a variety of compounds.<sup>160</sup> By comparing their double

Table 3.5  
 $C_{1s}$  Shifts Relative to Methane (eV)

	<u><math>\Delta E</math> experimental</u> <sup>17,103</sup>	<u><math>\Delta E</math> Koopmans' Theorem</u> <sup>159</sup>
$C_2H_6$	-0.2	0.2
$C_2H_4$	-0.1	0.9
$C_2H_2$	0.4	1.4
$C_2H_4O$	2.0	2.4
$CH_3OH$	1.9	2.0
$HCO_2H$	5.0	6.0
$CO_2$	6.8	8.3
$CO$	5.4	5.5
Cyclopropane	-0.2	0.4

zeta calculations on fluoromethanes with the single zeta calculations of Ha and Allen,<sup>161</sup> Brundle et al.<sup>162</sup> have concluded that for a reasonably quantitative description of binding energy shifts using Koopmans' theorem a basis set of double zeta quality, or better, is required. (The basis set should also be physically balanced). Also unless relaxation energies are constant, or vary in a regular manner, within the series of molecules studied a very good quantitative agreement

cannot be expected.

#### d) Hole State Calculations

The binding energy of a core electron in an atom or molecule M is the energy of the reaction



where \* indicates a vacancy in a core level. In the light of the previous discussion on correlation and relativistic corrections, the energy of this reaction may be obtained from Hartree-Fock calculations on the ground state molecule and on the core hole state of the ion. However, for the hole state calculations there is no absolute guarantee that variational upper bounds to the true total energies for the ions are obtained since the computed hole states are not necessarily orthogonal to all lower energy states of the same symmetry. This could introduce errors of both a systematic and/or non-systematic nature. However, the results reported in this work (in which the configurations were 'locked' to those of the ground state,<sup>163</sup> the eigen vectors of which were used for the initial trial molecular orbitals), and those of other workers indicate that such difficulties have not arisen.<sup>162</sup> Figure 3.2 shows the relationship between experimental, Koopmans' theorem and hole state binding energies.

The calculations of Bagus on the hole states of neon and argon show that while Koopmans' theorem yields inner shell ionization potentials

which are too large, hole state calculations give quite accurate ionization potentials.<sup>158</sup> The first direct calculations of this type on molecules were carried out by Schwartz<sup>164</sup> for first row hydrides. Contracted gaussian basis sets were used (10s, 5p /6s 3p) on the central atom and (5s/2s) on the hydrogen atoms.<sup>164</sup> The results are summarized in table 3.6.

Table 3.6

1s Electron Bindin Energies (eV)

<u>Molecule</u>	<u>-Orbital Energy</u> (Koopmans' theorem)	<u>Hole State</u>	<u>Experimental</u> <sup>17</sup>
BH <sub>3</sub>	207.3	197.5	-
CH <sub>4</sub>	304.9	291.0	290.7
NH <sub>3</sub>	422.8	405.7	405.6
H <sub>2</sub> O	559.4	539.4	539.7
HF	715.2	693.3	-
Ne	891.4	868.8	870.2

The hole state results are in very good agreement with the experimental values and appear to confirm Bagus' original contention that single configuration SCF wave functions can provide practical, but not rigorous, upper bounds to the energies of inner shell hole states.<sup>158</sup> The Koopmans' theorem binding energies overestimate the hole state (and experimental) binding energies by the electronic reorganisation energy

which occurs on photoionization. Gelius and Siegbahn<sup>165</sup> have tabulated the reorganization energies expected from different atomic shells by calculations on a series of atoms and hole states and comparing them with the Koopmans' theorem values.

In many molecules there are several equivalent sites for the core hole for example the two nitrogens of  $N_2$  or the six carbons of benzene. The problem therefore arises of whether the core hole is localized or delocalized over the equivalent sites. Snyder's model,<sup>166</sup> based on Slater's shielding constants, predicts that delocalization of the hole over  $t$  centres which would produce a hole charge of  $1/t$  and a relaxation energy per centre which is  $1/t^2$  that for the localized hole. This model also predicts a relaxation energy for ionization from a  $1s$  hole in a nitrogen atom to be 13.7eV (c.f. ref. 165 which predicts 16.6eV) and this would be reduced to 6.8 eV for  $N_2$  if the hole were delocalized. Shifts in core ionization potentials between  $N_2$  and  $NH_3$ , and  $CH_4$  and  $C_2H_2$  are both predicted to within about 1eV by Koopmans' theorem<sup>160</sup> and do not show the gross disagreement expected if delocalization over the two equivalent sites had occurred. The localization of hole states is also implicit in the thermodynamic equivalent cores method for predicting shifts where the hole bearing species of  $N_2$  is represented by  $NO^+$  and the electrons of  $NO^+$  are relaxed compared to  $N_2$ .<sup>50</sup> Further evidence for the localized hole state being correct has been obtained by Bagus and Schaefer<sup>167</sup> by direct calculations on  $O_2^+$  hole states when good agreement with experimental ionization potentials (i.e. within  $\sim 1.5$ eV) was

obtained only when the symmetry restriction that the molecular orbitals had g or u inversion symmetry had been removed. (The electronic structure of the valence electrons in the localized hole state then appeared to be that appropriate for  $\text{FO}^+$ ). The basis set used for these calculations was the large Slater basis set of 7s, 6p, 3d and 2f functions for each atom which had previously yielded very good agreement with the multiplet splittings and 1s ionization potentials in NO.<sup>168</sup> The observation of shake up satellites from the O1s peak of  $\text{CO}_2$ <sup>169</sup> and from the O1s and outer carbon  $\text{C}_{1s}$  peaks of  $\text{C}_3\text{O}_2$ <sup>26</sup> would not be expected for a delocalized hole since no change in the symmetry and the molecule would have occurred and the transitions are only monopole allowed.<sup>25</sup> This provides further evidence in favour of core hole states being localized.

Murrell and Ralston<sup>170</sup> have carried out a detailed study of hole localization in  $\text{He}_2^+$ . This system has the advantage that the 1s hole state is the ground state of the ion and therefore a rigorous variational bound on the energy can be obtained since the ionized state is orthogonal to all states of lower energy. By using suitable interatomic distances they extrapolated their results to  $\text{N}_2$  and their conclusions are that relaxation energy from a localized positive hole is appreciably more than that from two half charges even when core hole exchange is important. Thus for molecular orbital calculations on  $\text{N}_2^+$  and  $\text{NO}^+$  with inner shell holes the full relaxation energy would be allowed for in  $\text{NO}^+$  but not in  $\text{N}_2^+$ , and the stabilization for the electron contraction is underestimated for  $^*\text{N}_2^+$ . On the other hand applying

Koopmans' theorem to the neutral molecules no orbital contraction would be allowed for in either molecule and shifts in core electron binding energies are therefore reasonably well described.

#### e) Quantum Mechanical Potential at the Nucleus Model

The electron distribution within a molecule is continuous and it is therefore somewhat arbitrary to apportion electron densities to individual atoms. Therefore the population analyses on which the charge potential model is based are only a rough guide to the charge distribution. As an alternative to the charge potential model therefore Schwartz has developed the potential at the nucleus model<sup>171,172</sup> the main drawback of which, as far as the average chemist is concerned, is lack of conceptual simplicity. The model however still only considers ground state properties and does not take into account relaxation energies (the incorporation of relaxation effects within this model will be discussed later). The quantum mechanical generalization of the potential at nucleus  $n$  arising from the doubly occupied MO's  $\phi_j$  and the nuclei  $Z_m$  is given by

$$\phi = -2 \sum_j \langle \phi_j(1) | \frac{1}{r_{1n}} | \phi_j(1) \rangle + \sum_{m \neq n} \frac{Z_m}{R_{mn}}$$

The contribution of the 1s MO at the nucleus  $\phi_{1s}$  may be separated out leaving the external potential  $\phi_{ext}$ . Values of  $\phi_{1s}$ ,  $\phi_{ext}$  and Koopmans' theorem binding energies for a representative series of molecules are shown in table 3.7. The calculations were ab initio

Table 3.7

Calculated Potentials at the Nucleus and 1s Orbital Energies<sup>171</sup>(eV)

<u>C</u>	$-\bar{\phi}_{1s}$	$-\bar{\phi}_{ext}$	$-\epsilon_{1s}$
CH <sub>4</sub>	307.94	93.7517	304.8088
C <sub>2</sub> H <sub>2</sub>	307.97	92.4402	306.3680
HCN	307.93	91.2647	307.7807
CH <sub>3</sub> F	307.98	90.4456	307.9898
H <sub>2</sub> CO	307.97	89.1912	309.3639
CO	308.07	88.9872	310.4795
<u>O</u>			
H <sub>2</sub> O	415.6951	192.2463	559.2479
H <sub>2</sub> CO	415.7332	191.0082	560.6656
CO	415.7006	189.2477	562.6683
HO <sub>2</sub> F	415.7387	188.9538	562.8071

LCAO SCF MO calculations using a gaussian basis set of double zeta quality which had been found to give Koopmans' theorem shifts for the 1s core levels in accord with experimental values.  $\bar{\phi}_{1s}$  is essentially constant for a given atom and the non trivial changes in the potential at the nucleus are due to changes in  $\bar{\phi}_{ext}$ . The less negative the environment the greater is the 1s binding energy as

measured by Koopmans' theorem and table 3.8 shows binding energy shifts calculated by changes in the potential at the nucleus and Koopmans' theorem.

Table 3.8

Shifts in 1s Orbital Energies and External Potentials<sup>171</sup>(eV)

	<u><math>\Delta(-\epsilon_{1s})</math></u>	<u><math>\Delta\phi_{\text{ext}}</math></u>	<u><math>\Delta(-\epsilon_{1s})/\Delta(\phi_{\text{ext.}})</math></u>
<u>C</u>			
C <sub>2</sub> H <sub>2</sub>	1.56	1.31	1.19
HCN	3.00	2.49	1.20
CH <sub>3</sub> F	3.18	3.31	0.96
H <sub>2</sub> CO	4.55	4.56	1.00
CO	5.67	4.76	1.19
<u>O</u>			
H <sub>2</sub> CO	1.42	1.24	1.15
CO	3.43	3.00	1.14
FOH	3.56	3.29	1.08
<u>F</u>			
FOH	1.72	1.55	1.11
CH <sub>3</sub> F	-0.56	-0.59	0.95
<u>N</u>			
HCN	2.53	2.07	1.22

Shirley<sup>173</sup> has shown that the equivalent core method and the quantum mechanical potential at the nucleus approach represent the same level of approximation and depend essentially on residual integrals of the type

$$R = \sum_{\substack{\text{local} \\ i \neq N1s}} [2J(N1s, i) - K(N1s, i) - 2 \langle \phi_i(1) | \frac{1}{r_{1N}} | \phi_i(1) \rangle ]$$

(or Cls)

remaining constant. Where the summation is taken over local orbitals i.e. those localized molecular orbitals<sup>174</sup> which are connected to the atom under consideration. The potential at the nucleus model depends on R remaining essentially constant between molecules and the equivalent cores model requires this equality in the isoelectronic cations (the geometries of the ions having been constrained to the same as those of the molecules).

The potential at the nucleus approach may be extended to valence only treatments,<sup>175,176,177</sup> Since the core orbitals at other nuclei screen these nuclei as far as the potential at the given nucleus is concerned, the other core orbitals may be ignored in the potential calculation provided the nuclear charges are reduced appropriately. Thus only the potential at atom A due to the valence electrons need be considered.

$$\phi_{\text{val}} = -2 \sum_{i \neq \text{core}} \langle \phi_i | \frac{1}{r_A} | \phi_i \rangle + \sum_{B \neq A} \frac{Z_B^*}{R_{AB}}$$

where  $\phi_i$  are doubly occupied molecular orbitals,  $r_A$  is an electronic position from A and  $Z_B^*$  are the effective nuclear charges. It was

found, using CNDO calculations, that  $\Delta BE \neq \Delta \bar{\phi}_{val}$  although a linear correlation was obtained

$$\Delta BE = a \Delta \bar{\phi} + b$$

where  $a$  and  $b$  are parameters found from a least squares fit to the data. There is little improvement compared with the charge potential model. However, further improvement can be obtained by letting both the local- and other-atom contributions be adjustable in the form

$$\Delta BE = aq_A + bV + c$$

Davis and Shirley<sup>178</sup> have extended the potential at the nucleus model to allow for relaxation energies. The binding energy of a core electron may be written as<sup>178</sup>

$$-E_B(1s) \approx \epsilon(1s) + \frac{1}{2} \langle 1s | V_R | 1s \rangle \quad (1)$$

where  $V_R$  is a relaxation potential energy arising from the difference between the Hartree-Fock potential  $V_k$  of the passive orbitals in the final  $1s$  hole state and the initial state and this may be used to derive the relationship

$$-E_B(1s) = \frac{1}{2} [\epsilon(1s) + \epsilon(1s)^*] \quad (2)$$

where  $\epsilon(1s)^*$  is the orbital energy of a  $1s$  electron in the hole state.

Writing each orbital energy as the sum of the interaction energy of the 1s electron with its own nucleus plus a potential energy terms that includes interactions of the 1s electron with other electrons and other nuclei gives

$$\epsilon(1s) = \langle 1s | h | 1s \rangle + \langle 1s | V | 1s \rangle \quad (3)$$

Combining equations (2) and (3), taking differences (as between two compounds) and noting that the first terms of equation (3) are negligibly small<sup>171</sup> (cf. table 3.7) gives

$$\Delta E_B(1s) \approx -\frac{1}{2} \Delta \langle 1s | V + V^* | 1s \rangle \quad (4)$$

To a good approximation the right hand side of equation (4) can be replaced by the difference in the potential energy at the host nucleus,  $\phi$ , between one molecule and another. Thus for shifts in carbon 1s binding energies

$$\Delta E_B(C_{1s}) = \frac{e}{2} \Delta[\phi(C) + \phi(C^*)]$$

In CNDO calculations there is no way to calculate  $\phi(C^*)$  directly. The equivalent core approximation is therefore invoked to allow for the relaxation of electrons due to the increased core charge

$$\Delta E_B(C_{1s}) = \Delta \frac{e}{2} [\phi(C) + \phi(N)]$$

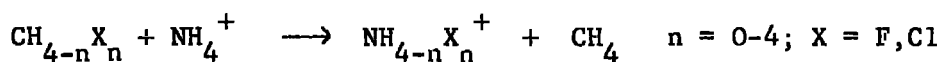
Results for carbon atoms show good agreement both with and without the relaxation correction but in the case of nitrogen compounds the inclusion of relaxation effects greatly improved the calculated shifts.

## 2) EQUIVALENT CORES SHIFTS FROM CNDO CALCULATIONS

The use of CNDO calculations for the calculation of shifts in core electron binding energies by the equivalent cores approach could represent an alternative to the charge potential model (Chapter IV) for the interpretation of shifts using semi-empirical SCF MO calculations which do not explicitly consider core electrons. The advantage of such calculations is that they are computationally relatively cheap and it is possible to investigate quite complex molecules for which ab initio treatments are not yet feasible.

Calculations were performed with the standard CNDO/2 parameterization to calculate energies for reactions of the type.

119



The energies for the nitrogen-containing cations were calculated both with geometries the same as the isoelectronic carbon species and also with geometries appropriate to the cations themselves. Optimum bond distances were obtained from energy minimizations for  $\text{CH}_4$ ,  $\text{NH}_4^+$ ,  $\text{CF}_4$ ,  $\text{NF}_4^+$ ,  $\text{CCl}_4$  and  $\text{NCl}_4^+$ . The energies calculated for these species are listed in table 3.9 and the calculated binding energy shifts together with the experimental gas phase values<sup>179,180</sup> of shifts relative to methane are shown in table 3.10. The trends within a

Table 3.9Total Energies from CNDO/2 Calculations (eV)

<u>n</u>	CH <sub>4-n</sub> F <sub>n</sub>	(1)	(2)
		NH <sub>4-n</sub> F <sub>n</sub> <sup>+</sup>	NH <sub>4-n</sub> F <sub>n</sub> <sup>+</sup>
0	- 275.263	- 390.721	- 390.953
1	- 1009.501	- 1125.622	- 1126.431
2	- 1744.018	- 1860.695	- 1862.126
3	- 2478.805	- 2595.936	- 2598.045
4	- 3213.891	- 3331.349	- 3334.201
	CH <sub>4-n</sub> Cl	NH <sub>4-n</sub> Cl <sup>+</sup>	NH <sub>4-n</sub> Cl <sup>+</sup>
1	- 694.580	- 810.833	- 810.838
2	- 1114.526	- 1231.603	- 1231.605
3	- 1535.130	- 1653.042	- 1653.260
4	- 1956.403	- 2075.159	- 2075.806

(1) Nuclei with some coordinates as corresponding carbon compound.

(2) Nuclei relaxed.

Table 3.10Equivalent Cores Results from CNDO/2 Calculations (eV)

<u>Compound</u>	<u>Heat of Reaction</u>		<u>Experimental Shift</u> <sup>179,180</sup>
	(1)	(2)	
CH <sub>4</sub>	0	0	0
CH <sub>3</sub> F	0.66	1.24	2.8
CH <sub>2</sub> F <sub>2</sub>	1.22	2.42	5.6
CHF <sub>3</sub>	1.68	3.55	8.3
CF <sub>4</sub>	2.00	4.62	11.0
CH <sub>3</sub> Cl	0.79	0.57	1.6
CH <sub>2</sub> Cl <sub>2</sub>	1.62	1.39	3.1
CHCl <sub>3</sub>	2.46	2.43	4.3
CCl <sub>4</sub>	3.30	3.71	5.5

- (1) Taking nuclei as fixed  
 (2) Assuming relaxation of nuclei

given series of molecules are well reproduced for both geometries of the nitrogen cation. However separate correlations are obtained for the fluoro- and chloro-methanes and the calculated shifts greatly underestimate the experimental shifts. These results indicate that equivalent core shifts calculated by the CNDO/2 method (without specific parameterization for reproducing thermodynamic data) should be viewed with caution even for a qualitative prediction of shifts. The use of semi-empirical calculations of the MINDO/1<sup>181,182</sup> type extends the correlation between calculated equivalent core shifts and experimental

shifts to a larger number of molecules of varying structure but, with the parameterization used, the experimental shifts are still greatly underestimated.<sup>150</sup>

### 3) A COMPARISON OF EQUIVALENT CORES, KOOPMANS' THEOREM AND CHARGE POTENTIAL SHIFTS FROM MINIMAL SLATER BASIS SET CALCULATIONS.

In the light of the previous discussion, and the partial success of the equivalent cores method using semi-empirical calculations, it is of interest to employ minimal Slater basis set LCAO MO SCF calculations to predict ESCA shifts by the equivalent cores method, and to compare these with shifts obtained using Koopmans' theorem and the charge potential model. The molecules chosen for this comparison were:-

$C_2H_2$ , HCN, FCN, CO,  $CO_2$ ,  $C_3O_2$ ,  $CS_2$ , OCS,  $N_2$   
and  $N_2O$ .

These molecules were chosen because there are several core levels to investigate, the relaxation energies may well be different for the variety of bonding situations and also for most of the molecules experimental gas phase data are available thus allowing a direct comparison of theory and experiment.

The calculations were performed using the ALCHEMY molecular orbital program for linear molecules. The basis sets used were minimal Slater sets employing single zeta best atoms exponents<sup>117</sup> (Appendix I) but with the inclusion of 3d orbitals ( $z = 1.2$ ) for the sulphur atoms and an exponent of 1.2 for hydrogen 1s orbitals. The

geometries of the molecules<sup>183</sup> (Appendix II) and the isoelectronic cations were taken to be the same thus eliminating energy changes due to nuclear relaxation. The total energies of the molecules and isoelectronic cations are listed in table 3.11 and the other calculated data are listed in table 3.12, together with the gas phase experimental binding energies and shifts for the C<sub>1s</sub>, N<sub>1s</sub> and O<sub>1s</sub> levels where known.<sup>17,26,103,160,184</sup> The agreement between the calculated equivalent core shifts and the experimental shifts is good for both inter and intra molecular shifts. A least squares fit to the data gives the relationship

$$\Delta E_{\text{exp.}} = -0.02 + 1.17 \Delta E_{\text{eq.core}} \\ (\pm 0.06)$$

with a correlation coefficient of 0.97. This is quite close to the ideal correlation of

$$\Delta E_{\text{exp}} = 0.00 + 1.00 \Delta E_{\text{eq.core}}$$

However a least squares fit to the Koopmans' theorem results obtained from the same calculations gives the relationship

$$\Delta E_{\text{exp}} = -0.03 + 0.84 \Delta E_{\text{Koopmans}} \\ (\pm 0.14)$$

Table 3.11

Total Energies of Molecules and Ions from Minimal Slater Basis Set Calculations (eV)

CO <sub>2</sub>	-5084.102	NO <sub>2</sub> <sup>+</sup>	-5521.216			OCF <sup>+</sup>	-5738.422		
CO	-3056.471	NO <sup>+</sup>	-3494.871			CF <sup>+</sup>	-3709.051		
C <sub>3</sub> O <sub>2</sub>	-7136.957	ONCCO <sup>+</sup>	-7575.628			OCCCF <sup>+</sup>	-7792.235		
		OCNCO <sup>+</sup>	-7579.153						
C <sub>2</sub> H <sub>2</sub>	-2084.247	HNCH <sup>+</sup>	-2526.453						
HCN	-2518.969	HNN <sup>+</sup>	-2959.744	HCO <sup>+</sup>	-3062.201				
FCN	-5195.622	FNN <sup>+</sup>	-5634.885	FCO <sup>+</sup>	-5739.263				
N <sub>2</sub>	-2953.978			NO <sup>+</sup>	-3494.666				
NNO	-4979.073			ONO <sup>+</sup>	-5521.084	NNF <sup>+</sup>	-5633.964		
				NOO <sup>+</sup>	-5517.453				
OCS	-13849.905	ONS <sup>+</sup>	-14288.440			FCS <sup>+</sup>	-14504.655	OCCl <sup>+</sup>	-15524.602
CS <sub>2</sub>	-22614.567	NS <sub>2</sub> <sup>+</sup>	-23055.045					SCCl <sup>+</sup>	-24289.822

Table 3.12

Calculated and Experimental Data for Carbon, Nitrogen and Oxygen (eV)

Compound	Equivalent core shift	orbital energy	Koopmans' theorem Shift	Experimental <sup>+</sup> Binding Energy(BE) shift	atomic charge $q_i$	Madelung Potential $\sum_{i \neq j} \frac{q_i}{r_{ij}}$	BE - $\sum \frac{q_i}{r_{ij}}$
<u>Carbon</u>							
HCCH	0	-309.56	0	291.3	0	1.88	289.4
HCN	1.43	-310.61	1.05	293.3	2.0	2.32	291.0
FCN	2.94	-313.29	3.73	-	-	-1.88	-
CO	3.81	-311.39	1.83	295.9	4.6	-2.22	298.1
CO <sub>2</sub>	5.09	-315.75	6.19	297.5	6.2	-5.37	302.9
OC <sub>2</sub> CO	3.54	-314.85	5.29	294.9	3.6	-4.00	298.9
OC <sub>2</sub> CO	0.01	-309.04	0.52	291.5	0.2	4.94	286.6
CS <sub>2</sub>	1.73	-312.82	3.26	293.1	1.8	-0.82	293.9
OCS	3.67	-314.39	4.83	295.2	3.9	-2.87	298.1
<u>Nitrogen</u>							
N <sub>2</sub>	0	-430.02	0	409.9	0	0	409.9
<u>NNO</u>	-1.32	-429.05	-0.97	408.5	-1.4	1.30	407.2
<u>NNO</u>	2.31	-434.93	4.91	412.5	2.6	-2.10	414.6
HCN	-2.54	-427.98	-2.04	406.1	-3.8	-0.34	406.4
FCN	-2.95	-421.42	-2.60	-	-	1.81	-

Table 3.12 - continued

Calculated and Experimental Data for Carbon, Nitrogen and Oxygen (eV)

Compound	Equivalent core shift	orbital energy	Koopmans' theorem shift	Experimental <sup>+</sup> Binding energy (BE)	shift	Atomic Charge $q_i$	Madelung Potential $\sum_{i \neq j} \frac{q_i}{r_{ij}}$	BE - $\sum \frac{q_i}{r_{ij}}$
<u>Oxygen</u>								
CO <sub>2</sub>	0	-563.94	0	540.8	0	-0.2161	4.02	538.1
CO	1.74	-566.30	2.36	542.1	1.3	-0.1740	2.22	538.6
OCS	-0.43	-565.60	1.66	-	-	-0.1469	2.63	-
NNO	-0.57	-562.92	-1.01	541.2	0.4	-0.1423	1.90	539.3
OCCCO	-0.96	-565.31	-1.37	539.7	-1.1	-0.1357	2.43	537.3

+ Refs. 17, 26, 103, 160, 184.

with a correlation coefficient of 0.75. Thus not only do the Koopmans' theorem shifts overestimate the magnitude of the experimental shifts, they also show a poorer correlation (i.e. more scatter) than the equivalent core calculations. Any non regular variation of reorganization energies between molecules will increase the scatter in this correlation between calculated and experimental shifts. The Koopmans' theorem binding energies overestimate the experimental binding energies and this illustrates mainly the neglect of electronic reorganization effects.

The Koopmans' theorem binding energies and shifts for the sulphur core levels are shown in table 3.13. For  $\text{CS}_2$  and  $\text{COS}$  there are predicted to be only slight differences in shifts between the corresponding 1s, 2s and 2p levels but the shifts themselves are also small. The equivalent cores calculations also predict a small shift between the sulphur core levels (the sulphur core levels in  $\text{OCS}$  being 0.56eV more tightly bound than in  $\text{CS}_2$ ) but this shift is in the opposite direction from that predicted by Koopmans' theorem.

Table 3.13

Orbital Energies and Shifts for Sulphur Core Levels (eV)

	<u>Orbital Energies</u>		<u>Shift</u> <sup>+</sup>
	$\text{CS}_2$	$\text{OCS}$	
S <sub>1s</sub>	-2502.54	-2501.71	-0.83
S <sub>2s</sub>	-240.49	-239.76	-0.73
S <sub>2p</sub>	-177.13	-176.46	-0.72

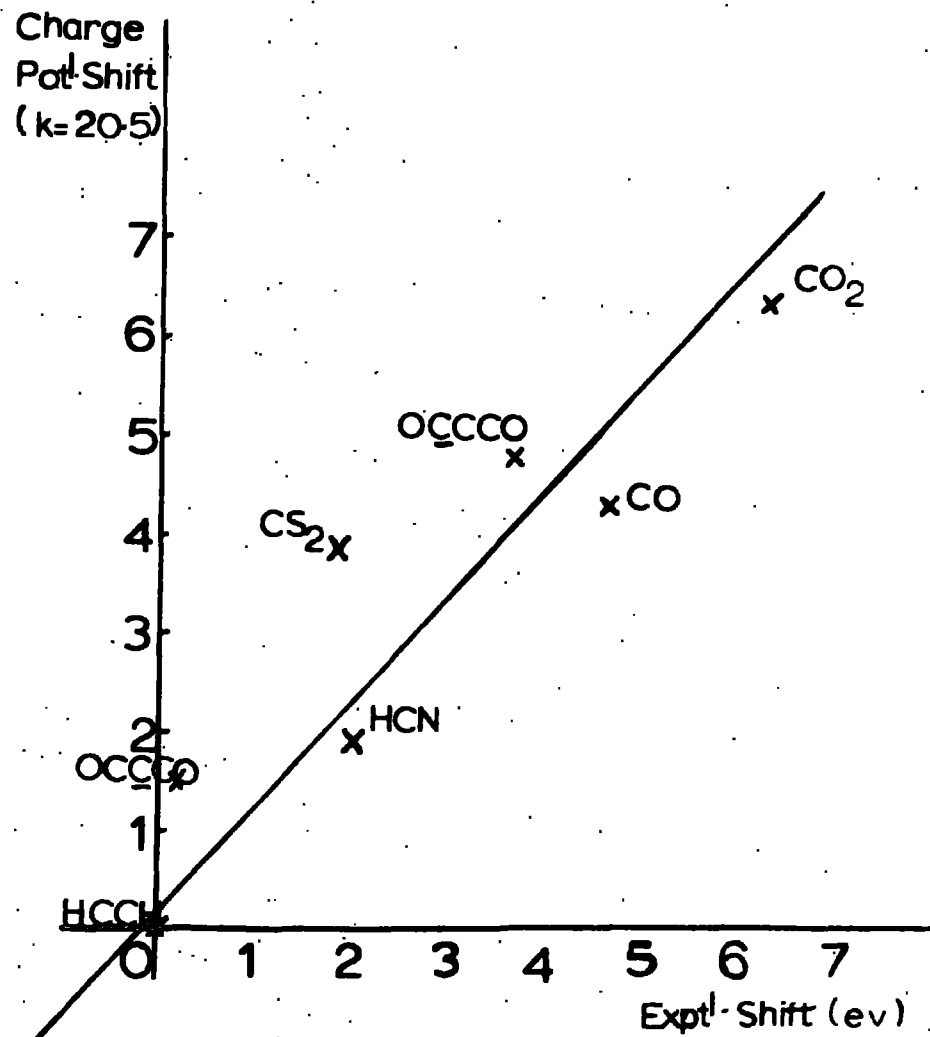
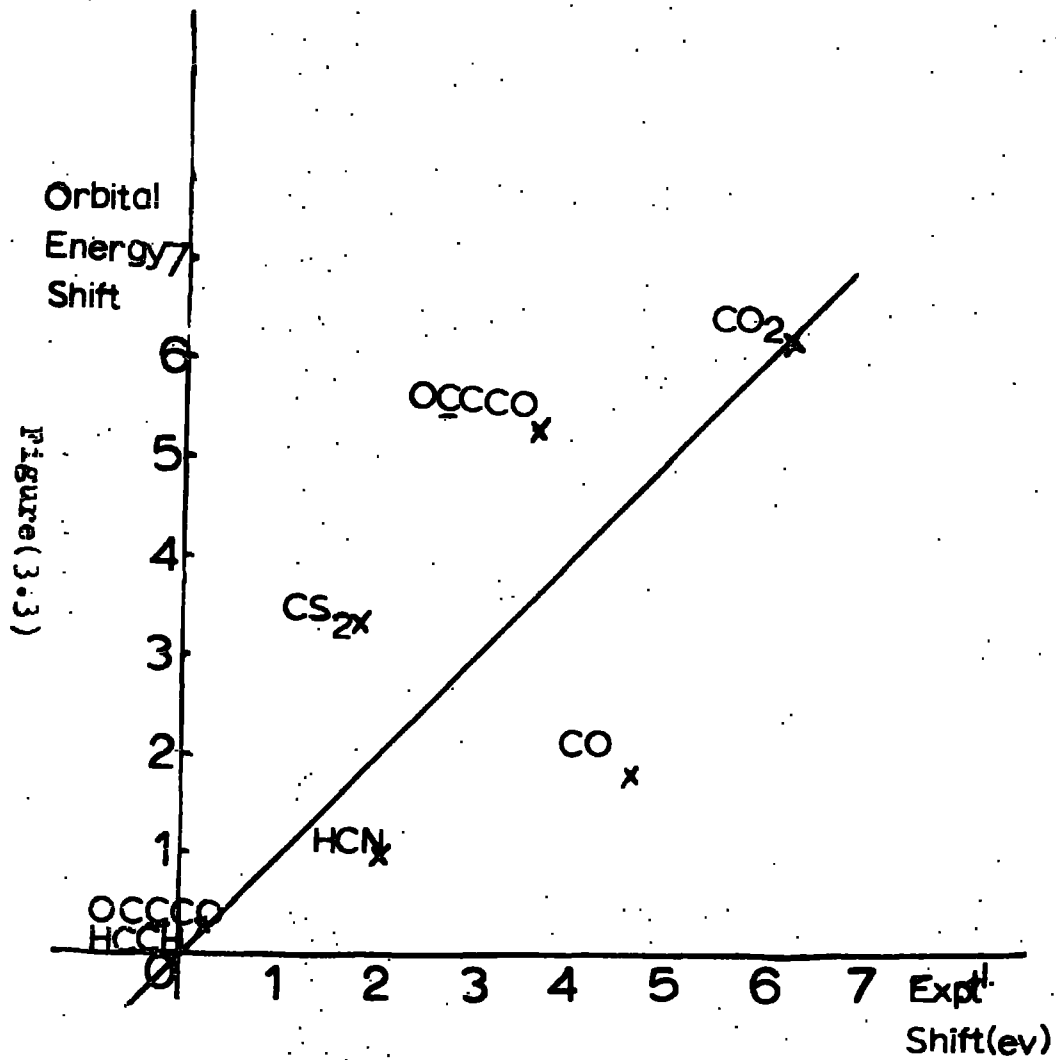
+ Shift of  $\text{OCS}$  relative to  $\text{CS}_2$

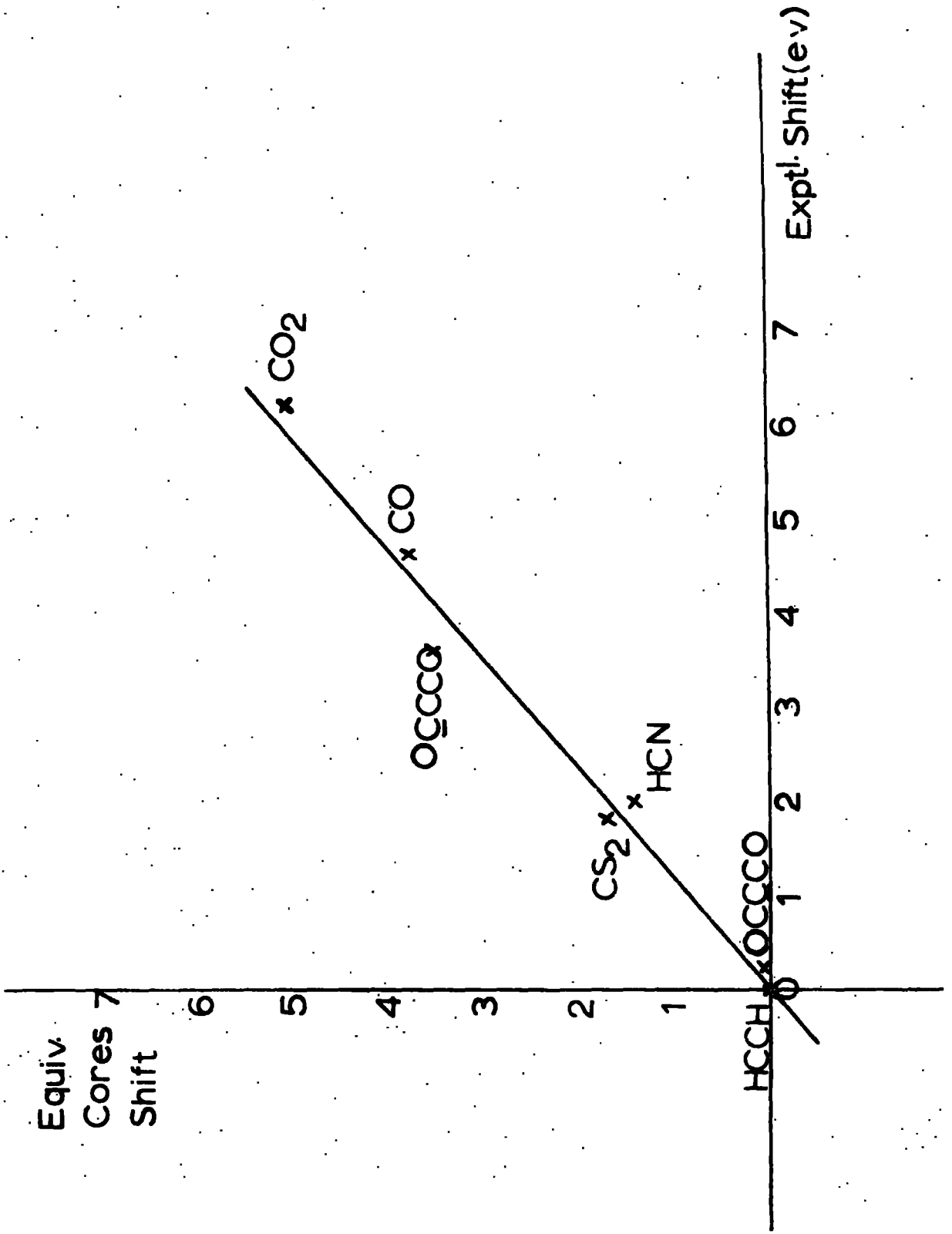
This provides a stringent test of the predictions obtained from the two methods. Intuitively, the equivalent core shift seems more reasonable since the greater electronegativity of oxygen compared with that of sulphur would be expected to increase the binding energies of the remaining atoms in the molecule. In fact recent experimental data<sup>184</sup> show that the  $S_{2p}$  electrons in OCS are more tightly bound than those in  $CS_2$  by 0.8eV in good agreement with the equivalent cores calculations.

The other most notable success of the equivalent cores model as compared with Koopmans' theorem is the prediction of the shift between the carbon atoms in OCCCO where the experimental shift is 3.4eV and the calculated equivalent core shift is 3.52eV. Koopmans' theorem estimates of this shift are 5.93 (Sabin and Kim<sup>185</sup>), 5.81 (this work) and 4.95 (Gelius et al<sup>26</sup>), this calculation being of double zeta quality.

#### Charge potential results from minimal Slater basis set calculations

A least squares analysis of the data for the  $C_{1s}$  binding energies gives the values  $E_c^0 = 293.6$  and  $k_c = 20.5 (\pm 1.5)$ . However, not enough data are available to obtain statistically significant  $E^0$  and  $k$  values for nitrogen and oxygen. The  $C_{1s}$  charge potential and Koopmans' theorem shifts are plotted against the experimental shifts (relative to acetylene) in figure 3.3. There is a large scatter around the ideal correlation line in both cases (c.f. the equivalent cores shifts figure 3.4).





Figure(3.4)

While some of this scatter may be attributable to the use of a minimal basis set, it is significant that the qualitative disagreements with the experimental results are similar in each case, thus illustrating the close relationship between the charge potential model and Koopmans' theorem. For example, both the charge potential model and Koopmans' theorem underestimate the experimental  $C_{1s}$  binding energy shifts in HCN and CO but overestimate it in the case of  $CS_2$ .

#### 4) A COMPARISON OF KOOPMANS' THEOREM, EQUIVALENT CORES CALCULATIONS AND HOLE STATE CALCULATIONS AS A FUNCTION OF BASIS SET

From the results presented in the previous section it is clear that even minimal Slater basis set calculations provide a good description of shifts in core electron binding energies using the equivalent cores model. Also these predictions are better than those obtained from Koopmans' theorem for a wide variety of molecules of differing electronic structures. This illustrates that the equivalent cores calculations do take some account of relaxation energy differences which occur on core electron ionization. It is therefore of interest to perform a detailed comparison of the shifts predicted by Koopmans' theorem, hole state calculations and equivalent cores calculations and to determine the sensitivity to basis set for each of the methods. No such detailed comparisons has previously been performed. The molecules chosen for this study were closely related - the fluoromethanes and mono and di chloromethane. These were chosen because they

have similar valence electron structures and the relaxation energies may therefore be expected to be similar or follow a regular trend. The hole state and Koopmans' theorem calculations allow a direct estimate of reorganization energies and the theoretical investigation of the equivalent cores model allows an examination of both the weak and strong forms of this model.

Ab initio LCAO MO SCF calculations on the molecules  $\text{CH}_{4-n}\text{F}_n$  ( $n = 0-4$ ),  $\text{CH}_3\text{Cl}$  and  $\text{CH}_2\text{Cl}_2$  together with the isoelectronic series  $\text{NH}_{4-n}\text{F}_n^+$ ,  $\text{NH}_3\text{Cl}^+$  and  $\text{NH}_2\text{Cl}_2^+$  were carried out using a better than double zeta basis set of optimised gaussian functions<sup>130</sup> (Appendix I). These consisted of 4s contracted to 3s for hydrogen (scale factor 1.2) and 9s 5p contracted to 5s 3p for carbon nitrogen fluorine. A 12s 9p<sup>186</sup> (Appendix I) basis set was used for chlorine and this was contracted to 7s, 5p according to the principles outlined by Dunning<sup>130</sup> (Greatest variational freedom is given (a) to those members of each group which are most strongly concentrated in the internuclear regions and (b) to those functions which contribute strongly to more than one orbital). For ease of reference this basis set will be referred to later as 'the large basis set'. These calculations, except for  $\text{CH}_2\text{Cl}_2$  and  $\text{NH}_2\text{Cl}_2^+$  were performed using the IBMOL V LCAO SCF MO program.<sup>187</sup> The calculations for  $\text{CH}_2\text{Cl}_2$  and  $\text{NH}_2\text{Cl}_2^+$  and the following calculations were performed using the ATMOL 2 group of programs.<sup>188</sup> Calculations on the series  $\text{CH}_{4-n}\text{F}_n$ ,  $\text{NH}_{4-n}\text{F}_n^+$  and  $^*\text{CH}_{4-n}\text{F}_n$  (where \* indicates a vacancy in the  $\text{C}_{1s}$  shell) were carried out using the following basis sets:

i) The core orbitals were represented by four contracted gaussians and the valence orbitals, including  $H_{1s}$  (scale factor 1.2) were represented by four gaussian functions contracted to groups of 3 and 1 thus allowing a flexible description of the valence orbitals (STO 4.31G basis set).

ii) Each orbital was represented by three contracted gaussian functions with a 1.2 scale factor for the  $H_{1s}$  (STO 3G basis set).

The exponents and coefficients used for these two basis sets were those obtained by Stewart<sup>189</sup> from a least squares fit of gaussian functions to Clementi's STO SCF atomic orbitals.<sup>127</sup>

a) Koopmans' theorem

Koopmans' theorem predictions of shifts are expected to be basis set dependent and even for a large basis set at the Hartree-Fock limit electronic relaxation is neglected. Therefore, unless the electronic relaxation energy is constant or varies in a regular manner for a particular series of molecules Koopmans' theorem cannot be expected to give a quantitative description of shifts in core electron binding energies.

The Koopmans' theorem prediction of the binding energies and shifts are compared with the experimental values in table 3.14. The accuracy with which the  $C_{1s}$  binding energy shifts are predicted, as would be expected, increases with increased flexibility of the basis set (Figure 3.5) but even the large basis set overestimates the shift between  $CH_4$  and  $CF_4$  by approximately 22%.

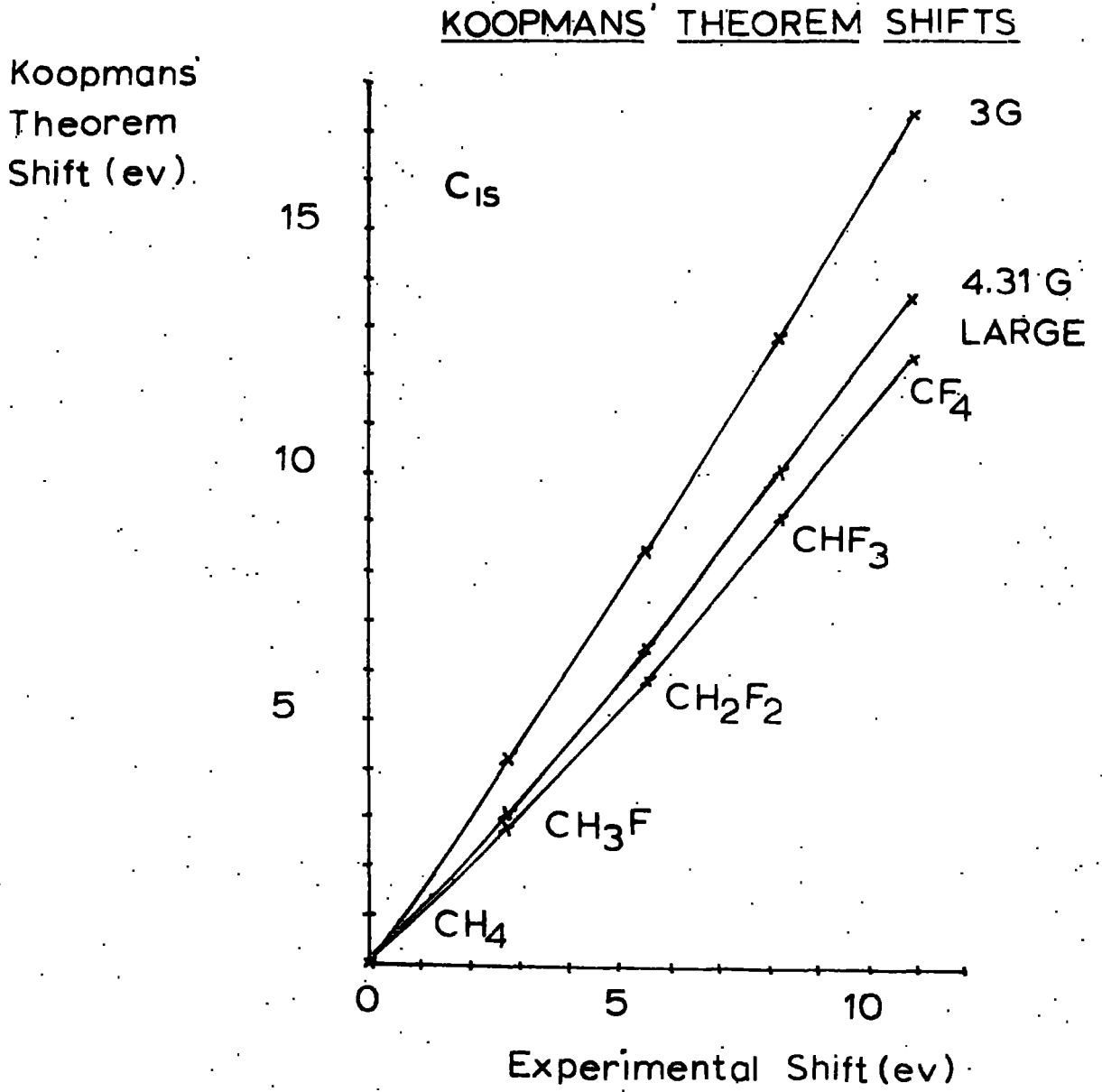
Table 3.14

Koopmans' Theorem Predictions for the HalomethanesC<sub>1s</sub> Shifts and Binding Energies (eV)

Molecule	<u>3G</u>		<u>4.31G</u>		<u>Large Basis</u>		<u>Experimental</u>	
	BE	Shift	BE	Shift	BE	Shift	BE	Shift
CH <sub>4</sub>	305.43	0.0	304.35	0.0	304.95	0.0	290.7	0.0
CH <sub>3</sub> F	309.64	4.21	307.43	3.08	307.75	2.80	293.5	2.8
CH <sub>2</sub> F <sub>2</sub>	313.90	8.47	310.82	6.47	310.81	5.86	296.3	5.6
CHF <sub>3</sub>	318.25	12.81	314.42	10.05	314.08	9.13	299.0	8.3
CF <sub>4</sub>	322.69	17.26	317.96	13.61	317.38	12.43	301.7	11.0
CH <sub>3</sub> Cl	-	-	-	-	307.49	2.54	292.3	1.6
CH <sub>2</sub> Cl <sub>2</sub>	-	-	-	-	309.77	4.82	293.9	3.1

F<sub>1s</sub> Shifts and Binding Energies

CH <sub>3</sub> F	704.50	0.0	713.24	0.0	714.90	0.0	692.4
CH <sub>2</sub> F <sub>2</sub>	705.70	1.20	714.41	1.17	716.13	1.23	693.1
CHF <sub>3</sub>	706.91	2.41	715.60	2.36	717.31	2.41	694.1
CF <sub>4</sub>	708.17	3.67	716.76	3.52	718.46	3.56	695.0



Figure(3.5)

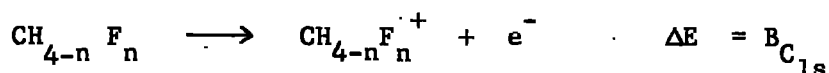
Gelius and Siegbahn<sup>38</sup> have divided the molecular electronic reorganization energy from an atom A,  $E_A^{\text{reorg}}(\text{mol})$ , into two components

$$E_A^{\text{reorg}}(\text{mol}) = E_A^{\text{contr}} + E_A^{\text{flow}}$$

where the first term is the reorganization energy gained from the contraction of the local charge distribution around nucleus A and is essentially atomic. The second term represents the redistribution of electron density in the rest of the molecule. Using the differences between the calculated binding energies from the negative of the Hartree-Fock orbital energies (Koopmans' theorem), and the differences between the total energies of the atom and ion Gelius and Siegbahn estimated the atomic reorganization energy for 1s ionization of carbon to be 13.7eV. This value accounts for most of the difference between the experimental and Koopmans' theorem values in the cases of the 4.31G and large basis set calculations while the differences for the 3G calculations are slightly larger. The estimate of a reorganization energy of 22.0 (or 22.1eV employing a relativistic calculation)<sup>38</sup> for  $F_{1s}$  ionization accounts for most of the observed difference between experimental binding energies and the large basis set calculations but overestimates the difference in the cases of the 4.31G and 3G calculations. This may be a result of the poorer description of the system by the smaller basis sets. However, the fact that with an improved basis set the shifts are quite well described by Koopmans' theorem suggests that reorganization energy differences contribute to only a minor extent for these closely related molecules (c.f. Chapter III.4d).

### b) Hole State Calculations

Hole state calculations, unlike Koopmans' theorem calculations, take electronic reorganization into account. Where there is more than one equivalent centre in a molecule the question of localized versus non localized hole states presents computational problems. The available evidence is compelling in favour of the description of the core hole state in such systems being localized on the time scale of the ESCA experiment (c.f. Chapter III.1.d). However, the theoretical treatment of such states is more difficult than for the delocalized hole states. The hole state calculations on the halomethanes have therefore been restricted to the carbon atoms for which there are unique hole states. The carbon 1s binding energies were calculated, using the STO 3G and STO 4.31G basis sets, for the series  $\text{CH}_{4-n}\text{F}_n$   $n = 0-4$  by taking the energy differences between the neutral molecule and the core ionized species.

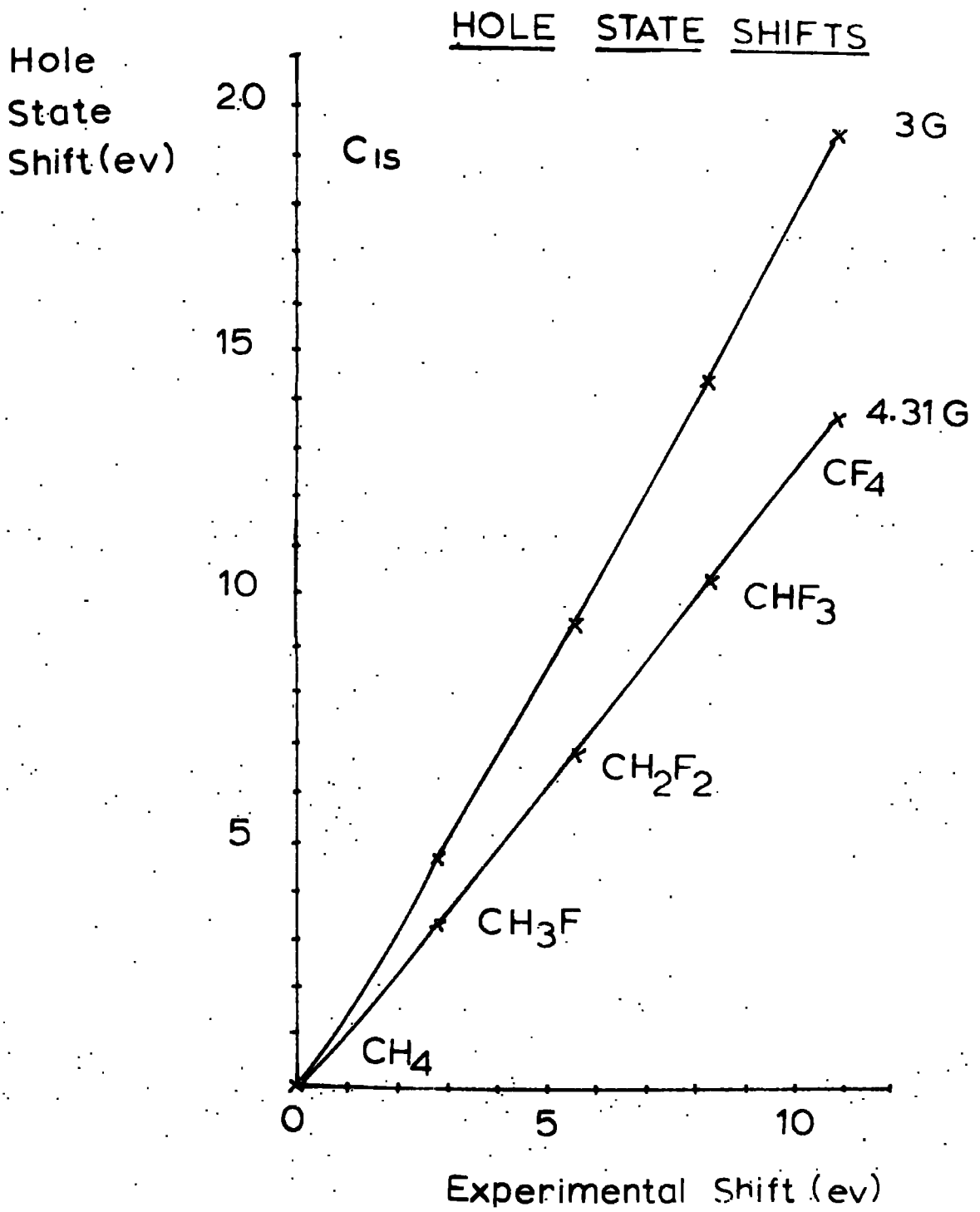


The total energies for the species involved are shown in table 3.15 and the calculated binding energies and shifts are listed in table 3.16. The binding energies are in better agreement with the experimental values than were the Koopmans' theorem values. However, for the 3G and 4.31G calculations the predictions of shifts are not as good as the Koopmans theorem predictions, but for double zeta calculations on the ground states and core hole states of  $\text{CH}_{4-n}\text{F}_n$  ( $n = 0-3$ ) Brundle, Robin and Basch<sup>162</sup> have shown that the shifts are predicted with about

Table 3.15

Total Energies (eV)

n	CH <sub>4-n</sub> F <sub>n</sub>			*CH <sub>4-n</sub> F <sub>n</sub> <sup>+</sup>		NH <sub>4-n</sub> F <sub>n</sub> <sup>+</sup>		
	3G.	431G.	Large	3G.	4.31G.	3G.	4.31G.	Large
0	-1078.1863	-1089.0380	-1093.4785	-780.6724	-796.1041	-1514.4967	-1531.2662	-1537.7923
1	-3720.4685	-3776.3545	-3783.1361	-3418.3047	-3470.1125	-4153.8329	-4205.5299	-4224.5316
2	-6363.0474	-6443.9813	-6473.2378	-6056.0838	-6144.2386	-6739.0207	-6879.8908	-6911.4577
3	-9005.7991	-9121.6151	-9163.4585	-8693.8839	-8818.3430	-9431.9449	-9554.1786	-9598.3631
4	-11648.5597	-11798.8994	-11852.3984	-11331.5514	-11492.2842	-12070.5013	-12228.2038	-12283.9676
		CH <sub>3</sub> Cl	-13580.5603				NH <sub>3</sub> Cl <sup>+</sup>	-14023.0044
		CH <sub>2</sub> Cl <sub>2</sub>	-26067.4141				NH <sub>2</sub> Cl <sub>2</sub> <sup>+</sup>	-26508.2375



Figure(3.6)

equal accuracy by both methods. The hole state shifts show a large dependency on the basis set used (Figure 3.6).

Table 3.16  
Hole State Calculations

	<u>C<sub>1s</sub> Binding Energies and Shifts<sup>+</sup></u>					
	<u>3G</u>		<u>4.31G</u>		<u>Experimental<sup>180</sup></u>	
	<u>BE</u>	<u>Shift</u>	<u>BE</u>	<u>Shift</u>	<u>BE</u>	<u>Shift</u>
CH <sub>4</sub>	297.51	0.0	292.93	0.0	290.7	0.0
CH <sub>3</sub> F	302.16	4.65	296.24	3.31	293.5	2.8
CH <sub>2</sub> F <sub>2</sub>	306.96	9.45	299.74	6.81	296.3	5.6
CH <sub>3</sub> F	311.92	14.41	303.27	10.34	299.0	8.3
CF <sub>4</sub>	317.01	19.05	306.62	13.69	301.7	11.0

+ relative to CH<sub>4</sub>

### c) Equivalent Cores Calculations

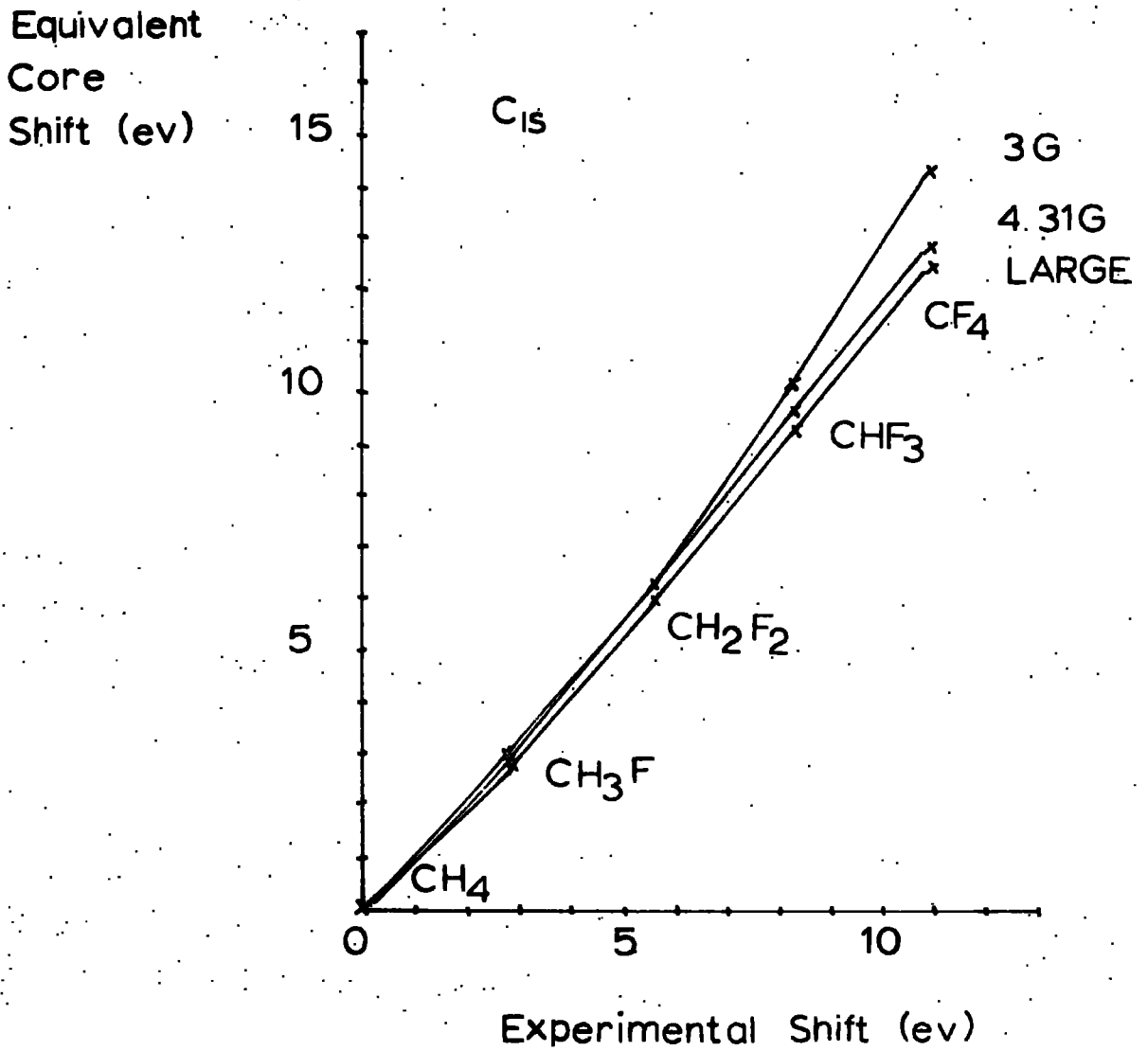
The carbon 1s binding energies in CH<sub>4-n</sub>F<sub>n</sub> (n = 0-4) were calculated using the STO-3G, STO-4.31G and large basis sets and for CH<sub>3</sub>Cl and CH<sub>2</sub>Cl<sub>2</sub> using the large basis set. The total energies for these species and their isoelectronic nitrogen cations are listed in table 3.15. The results are shown in table 3.17 and show an increase

Table 3.17Equivalent Cores Shifts<sup>+</sup> (eV)

	<u>3G</u>	<u>4.31G</u>	<u>Large</u>	<u>Experimental</u> <sup>179,180</sup>
CH <sub>4</sub>	0.0	0.0	0.0	0.0
CH <sub>3</sub> F	2.95	3.05	2.82	2.8
CH <sub>2</sub> F <sub>2</sub>	6.34	6.31	5.99	5.6
CHF <sub>3</sub>	10.16	9.66	9.31	8.3
CF <sub>4</sub>	14.37	12.92	12.64	11.0
CH <sub>3</sub> Cl	-	-	1.77	1.6
CH <sub>2</sub> Cl <sub>2</sub>	-	-	3.39	3.1

+ relative to CH<sub>4</sub>

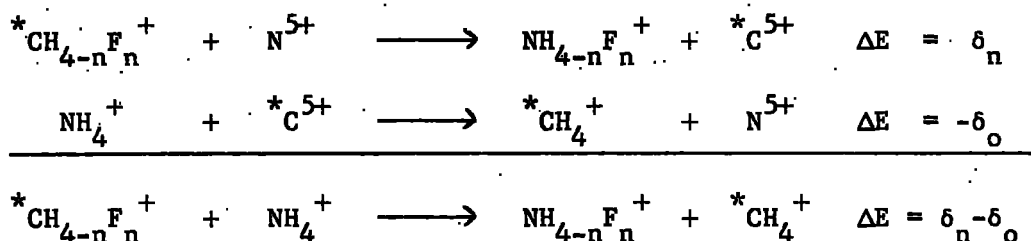
in accuracy with the increase in flexibility of the basis set used. There is, however, a much smaller dependence on the basis set used (figure 3.7) than is the case for either the Koopmans' theorem or hole state calculations and even the STO-3G. basis set gives a good prediction of the shifts. There is still a tendency to overestimate the shifts and for the large basis set calculations the equivalent cores shifts are closely similar to the Koopmans' theorem shifts. The equivalent core predictions for the C<sub>1s</sub> shifts in CH<sub>3</sub>Cl and CH<sub>2</sub>Cl<sub>2</sub> (table 3.17) are in good agreement with the experimental values: this is in contrast to the Koopmans' theorem predictions which are poorer than the corresponding large basis set Koopmans' theorem

EQUIVALENT CORE SHIFTS

Figure(3.7)

predictions for the  $C_{1s}$  shifts in the fluoromethanes (table 3.14). This provides further evidence for the comparative lack of sensitivity to the basis set used for the equivalent cores method.

The accuracy with which the equivalent cores method predicts shifts depends on the constancy of the energy of core exchange  $\delta$ . An expression for the constancy of  $\delta$  may be obtained by considering the following processes



where  $\delta_n - \delta_o$  is the difference in the energies of core exchange. Using the total energies listed in table 3.15 values of  $\delta_n - \delta_o$  were calculated for the fluoromethanes using the STO-3G and STO 4.31G basis sets and these are shown in table 3.18.

Table 3.18  
Calculated Values of  $\delta_n - \delta_o$  (eV)

	$\delta_n - \delta_o$		
	$\delta_n - \delta_o$	<u>STO. 3G</u>	<u>STO 4.31G</u>
	<u>n</u>		
CH <sub>4</sub>	0	0.0	0.0
CH <sub>3</sub> F	1	-1.70	-0.26
CH <sub>2</sub> F <sub>2</sub>	2	-3.11	-0.49
CHF <sub>3</sub>	3	-4.24	-0.67
CF <sub>4</sub>	4	-5.31	-0.76

Large deviations of  $\delta_n - \delta_o$  from zero are predicted by the STO-3G calculations but an improvement in the basis set to STO-4.31G greatly reduces the deviation of  $\delta_n - \delta_o$  from zero and it is likely that a further improvement in basis set would predict the values of  $\delta_n - \delta_o$  to be nearer zero. Using the same basis sets values of the total energies of  $^*C^{5+}$  and  $N^{5+}$  may also be obtained and these are shown in Table 3.19 and this was used to obtain values for the energy of core exchange in methane ( $\delta_o$ ).



Table 3.19

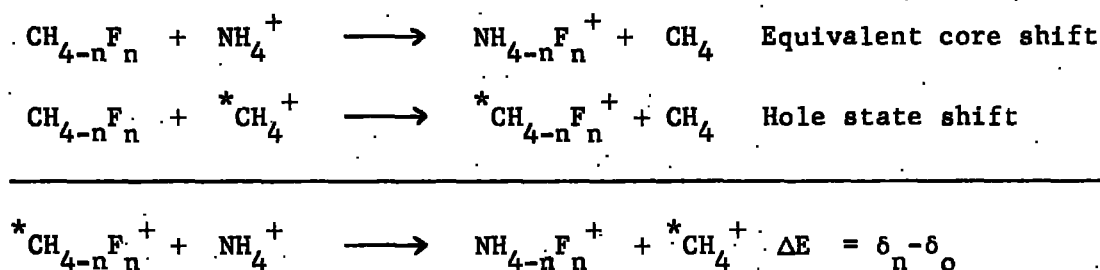
Total Energies of Cores (eV)

	<u>3G</u>	<u>4.31G</u>
$^*C^{5+}$	-483.6457	-486.7477
$N^{5+}$	-1202.5878	-1212.6848

This gives values of -13.7812 and -9.2350eV for  $\delta_o$  using the STO-3G and STO-4.31G basis sets. These values are obviously strongly basis set dependent but appear to approach zero, or at least a value closer to zero, as the basis set improves. Although the STO-3G and STO-4G descriptions of the cores are not good they are consistent with the calculations reported above. These calculations suggest that

the weak form of the equivalent cores approximation ( $\delta_n - \delta_o = a$  constant) is a reasonable description of the situation but that the strong form ( $\delta_n = \delta_o = 0$ ) may not be valid. This latter point will be mentioned later from an experimental point of view (Chapter III.5).

The values of  $\delta_n - \delta_o$  are equal to the differences between the hole state shifts and the equivalent core shifts



The energy of core exchange would therefore be predicted to be independent of molecular environment when equivalent core and hole state calculations predict the same values of shifts.

#### d) Reorganization Effects.

These calculations on the fluoromethanes, together with those of Brundle et al.<sup>162</sup> show that for these closely related molecules there is very little difference between binding energy shifts predicted by Koopmans' theorem, hole state, and equivalent cores calculations if a large flexible basis set is used. Since the hole state and equivalent core calculations take electronic reorganization into account but Koopmans' theorem does not, then for this closely related series of molecules, differences in reorganization energies therefore can make only minor contributions to the binding energy shifts. In this

connection it is of interest to pursue the analysis of the reorganization energies using the model suggested by Gelius and Siegbahn.<sup>38</sup> The dominant contribution is that arising from the local charge distribution ( $E_A^{\text{contr}}$ ) and this may be expressed as

$$E_A^{\text{contr}} = k'q_A + l'_A$$

where  $q_A$  is the charge on atom A before ionization,  $k'$  is a constant (2.5 eV in an atom<sup>38,166</sup>) and  $l'_A$  is the reorganization energy due to orbital contraction around a neutral atom in the molecule (13.7eV for a carbon atom<sup>38</sup>). Estimates of the reorganization energy obtained from differences between Koopmans' theorem and hole state binding energies are shown in table 3.20 together with atomic charges for the 4.31G-basis set calculations. These overall relaxation energies, which include effects from the redistribution of electron density in the remainder of the molecule ( $E_A^{\text{flow}}$ ), are essentially constant.

It is unrealistic to compare directly the atomic reorganization energy data of Gelius and Siegbahn with that calculated for the fluoromethanes because of the differences in basis sets used. However the prediction of a near constancy of relaxation energies for the fluoromethanes is interesting since from the analysis of Gelius and Siegbahn this would only be expected if the sum of the charge dependent term in  $E_A^{\text{contra}}$  and the change in  $E_A^{\text{flow}}$  was a constant. This implies that  $E_A^{\text{flow}}$  shows a similar but opposite dependency on the charge on the atoms bonded to carbon such that the sum total remains essentially constant.

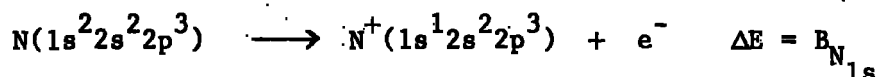
Table 3.20Charges and Relaxation energies (4.31G Basis Set)

<u>Molecule</u>	<u>Atom</u>	<u>Charge</u>	<u>Relaxation Energy (eV)</u> (Koopmans' BE - Hole State BE)
CH <sub>4</sub>	C	-0.875	11.4
	H	+0.219	-
CH <sub>3</sub> F	C	-0.281	11.2
	H	+0.226	-
	F	-0.399	-
CH <sub>2</sub> F <sub>2</sub>	C	+0.373	11.1
	H	+0.251	-
	F	-0.379	-
CHF <sub>3</sub>	C	+0.754	11.1
	H	+0.308	-
	F	-0.354	-
CF <sub>4</sub>	C	+1.328	11.3
	F	-0.332	-

5) EQUIVALENT CORE ESTIMATES OF CORE ELECTRON BINDING ENERGIES IN ATOMS FROM IONIZATION POTENTIAL DATA

Besides the use of the equivalent cores approximation for obtaining estimates of shifts in core electron binding energies it may also be used to obtain estimates of core electron binding energies for free atoms using experimental ionization potential data. In favourable cases this may be used to obtain an experimental estimate of the energy of core exchange  $\delta$ . For example consider the following processes for a nitrogen atom.

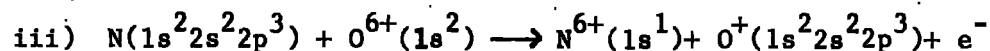
i) Photoionization of a 1s electron



ii) Exchange of the electron deficient nitrogen core and the equivalent oxygen core

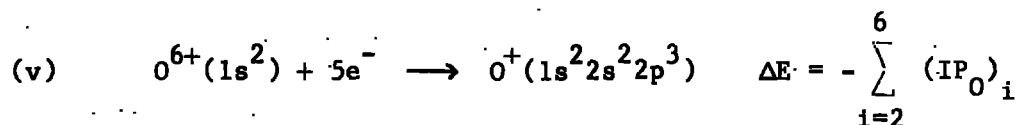
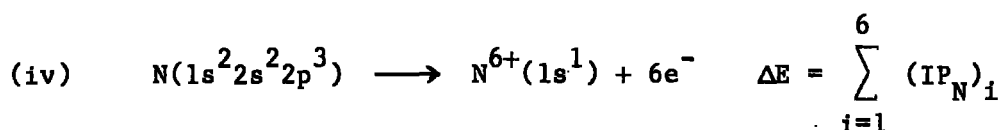


Summing reactions (i) and (ii) reaction (iii) is obtained:



$$\Delta E = B_{N1s} + \delta$$

The energy of this reaction differs from the 1s electron binding energy in a nitrogen atom by the energy of core exchange  $\delta$ . The energy of reaction (iii) may be obtained by splitting it into two processes, (iv) and (v) the energies of which may be obtained from the sum of successive ionization energies.



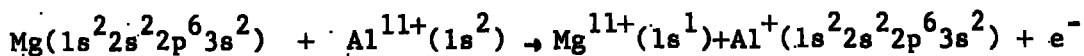
$$\text{Hence} \quad B_{N_{1s}} + \delta = \sum_{i=1}^6 (IP_N)_i - \sum_{i=2}^6 (IP_O)_i$$

Using ionization potential data from Moore's tables<sup>190</sup> gives a value of 399.4 eV for the energy of reaction (iii). The nitrogen 1s binding energy for molecular nitrogen is 409.9 eV<sup>17</sup> and that for the atom would not be expected to be significantly different and hence the estimated value of  $\delta$  is -10.5 eV. (Since the atom has zero charge in both instances the charge potential model<sup>17</sup> predicts the binding energies to be the same. There may be differences in electronic reorganization energies on photoionization between the atom and molecule but the analysis of Gelius and Siegbahn suggests that such differences are likely to be small and arise from the inclusion of the term  $E_A^{\text{flow}}$ ). The only relevant experimental data is from a study of high temperature molecular beams of bismuth which shows that molecular bismuth has a 4f binding energy 1eV less than atomic bismuth.<sup>191</sup>

For the majority of elements ionization from more than one core level is possible. In magnesium, for example, core ionizations from the 1s, 2s and 2p levels are possible and the binding energies may be

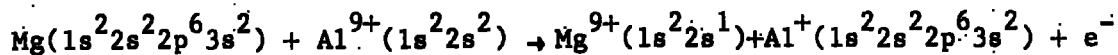
estimated from the following reactions:

Mg 1s



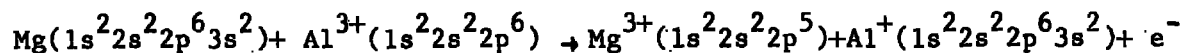
$$B_{1s} + \delta = \sum_{i=1}^{11} (\text{IP}_{\text{Mg}})_i - \sum_{i=2}^{11} (\text{IP}_{\text{Al}})_i$$

Mg 2s



$$B_{2s} + \delta = \sum_{i=1}^9 (\text{IP}_{\text{Mg}})_i - \sum_{i=2}^9 (\text{IP}_{\text{Al}})_i$$

Mg 2p



$$B_{2p} + \delta = \sum_{i=1}^3 (\text{IP}_{\text{Mg}})_i - \sum_{i=2}^3 (\text{IP}_{\text{Al}})_i$$

There is no reason to assume that the values of  $\delta$  will be the same for these three reactions. Subject to the availability of ionization potential data<sup>190,192</sup> the core electron binding energies for the elements Li to Ar have been estimated using the equivalent cores approximation. These estimates, together with an approximate value taken from the compilation of binding energies (for solid samples) given by Siegbahn et al.<sup>1</sup> are shown in table 3.21. For oxygen

Table 3.21

Equivalent Core Binding Energies from Ionization Potential Data (eV)

	Li	Be	B	C	N	O	F	Ne
Equivalent Core	62.8	118.3	194.6	287.6	399.4	530.9	-	-
Approximate B.E. <sup>a</sup>	55	111	188	284	399	532		
				290.4 <sup>b</sup>	409.9 <sup>c</sup>	543.5 <sup>d</sup>		
				$\delta = -2.8$	$\delta = -10.5$	$\delta = -12.6$		
	Na	Mg	Al	Si	P	S	Cl	Ar
1s Equivalent core	-	1279.0	1531.0	-	-	-	-	-
Approximate B.E. <sup>a</sup>		1305	1560					
2s Equivalent core	-17.3	- 9.3	2.87	17.8	-	-	-	-
Approximate B.E. <sup>a</sup>	63	89	118	149				
2p Equivalent core	37.4	55.5	78.3	103.4	131.4	161.6	195.2	228.9
Approximate B.E. <sup>a</sup>	31	52	73	99	135	164	200	245
(2p <sub>3/2</sub> )						170.3 <sup>e</sup>		248.5 <sup>f</sup>
						$\delta = -8.7$		$\delta = -19.6$

(a) Ref 1 (b) C<sub>1s</sub> binding energy in benzene, ref. 103 (c) N<sub>1s</sub> binding energy in N<sub>2</sub> ref. 17

(d) 1s binding energy in O<sub>2</sub> (weighted mean of multiplet states) ref. 17 (e) 2p<sub>3/2</sub> binding energy for zero atomic charge estimated from ref. 17 (f) 2p<sub>3/2</sub> binding energy for free atom ref. 17.

nitrogen and argon the gas phase value for the molecule<sup>17</sup> is also listed and for carbon and sulphur an estimate of the gas phase binding energy for an atom of zero charge has been made. These values permit a direct estimate of the energy of core exchange ( $\delta$ ) and these are also shown in Table 3.21. The core electron binding energies for the 1s and 2p electrons are predicted well. The estimates of  $\delta$  are negative and increase in magnitude with increasing atomic number along a row of the periodic table. It does, however, appear that  $\delta$  may be positive for the more metallic elements.

The predicted binding energies for the 2s levels range from -17.3eV for sodium to +17.7eV for silicon. This incorrect prediction of 2s binding energies is initially rather surprising since 2s binding energies are intermediate between 1s and 2p binding energies which are both predicted well. The equivalent core reactions for the interpretation of the 1s and 2p electrons for the second row elements involve the assumption that the potential experienced by the electrons in the 2s, 2p and 3s orbitals for the former and 3s for the latter are comparable for the hole state and its corresponding equivalent core species. Since, for the 1s and 2p levels the radial maxima (e.g. for Mg 1s 0.0854, 2s 0.5464, 2p 0.4838 and 3s 2.5862 a.u.<sup>193</sup>) for the levels in which the holes are created are much smaller than for the relevant 'outer orbitals' than the net effect as far as the outer orbitals are concerned is the same as increasing the nuclear charge by one unit. For the equivalent core reactions for the 2s electrons, however, the radial maxima of the orbitals are closely similar to those for the 2p orbitals and therefore the screening of the 2p electrons

from the nucleus by the 2s electrons is much smaller. In the case of 2s ionization therefore, the 2p electrons will not relax as if the nuclear charge had been increased by one unit so that the basic assumption of the equivalent core approach is invalidated.

The 2p ionization energies used in the calculation of 2s binding energies for Na, Mg and Al were therefore re-examined using Burns' atomic shielding parameters<sup>194</sup> and Slater's rules.<sup>109</sup> A quadratic fit to the dependence of the ionization energies on effective nuclear charge<sup>195</sup> was taken (e.g. for Mg the corresponding ionization energies of Na, Mg and Al were considered for the quadratic fit and as a further check the series Ne, Mg, Si was also taken. Excellent agreement between the two was found). The relationship obtained was used to estimate the ionization energies of the 2p electrons when there is vacancy in the 2s level. These estimates of the 2p ionization energies were then used in place of the corresponding equivalent core ionization energies but otherwise the calculations were as before. Burns' shielding parameters, which assume that one 2s electron shields a 2p electron from the nucleus by 0.5e gave estimates of the 2s binding energies for Na, Mg and Al to be 123.8, 152.2 and 185.0 eV respectively. This overestimates the binding energies somewhat but does give much more realistic values than the straightforward equivalent cores approach. The Slater's rule analysis, which predicts a shielding of a 2p electron by one 2s electron of 0.35e, overestimates the 2s binding energies further with values of 164.1, 198.6 and 237.6eV for Na, Mg and Al respectively. By incrementing the values of the shielding of a 2p

electron by a 2s electron in units of 0.1 the best value of the shielding constant was found to be 0.7. This gave values of 68.6, 88.8 and 113.4 eV for the 2s binding energies in Na, Mg and Al. These results illustrate that, as would be expected, the equivalent cores method gives accurate results for core electrons which are highly shielding with respect to electrons of lower binding energy and a qualitative description of the deviations from this is obtained by using shielding constants.

#### 6) A COMPARISON OF ASSIGNMENTS OF $C_{1s}$ BINDING ENERGIES BASED ON KOOPMANS' THEOREM AND THE CHARGE POTENTIAL MODEL

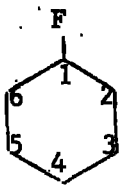
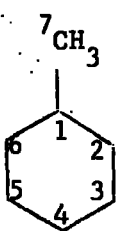
The results presented in this chapter have shown that good predictions of core electron binding energies can be obtained from non-empirical calculations using Koopmans' theorem, equivalent cores calculations and hole state calculations, but that the accuracies of the predictions from these methods have different basis set dependancies. For accurate predictions by Koopmans' theorem, calculations of double zeta quality are required and are obtained only if relaxation contributions to shifts are negligible. However, there are severe limitations on the size of molecules which can be studied by non-empirical calculations especially if double zeta quality is required. Therefore computationally inexpensive, but theoretically valid, models are required. The most widely used of these is the

charge potential model in conjunction with charges obtained from CNDO calculations. (The charge potential model will be discussed in more detail in chapter IV). However, with increased computer power and efficient programs the range of molecules which can be studied at the non-empirical level is expanding. As particular examples fluorobenzene and toluene have been studied with double zeta quality basis sets of optimized 9s and 5p gaussian functions for carbon and fluorine contracted to 4s and 2p, and 4s functions contracted to 2s for hydrogen (scale factor 1.2) (Appendix I). These calculations were carried out using the IBMOL 5<sup>187</sup> computer program. CNDO/2 calculations have also been carried out on these molecules. A comparison of the predicted shifts between the computationally expensive ab initio calculations and the computationally inexpensive CNDO/2 calculations provides a stringent test for the assignments obtained from the charge potential model. The ab initio and charge potential ( $k_1 = 25$ ) results are listed in table 3.22. The shifts relative to  $C_1$  and the order of the predicted assignments (in decreasing binding energy) are also shown in table 3.22. There is found to be good agreement between the order predicted by both methods. The only exception is the predicted ordering of the ortho and para carbon atoms in toluene but in both cases these are predicted to be the same to the first decimal place and this is well within the experimental error of measurements of core electron binding energies. This close agreement between assignments predicted by double zeta

ab initio calculations and by the charge potential model using semi-empirical CNDO/2 calculations allows the charge potential model to be used with confidence for larger molecules for which ab initio calculations are not yet possible. The two examples given above, especially toluene, provide very stringent tests since the shifts in core electron binding energies are very small.

Table 3.22

A comparison of ab initio and semi-Empirical Calculations

Molecule	<u>Ab initio</u>			<u>CNDO/2</u>		
	Atom	BE.	Shift	Order	Shift	Order
	1	309.81	0	1	0	1
	2,6	307.37	- 2.44	3	- 2.83	3
	3,5	307.50	- 2.31	2	- 2.58	2
	4	307.25	- 2.56	4	- 2.93	4
	1	307.13	0	1	0	1
	2,6	306.72	- 0.41	4	- 0.71	3
	3,5	306.88	- 0.25	2	- 0.57	2
	4	306.75	- 0.38	3	- 0.73	4
	7	306.51	- 0.62	5	- 0.76	5

† An average value of  $k = 25$  found from extensive studies of closely related molecules (c.f. Chapter IV) was employed in the charge potential calculations. With slight adjustment of parameters better overall agreement in detail could undoubtedly be obtained between the shifts for these two molecules obtained from the charge potential model and Koopmans' theorem.

CHAPTER IV

THE CHARGE POTENTIAL MODEL AND MOLECULAR

CHARGE DISTRIBUTIONS

1) BACKGROUND AND DEVELOPMENT

It was observed at an early stage in the development of ESCA that the binding energy of a core level tended to increase with increase in oxidation state of the element. Some typical shifts in binding energies for a few elements in solid samples are shown in table (4.1) and were compiled<sup>196</sup> from some of the early data obtained from the ESCA groups in Uppsala and Berkeley.

Table 4.1  
Oxidation State

<u>Element</u>	-2	-1	0	+1	+2	+3	+4	+5	+6	+7
N <sub>1s</sub>	-	0	-	+4.5	-	+5.1	-	+8.0	-	-
S <sub>1s</sub>	-2.0	-	0	-	-	-	+4.5	-	+5.8	-
Cl <sub>2p</sub>	-	0	-	-	-	+3.8	-	+7.9	-	+9.5
Cu <sub>1s</sub>	-	-	0	+0.7	+4.4	-	-	-	-	-
I <sub>4s</sub>	-	0	-	-	-	-	-	5.3	-	6.5
Eu <sub>3d</sub>	-	-	-	-	0	9.6	-	-	-	-

While there is a general increase in the binding with increasing oxidation state this increase is not smooth and varies between elements. Chemical shifts were first interpreted in terms of an ionic model<sup>1,197</sup> If charge is added to or removed from the valence shell, as in the case of bond or ion formation, the electrostatic potential within the valence shell is changed. If, for example,  $q$  electronic charges are

removed from the valence shell to infinity the potential energy is lowered by the amount

$$\Delta E = \frac{q}{r} \quad (1)$$

where  $r$  is the radius of the valence shell. However, the electron is not removed to infinity but to a finite distance  $R$  within the molecule. The shift is then given by

$$\Delta E = \left( \frac{1}{r} - \frac{1}{R} \right) q \quad (2)$$

although in a crystal the lattice contribution has to be calculated.

For higher states of oxidation the valence electrons contract ( $r$  decreases) and the shift per degree of oxidation should increase.

(Siegbahn et al.<sup>17</sup> have carried out some SCF calculations using modified Hartree-Fock-Slater wave functions which agree with this).

Also, provided the valence electrons do not penetrate the atomic core, the model predicts the same shifts for all core electrons, but if there is penetration of valence electrons into the core different shifts for different core levels may occur. As far as inner electrons are concerned, neighbouring ions can, to a first approximation, be regarded as point charges since the overlap is negligibly small. Therefore, in a crystal, to evaluate the direct effect of the lattice charges on the binding energy a summation of potentials from the point charges in the crystal is required. In the point charge model the crystal potential  $V_i$

at the nucleus of atom  $i$  is

$$V_i = \sum_{j \neq i} \frac{q_j}{r_{ij}} \quad \text{where } r_{ij} \text{ are inter-ionic distances} \\ \text{and } q_j \text{ is the charge anion } j \quad (3)$$

These arguments may be extended in more detail to covalent compounds<sup>17</sup> and figure 4.1<sup>17</sup> shows the radial distribution of an electron in a carbon 1s and 2s Slater orbital and the potential electrostatic component  $V_{2s}$  from the spherical component of the L-shell electron distribution. This potential levels off near the nucleus and is almost constant in the region of maximum K-electron density. A redistribution of the valence electrons in the molecule compared to the atom, which involves the partial removal or addition of a valence electron on a particular atomic site, thus gives rise to an almost uniform change of the effective potential experienced by the core electrons on that atom. The change in potential as a consequence of redistribution of the valence electrons on the formation of a molecule may be split into two components, one associated with the change of the valence electron population on the atom under consideration and the other, a two centre interaction, originating from the electron distribution in the remainder of the molecule which is considered as an array of point charges centred on the atoms. Thus the binding energies  $E_i$  may be written as

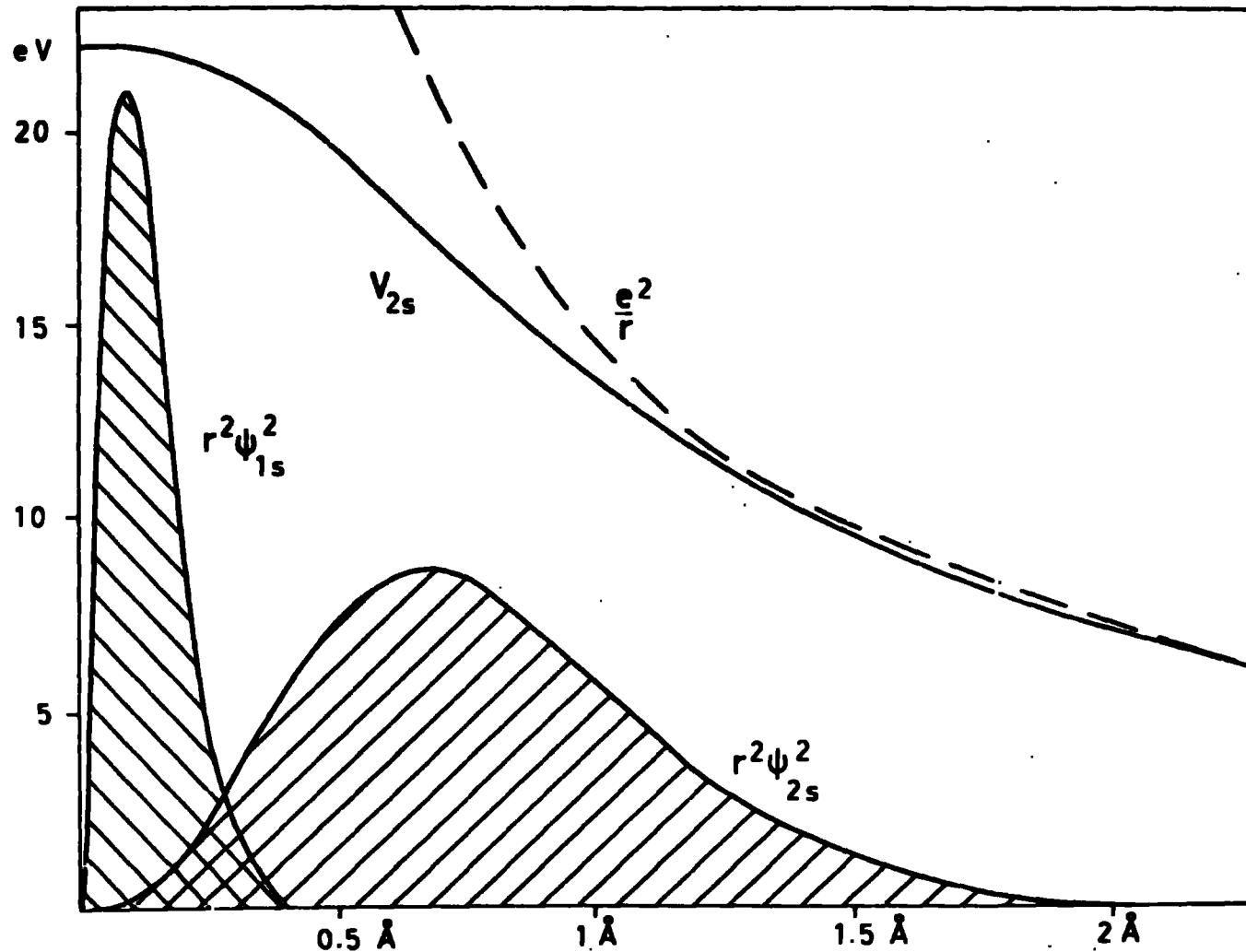
$$E_i = E_i + kq_i + \sum_{j \neq i} \frac{q_j}{r_{ij}} \quad (4)$$

where:  $q_i$  is the charge on atom  $i$

$k$  represents the average interaction between a core and valence electron on the atom

$r_{ij}$  are the interatomic distances (the summation is an

Figure(4.1)



1s and 2s electron densities in carbon calculated from Slater orbital wavefunctions (different normalisations). The potential function from a 2s electron and the Coulomb potential from a unit point charge at the nucleus are also shown. As shown by these diagrams a 2s electron contributes about 22 eV to the potential energy of a 1s electron in carbon.

intra-molecular Madelung type potential)

and  $E^0$  is a reference level.

The assumption of point charges is equivalent to assuming that there is no overlap between the core electron density on atom A and the valence electron densities on the other atoms in the molecule and this approach forms a natural basis for relating ESCA chemical shifts with CNDO molecular orbital calculations.<sup>17</sup>

Some earlier ESCA work considered shifts to be proportional only to the charge on the atom<sup>1,196,198.</sup>

$$\Delta E = k'q \quad (5)$$

however, the term  $\sum_{j \neq i} \frac{q_j}{r_{ij}}$  is not negligible and the proportionality constant  $k'$  was considerably modified with respect to  $k$  in equation (4). However, results obtained from equation (5) do often give good correlations between calculated charges and chemical shifts<sup>17</sup> and this is useful in conjunction with charges obtained from Pauling's relation between electronegativity and the partial ionic character of a bond.<sup>199</sup>

$$I = 1 - \exp [-0.25(x_A - x_B)^2] \quad (6)$$

However, Thomas<sup>179</sup> has found that for a series of halomethanes the  $C_{1s}$  binding energy shifts (relative to methane) are proportional to the sums of electronegativity differences, where the difference is between the electronegativity of the ligand and hydrogen and the sum

is over all ligands

$$(B_M - B_{CH_4}) \propto \sum_{i=1}^4 (x_A - x_H) \quad (7)$$

The correlation is better than that obtained using equation (6) since it extends over fluoro, chloro and bromo methanes<sup>179</sup> rather than giving separate correlations.<sup>17</sup>

When using equation (4) it is usual to treat  $k$  and  $E^0$  as empirical parameters and to obtain them from a least squares fit between

$$E - \sum_{j \neq i} \frac{q_j}{r_{ij}} \quad \text{and} \quad q_i \quad (E \text{ being the measured binding energy and the } q\text{'s}$$

the calculated charges). A representative tabulation of data obtained by Siegbahn et al.<sup>17</sup> is shown in table 4.2. The values refer to gas phase data and a value of  $k_c$  equal to 21.9 eV/unit charge was used.

Elison and Larcom<sup>200</sup> have slightly improved the correlations obtained from the charge potential model by considering  $s$  and  $p$  charges separately and using different  $k$  values for the  $s$  and  $p$  charges. However, the only really significant improvement obtained with this increase in parameters occurs in the case of carbon monoxide where the predicted  $C_{1s}$  binding energy shift is now in good agreement with the experimental value. However, the calculations discussed previously (Chapter III) and the following discussion would seem to suggest that the deviations may be due to differences in relaxation energy which the additional parameters encompass.

Table 4.2

C<sub>1s</sub> Binding Energies of Compounds referred to CH<sub>4</sub> (290.7 eV)<sup>17</sup>

	$\Delta E$	Pauling Charge		CNDO charges		Calculated Shift(4)
		$q_p$	$q_i$	$\sum_{j \neq i} \frac{q_j}{r_{ij}}$		
CH <sub>4</sub>	0	-0.16	-0.08	1.00		-0.1
CH <sub>3</sub> CH <sub>2</sub> OH	0.2	-0.12	-0.16	2.95		0.0
CH <sub>3</sub> C(=O)H	0.6	-0.12	-0.14	2.93		0.5
CH <sub>3</sub> OH	1.6	0.10	0.17	-2.39		2.1
(CH <sub>3</sub> ) <sub>2</sub> C=O	3.1	0.44	0.30	-4.21		3.2
CH <sub>3</sub> C(=O)H	3.2	0.40	0.30	-4.12		3.3
CO	5.2	0.55	0.02	-0.32		0.9
CO <sub>2</sub>	6.8	0.88	0.61	-7.53		6.8
HCF <sub>3</sub>	8.1	1.26	0.68	-7.52		8.4

The charge potential model may be derived directly from Koopmans' theorem (c.f. Chapter III.1.b) and therefore suffers from the same deficiencies as Koopmans' theorem predictions i.e. the neglect of relaxation energy effects. However, by treating  $E^0$  and  $k$  as empirical parameters these deficiencies are largely accounted

for within a series of closely related molecules. In fact values of  $k$  for a given element do vary slightly between different series of related compounds. The values of  $k$  and  $E^0$  also depend on the definition of atomic charge and, in an SCF-MO treatment, on the basis set used. Values of  $k$  for carbon reported by Clark et al.<sup>93</sup> for some series of organic compounds studied in the condensed phase are shown in table (4.3). Charges obtained from CNDO/2 calculations were used.

Table 4.3

$k$  Values for Carbon (eV/unit charge)

<u>Class of Compound</u>	<u><math>k</math></u>
halogenated monosubstituted benzenes	24.6
acetyl compounds	25.0
aromatic hydrocarbons and perfluoroanalogues	25.0
halogenated methanes	28.7 <sup>a</sup>
	26.6 <sup>b</sup>
pyridine and the six-membered ring diazines	22.4 (all)
	25.5 (hydro)
	24.3 (chloro)
	20.9 (fluoro)
five membered ring heterocycles	25.4
the fluorobenzenes	23.5
the chlorobenzenes	31.3 <sup>a</sup>
	23.2 <sup>b</sup>

a including d orbitals on chlorine

b excluding d orbitals on chlorine

For a series of closely related compounds relaxation energies are likely to be similar and relaxation effects are accounted for by treating  $k$  and  $E^0$  as empirical parameters as mentioned previously. When a  $1s$  electron is ejected the remaining electrons in the molecule contract towards the positive hole to minimize the total energy and the amount of relaxation may depend markedly on the bonding situation e.g. contract halomethanes where there are four single bonds from which the positive hole can draw electron density without creating positive centres elsewhere, with carbon monoxide from which electron density can only flow from the oxygen atom and the bond. Attempts have therefore been made to account for the relaxation of valence electrons which occurs during the photoionization process.<sup>178,201</sup> Both these methods invoke the equivalent cores approximation to simulate the final core hole state. The analysis of Davis and Shirley<sup>178</sup> is based essentially on the quantum mechanical potential at the nucleus approach (c.f. Chapter III.1.e) while that of Jolly<sup>201</sup> is based more directly on the charge potential model and is outlined in some detail below.

The charge potential model is initially considered in the form

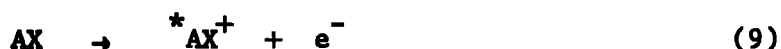
$$E_B = kQ + V + I \quad (8)$$

( $V$  corresponds to  $\sum_{j \neq i} \frac{q_j}{r_{ij}}$  and  $I$  to  $E^0$  in the previous formulation

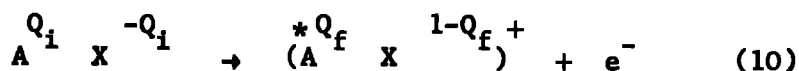
(Equation 4) and  $Q$  is the charge on the atom which loses the core electron).

Q and V depend only on the initial state of the molecule. However during the time required for the ejection of a core electron from an atom in a molecule the valence electrons shift towards the nucleus of the atom in which the hole is created,<sup>44,50,158,166,167.</sup> This concurrent valence electron relaxation is believed to be essentially complete in the time of the photoionization process. Therefore, if it is required to calculate accurately the binding energy by a hypothetical 'sudden process' in which the valence electrons are assumed to remain fixed, neither the valence electron distribution of the initial molecule nor that of the final core hole state ion can be used. A valence electron distribution, probably close to the average of the two extremes, should give the correct energy.

Ionization of a core electron from atom A in the molecule AX is represented by

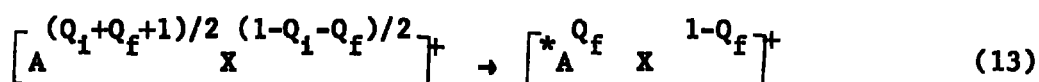
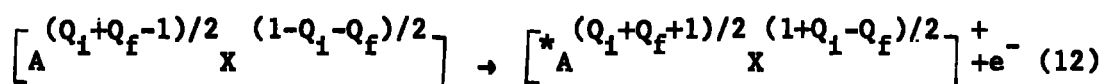
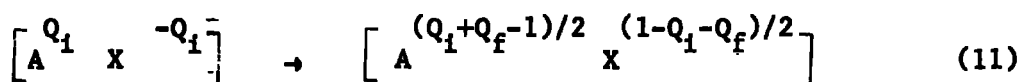


Assigning valence electron charges in the initial and final states on atom A as  $Q_i$  and  $Q_f$  leads to



Assuming that the appropriate valence electron populations for calculating the energy of a sudden electron ejection are the average of the initial and final populations the photoelectric process may be

divided into three parts



It is assumed that reactions (10) and (12) have the same energy i.e. the binding energy  $E_B$ . (Reactions (11) and (13) are therefore of equal energy but opposite sign.)

The energy of reactions (12) may be evaluated as the sum of the core binding energy for a free  $A^{(Q_i+Q_f-1)/2}$  ion and the electrostatic removal of an electron from that site in the molecule

$$E_B = E_B \left( A^{(Q_i+Q_f-1)/2} \right) + V \left( X^{(1-Q_i-Q_f)/2} \right) \quad (14)$$

Relating the core binding energy of a free monatomic ion to the ionic charge  $Q$ <sup>17</sup>

$$E_B (A^Q) = kQ + 1 \quad (15)$$

By setting  $Q = (Q_i + Q_f - 1)/2$  and combining equations (14) and (15) the following relationship is obtained.

$$E_B = k(Q_i + Q_f - 1)/2 + V_{av} + 1 \quad (16)$$

This half ionized core model differs from the charge potential model in that the charges used correspond to the average of the initial and final valence electron distributions instead of the ground state atomic charges. The final state charges are estimated from the charges in the corresponding isoelectronic equivalent core cation. Using this method with CNDO charges improvements were found for  $C_{1s}$  binding energies but slightly poorer correlations were obtained for  $N_{1s}$  and  $O_{1s}$  binding energies. Equation (16) could be modified by use of a weighted average rather than the simple average.

However from the point of view of the practical chemist it is preferable to predict properties from the ground states of molecules and also to be able to predict ground state properties from other observations. The charge potential model in its standard form

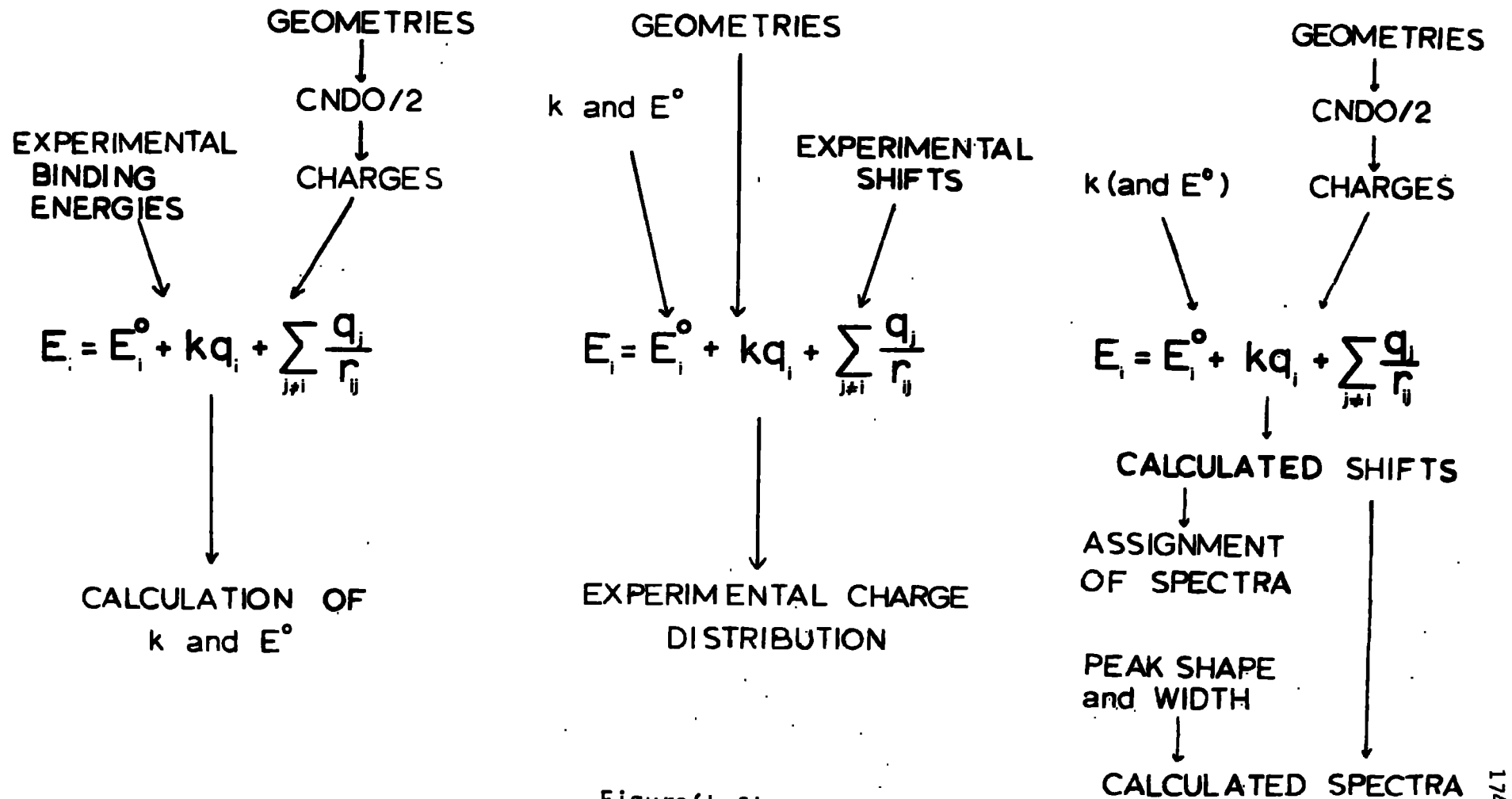
$$E_i = E_i^0 + kq_i + \sum_{j \neq i} \frac{q_j}{r_{ij}}$$

is conceptually simple and relates to ground state properties. It may also be inverted to yield ground state charge distributions from measured binding energy shifts (this work). It is this form of the charge potential model which will be considered in this work.

## 2) USES OF THE CHARGE POTENTIAL MODEL

Figure 4.2 demonstrates how the charge potential model may be used by chemists and illustrates the data required and information obtained from its use. For a particular core level values of  $k$  and  $E^0$

# USES OF THE CHARGE POTENTIAL MODEL



Figure(4.2)

are obtained from the measured binding energies  $E_i$  and the charge distribution is usually obtained from CNDO/2 calculations. Both the charge potential equation and the CNDO program require a knowledge of the geometry of the molecule (i.e. the atomic coordinates). Since this information is not usually available, especially for complex systems, standard bond lengths and angles<sup>183</sup> are employed. (In principle an optimized geometry could be obtained by minimizing the total energy obtained from the CNDO calculations. However, for most systems of interest to organic chemists such geometry optimizations are completely impracticable on the grounds of the number of variables involved, the computational expense, and time which would be involved).

Once values of  $k$  and  $E^0$  have been established for a system the charge potential model may be used, in conjunction with calculated charges, to assign peaks within a spectrum. This is particularly useful when assigning binding energies, which differ only slightly, to various atoms within a molecule. Knowledge of  $E^0$  is not essential for assignment since it is the ordering of the binding energies which is important. Clark et al.<sup>72,85,86</sup> have made extensive use of this method of assigning binding energies. If also, from a study of similar compounds under the same experimental conditions, peak shapes and line widths are known to a high degree of accuracy, (knowledge also required for detailed deconvolutions of partially resolved peaks), then the charge potential model may be used to calculate spectra and these may be simulated and plotted out by use of the Du Pont 310 curve resolver (c.f. chapter V). Comparison between experimental spectra and spectra

calculated for several possible structures may sometimes be used as an aid to differentiate between the structures. The Madelung type potential terms  $\sum_{j \neq i} \frac{q_j}{r_{ij}}$  and theoretical values of  $E-E^0$  were calculated using the versatile program NEWPOT described in appendix III.

Since the charge potential model has proved successful in predicting chemical shifts from charge distributions the main aims of the work presented in the remainder of this chapter are to determine

- i) whether the charge potential model can be used in an inverted form in order to obtain detailed charge distributions within molecules from experimental ESCA data as an alternative to molecular orbital calculations: and if so:-
  - ii) Whether a detailed or simple deconvolution of the spectrum is required (if a detailed deconvolution were required a molecular orbital calculation would be required to assign the binding energies thus rendering the technique of little practical value).
  - iii) Whether the shifts involved need to be large, as with fluorocarbon compounds or whether good results may be obtained from molecules in which the shifts are small (e.g. hydrocarbons) or moderate (e.g. chlorobenzenes).
  - iv) Whether the technique can be applied to large molecules with complex structures (even CNDO/2 calculations on moderate to large sized organic molecules become computationally expensive).

### 3) CHARGE DISTRIBUTIONS - THE INVERSION OF THE CHARGE POTENTIAL MODEL

A description of the charge distribution within a molecule is often a useful rule of thumb guide in discussing the chemistry of complex systems e.g. the prediction of probable sites of reactions or for preliminary assignment of other spectroscopic data where the interpretation may not be straightforward but may depend to some extent on the charge distribution. The charge potential model provides a possible method for obtaining charge distributions in molecules directly from experimental data

$$E_i = E^{\circ} + kq_i + \sum_{j \neq i} q_j / r_{ij}$$

Consider, for example, a molecule containing four atoms. The charge potential model leads to the equations (values in atomic units)

$$\begin{aligned} E_1 - E^{\circ}_1 &= k_1 q_1 + \frac{q_2}{r_{12}} + \frac{q_3}{r_{13}} + \frac{q_4}{r_{14}} \\ E_2 - E^{\circ}_2 &= \frac{q_1}{r_{21}} + k_2 q_2 + \frac{q_3}{r_{23}} + \frac{q_4}{r_{24}} \\ E_3 - E^{\circ}_3 &= \frac{q_1}{r_{31}} + \frac{q_2}{r_{32}} + k_3 q_3 + \frac{q_4}{r_{34}} \\ E_4 - E^{\circ}_4 &= \frac{q_1}{r_{41}} + \frac{q_2}{r_{42}} + \frac{q_3}{r_{43}} + k_4 q_4 \end{aligned}$$

The  $E^{\circ}$  and  $k$  values are characteristic of the core level concerned and have previously been determined by a study of similar compounds. The geometry of the molecule is known, or estimated, and therefore the internuclear distances  $r_{ij}$  are known and  $E$  is just the measured experimental binding energy. There is therefore a series of four equations with four unknowns, the charges, and these may be solved uniquely to

obtain the charge distribution in the molecule. This may obviously be extended to any number of atoms. For a neutral molecule, however, there is the additional equation

$$\sum_i q_i = 0$$

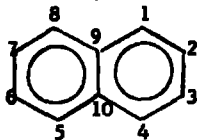
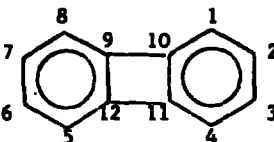
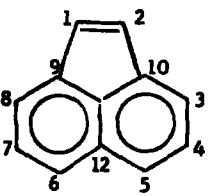
This condition will not be imposed on the charges but will be mentioned later. The charge distributions were obtained with the aid of the program CHARGES (Appendix III), and the standard IBM program SOLN<sup>202</sup>, although a new and more versatile program ATCH has since been written (Appendix III).

a) Charge Distributions in Aromatic Hydrocarbons and their Perfluoro Analogues

Clark and Kilcast<sup>71</sup> have reported binding energy data, CNDO/2 charges and detailed assignments for a series of aromatic compounds and their perfluoro analogues. Their data are shown in table 4.4. An analysis of these data by linear least squares regression gives the values  $E_c^0 = 284.6\text{eV}$  and  $K_c = 25.0 (\pm 0.6)\text{ eV/unit charge}$ . However the  $F_{1s}$  binding energy shifts are very small and the  $F_{1s}$  spectra appear as single peaks which are only slightly broadened compared with perfluorobenzene as standard. It is therefore not possible meaningfully to deconvolute the  $F_{1s}$  spectra and the fluorine atoms within a molecule were all assigned the same binding energy. The shifts in  $F_{1s}$  binding energies between molecules were also very small. It was therefore not possible to obtain reliable values of  $k_F$  and  $E_F^0$  from a least squares

Table 4.4

Detailed binding energies, assignments and CNDO charges for a series of hydrocarbons and fluorocarbons<sup>71</sup>

	Position	Hydrocarbons			Fluorocarbons			
		$q_C$	$q_H$	$BE_C$	$q_C$	$q_F$	$BE_C$	$BE_F$
	1	0.006	-0.006	284.9	0.155	-0.155	289.5	690.9
	1,4,5,8	-0.004	-0.006	284.8	0.180	-0.167	289.3	690.9
	2,3,6,7	0.001	-0.008	284.5	0.154	-0.161	288.7	690.9
	9,10	0.034	-	285.3	-0.016	-	287.4	-
	1,4,5,8	-0.007	-0.002	284.8	0.186	-0.171	288.7	690.6
	2,3,6,7	0.002	-0.006	285.3	0.152	-0.163	289.0	690.6
	9,10,11,12	0.014	-	285.6	-0.004	-	286.8	-
	1,2	-0.009	0.009	283.9	0.169	-0.179	288.3	690.6
	3,8	0.029	0.008	284.9	0.248	-0.167	289.5	690.6
	4,7	-0.011	0.004	284.5	0.115	-0.162	288.8	690.6
	5,6	0.013	0.007	284.9	0.227	-0.165	289.0	690.6
	9,10	-0.008	-	284.5	-0.078	-	286.4	-
	11	0.011	-	284.9	0.046	-	287.2	-
	12	0.019	-	284.9	-0.061	-	287.2	-

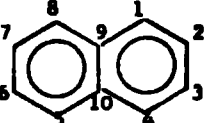
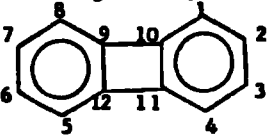
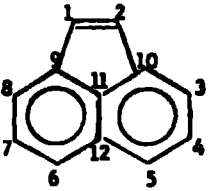
fit to these data. From a study of the fluoromethanes<sup>179</sup> for which the shifts in  $F_{1s}$  binding energy are appreciable, however, a value of  $k_F \approx 30$  eV/unit charge was obtained. Taken in conjunction with the absolute binding energies and computed CNDO/2 charge distributions for the perfluoro aromatic compounds the value  $k_F = 30$  yielded a value of  $E_F^0 \approx 693.2$  eV.

For a solution of the equations yielding the charge distribution within a molecule values of  $k$  and  $E^0$  are required for all the elements in the molecule. In the particular case of hydrogen a problem arises since the  $1s$  orbital is simultaneously a core and valence orbital. In hydrogen-containing molecules therefore there are no energy levels characteristic of the  $H_{1s}$  orbitals and hence direct evaluations of  $E_H^0$  and  $k_H$  cannot be made. The values used below ( $E_H - E_H^0 = 0.1$  and  $k_H = 25.0$ ) were obtained by trial and error with calculations on methane and benzene taking the relationship  $\sum_i q_i = 0$  as the criterion of good values. The value of  $k_H$  is not critical and in benzene, for example, the use of  $k_H = 30$  rather than 25 changes the charge on hydrogen by only 0.001.

Using the parameters  $E_C^0 = 284.6$ ,  $E_F^0 = 693.2$ ,  $(E - E^0)_H = 0.1$ ,  $k_C = 25.0$ ,  $k_F = 30.0$  and  $k_H = 25.0$  together with the binding energies and assignments in table 4.4 the charge distributions in the aromatic hydrocarbons and their perfluoro analogues were calculated. Table 4.5 shows a comparison of these 'experimental charges' with those obtained from the CNDO/2 SCF MO calculations. (The same molecular geometries were used for the two methods). The CNDO charges are well reproduced and

Table 4.5

Experimental and CNDO/2 Charges for a Series of Hydrocarbons and Fluorocarbons

<u>Molecule</u>	<u>Position</u>	<u>Hydrocarbons</u>						<u>Fluorocarbons</u>					
		<u>Carbon</u>			<u>Hydrogen</u>			<u>Carbon</u>			<u>Fluorine</u>		
		<u>Exptl.</u>	<u>CNDO</u>	<u>Difference</u>	<u>Exptl.</u>	<u>CNDO</u>	<u>Difference</u>	<u>Exptl.</u>	<u>CNDO</u>	<u>Difference</u>	<u>Exptl.</u>	<u>CNDO</u>	<u>Difference</u>
	1	+0.007	+0.006	0.001	-0.004	-0.006	0.002	0.168	0.155	0.013	-0.164	-0.155	-0.009
	1,4,5,8	0.001	-0.004	0.005	-0.002	-0.006	-0.004	0.201	0.180	-0.021	-0.163	-0.167	0.004
	2,3,6,7	-0.013	0.001	-0.014	0.006	-0.008	0.014	0.138	0.154	-0.016	-0.152	-0.161	0.009
	9,10	0.025	0.034	-0.009	-	-	-	-0.035	-0.016	-0.017	-	-	-
	1,4,5,8	-0.018	-0.007	-0.011	-0.005	-0.002	-0.003	0.178	0.186	-0.010	-0.169	-0.171	0.002
	2,3,6,7	0.028	0.002	0.026	-0.017	-0.006	-0.011	0.168	0.152	0.016	-0.167	-0.163	-0.004
	9,10,11,12	0.025	0.014	0.011	-	-	-	-0.007	-0.004	-0.003	-	-	-
	1,2	-0.040	-0.009	-0.031	0.023	0.009	0.014	0.171	0.169	-0.002	-0.162	-0.179	0.017
	3,8	0.020	0.029	-0.009	-0.003	0.008	-0.011	0.237	0.248	-0.011	-0.178	-0.167	-0.011
	4,7	-0.020	-0.011	-0.009	0.007	0.004	0.003	0.144	0.115	0.029	-0.165	-0.162	-0.003
	5,6	0.014	0.013	0.001	-0.004	0.007	-0.011	0.195	0.227	-0.032	-0.169	-0.165	-0.004
	9,10	-0.006	-0.008	0.002	-	-	-	-0.067	-0.078	0.011	-	-	-
	11	0.019	0.011	0.008	-	-	-	0.029	0.046	-0.017	-	-	-

there is generally agreement to within  $\pm 0.02e$ . The overall correlations between the experimental and CNDO charges, as found by a least squares fit to the data, are:-

$$\begin{array}{ll} \text{fluorocarbons} & q_{\text{exp}} = 0.000 + 0.99q_{\text{CNDO}} \\ \text{(carbon and fluorine)} & (\pm 0.02) \end{array}$$

$$\begin{array}{ll} \text{hydrocarbons} & q_{\text{exp}} = 0.002 + 0.97q_{\text{CNDO}} \\ \text{(carbon and hydrogen)} & (\pm 0.22) \end{array}$$

$$\begin{array}{ll} \text{all molecules} & q_{\text{exp}} = 0.001 + 1.00q_{\text{CNDO}} \\ \text{(carbon, hydrogen and fluorine)} & (\pm 0.01) \end{array}$$

The correlation for the hydrocarbons is not quite as good as that for the fluorocarbons and this illustrates not only the difficulty in obtaining suitable parameters for hydrogen, but also the fact that much smaller shifts and ranges of charges occur in the hydrocarbon series.

In order to obtain the charge distribution an initial assignment of binding energies is required. For example, in the case of perfluorobiphenylene there are three distinct environments for carbon and hence six possible assignments of binding energies. Table 4.6 shows the charge distributions obtained from each possible assignment. It should be noted that comparatively small charges are obtained on bridgehead carbons (i.e. those not bonded to fluorine) even when they are assigned high binding energies and that small charges are obtained on

Table 4.6

Charge Distributions in Perfluorobiphenylene from various assignments of the C<sub>1s</sub> Binding Energies.

	<u>(E-E<sup>o</sup>)<sub>c</sub></u>			<u>CHARGES</u>					
	A	B	C	<u>Carbon</u>			<u>Fluorine</u>		
(a)	A	B	C	A	B	C	B	C	
	4.1	4.4	2.2	0.053	0.198	0.060	-0.176	-0.135	
	4.1	2.2	4.4	0.085	0.034	0.193	-0.145	-0.165	
	4.4	4.1	2.2	0.067	0.175	0.064	-0.172	-0.135	
	4.4	2.2	4.1	0.095	0.032	0.179	-0.145	-0.161	
(b)	2.2	4.1	4.4	-0.007	0.178	0.168	-0.169	-0.167	
	2.2	4.4	4.1	-0.011	0.200	0.150	-0.173	-0.163	
(c)	2.2	4.25	4.25	-0.009	0.189	0.159	-0.171	-0.165	
	CNDO/2 Charges			-0.004	0.186	0.152	-0.171	-0.163	

(a) A = ring positions 9,10,11,12,

B = ring positions 1,4,5,8

C = ring positions 2,3,6,7

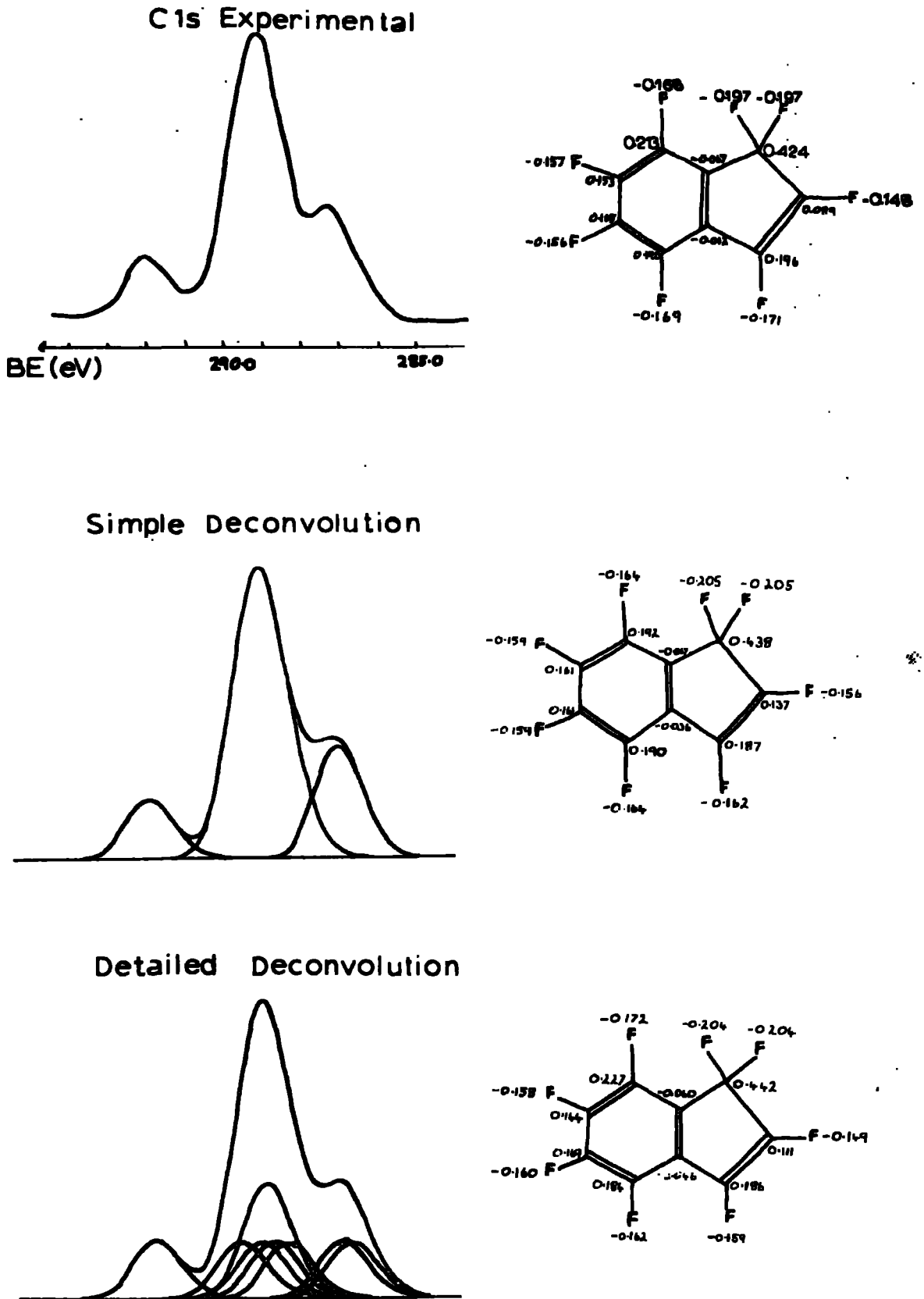
(b) Assignment obtained from CNDO charges

(c) Average deconvolution

carbon atoms bonded to fluorine if they are assigned low binding energies. The only two reasonable assignments are those which assign the lowest binding energy to the bridgehead carbons. Without a direct comparison with the charges and assignments obtained from the CNDO calculations it would be difficult to state unambiguously which of these two assignments was correct. It is therefore of interest to calculate the charge distribution assuming an average shift for the carbon atoms bonded to fluorine. This is also shown in table 4.6 and is itself in very good agreement with the CNDO charges. This implies that it should be possible to obtain good charge distributions within a molecule without making detailed deconvolutions of spectra.

Figure 4.3 shows the  $C_{1s}$  spectrum of perfluoroindene (normalized to a horizontal base line) and two deconvolutions of this spectrum. The first deconvolution simply splits the spectrum into three peaks which have the area ratio, in order of decreasing binding energy, 1:6:2 and these peaks may readily be assigned to the  $CF_2$  carbon, the CF carbons and the bridgehead carbons respectively. The second deconvolution is more detailed and was obtained by fitting nine gaussian type curves of equal area and half width (1.4eV) to the spectrum. (The line shape, widths and areas were taken from the relatively well resolved peak at highest binding energy corresponding to the  $CF_2$  carbon). The individual  $C_{1s}$  levels are now less readily assigned and a CNDO charge distribution has to be obtained. The charges thus obtained were used in conjunction with the charge potential model ( $k_c = 25.0$ ) to obtain theoretical shifts

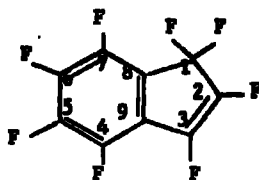
CHARGE DISTRIBUTION IN PERFLUOROINDENE



Figure(4.3)

Table 4.7

Charge distributions in prefluoroindene



<u>Position</u>	<u>CNDO Charges</u>		<u>Simple Assignment<sup>(a)</sup></u>			<u>Detailed Assignment<sup>(a)</sup></u>			
	C	F	$(E-E^0)_C$	C	Charges	F	$(E-E^0)_C$	C	Charges
1	0.424	-0.197	7.4	0.438	-0.205	7.4	0.442	-0.204	
2	0.098	-0.148	4.4	0.137	0.156	3.9	0.111	-0.149	
3	0.196	-0.171	4.4	0.187	-0.162	4.2	0.186	-0.159	
4	0.190	-0.169	4.4	0.190	-0.164	4.3	0.184	-0.162	
5	0.168	-0.156	4.4	0.161	-0.159	4.5	0.169	-0.160	
6	0.153	-0.157	4.4	0.161	-0.159	4.3	0.144	-0.158	
7	0.213	-0.168	4.4	0.192	-0.164	5.0	0.227	-0.172	
8	-0.067	-	2.4	-0.067	-	2.6	-0.060	-	
9	-0.012	-	2.4	-0.036	-	2.2	-0.046	-	

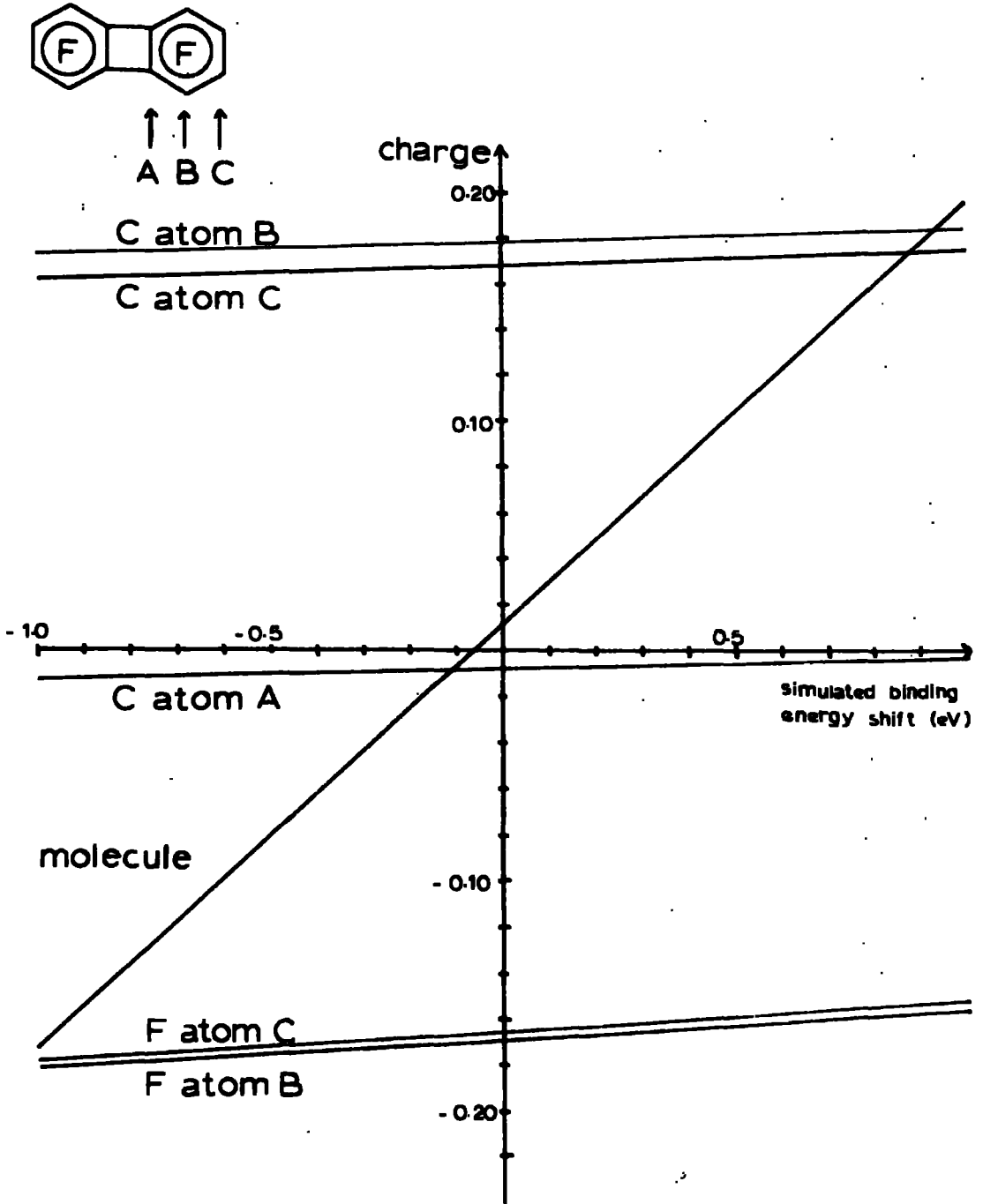
(a)  $(E-E^0)_F = -2.4$

for each carbon atom and were then compared with the experimental values to obtain the detailed assignment. The charge distributions for perfluoroindene obtained from the CNDO calculations, from the simple deconvolution and from the detailed deconvolution are shown in table 4.7 and figure 4.3. The experimental charge distributions obtained are both in very good agreement with the CNDO charges and that for the first deconvolution is extremely good considering the simplicity of the deconvolution and assignments involved. These calculations show clearly that reasonable charge distributions within quite complex molecules can readily be obtained by simple deconvolutions and assignments, although some slight loss of detail may occur compared with detailed assignments.

b) Use of Experimental Charge Distributions for Detecting Sample Charging Effects

One important source of error in determining absolute binding energies using the ESCA technique is the slight build up of charge which may occur when studying insulating solids. This has been discussed previously (Chapter I.5). Calibration with respect to hydrocarbon contamination and sample backing are methods which have been used to overcome this. However, when studying organic molecules these approaches obviously have very limited applicability and the usual technique employed in this laboratory has been to study very thin films of the sample on a conducting gold backing. This technique minimizes

SIMULATED SAMPLE CHARGING FOR PERFLUOROBIPHENYLENE



Figure(4.4)

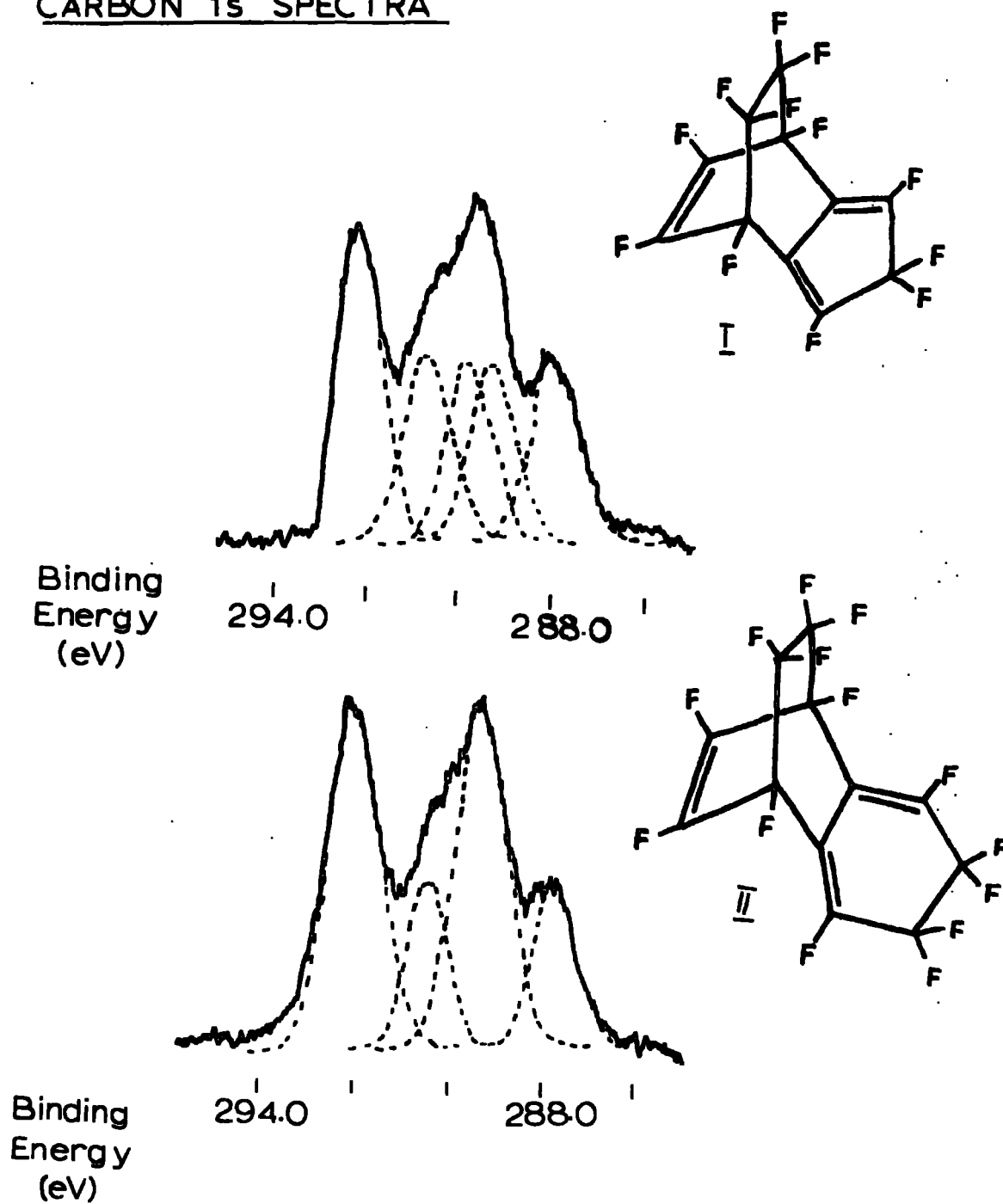
sample charging effects, although in some cases some uncertainty may still remain. It is therefore of interest to simulate this effect and to determine its effect on the experimental charges by changing the binding energies of all the atoms within a molecule by the same amount (an increase in binding energy implies a positive charge on the sample). This has been carried out for the particular case of perfluorobiphenylene by incrementing the experimentally determined core binding energies in steps of 0.2eV to simulate changes in binding energies caused by sample charging of between  $\pm 1$ eV. The results are shown in figure 4.4. There is a slight linear increase of experimental charge with increased positive charging effect for each atom in the molecule, the rate of increase for the fluorine atoms being slightly larger than that for the carbon atoms. Although there is little effect on the experimental charge of each individual atom, the total effect on the apparent charge of the whole molecule is quite significant and this ranges between -0.172 and + 0.196. Thus once reliable values of  $k$  and  $E^0$  have been obtained, it should be possible to use the 'total experimental charge' on a molecule (i.e.  $\sum_i q_i$ ) to estimate the extent to which sample charging has occurred. (For no charge build up  $\sum_i q_i \approx 0$ ).

### c) Charge Distributions in Large Molecules

The inverted charge potential model yields very good results for simple fluorocarbon compounds of moderate size as was shown by comparison with the CNDO results (Chapter IV.3a). The compounds dodecafluorotricyclo[5,2,2,0<sup>2,6</sup>] undeca-2,5,8triene(I) and

tetradecafluorotricyclo[6,2,2;<sup>2,7</sup>] dodeca2,6,9triene<sup>203</sup> (II) provide examples of complex systems containing a wider variety of bonding situations. The size of these molecules means that the CNDO charge distributions are computationally expensive to obtain and they are also near the size limit imposed by the CNDO/2 program presently in use. They therefore present a rigorous test of this experimental method of determining charge distributions.

The samples, liquids, were condensed as thin films on a gold backing on a cooled probe. The line shapes used for the deconvolutions were derived from the relatively well resolved peak at highest binding energy for both (I) and (II) and were approximately gaussian. The  $C_{1s}$  spectra are quite well resolved and are shown in figure 4.5 together with the deconvolutions into their component peaks. Compound (II) has four component peaks with area ratio, in order of decreasing binding energy, 4:2:4:2. By comparison with the known molecular formula, together with the fact that increasing the number of fluorines bonded to a carbon atom increases its  $1s$  binding energy these are assigned to the ( $>CF_2$ ) carbons, the tertiary ( $-CF$ ) carbons, the vinylic ( $-C^H-F$ ) carbons and the bridgehead ( $=C<$ ) carbons respectively. Compound (I) has five component peaks in the area ratio 3:2:2:2:2. The two types of vinylic  $-C^H-F$  carbons have slightly different binding energies (289.9 and 289.4eV) but are still readily distinguishable from the tertiary  $-CF$  carbons at higher binding energy (290.9eV). The experimental binding energies and assignments are listed in table 4.8. Using these binding energies and assignments, (the average vinylic  $CF$  binding energy being

CARBON 1s SPECTRA

Figure(4.5)

used for compound (I)) together with the parameters derived previously (Chapter IV.3.a) the experimental charge distributions were determined

Table 4.8

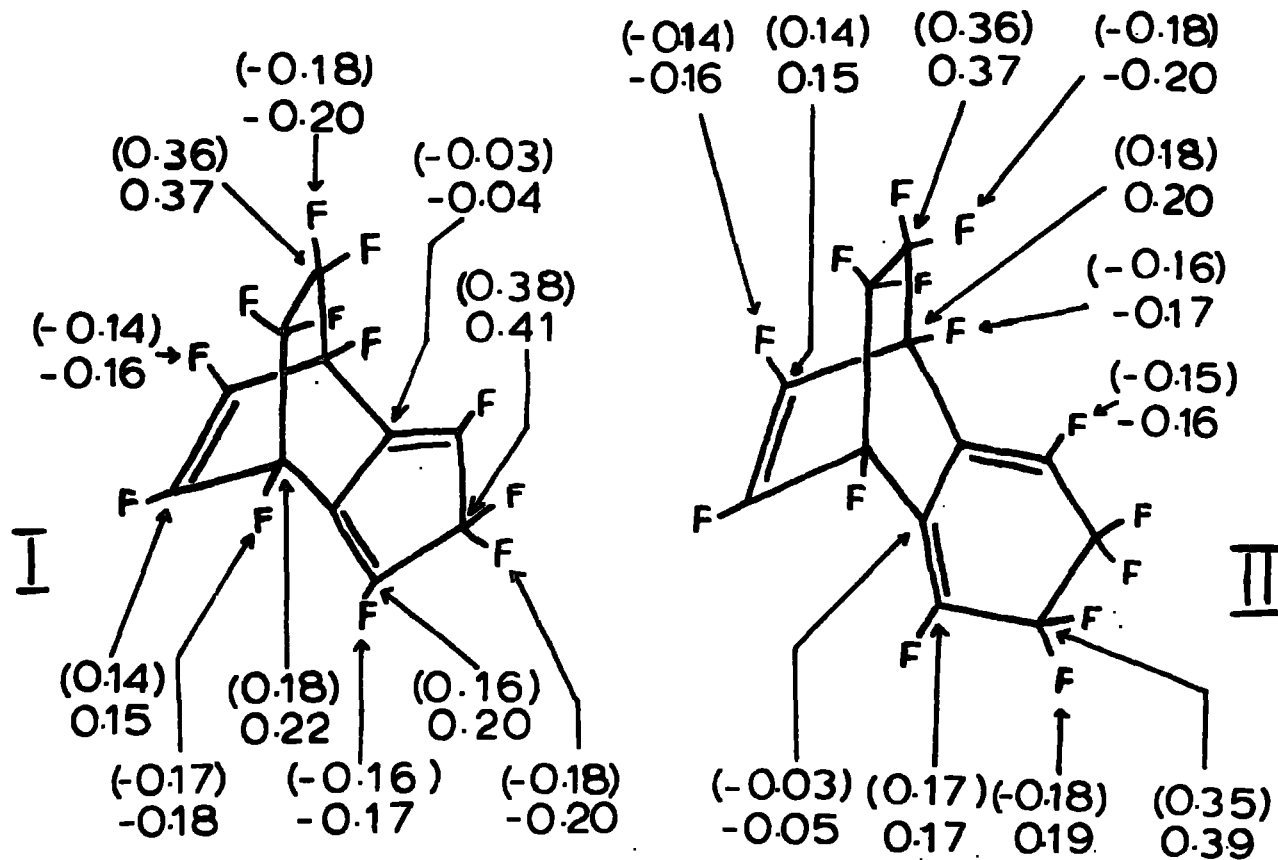
Experimental binding energies and assignments for compounds I and II

Environment of atom	Compound (I)		Compound (II)	
	Binding energy (eV)	Area ratio	Binding energy (eV)	Area ratio
	$C_{1s}$		$C_{1s}$	
	292.3	3	292.3	4
	290.9	2	290.6	2
	289.9	2	289.4	4
	289.65			
	289.4	2		
	288.0	2	287.8	2
	$F_{1s}$		$F_{1s}$	
All F atoms	690.9		691.0	

and are shown in figure 4.6. In order to obtain the direct comparison between experimental and theoretical charge distributions required to test the method for these complex systems CNDO calculations were carried

# EXPERIMENTAL CHARGE DISTRIBUTIONS IN LARGE MOLECULES

Figure(4.6)



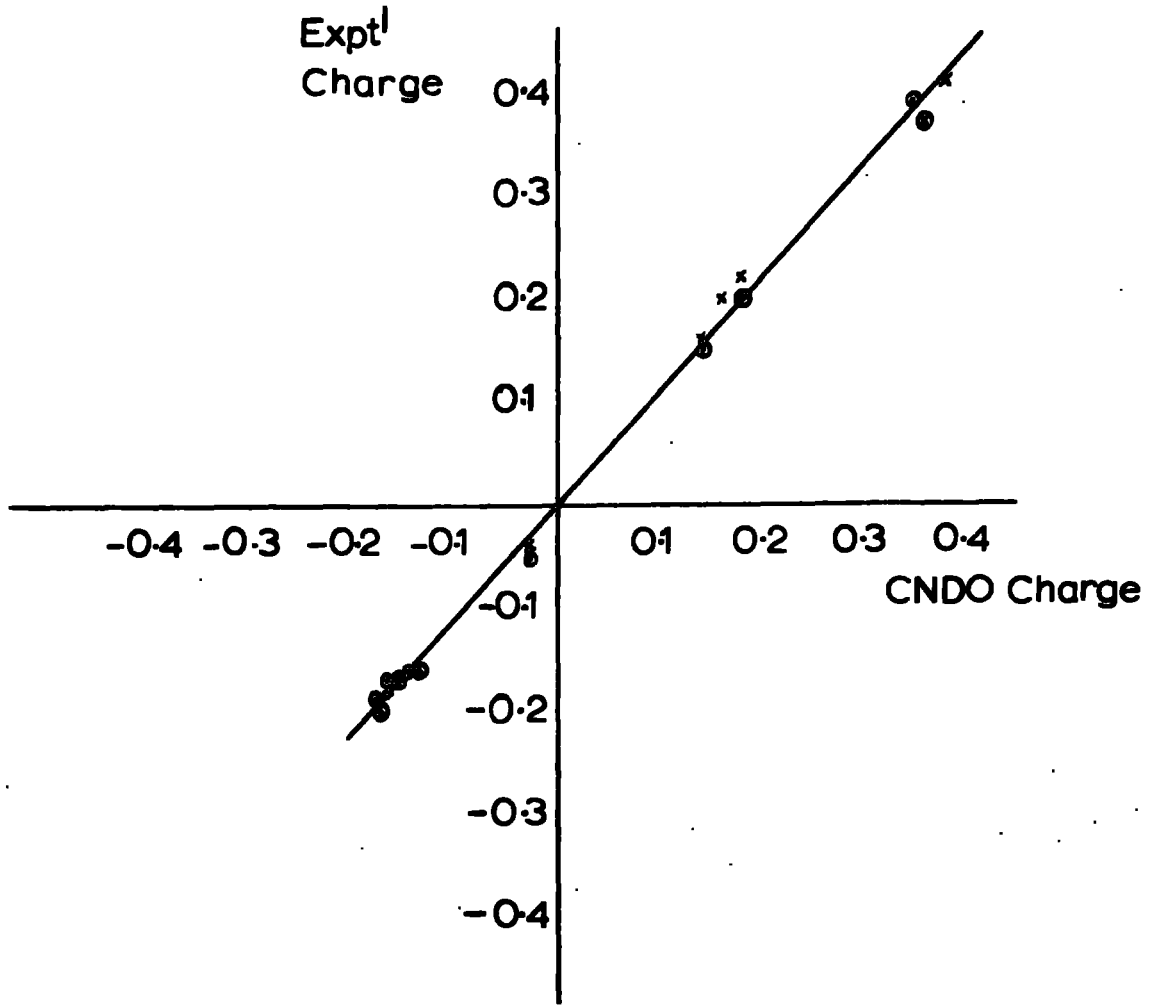
( ) CNDO/2 Charges

# Charge distributions in Perfluoro Tricyclic compounds.

x = 5 membered ring

⊙ = 6 " "

Figure (4.7)



$$q_{\text{exp}} = -0.003 + 1.079 q_{\text{CNDO}} \quad (\pm 0.008)$$

$$R^2 = 0.99$$

out and the results are also shown in figure 4.6. However, the calculations were rather lengthy and required about 12 minutes of c.p.u. time on an IBM 360/67 using an energy convergence limit of 0.0002 a.u.

A least squares fit between experimental and CNDO/2 charges gives the relationships

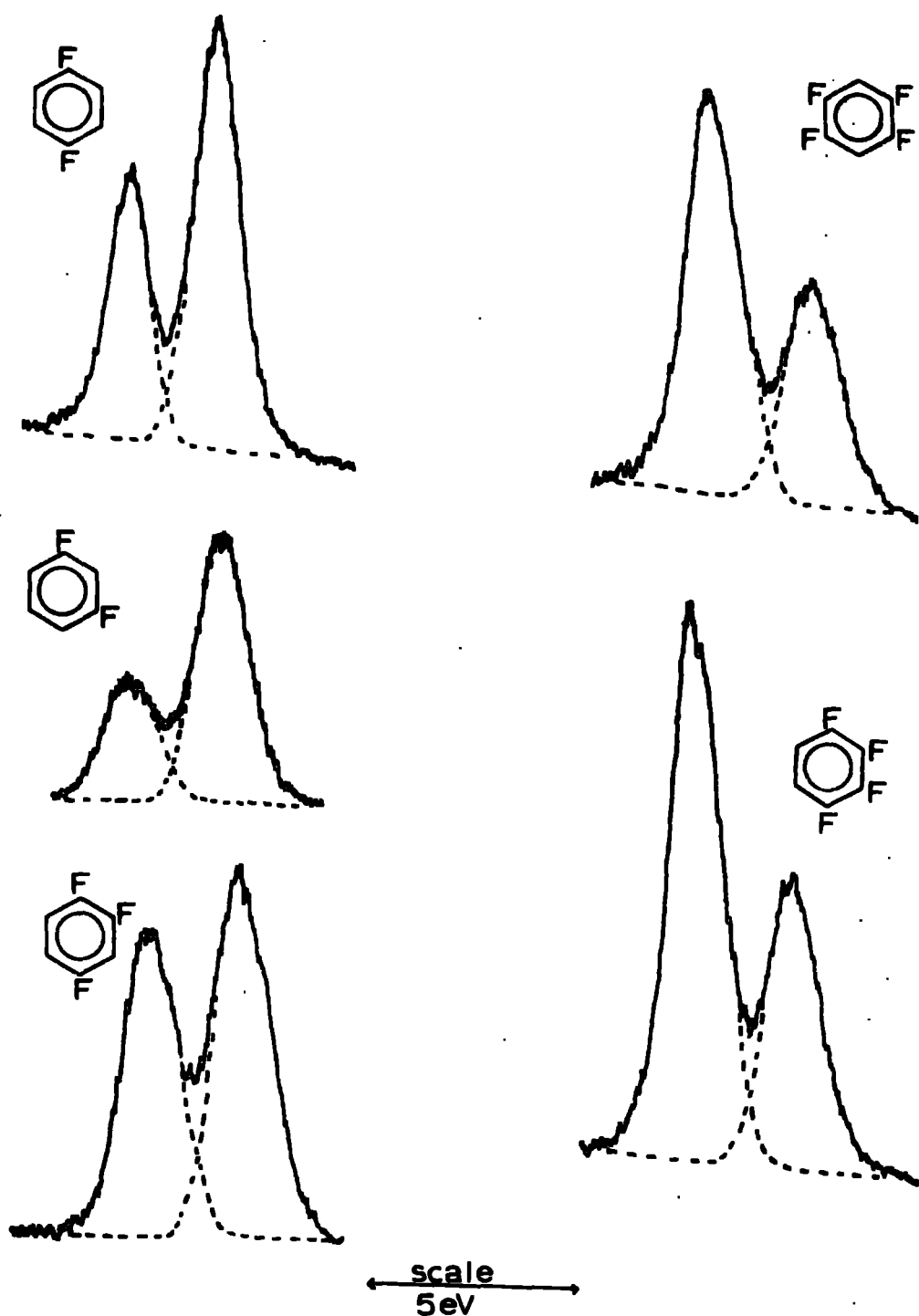
$$q_{\text{exp}} = 0.00 + 1.10 q_{\text{CNDO}} \quad \text{for compound I} \\ (\pm 0.01)$$

$$q_{\text{exp}} = 0.00 + 1.08 q_{\text{CNDO}} \quad \text{for compound II} \\ (\pm 0.01)$$

This is remarkably good considering both the size and complexity of the molecules and the correlation coefficient in both cases is better than 0.99. The overall correlation for the two molecules is shown figure 4.7.

#### d) Experimental Charge Distributions in the Fluorobenzenes

The fluorobenzenes represent systems which contain three elements per compound and therefore provide a more stringent test of the parameters  $k$  and  $E^0$  previously determined. Clark et al.<sup>72</sup> have carried out binding energy measurements, CNDO/2 calculations and detailed deconvolutions on the complete series of fluorobenzenes studied in the condensed phase. The peaks corresponding to the C-H and C-F carbon atoms were well resolved with an average shift of about 2.3eV between them. Typical  $C_{1s}$  spectra and their simple deconvolutions into C-H and C-F peaks are shown in figure 4.8. Since average binding energies have been shown to give

TYPICAL C1s SPECTRA of FLUOROBENZENES†

† Spectra recorded by Dr. D. Kilcast

Figure(4.8)

experimental charge distributions in good agreement with CNDO/2 calculations (Chapter IVa,c) the binding energies used for these calculations were obtained from the centroids of the C-H and C-F peaks even in cases of low symmetry. In many cases of high symmetry, (e.g. 1,4 difluorobenzene) there is only one possible assignment but in other cases (e.g.  $C_6F_5H$  where there are three environments of C-F carbons) detailed deconvolutions and CNDO/2 calculations would be required for a detailed assignment. However, the experimental charges are required to be determined independently of any molecular orbital calculations.

The parameters for carbon and fluorine used in these calculations were those previously obtained from the study of the aromatic hydrocarbons and fluorocarbons (Chapter IV.3.a).

$$\begin{array}{ll}
 E_F^{\circ} = 693.2 \text{ eV} & E_C^{\circ} = 284.6 \text{ eV} \\
 k_F = 30 \text{ eV/unit charge} & k_C = 25 \text{ eV/unit charge}
 \end{array}$$

The experimental binding energies and  $E-E^{\circ}$  values used in the calculations are listed in table 4.9. The calculations of the binding energies were carried out initially using the same parameters for hydrogen as previously i.e.  $k_H = 25.0$ ,  $(E-E^{\circ})_H = 0.1$ . However, a direct comparison with the CNDO results indicated that while the fluorine charges and the charges for the C-F carbon atoms were in good agreement with the CNDO/2 charges the charges for the C-H carbons were too high

Average Experimental Binding Energies for the Fluorobenzenes

Compound	<u>C-F</u>		<u>C-H</u>		F	
	BE	$E-E_c^0$	BE	$E-E_c^0$	BE	$E-E_F^0$
1-F	287.8	+ 3.2	285.6	+ 1.0	689.6	- 3.6
1,2-F	288.2	+ 3.6	285.8	+ 1.2	689.8	- 3.4
1,3-F	288.4	+ 3.8	286.1	+ 1.5	689.8	- 3.4
1,4-F	288.3	+ 3.7	286.2	+ 1.6	689.8	- 3.4
1,2,3-F	288.2	+ 3.6	286.0	+ 1.4	690.1	- 3.1
1,2,4-F	288.5	+ 3.9	286.3	+ 1.7	690.1	- 3.1
1,3,5-F	288.8	+ 4.2	286.3	+ 1.7	690.3	- 2.9
1,2,3,4-F	290.0	+ 5.4	286.7	+ 2.1	690.5	- 2.7
1,2,3,5-F	289.2	+ 4.6	286.9	+ 2.3	690.5	- 2.7
1,2,4,5-F	288.8	+ 4.2	286.4	+ 1.8	690.4	- 2.8
1,2,3,4,5-F	289.2	+ 4.6	286.9	+ 2.3	690.7	- 2.5
Perfluorobenzene	289.5	+ 4.9	-	-	690.9	- 2.3

(+ ve) while those for hydrogen were too low (-ve). However the trends in the charges were followed. Table 4.10 shows the typical case of

Table 4.10

Experimental Charge Distributions in 1,3 Difluorobenzene as a Function of  $(E-E^0)_H$ .

	$(E-E^0)_H$					<u>CNDO/2</u>
	<u>0.1</u>	<u>0.5</u>	<u>1.0</u>	<u>2.0</u>	<u>3.0</u>	
$C_{1,3}$	0.228	0.227	0.226	0.222	0.220	0.255
$C_2$	-0.022	-0.034	-0.050	-0.075	-0.103	-0.104
$C_{4,6}$	0.010	-0.001	-0.015	-0.043	-0.070	-0.070
$C_5$	0.046	0.035	0.021	-0.006	-0.034	0.043
$F_{1,3}$	-0.196	-0.199	-0.204	-0.212	-0.221	-0.200
$H_2$	-0.018	0.003	0.031	0.085	0.139	0.041
$H_{4,6}$	-0.027	-0.007	0.018	0.069	0.119	0.023
$H_5$	-0.035	-0.016	0.007	0.054	0.101	0.006

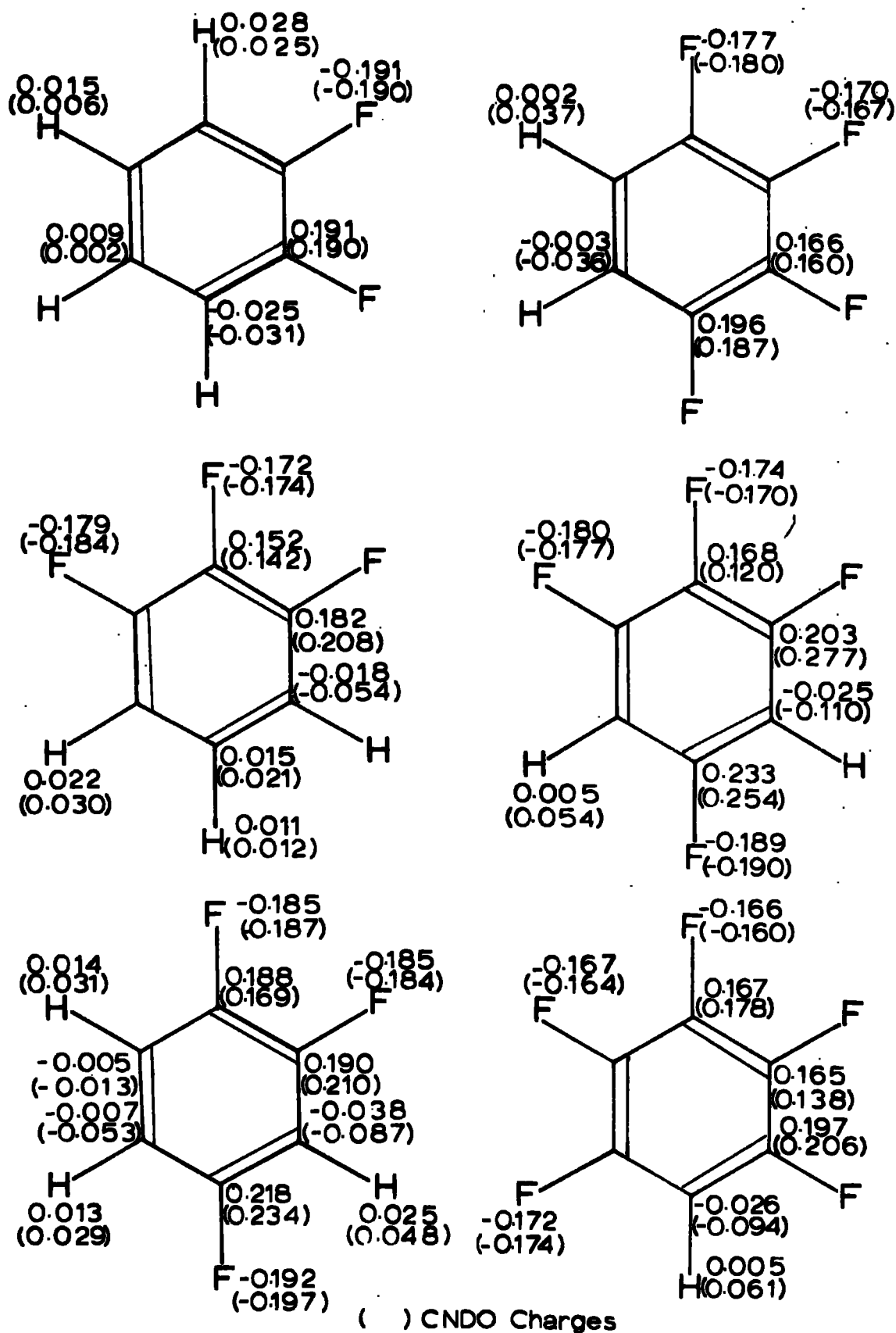
1,3difluorobenzene. Since the discrepancy occurred in connection with the hydrogen and carbon atoms attached to hydrogen, (for hydrogen values of  $k$  and  $(E-E^0)$  are somewhat arbitrary), the charge distribution was recalculated using various values of  $(E-E^0)_H$  and these results are also listed in table 4.10. The values  $(E-E^0)_H = 1.0\text{eV}$  and  $k_H = 25.0$  were taken as a reasonable overall compromise although the deviations were slightly greater than those of the previous compounds.

Table 4.11

## Charge Distributions in the Fluorobenzenes

Compound	Position	Carbon		Hydrogen		Fluorine	
		CNDO/2	Expt.	CNDO/2	Expt.	CNDO/2	Expt.
1-F	1	0.229	0.209	-	-	-0.205	-0.203
	2,6	-0.049	-0.028	0.017	0.032	-	-
	3,5	0.027	0.005	0.000	0.020	-	-
	4	-0.012	0.003	-0.001	0.019	-	-
1,2-F	1,2	0.190	0.191	-	-	-0.190	-0.191
	3,6	-0.031	-0.025	0.025	0.028	-	-
	4,5	0.002	0.009	0.006	0.015	-	-
1,3-F	1,3	0.255	0.226	-	-	-0.200	-0.204
	2	-0.104	-0.050	0.041	0.031	-	-
	4,6	-0.070	-0.015	0.023	0.018	-	-
	5	0.043	0.021	0.006	0.007	-	-
1,4-F	1,4	0.214	0.214	-	-	-0.203	-0.203
	2,3,5,6	-0.029	-0.006	0.024	0.016	-	-
1,2,3-F	1,3	0.208	0.182	-	-	-0.184	-0.179
	2	0.142	0.152	-	-	-0.174	-0.172
	4,6	-0.054	-0.018	0.030	0.022	-	-
	5	0.021	0.015	0.012	0.011	-	-
1,2,4-F	1	0.169	0.188	-	-	-0.187	-0.185
	2	0.210	0.190	-	-	-0.184	-0.185
	3	-0.087	-0.038	0.048	0.025	-	-
	4	0.234	0.218	-	-	-0.197	-0.192
	5	-0.052	-0.007	0.029	0.013	-	-
	6	-0.013	-0.005	0.031	0.014	-	-
1,3,5	1,3,5	0.274	0.234	-	-	-0.194	-0.189
	2,4,6	-0.126	-0.051	0.046	0.022	-	-
1,2,3,4-F	1,4	0.187	0.196	-	-	-0.180	-0.177
	2,3	0.160	0.166	-	-	-0.167	-0.170
	5,6	-0.036	-0.003	0.037	0.002	-	-
1,2,3,5-F	1,3	0.227	0.203	-	-	-0.177	-0.180
	2	0.120	0.168	-	-	-0.170	-0.174
	4,6	-0.110	-0.025	0.054	0.005	-	-
	5	0.254	0.233	-	-	-0.190	-0.189
1,2,4,5-F	1,2,4,5	0.188	0.194	-	-	-0.180	-0.177
	3,6	-0.070	-0.043	0.056	0.021	-	-
1,2,3,4,5	1,5	0.206	0.197	-	-	-0.174	-0.172
	2,4	0.138	0.165	-	-	-0.164	-0.167
	3	0.178	0.167	-	-	-0.160	-0.166
	6	-0.094	-0.026	0.061	0.005	-	-
Per F benzene		0.155	0.168	-	-	-0.155	0.164

# EXPERIMENTAL CHARGE DISTRIBUTIONS in some FLUOROBENZENES



Figure(4.9)

The charge distributions for the remainder of the fluorobenzenes were therefore calculated using this parameter set and are shown in table 4.11. The correlation between CNDO/2 and experimental charges is extremely good and a least squares analysis of the data gives the relationship

$$q_{\text{exp}} = 0.004 + 0.913 q_{\text{CNDO}} \\ (\pm 0.024)$$

With the exception of the para carbon atom in monofluorobenzene, the signs of the charges are all correctly predicted. Fluorine charges are predicted with great accuracy and the experimental and CNDO/2 charges on the carbons attached to fluorine are also very close. The trends in the ordering of charges are also reproduced well and some examples are illustrated in figure 4.9. Some of these examples have been taken from molecules of low symmetry to emphasise that the order of the charges is well reproduced for all atoms including hydrogen. (These examples also include molecules for which detailed deconvolutions would have been required for a complete assignment).

#### e) Experimental Charge Distributions in the Chlorobenzenes

The chlorobenzenes represent an interesting series of compounds to study from the point of view of experimental charge distributions since the shifts in  $C_{1s}$  binding energies are less than those obtained in the fluorobenzenes, (about 1.4eV compared with about 2.3eV between substituted and unsubstituted carbon atoms). In second row elements,

such as sulphur or chlorine, there is also the question of whether or not 3d orbital participation in bonding is important. Where comparisons are available with non-empirically calculated wave functions, as for example in the case of thiophen,<sup>204</sup> they show that CNDO/2 calculations over emphasise the importance of 3d orbitals in the bonding of second row atoms. This factor must be borne in mind when using CNDO/2 calculations as a model for interpreting ESCA chemical shifts.

Molecular core binding energies have been measured and detailed deconvolutions carried out for the chlorobenzenes studied in the condensed phase.<sup>205</sup> CNDO/2 calculations have also been performed on these molecules using basis sets which included<sup>205</sup> and excluded 3d orbitals (this work). These data, together with a recalculation of the CNDO/2 charges excluding 3d orbitals for a series of halomethanes<sup>77c</sup> show that the inclusion, or exclusion, of 3d orbitals may affect the k values of both chlorine and carbon (Table 4.12).

Table 4.12

k-Values in Chloro compounds

Halogenated methanes	$k_c = 28.7,$	$k_{Cl} \approx 31$	(a)
	$k_c = 26.6,$	$k_{Cl} \approx 24.5$	(b)
Chlorobenzenes	$k_c = 31.3,$	$k_{Cl} \approx 30$	(a)
	$k_c = 23.2,$	$k_{Cl} \approx 31$	(b)

(a) Including 3d orbitals on chlorine

(b) Excluding 3d orbitals on chlorine

The  $k$  values for chlorine are subject to much larger errors than those for carbon, especially in the case of the chlorobenzenes where the range of shifts was extremely small. The  $k$  values found for carbon when  $d$  orbitals are included in the chlorine basis set are significantly larger than when  $d$  orbitals are excluded. Since the role of  $3d$  orbitals in second row atoms is overemphasised by CNDO/2 calculations, the discussion of the charge distribution is based on the analysis which excludes  $3d$  orbitals from the chlorine basis set.

The parameters used were

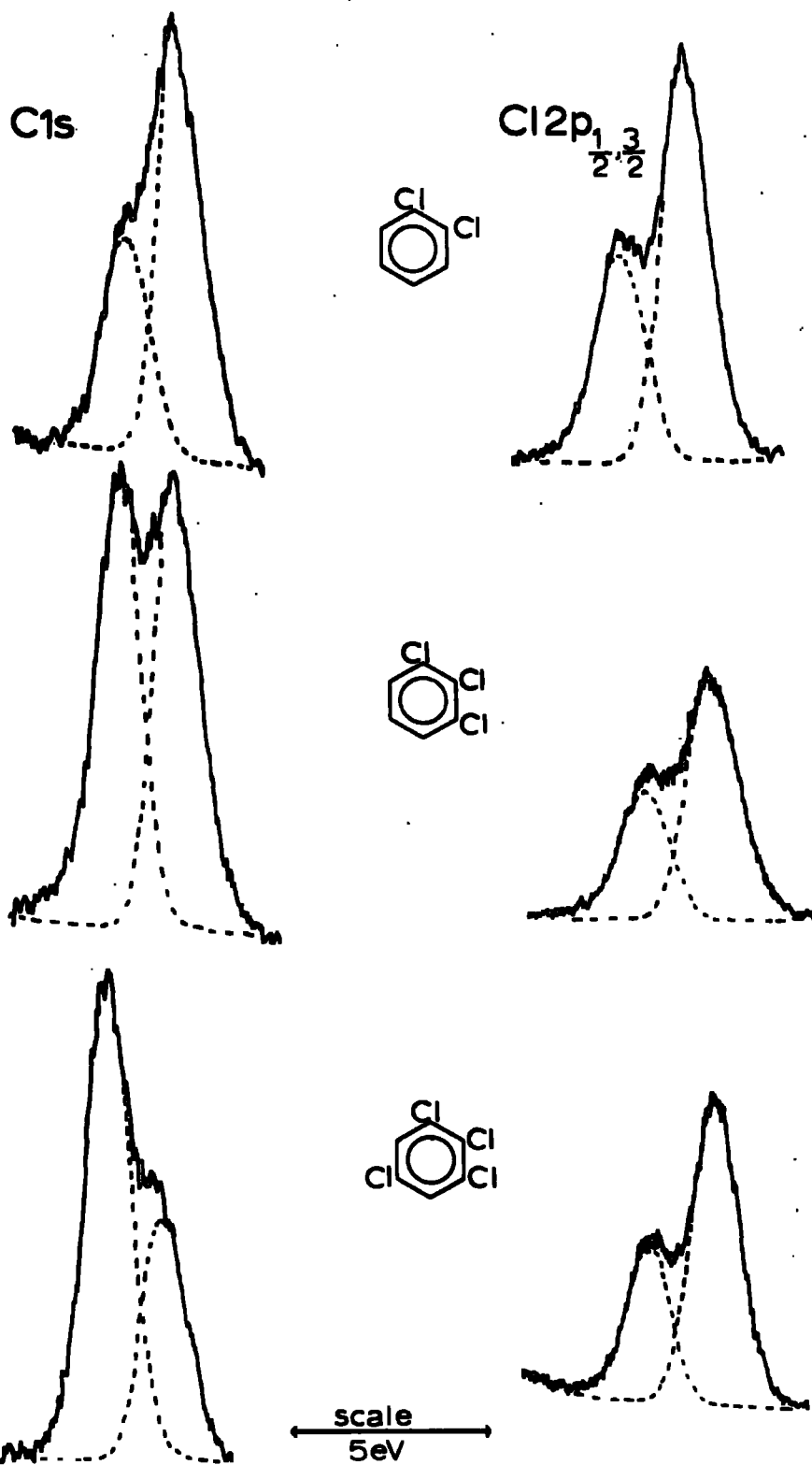
$$\begin{array}{ll} E_c^0 = 284.6 & (E-E^0)_H = 1.0 \\ k_c = 25 & k_H = 25 \end{array}$$

These maintain consistency with the previously used values which have been shown to give good results for fluorobenzenes and aromatic fluorocarbon compounds. The parameters for chlorine

$$E_{Cl}^0 = 203 \quad k_{Cl} = 24.5$$

were taken from the analysis of the chlorine-containing halomethanes when the  $3d$  orbitals had been excluded from the basis set. These values, although still subject to large error, are more reliable than those obtained from the study of the chlorobenzenes themselves since a greater range of shifts in chlorine core electron binding energies

# TYPICAL C1s and Cl 2p SPECTRA of CHLOROBENZENES†



†Spectra recorded by Dr. D.Kilcast

**Figure(4.10)**

Average Binding energies for the chlorobenzenes

Compound	C-H		C-Cl		Cl <sub>2</sub> P <sub>3/2</sub>	
	BE	E-E <sup>o</sup>	BE	E-E <sup>o</sup>	BE	E-E <sup>o</sup>
1-Cl	285.7	1.1	287.1	2.5	201.0	-2.0
1,2-Cl	285.4 <sub>5</sub>	0.8 <sub>5</sub>	286.8	2.2	201.3	-1.7
1,3-Cl	285.9	1.3	287.2	2.6	201.2	-1.8
1,4-Cl	285.8	1.2	286.9	2.3	201.1	-1.9
1,2,3-Cl	285.9	1.3	287.4	2.8	201.4	-1.6
1,2,4-Cl	285.9	1.3	287.2	2.6	201.1	-1.9
1,3,5-Cl	285.6	1.0	287.1	2.5	201.4	-1.6
1,2,3,4-Cl	286.1	1.5	287.6	3.0	201.4	-1.6
1,2,3,5-Cl	286.1	1.5	287.5	2.9	201.3	-1.7
1,2,4,5-Cl	286.1	1.5	287.4	2.8	201.4	-1.6
1,2,3,4,5-Cl	286.2	1.6	287.5	2.9	201.4	-1.6
1,2,3,4,5,6-Cl	-	-	287.6	3.0	201.4	-1.6

$$E_c^o = 284.6$$

$$E_{Cl_2P_{3/2}}^o = 203.0$$

is involved. The use of these parameters for carbon and chlorine also maintains complete independence of the experimental charges for the chlorobenzenes and the CNDO/2 calculations performed on them.

The  $C_{1s}$  spectra are readily deconvoluted into the components corresponding to  $\underline{C}$ -Cl and  $\underline{C}$ -H carbons using the Du Pont 310 curve resolver and are in the area ratio corresponding to that of the numbers of the two types of carbon. It was these average  $\underline{C}$ -Cl and  $\underline{C}$ -H binding energies which were used in the following analysis of the charge distributions. This again maintains the independence from the CNDO/2 calculations which would be required for a detailed assignment and also average binding energies provided good results in the fluorocarbon cases. The chlorine binding energies used are the  $Cl_{2p_{3/2}}$  components of the  $2p_{1/2,3/2}$  doublet, the resolution of the two components being the same in both symmetrical and unsymmetrical cases. Typical  $C_{1s}$  and  $Cl_{2p}$  spectra are shown in figure 4.10 together with the deconvolutions into their component peaks. The average experimental binding energies for the chlorobenzenes and the values of  $E-E^0$  used are listed in table 4.13. The experimental charge distributions and the CNDO charges calculated excluding 3d orbitals are shown in table 4.14. The comparison with CNDO charges is not as good as those found previously but the ordering of the charges within molecules and general trends are still reproduced quite well. The correlation between calculated and experimental charges is

$$q_{\text{exp}} = 0.002 + 0.951 q_{\text{CNDO}} \\ (\pm 0.015)$$

Table 4.14

## Charge Distributions in the Chlorobenzenes

Compound	Position	CARBON		HYDROGEN		CHLORINE	
		CNDO/2	Expt'	CNDO/2	Expt'	CNDO/2	Expt'
1-Cl	1	0.125	0.130	-	-	-0.155	-0.141
	2,6	-0.022	-0.011	0.013	0.031	-	-
	3,5	0.023	0.009	0.000	0.017	-	-
	4	0.004	0.007	-0.002	0.002	-	-
1,2-Cl	1,2	0.120	0.100	-	-	-0.136	-0.114
	3,6	-0.008	-0.019	0.017	0.033	-	-
	4,5	0.003	-0.001	0.005	0.024	-	-
1,3-Cl	1,3	0.140	0.127	-	-	-0.144	-0.132
	2	-0.051	-0.022	0.031	0.029	-	-
	4,6	-0.024	-0.004	0.017	0.020	-	-
	5	0.038	0.016	0.006	0.013	-	-
1,4-Cl	1,4	0.123	0.113	-	-	-0.148	-0.133
	2,3,5,6	-0.006	-0.003	0.0183	0.025	-	-
1,2,3-Cl	1,3	0.127	0.116	-	-	-0.127	-0.117
	2	0.098	0.096	-	-	-0.114	-0.111
	4,6	-0.022	-0.008	0.021	0.021	-	-
	5	0.011	0.014	0.010	0.013	-	-
1,2,4-Cl	1	0.105	0.111	-	-	-0.128	-0.127
	2	0.127	0.112	-	-	-0.124	-0.126
	3	-0.032	-0.022	0.034	0.032	-	-
	4	0.133	0.127	-	-	-0.139	-0.135
	5	-0.021	-0.004	0.022	0.023	-	-
	6	0.001	-0.003	0.022	0.024	-	-
1,3,5-Cl	1,3,5	0.155	0.129	-	-	-0.134	-0.118
	2,4,6	-0.054	-0.040	-0.034	-0.037	-	-
1,2,3,4-Cl	1,4	0.111	0.119	-	-	-0.120	-0.120
	2,3	0.104	0.101	-	-	-0.106	-0.112
	5,6	-0.014	-0.017	0.025	0.017	-	-
1,2,3,5-Cl	1,3	0.134	0.118	-	-	-0.116	-0.121
	2	0.083	0.099	-	-	-0.108	-0.115
	4,6	-0.047	-0.020	0.036	0.025	-	-
	5	0.139	0.135	-	-	-0.130	-0.128
1,2,4,5-Cl	1,2,4,5	0.111	0.112	-	-	-0.118	-0.116
	3,6	-0.024	-0.015	0.038	0.025	-	-
1,2,3,4,5-Cl	1,5	0.117	0.114	-	-	-0.111	-0.114
	2,4	0.089	0.097	-	-	-0.101	-0.110
	3	0.111	0.098	-	-	-0.098	-0.110
	6	-0.040	-0.013	0.040	0.023	-	-

Considering the uncertainties involved in the  $k$  and  $E^0$  values for chlorine and the rather arbitrary way in which the parameters  $k_H = 25$  and  $(E-E^0)_H = 1.0$  were assumed this relationship is surprisingly good. Further studies of related systems should provide more reliable values of  $k$  and  $E^0$  for the elements involved.

4) A NOTE ON THE USE OF CNDO/2 CALCULATIONS ON MOLECULES CONTAINING SECOND ROW ELEMENTS FOR THE ASSIGNMENT OF SHIFTS IN MOLECULAR CORE BINDING ENERGIES.

As has been shown in this and other work<sup>17,71,72</sup> the charge potential model used in conjunction with charges obtained from CNDO/2 calculations forms an excellent basis for the discussion of ESCA results for molecules containing first row atoms. However for second row elements the charges calculated by the CNDO method are dependant on the inclusion, or exclusion, of 3d orbitals from the basis set.<sup>147</sup> There is the possibility that calculations employing different basis sets may lead to different assignments of binding energies within a molecule. That such differences in the predicted order of binding energies can, and often do, occur is illustrated by the examples in table 4.15 which shows the predicted orders of binding energies and the CNDO charge distributions using the two basis sets.

Such differences in the predicted orders of binding energies only occur, however, for atoms which have small differences in binding energy and with the present instrumentation (A.E.I. ES100) the

Table 4.15

Comparison of Orders of Binding Energies and Charge Distributions in some Chlorobenzenes using  
CNDO calculations including and excluding 3d orbitals

Molecule	Position	<u>INCLUDING d ORBITALS</u>				<u>EXCLUDING d ORBITALS</u>			
		Calculated Order of C <sub>1s</sub> Binding Energies	C	Cl	H	Calculated Order of C <sub>1s</sub> Binding Energies	C	Cl	H
1,3 Cl	1,3	1	0.091	-0.159	-	1	0.140	-0.144	-
	2	2	0.030	-	0.025	4	-0.051	-	0.031
	4,6	3	0.020	-	0.016	3	-0.024	-	0.017
	5	4	0.010	-	0.009	2	0.038	-	0.006
1,2,3 Cl	1,3	2	0.098	-0.136	-	1	0.127	-0.127	-
	2	1	0.113	-0.124	-	2	0.098	-0.114	-
	4,6	3	0.016	-	0.020	4	-0.022	-	0.020
	5	4	0.004	-	0.013	3	0.011	-	0.010
1,2,4 Cl	1	2	0.082	-0.123	-	3	0.105	-0.127	-
	2	3	0.073	-0.121	-	1	0.127	-0.124	-
	3	5	0.018	-	0.033	5	-0.032	-	0.034
	4	1	0.088	-0.141	-	2	0.134	-0.139	-
	5	4	0.027	-	0.023	6	-0.021	-	0.022
	6	6	0.017	-	0.024	4	0.001	-	0.022
1,2,3,5	1,3	2	0.098	-0.128	-	1	0.134	-0.116	-
	2	1	0.117	-0.117	-	3	0.083	-0.108	-
	4,6	4	0.025	-	0.033	4	-0.047	-	0.036
	5	3	0.082	-0.137	-	2	0.140	-0.130	-

calculated differences are generally within the experimental error of the binding energy measurements (approximately  $\pm 0.2\text{eV}$ ). The different theoretical assignments sometimes obtained by use of these different basis sets should not, therefore, lead to any serious misinterpretation of any results previously obtained.

## 5) DISCUSSION

The above analysis of charge distributions from ESCA data was a direct attempt to reproduce the charge distributions obtained from CNDO/2 calculations and very good results were obtained even for complex molecules using simple assignments of binding energies. Since in an SCF MO treatment the values of  $k$  and  $E^{\circ}$  depend on the definition of atomic charge and the basis set used there is the possibility that by use of suitable  $k$  and  $E^{\circ}$  parameters it may be possible to predict the charges which would have been obtained from computationally much more expensive ab initio treatments of the molecules.

The parameterization used for hydrogen is somewhat arbitrary and a value of  $(E-E^{\circ})_{\text{H}} = 1.0$  was found to give a better fit to the CNDO charges for the fluorobenzenes than the value  $(E-E^{\circ})_{\text{H}} = 0.1$  used with the aromatic hydrocarbon compounds. The binding energies of the C-H carbons in the fluorobenzenes are greater than those in the aromatic hydrocarbons and this suggests that the optimum value of  $(E-E^{\circ})_{\text{H}}$  to use may depend somewhat on the binding energy shift of the atom to which the hydrogen is bonded. In an independent, but essentially similar,

calculation of the charge distributions in some fluorobenzenes<sup>87</sup> Davis et al. eliminated the problem of parameterization for hydrogen by considering that all the hydrogen atoms in a molecule had the same charge and imposing the condition that  $\sum_i q_i = 0$ . While this procedure circumvents the problem, the values of  $k_H$  and  $(E-E^0)_H$  used above predict the correct ordering of the hydrogen charges within molecules of low symmetry where the hydrogen atoms do not have equal charges (Figure 4.9). With solid samples the imposition of the condition  $\sum_i q_i = 0$  also has the disadvantage that large deviations from this relationship could not be used to detect charging effects. The  $k$  values used by Davis et al.<sup>87</sup> were  $k_C = 22.0$  and  $k_F = 32.5$  and the sensitivity of the derived charge with change in  $k$  value was found to be slight. (This is in qualitative agreement with the work reported here where the initially determined values of  $k_C$  (and  $k_F$ ) reproduced the CNDO/2 charge distributions well for other series of molecules even when a detailed analysis of that series of molecules in terms of CNDO/2 charges gave slightly different  $k$  values. The  $E^0$  values are not directly comparable since gas phase measurements were used by Davis et al., however  $E^0_C$  was taken to be the  $C_{1s}$  binding energy in benzene. There is generally good agreement between the charges derived in this work, those of Davis et al. and the CNDO/2 charges. Stuckey et al.<sup>206</sup> have also successfully used the charge potential model for obtaining empirical charge distributions in molecules which contain carbon, nitrogen and oxygen or these elements and one other chemically unique atom. The parameters for carbon and

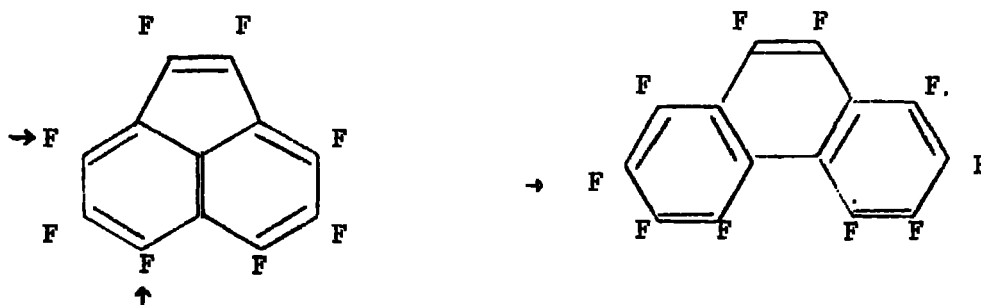
## INTRODUCTION

The work presented in this chapter illustrates how ESCA may be used to solve structural problems in chemistry which are not readily amenable to solution by other methods. The application of ESCA to these structural problems may require the use of the charge potential model and CNDO calculations but in other, even quite complex cases, ESCA spectra may be used to distinguish between various possible structures. The examples presented in this chapter consist essentially of distinguishing between various isomers on the basis of the  $C_{1s}$  ESCA spectra of the compounds. All the samples studied in these investigations were liquids and the sample handling method was that outlined in chapter (I.5.b).

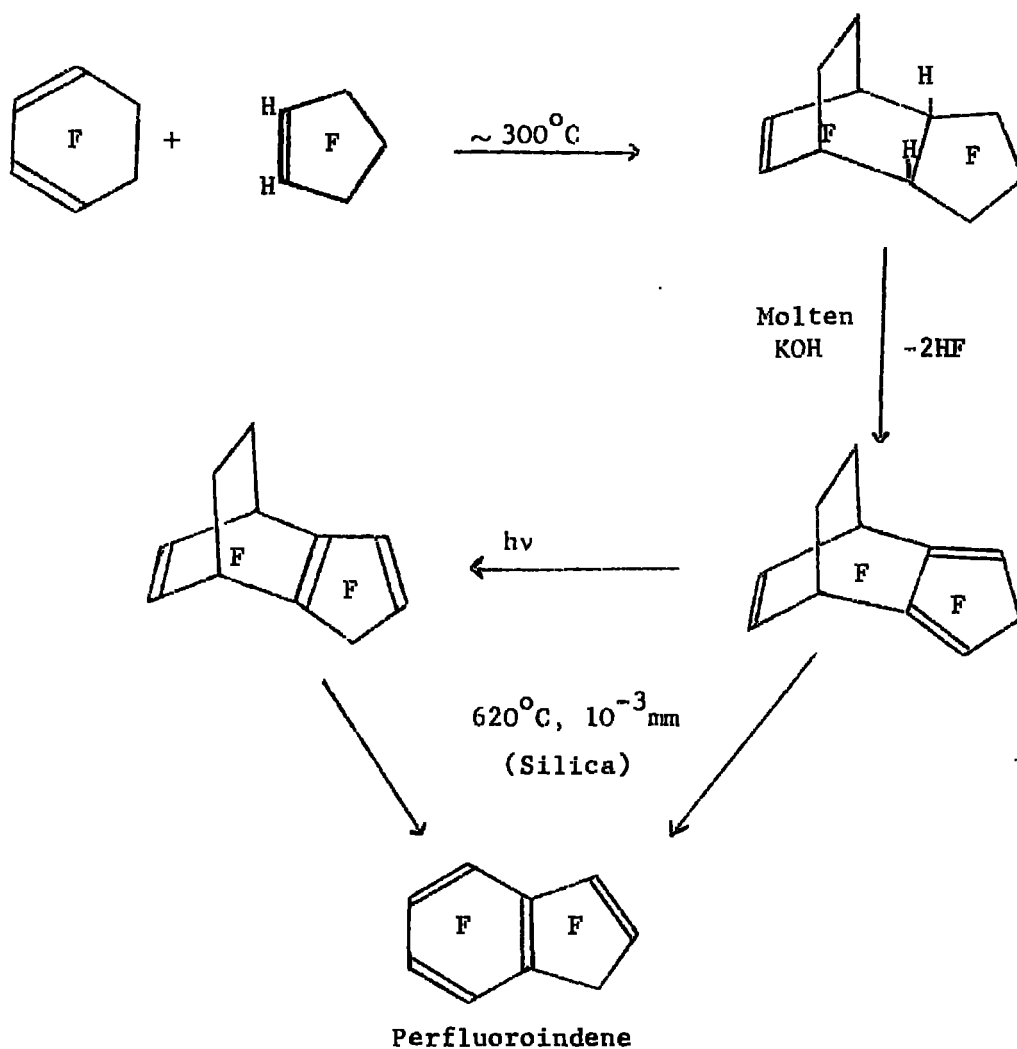
### 1) ORIENTATION OF NUCLEOPHILIC SUBSTITUTION IN PERFLUOROINDENE

#### a) Background

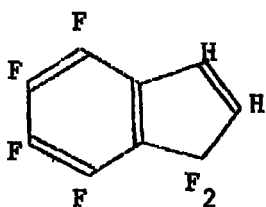
The reactions of polyfluoropolynuclear aromatic compounds with nucleophiles have occupied the practical and theoretical interests of a number of workers for several years.<sup>215,216,217,218.</sup> The positions at which nucleophilic attack occurs in two such compounds are shown below.<sup>217,218</sup>



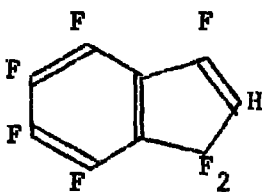
As is general with fluoroaromatic compounds substitution occurs at a position such that the carbon para to the position of substitution in the Wheland intermediate formed (approximation to the transition state) does not carry a fluorine atom,<sup>216</sup> (Such substitution would cause a large  $I_{\pi}$  repulsion between the fluorine p electrons and the ring  $\pi$  electrons on the neighbouring carbon atoms).<sup>216,219.</sup> However, in the above cases, substitution occurs in the aromatic rings and not at the most olefinic sites in the compounds. Feast and Preston<sup>203</sup> have recently synthesized perfluoroindene according to the following reaction scheme



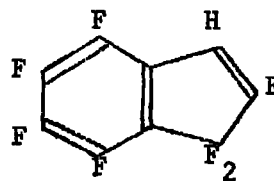
It is therefore of interest to determine the site nucleophilic substitution in this compound which also contains an aromatic ring conjugated with a more olefinic double bond. Perfluoroindene reacted cleanly with sodium borohydride in diglyme and the reaction could be regulated to give either the mono ( $C_9HF_7$ ) or di( $C_9H_2F_6$ ) replacement products.<sup>220,221</sup> The di-replacement product was readily shown to be 1,1,4,5,6,7 hexa-fluoroindene by conventional spectroscopic examination<sup>222</sup> while the mono-displacement product was shown by  $^1H$  and  $^{19}F$  n.m.r. spectroscopies to be a mixture of two isomers in a 4:1 ratio.<sup>222</sup> However, these isomers were inseparable on available gas chromatography packings. The infrared spectrum of the mixture showed that the strong absorption at  $1,750cm^{-1}$  ( $-CF=CF-$ ) present in perfluoroindene had been replaced by two bands at  $1672$  and  $1628cm^{-1}$  ( $-CH=CF-$ ) indicating that the mono displacement product was a mixture of 1,1,3,4,5,6,7- and 1,1,2,4,5,6,7 heptafluoroindenenes (II) and (III).



I



II



III

Identification of the major component in the mixture of II and III was not possible by  $^{19}F$  n.m.r. since the easily identified peri F-F coupling commonly found in other polycyclic aromatics does not occur in perfluoroindene, and arguments based on chemical shift

correlations with those of the most nearly analogous structures for which data are available were unconvincing.<sup>222</sup> Thus in this compound substitution with hydride ion occurs exclusively with the vinylic fluorines.

b) Simulation of the C<sub>1s</sub> Spectra of Monosubstituted Perfluoroindenes and Identification of the Major Component.

As was demonstrated in chapter (IV) and other work<sup>17,71,77c,86</sup> an excellent correlation exists between experimentally determined C<sub>1s</sub> shifts in fluorocarbon and other organic molecules and the shifts derived from charge potential model using CNDO/2 SCF MO charge distributions. Further reliance can be placed on the model since it can be used to calculate charge densities for large complex molecules (Chapter IV.3c). The charge potential model was therefore used to simulate the C<sub>1s</sub> spectra of isomers II and III (cf. Chapter IV figure 4.1) and 4:1 and 1:4 mixtures of the isomers in the following manner.

- i) CNDO/2 calculations were performed on isomers II and III to obtain the charge distributions in the two isomers.
- ii) The charges obtained were used in conjunction with the charge potential model

$$E - E^0 = kq_i + \sum_{j \neq i} \frac{q_j}{r_{ij}}$$

to calculate the C<sub>1s</sub> binding energies and shifts. The parameters used in the charge potential model were  $k_c = 25$  and  $E_c^0 = 284.6\text{eV}$

and were those previously derived from the study of aromatic and perfluoroaromatic compounds (Chapter IV.3.a).

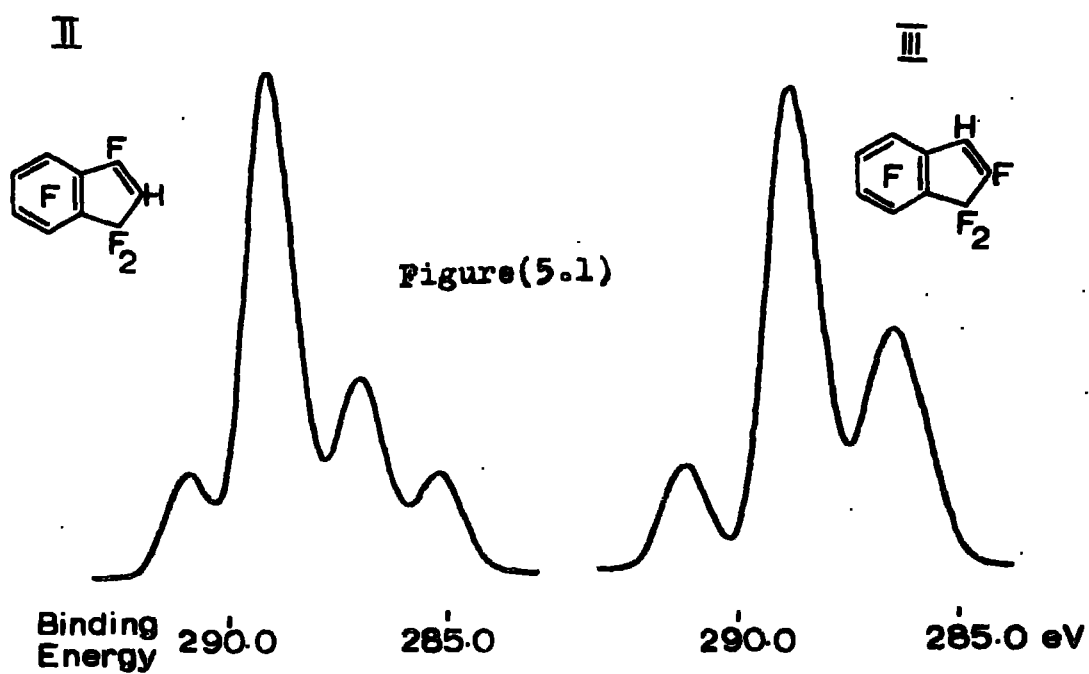
- iii) From the previous study of perfluoroindene (Chapter IV.3a) and other fluorocarbon compounds<sup>71,72</sup> studied under the same experimental conditions, the peak shapes were taken to be gaussian with a width of 1.4eV at half maximum height.
- iv) Computer simulated  $C_{1s}$  spectra of both isomers II and III were obtained by superimposition of nine such peaks of equal area at the calculated binding energy for each.

The relevant results of the CNDO/2 and charge potential calculations used for the simulation of the spectra are shown in table 5.1 and the simulated spectra of compounds II and III are shown in figure 5.1. The two calculated spectra are sufficiently different to enable a distinction to be made between the two isomers. The major distinguishing feature is the low binding energy shoulder caused by  $C_2$  in isomer II. This is caused by the large negative charge (-0.159) on the  $C_2$  carbon which is only partially offset by the positive Madelung potential of + 4.5eV. This large negative charge is caused essentially by the large build up of  $\pi$ -electron density ( $\pi$  charge = -0.127) while the  $\sigma$ -charge is comparatively small (-0.032). In the case of isomer III the negative charge on the  $C-H$  carbon is much less (-0.048) and, although the Madelung potential contribution is also

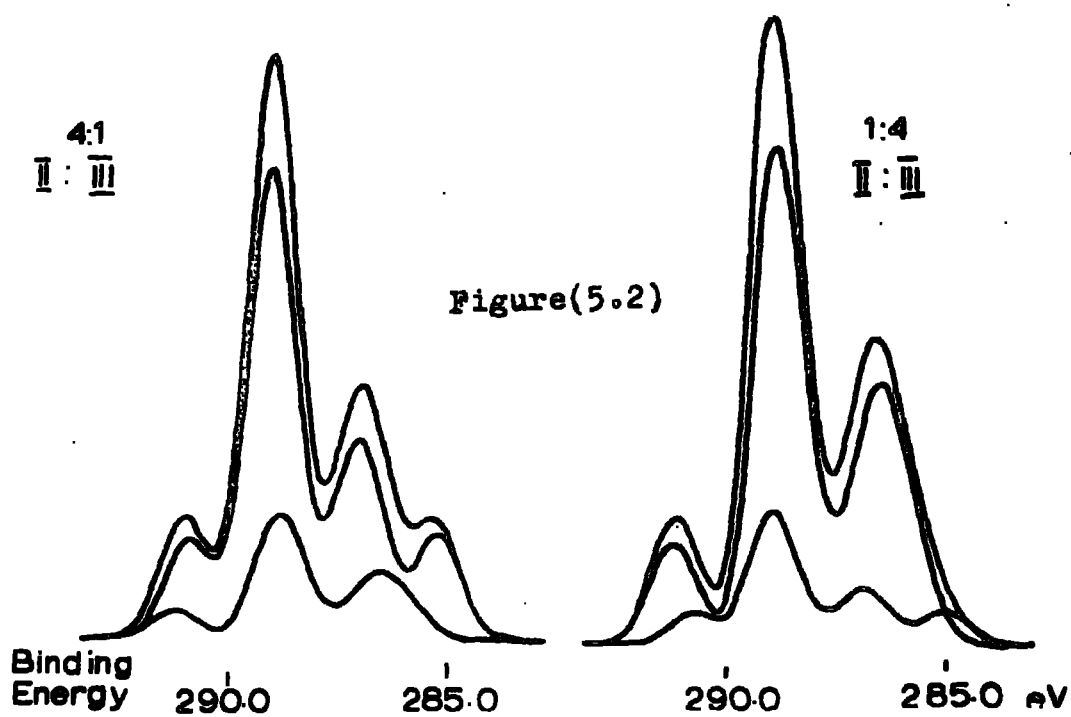
TABLE 5.1DO/2 and Charge Potential Results for 1,1,3,4,5,6,7- and 1,1,2,4,5,6,7-Heptafluoroindenes (II and III respectively).

<u>Position</u>	<u>Charge on C atom</u>	<u>Madelung Potential</u>	<u>Calculated Shift</u>	<u>Calculated Binding Energy</u>
	$q_i$	$\sum_{i \neq j} \frac{q_j}{r_{ij}}$	$E - E^0$	$E$
<b>ISOMER II</b>				
1	0.449	-4.61	6.6	291.2
2	-0.159	4.49	0.5	285.1
3	0.271	-2.13	4.7	289.3
4	0.197	-0.38	4.5	289.1
5	0.164	0.37	4.5	289.1
6	0.156	0.45	4.4	290.0
7	0.205	-0.62	4.5	289.1
8	-0.067	3.88	2.2	286.8
9	-0.025	3.19	2.6	287.2
<b>ISOMER III</b>				
1	0.419	-3.62	6.9	291.5
2	0.173	-0.30	4.0	288.6
3	-0.048	2.57	1.4	286.0
4	0.173	-0.20	4.1	288.7
5	0.173	0.15	4.5	289.1
6	0.149	0.52	4.3	288.9
7	0.215	-0.77	4.6	289.2
8	-0.078	4.00	2.1	286.7
9	0.010	2.11	2.4	287.0

SIMULATED C1s SPECTRA for ISOMERS II and III



SIMULATION of 4:1 and 1:4 MIXTURES of ISOMERS II and III

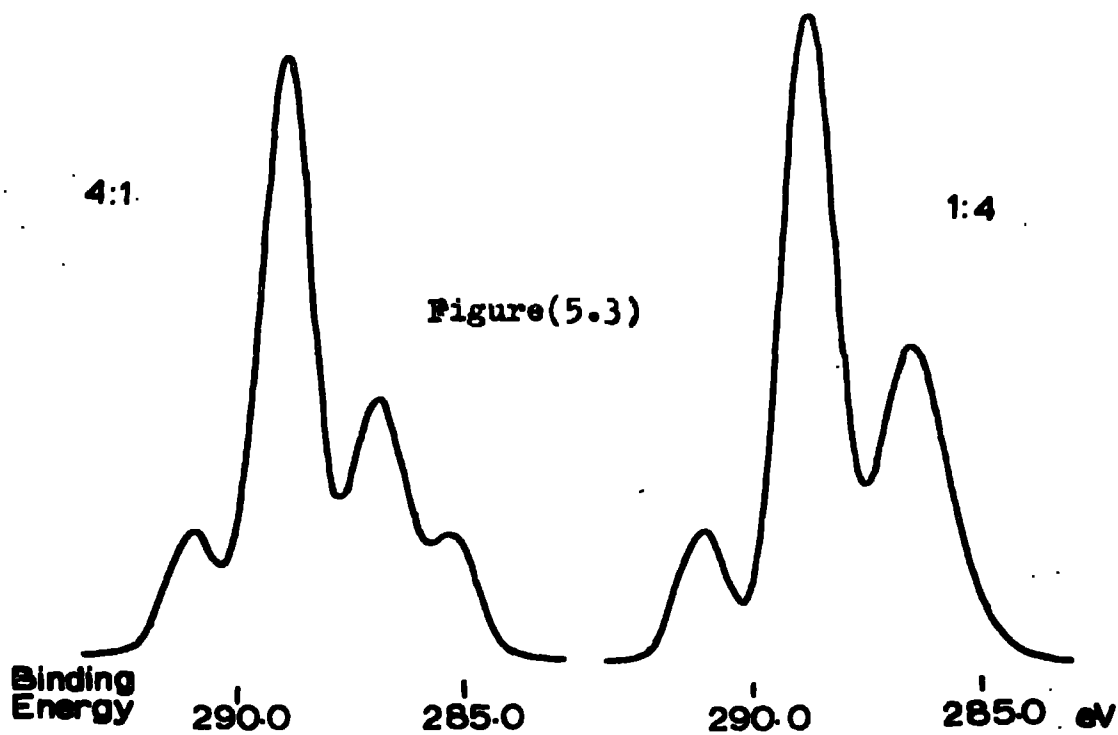


smaller (+ 2.6eV), the shift between the C-H and the bridge-head carbons is not great enough to give rise to a distinct shoulder at low binding energy. The magnitude of the  $\pi$ -charge on the C-H carbon is much smaller (-0.058) than in isomer II and there is also a slight reduction in the  $\sigma$ -charge (-0.010).

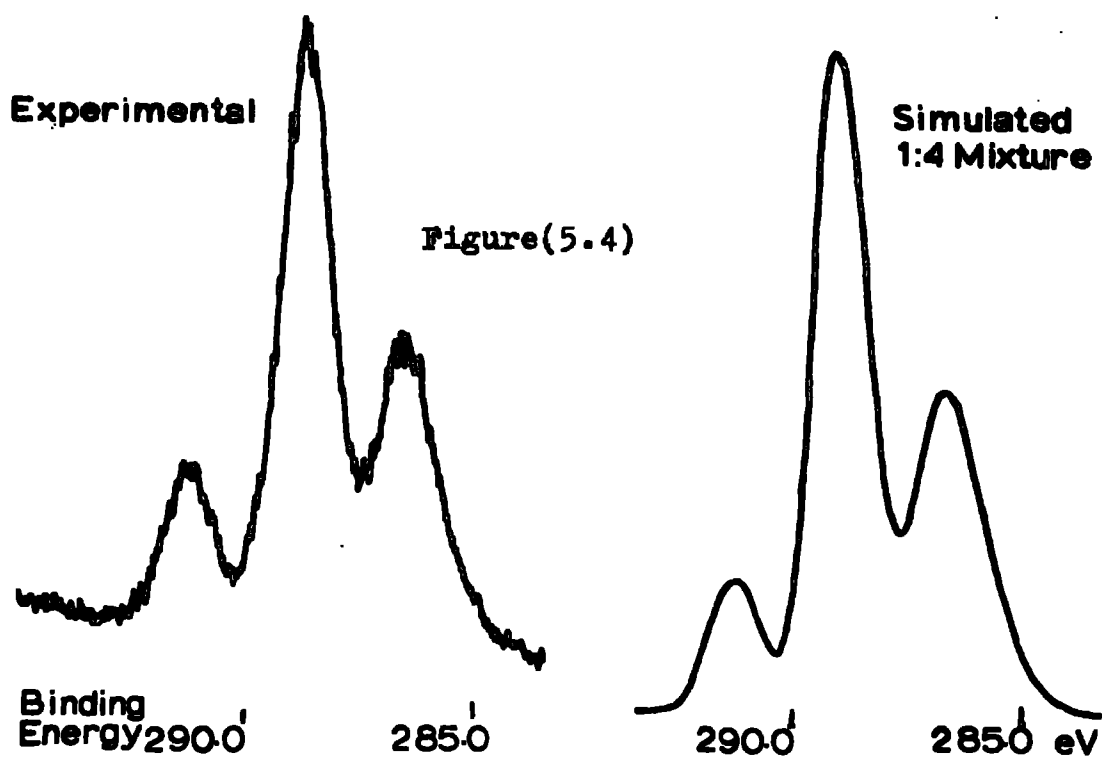
However, since the mono-displacement product was a mixture of isomers II and III in either a 4:1 or 1:4 ratio the theoretical  $C_{1s}$  spectra for these mixtures were computed as shown in figure 5.2. The distinguishing features between the two simulated spectra for the mixtures (figure 5.3) are the peak at low binding energy due to  $C_2$  in isomer II and the separations between the major peaks at higher binding energy (e.g. the CF<sub>2</sub> peak is better resolved in the mixture in which isomer III is the major component).

The experimental  $C_{1s}$  spectrum is in excellent agreement with the theoretical spectrum computed for the 1:4 mixture of isomers II and III respectively (figure 5.4). Agreement between the theoretical and experimental spectrum is complete not only in terms of binding energies and shifts but also in the shape of the overall spectral envelope. (When normalized to a horizontal baseline the experimental spectrum is exactly superimposable on the calculated spectrum). This provides very strong evidence that the vinylic fluorine atom adjacent to the aromatic ring in perfluoroindene is the most susceptible to nucleophilic replacement by hydrogen in the reaction with sodium borohydride in diglyme.

SIMULATED C1s SPECTRA of 4:1 and 1:4 MIXTURES of II and III



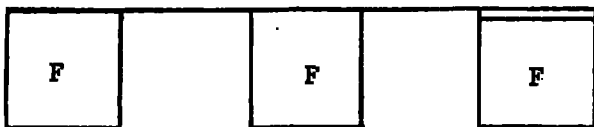
COMPARISON of EXPERIMENTAL and SIMULATED C1s SPECTRA



2) DETERMINATION OF THE PRODUCT OF THE FLUORIDE ION INITIATED TRIMERIZATION OF PERFLUOROCYCLOBUTENE

a) Background

The formation of a trimeric compound from perfluorocyclobutene was first reported in 1952.<sup>223</sup> The trimer was formed when a mixture of perfluorocyclobutene and pyridine was allowed to stand overnight. The trimer  $C_{12}F_{18}$  was the only compound isolated when the ratio of pyridine to perfluorocyclobutene was high ( $\sim 1:1$  molar) but if only a small amount of pyridine was used a small amount of a mixture of dimers was also formed. In all cases separation was difficult due to the formation of black tars. The structure

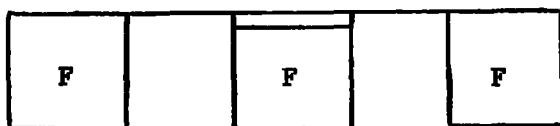


was postulated.

The fluoride ion initiated trimerization of perfluorocyclobutene was reported in 1965<sup>224</sup> when treatment of perfluorocyclobutene with fluoride ion yielded the dimers

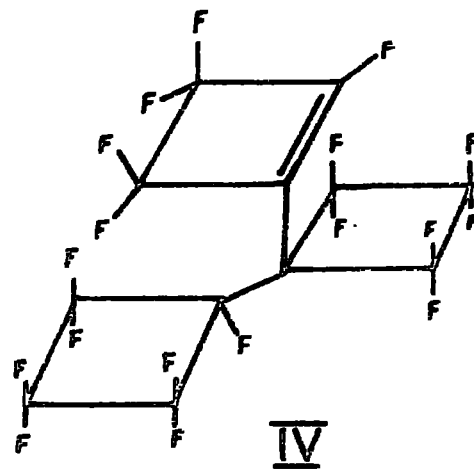
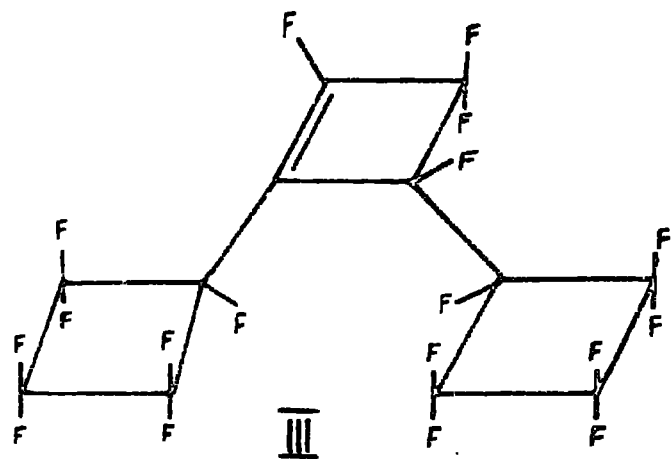
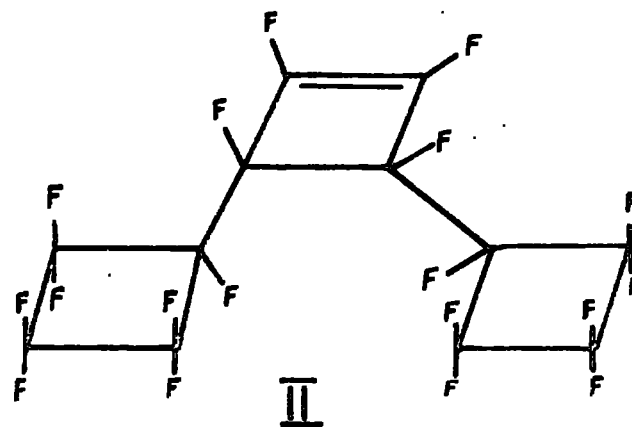
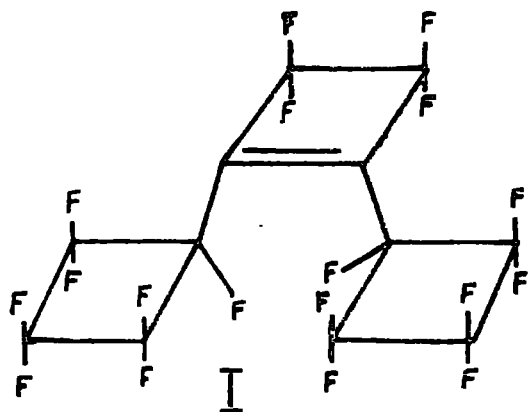


together with a trimer  $C_{12}F_{18}$  which was assigned the structure



(I)

Figure(5.5)



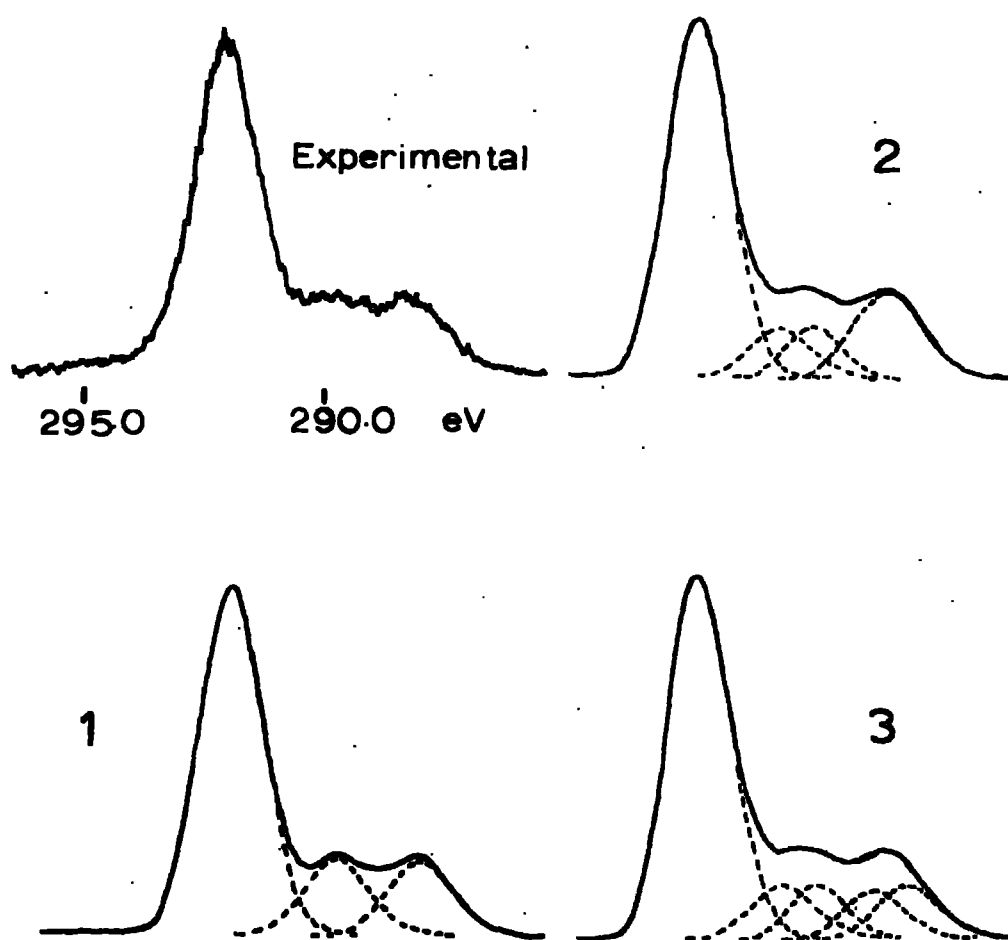
More recently Chambers et al.<sup>225</sup> have studied fluoride ion initiated reactions of some perfluorocycloalkenes and have obtained the trimerization product of perfluorocyclobutene in good yield with only a trace of the dimerization products. However, the structure previously assigned to this trimerization product (I) was not in good agreement with the  $^{19}\text{F}$  n.m.r. spectrum of the trimer.<sup>225</sup> Some possible structures of a trimer of perfluorocyclobutene are shown in figure 5.5. It is therefore of interest to determine whether the structure may be identified on the basis of ESCA data.

#### b) Experimentally Based Identification

The  $\text{C}_{1s}$  ESCA spectrum of the compound  $\text{C}_{12}\text{F}_{18}$  was recorded (figure 5.6) as were the  $\text{C}_{1s}$  ESCA spectra of four model compounds of known structure (figures 5.7 and 4.5). The  $\text{F}_{1s}$  spectra of these compounds were also recorded. The model compounds used in this study were chosen because:

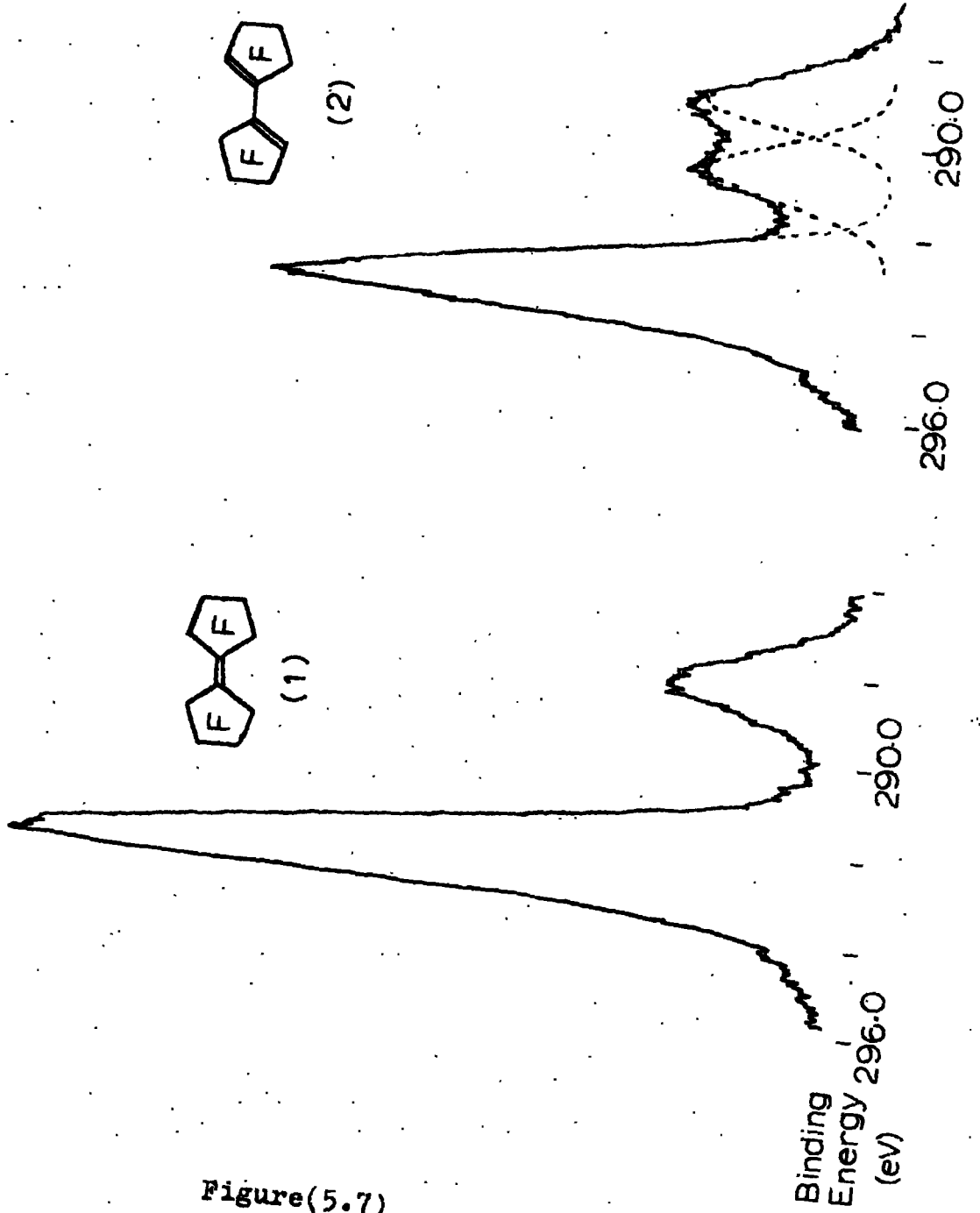
- i) Like  $\text{C}_{12}\text{F}_{18}$  they contain only carbon and fluorine.
- ii) They are volatile liquids, as is  $\text{C}_{12}\text{F}_{18}$ , and they could therefore be studied under the same experimental conditions as  $\text{C}_{12}\text{F}_{18}$  (i.e. injected into the reservoir shaft and condensed onto a cooled piece of gold on the tip of the probe).
- iii) They contain bonding situations found in the various proposed isomers of  $\text{C}_{12}\text{F}_{18}$  and the  $\text{C}_{1s}$  levels in the model compounds are

DECONVOLUTIONS of the EXPERIMENTAL C1s  
SPECTRUM of C<sub>12</sub>F<sub>18</sub>



Figure(5.6)

# CARBON 1s SPECTRA



Figure(5.7)

Binding Energy 296.0 (eV)

readily assigned. The environments of the carbon atoms in the model compounds are  $\text{>CF}_2$ , tertiary  $\begin{array}{c} | \\ -\text{C}-\text{F} \\ | \end{array}$ , vinylic  $\begin{array}{c} || \\ -\text{C}-\text{F} \end{array}$  and vinylic  $\begin{array}{c} \diagup \\ \text{C}=\end{array}$ .

The binding energy data for the model compounds are listed in table 5.2 and table 5.3 shows the shifts in these compounds relative to the  $\begin{array}{c} \diagup \\ \text{C}=\end{array}$  carbon atoms which each of these compounds contains. The use of these internal shifts compensates for any charging effects which may have occurred and forms a sound basis for the comparison of shifts between these compounds. (The near constancy of the  $\text{F}_{1s}$  binding energies for these compounds, however, suggests that charging effects for the samples are slight).

The experimental  $\text{C}_{1s}$  spectrum of the trimer  $\text{C}_{12}\text{F}_{18}$ , figure 5.6, immediately eliminates structures II and III, as well as the structure initially postulated for the trimerization in the presence of pyridine, since the  $\text{C}_{1s}$  spectrum clearly shows an overall  $\text{CF}_2:\text{CF}:\text{C}$  ratio of 4:1:1 (8:2:2). (The other structures would show peak area ratios of 6:6:0, 7:4:1 and 7:4:1 respectively). Isomer I has high symmetry and therefore its  $\text{C}_{1s}$  spectrum would be expected to be well resolved into  $\text{CF}_2$ ,  $\begin{array}{c} | \\ -\text{C}-\text{F} \\ | \end{array}$  and  $\begin{array}{c} \diagup \\ \text{C}=\end{array}$  peaks. However, isomer IV has much less symmetry and contains  $\text{CF}_2$ ,  $\begin{array}{c} | \\ -\text{C}-\text{F} \\ | \end{array}$ ,  $\begin{array}{c} || \\ -\text{C}-\text{F} \end{array}$ ,  $\begin{array}{c} \diagup \\ \text{C}=\end{array}$  and  $\begin{array}{c} | \\ -\text{C}- \\ | \end{array}$  bonding situations and therefore its  $\text{C}_{1s}$  spectrum would be expected to have poorer resolution. The experimental spectrum is poorly resolved in the  $\text{CF}$  and  $\text{C}$  region indicating that structure IV is more probable than structure I. However further analysis is required before a definite assignment can be made.

Table 5.2

Binding Energies in Model Fluorocarbon Compounds

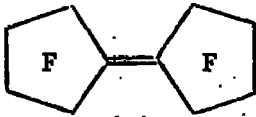
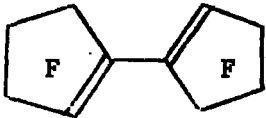
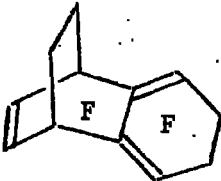
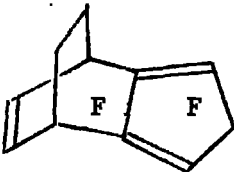
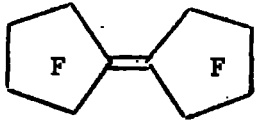
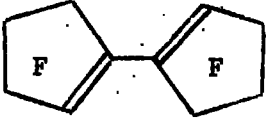
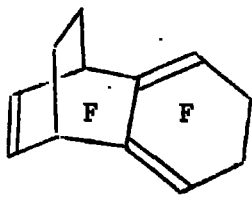
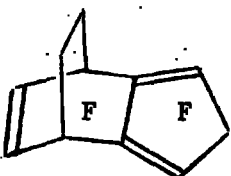
	<u>Atom</u>	<u>BINDING ENERGY</u> (eV)
 <p>(1)</p>	C=	288.1
	CF <sub>2</sub>	292.2
	F	691.0
 <p>(2)</p>	C=	287.8
	=CF	289.3
	CF <sub>2</sub>	291.9
	F	690.8
 <p>(3)</p>	C=	287.8
	=C-F	289.4
	 -C-F	290.6
	CF <sub>2</sub>	292.3
	F	691.0
 <p>(4)</p>	C=	288.0
	=CF	289.6 <sub>5</sub> (average)
	 -CF	290.9
	CF <sub>2</sub>	292.3
	F	690.9

Table 5.3

C<sub>1s</sub> Internal Shifts in Fluorocarbon Compounds

				
	0	-	-	4.1
	0	1.5	-	4.1
	0	1.6	2.6	4.5
	0	1.6 <sub>5</sub> (av.)	2.9	4.3

Three deconvolutions of the  $C_{1s}$  spectrum of the trimer were carried out by fitting gaussian curves in the area ratio of 8:2:2, 8:1:1:2 and 8:1:1:1:1. The line width used for the curve fitting, 1.4 eV, was taken from the well resolved  $C_{1s}$  spectra of model compounds numbers (1) and (2) which had been obtained under the same experimental conditions. These deconvolutions are also shown in figure 5.6 and are the best fits to the experimental spectrum obtainable within the imposed line widths and area ratios. (Since the  $CF_2$  peak is well resolved in the  $C_{1s}$  spectrum of  $C_{12}F_{18}$  it was not necessary to impose the line width restriction on this peak but the line width obtained was found to be consistent with that obtained from the model compounds). The accuracy of the fit increased along the series of deconvolutions and the results of these deconvolutions are listed in table 5.4.

Deconvolution number 1, which would correspond to isomer I, gives a shift of 1.7 eV between the  $\text{>C=}$  carbon atoms and the CF carbon atoms. By comparison with the model compounds, table 5.3, this internal shift is typical of a  $\text{-}\overset{\parallel}{\text{C}}\text{-F}$  carbon atom but not a  $\text{-}\overset{|}{\text{C}}\text{-F}$  carbon atom. Since there are no  $\text{-}\overset{\parallel}{\text{C}}\text{-F}$  bonding situations in isomer I, (and also a shift of 3.9eV between  $\text{>C=}$  and  $\text{>CF}_2$  is a little low), this structure may be excluded. Deconvolution number 2 shows internal shifts of 3.9, 2.5 and 1.7eV relative to the unsubstituted carbon atoms and these shifts are fairly typical of  $CF_2$ ,  $\text{-}\overset{|}{\text{C}}\text{-F}$  and  $\text{-}\overset{\parallel}{\text{C}}\text{-F}$  carbon atoms and these bonding situations occur in isomer IV. The value of 3.9eV for the internal shift between  $CF_2$  carbon atoms and an unsubstituted carbon atom of the type  $\text{>C=}$  is a little low, however, isomer IV contains both a  $\text{>C=}$  carbon atom and a  $\text{-}\overset{|}{\text{C}}\text{-}$  carbon atom and these may well have slightly

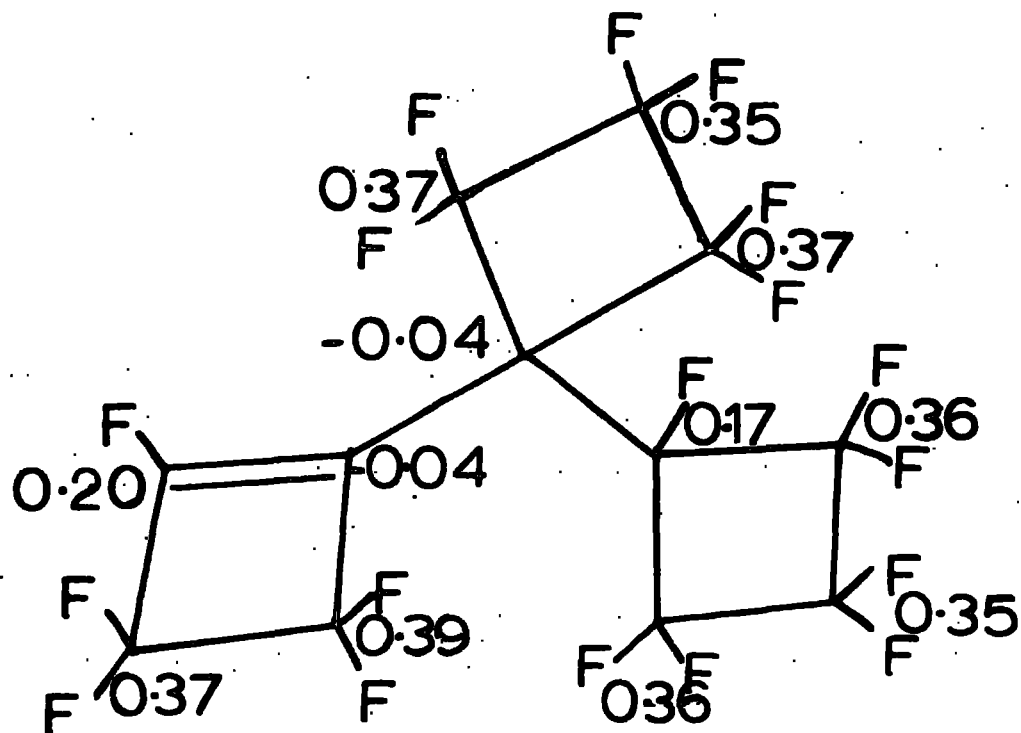
Table 5.4Deconvolutions of the C<sub>1s</sub> Spectrum of C<sub>12</sub>F<sub>18</sub>

<u>Area Ratio</u>	<u>Binding Energy</u> <sup>†</sup> (eV)	<u>Internal Shift</u> <sup>*</sup> (eV)	<u>Assignment</u>
<u>Deconvolution (1)</u>			
2	288.1	0	$\text{>C=}$
2	289.8	1.7	CF
8	292.0	3.9	CF <sub>2</sub>
<u>Deconvolution (2)</u>			
2	288.1	0	$\text{>C=}$
1	289.8	1.7	$\text{-}\overset{\parallel}{\text{C}}\text{F}$
1	290.6	2.5	$\text{-}\overset{ }{\text{C}}\text{F}$
8	292.0	3.9	CF <sub>2</sub>
<u>Deconvolution(3) Assignment (a)</u>			
1	287.9	0	$\text{>C=}$
1	288.6	0.7	$\text{-}\overset{ }{\text{C}}\text{-}$
1	289.8	1.9	$\text{-}\overset{\parallel}{\text{C}}\text{F}$
1	290.6	2.7	$\text{-}\overset{ }{\text{C}}\text{F}$
8	292.0	4.1	CF <sub>2</sub>
<u>Assignment (b)</u>			
1	287.9	-0.7	$\text{-}\overset{ }{\text{C}}\text{-}$
1	288.6	0.0	$\text{>C=}$
1	289.8	1.2	$\text{-}\overset{\parallel}{\text{C}}\text{F}$
1	290.6	2.0	$\text{-}\overset{ }{\text{C}}\text{F}$
8	292.0	3.4	CF <sub>2</sub>

† F<sub>1s</sub> binding energy = 691.1 eV

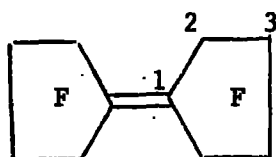
\* relative to  $\text{>C=}$

Figure (5.8)

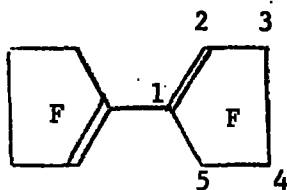


$$Q_{\text{expt}} = 0.007 + 1.004 Q_{\text{CNDO}}$$

Experimental Charge Distributions

Table 5.5Experimental Charge Distributions in Model Compounds 1 and 2

<u>Position</u>	$q_c$	$q_F$
1	-0.034	-
2	0.392	-0.193
3	0.355	-0.188



1	-0.038	-
2	+0.229	-0.175
3	0.362	-0.197
4	0.349	-0.192
5	0.387	-0.199

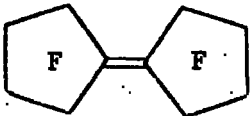
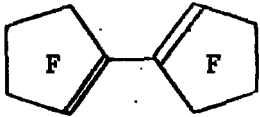
Table 5.6Data Used for Calculation of Experimental Charge Distributions

$k_c = 25$

$k_F = 30$

$E_c^{\circ} = 284.6$

$E_F^{\circ} = 693.1$

<u>Molecule</u>	<u>Atom</u>	<u>E-E<sup>o</sup></u>
ISOMER IV	C=	3.3
	-C-	4.0
	<u>C-F</u>	5.2
	<u>CF</u>	6.0
	<u>CF<sub>2</sub></u>	7.4
	F	-2.1
	C=	3.5
	<u>CF<sub>2</sub></u>	7.6
	F	-2.2
	C=	3.2
	<u>CF</u>	5.7
	<u>CF<sub>2</sub></u>	7.3
	F	-2.4

different binding energies. Deconvolution number 3 (area ratio 8:1:1:1:1) does, in fact, show an improved fit to the experimental spectrum and table 5.4 shows internal shifts for both possible assignments of the  $\text{>C=}$  and  $\text{-C-}$  carbon atoms. Assignment (b) gives internal shifts which are not in agreement with any of the internal shifts expected on the basis of the model compounds and may therefore be rejected. Assignment (a), however, gives internal shifts which are in good agreement with those expected for isomer IV. The product of fluoride ion initiated trimerization of perfluorocyclo-butene is therefore identified as isomer IV.

Shifts in core electron binding energies may be used to predict accurately the charge distributions in fluorocarbon compounds of quite complex structure (Chapter IV.3.c). The  $C_{1s}$  charge distributions for isomer IV is shown in figure 5.8 and the charge distributions for model compounds 1 and 2 are given in table 5.5. (The experimental charge distributions for model compounds 3 and 4 are shown in Chapter IV figure 4.6). The binding energy data and parameters used for these calculations are listed in table 5.6.

### c) Theoretical Determination of the Structure of $C_{12}F_{18}$

As an alternative to the experimental approach for distinguishing between isomers I to IV (figure 5.5) CNDO/2 calculations may be performed on the possible isomers and the calculated  $C_{1s}$  spectrum compared with the experimental  $C_{1s}$  spectrum. The  $CF_2:CF:C$  area ratio of the experimental  $C_{1s}$  spectrum, as described previously (Chapter V.2.b)

eliminates isomers II and III. CNDO/2 calculations were therefore carried out on isomers I and IV. The charges and intramolecular Madelung potentials for the carbon atoms are listed in table 5.7 and these were used to calculate the theoretical shifts ( $E-E^0$ ) using the charge potential model ( $k_c = 25.0$ ). These shifts were then taken in conjunction with a line width of 1.4eV to obtain the theoretical  $C_{1s}$  spectra for isomers I and IV (cf. figure 4.2). These are shown together with the experimental  $C_{1s}$  spectrum (normalized to a horizontal baseline) in figure 5.9. The experimental spectrum agrees closely with that calculated for isomer IV but not with that calculated for isomer I. This provides strong evidence that isomer IV is the correct structure.

The main drawbacks to this theoretical identification of the isomer are (i). Calculating the coordinates of the atoms in such complex systems (This was carried out with the aid of the computer program GEOMI, appendix III, and the coordinates are listed in appendix II).

(ii). The large amount of computer time required for these systems and they are in fact the largest systems (120 basis functions) which can be studied with our present CNDO/2 program.

(iii). Although the differences in the calculated spectra are quite noticeable and the similarity between that of isomer IV and the experimental spectrum is obvious, much greater confidence could be placed on the assignment if better resolution were obtainable. However, with the introduction of monochromators the consequent reduction in line widths will greatly facilitate the distinction between such isomers.

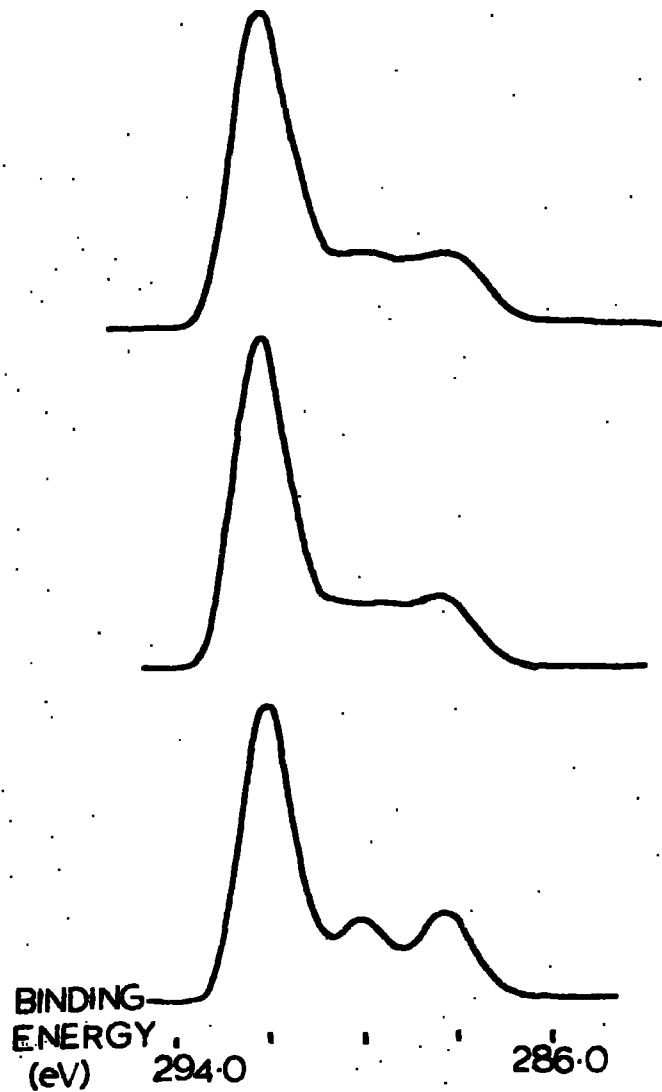
Table 5.7

CNDO/2 Calculations on isomers I and IV

ISOMER I	C atom N <sup>o</sup> .	q <sub>i</sub>	$\sum_{j \neq i} \frac{q_j}{r_{ij}}$	$25q_i + \sum_{j \neq i} \frac{q_j}{r_{ij}}$ (E-E <sup>0</sup> )
	1	-0.0039	3.99	3.89
	2	0.3794	-2.03	7.46
	3	0.1384	2.27	5.72
	4	0.3293	-0.67	7.57
	5	0.3495	-1.07	7.65
	6	0.3483	-1.02	7.69
	1	-0.0325	4.47	3.66
	2	0.3833	-2.00	7.59
	3	0.1868	0.68	5.35
	4	0.3615	-1.58	7.46
	5	-0.0464	5.49	4.33
	6	0.3291	-0.60	7.63
	7	0.3772	-1.38	8.05
	8	0.3794	-1.52	7.96
	9	0.1496	2.44	6.18
	10	0.3321	-0.70	7.60
	11	0.3494	-0.93	7.75
	12	0.3472	-0.93	7.75

# CALCULATED and EXPERIMENTAL C1s SPECTRA of C<sub>12</sub>F<sub>18</sub>

Figure(5.9)



C<sub>12</sub>F<sub>18</sub> Experimental spectrum

Theoretically simulated spectra

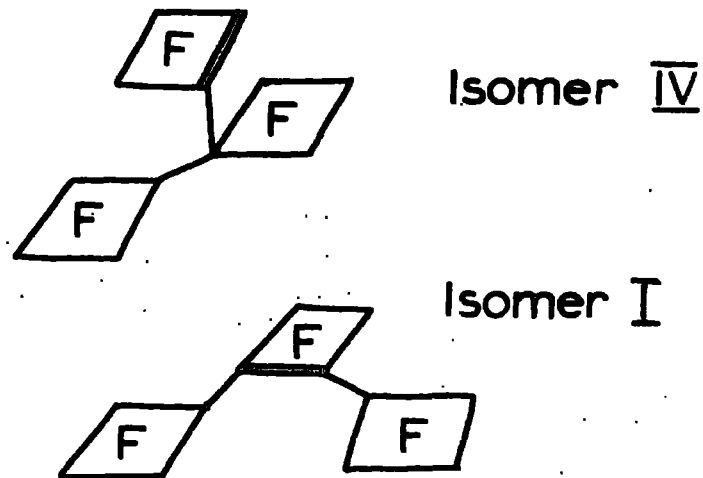


Table 5.8Charge Distribution in C F Isomer IV  
12 18

		<u>Charge</u>				<u>Charge</u>	
<u>Atom</u>		<u>CNDO/2</u>	<u>Experimental</u>	<u>Atom</u>		<u>CNDO/2</u>	<u>Experimental</u>
1	C	-0.0325	-0.037	16	F	-0.1683	-0.182
2	C	0.3833	0.391	17	F	-0.1639	-0.175
3	C	0.1868	0.199	18	F	-0.1859	-0.201
4	C	0.3615	0.374	19	F	-0.1794	-0.192
5	F	-0.1812	-0.184	20	C	0.3321	0.350
6	F	-0.1846	-0.189	21	C	0.3494	0.356
7	F	-0.1798	-0.186	22	C	0.3472	0.356
8	F	-0.1798	-0.187	23	F	-0.1648	-0.178
9	C	-0.0464	-0.039	24	F	-0.1828	-0.199
10	C	0.3291	0.352	25	F	-0.1797	-0.194
11	C	0.3772	0.370	26	F	-0.1665	-0.181
12	C	0.3794	0.375	27	F	-0.1647	-0.175
13	C	0.1496	0.167	28	F	-0.1652	-0.181
14	F	-0.1831	-0.195	29	F	-0.1600	-0.179
15	F	-0.1800	-0.190	30	F	-0.1469	-0.158

The agreement between the independent experimental and theoretical identification of isomer IV being the product formed is very encouraging and illustrates that detailed theoretical calculations are not always required for the interpretation of ESCA data in complex systems. The relationship between the experimental and CNDO/2 charge distributions in isomer IV is

$$q_{\text{exp}} = -0.004 + 1.039q_{\text{CND}} \\ (\pm 0.006)$$

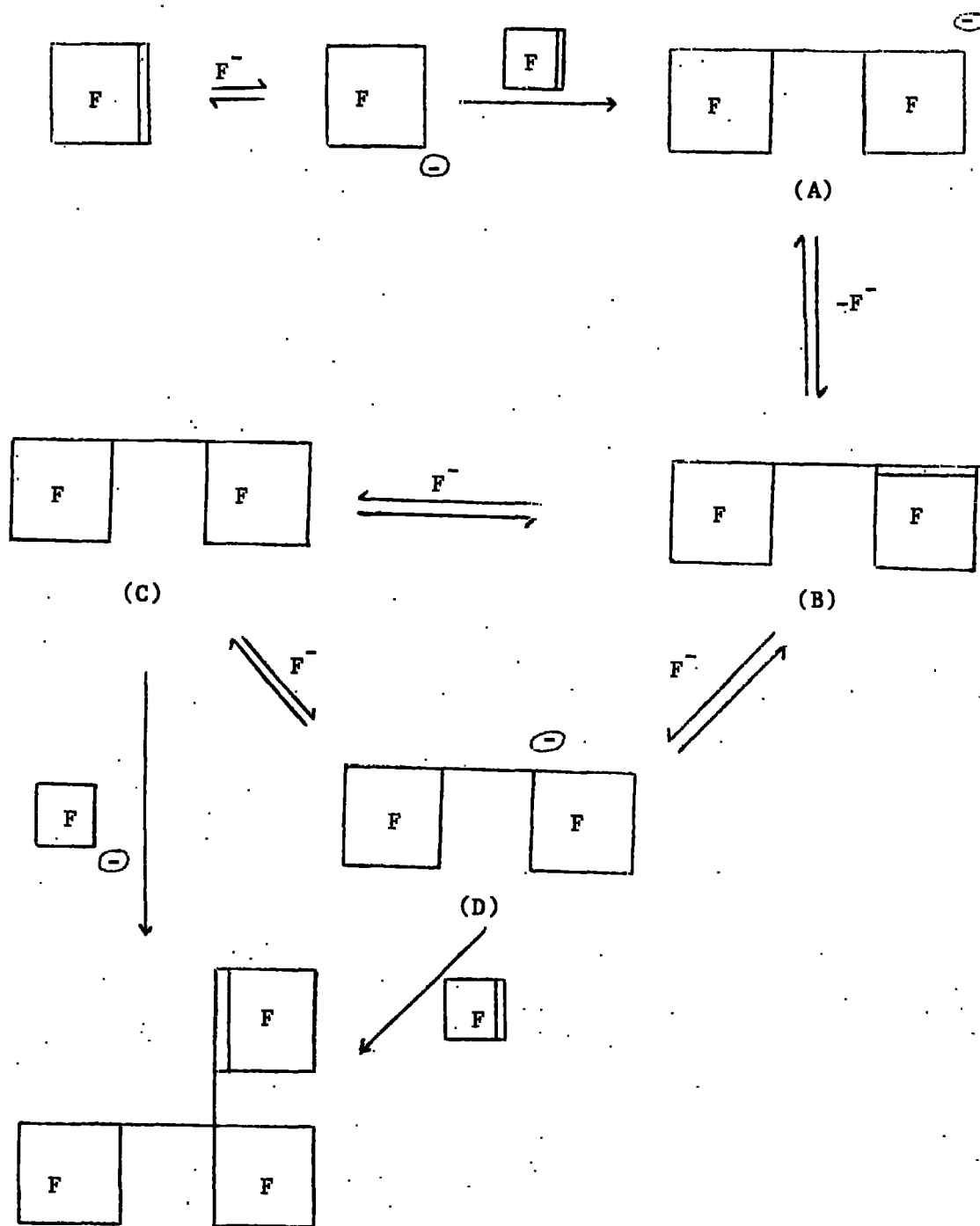
and the CNDO/2 and experimental charges are given in table 5.8.

(The atoms are listed in the same order that was used for the CNDO/2 input, appendix II).

#### d) Discussion

The assignment of isomer IV as the structure of the fluoride ion initiated trimerization is at variance with that proposed by Fraticelli<sup>224</sup> (I). However the <sup>19</sup>F n.m.r. spectrum of structure IV, although complex, shows a fluorine resonance, integrating to one fluorine, which is characteristic of a single fluorine atom attached to a saturated carbon atom and also shows a clearly defined resonance, due to one fluorine, which is only consistent with fluorine attached to vinylic carbon.<sup>225</sup>

These observations are consistent only with isomer IV and therefore both ESCA and <sup>19</sup>F n.m.r. data indicate that structure IV is the product of fluoride ion induced trimerization of perfluorocyclobutene and not structure I as proposed by Fraticelli. Chambers et al.<sup>225</sup> have proposed the following reaction scheme to account for the formation of isomer IV:



IV

although they could not determine by which of the above routes the formation occurred. (Dimers (B) and (C) are those previously identified by other workers).<sup>223,224</sup> However, the formation of

carbanion (D) is expected to be favoured in the equilibrium between carbanions (A) and (D) since the negative charge in (D) is stabilized by a  $\underline{\text{CF}}$  and two  $\underline{\text{CF}}_2$  groups whereas the negative charge in (A) is stabilized by only one  $\underline{\text{CF}}$  and one  $\underline{\text{CF}}_2$  group. (Fluorine atoms  $\beta$  to a negative charge strongly stabilize the negative charge in fluorocarbanions). Thus on the basis of the chemistry of the system carbanion (D) may be expected to be formed and it was on this basis that structure IV was initially postulated as a possible structure of the trimerization product.

This example of structure determination clearly illustrates the use of ESCA as a powerful method of distinguishing between possible isomers and was undertaken because the structure could not be unambiguously assigned using other techniques.

APPENDIX I

ORBITAL EXPONENTS AND CONTRACTION COEFFICIENTS USED FOR

AB INITIO MOLECULAR ORBITAL

CALCULATIONS

Slater Single Zeta Best Atom Exponents<sup>117</sup>

	1s	2s	2p	3s	3p
C	5.6727	1.6083	1.5679		
N	6.6651	1.9237	1.9170		
O	7.6579	2.2458	2.2266		
F	8.6501	2.5638	2.5500		
S	15.5409	5.3144	5.9885	2.1223	1.8273
Cl	16.5239	5.7152	6.4966	2.3561	2.0387

Gaussian Orbital Exponents and Contraction Coefficients for 'Large Basis Set' Calculations on Halomethanes (Carbon, Nitrogen and Fluorine)<sup>130</sup>

<u>Exponent</u>	<u>Coefficient</u>	<u>Exponent</u>	<u>Coefficient</u>	<u>Exponent</u>	<u>Coefficient</u>
<u>Carbon S</u>		<u>Nitrogen S</u>		<u>Fluorine S</u>	
4232.6100	0.006228	5909.4400	0.006240	9994.7900	0.006431
634.8820	0.047676	887.4510	0.047669	1506.0300	0.048757
146.0970	0.231439	204.7490	0.231317	350.2690	0.233065
42.4974	0.789108	59.8376	0.788869	104.0530	0.785549
<hr/>		<hr/>		<hr/>	
14.1892	0.791751	19.9981	0.792912	34.8432	0.802728
1.9666	0.321870	2.6860	0.323609	4.3688	0.317752
<hr/>		<hr/>		<hr/>	
5.1477	1.0	7.1927	1.0	12.2164	1.0
<hr/>		<hr/>		<hr/>	
0.4962	1.0	0.7000	1.0	1.2078	1.0
<hr/>		<hr/>		<hr/>	
0.1533	1.0	0.2133	1.0	0.3634	1.0
<hr/>		<hr/>		<hr/>	
<u>Carbon P</u>		<u>Nitrogen P</u>		<u>Fluorine P</u>	
18.1557	0.039196	26.7860	0.38244	44.3555	0.042011
3.9864	0.244144	5.9564	0.243846	10.0820	0.261899
1.1429	0.816775	1.7074	0.817193	2.9959	0.797662
<hr/>		<hr/>		<hr/>	
0.3594	1.0	0.5314	1.0	0.9383	1.0
<hr/>		<hr/>		<hr/>	
0.1146	1.0	0.1654	1.0	0.2733	1.0
<hr/>		<hr/>		<hr/>	



STO 4.31G Basis Sets used in the Calculations on Fluoromethanes <sup>189</sup>

<u>Exponent</u>	<u>Coefficient</u>	<u>Exponent</u>	<u>Coefficient</u>	<u>Exponent</u>	<u>Coefficient</u>
<u>Carbon 1s</u>		<u>Carbon 2s</u>		<u>Carbon 2p</u>	
158.79200	0.0648888	32.165900	-0.0874263	4.620170	0.0997415
28.86820	0.2815200	5.550890	-0.2444120	1.057310	0.3559750
7.82464	0.5338980	0.425297	0.6464920	0.311279	0.5258960
2.49060	0.2707320	0.134626	1.0	0.0988179	1.0
<u>Nitrogen 1s</u>		<u>Nitrogen 2s</u>		<u>Nitrogen 2p</u>	
217.66700	0.0648326	45.291200	-0.0885431	6.812820	0.1019300
39.60980	0.2825690	7.899950	-0.2498910	1.567510	0.3606460
10.771100	0.5353110	0.610336	0.6453280	0.461632	0.5160080
3.423800	0.2677920	0.190161	1.0	0.145557	1.0
<u>Fluorine 1s</u>		<u>Fluorine 2s</u>		<u>Fluorine 2p</u>	
361.73200	0.0651740	79.444500	-0.0889846	10.907700	0.1225110
65.87110	0.2850680	13.987600	-0.2592360	2.515680	0.3950710
17.96720	0.5385960	1.069980	0.6603240	0.708224	0.5037310
5.70045	0.2609610	0.326013	1.0	0.208634	1.0
<u>Hydrogen 1s</u>					
5.216845	0.0567524				
0.954618	0.2601414				
0.265203	0.5328461				
0.088019	1.0				

STO-3G Basis Sets used in the Calculations on Fluoromethanes <sup>189</sup>

<u>Exponent</u>	<u>Coefficient</u>	<u>Exponent</u>	<u>Coefficient</u>	<u>Exponent</u>	<u>Coefficient</u>
<u>Carbon 1s</u>		<u>Carbon 2s</u>		<u>Carbon 2p</u>	
69.672300	0.167701	8.365170	-0.288780	2.323490	0.233214
12.44250	0.54355	0.379382	0.700773	0.501410	0.574322
3.22218	0.431954	0.122254	0.373432	0.131779	0.413243

<u>Nitrogen 1s</u>		<u>Nitrogen 2s</u>		<u>Nitrogen 2p</u>	
95.57200	0.167753	11.852700	-0.29507	3.446690	0.237401
17.11730	0.545580	0.544801	0.696797	0.746574	0.572017
4.44008	0.429160	0.173200	0.378818	0.192196	0.415644

<u>Fluorine 1s</u>		<u>Fluorine 2s</u>		<u>Fluorine 2p</u>	
159.51900	0.168066	20.674900	-0.304865	5.741040	0.267160
28.64360	0.548963	0.959828	0.708218	1.217890	0.576108
7.45505	0.424739	0.296800	0.369033	0.291822	0.400331

<u>Hydrogen 1s</u>	
2.227661	0.154329
0.405771	0.535328
0.109818	0.444635

Basis Sets used for Calculations on Fluorobenzen and Toluene<sup>130</sup>

<u>Exponent</u>	<u>Coefficient</u>	<u>Exponent</u>	<u>Coefficient</u>
<u>Carbon S</u>		<u>Hydrogen S</u>	
4232.61	0.00122	19.2406	0.01906
634.882	0.00934	2.8992	0.13424
146.097	0.04534	0.6534	0.47449
42.4974	0.15459	0.1776	0.50907
14.1892	0.35867	<u>Carbon P</u>	
5.14773	0.43809	18.1557	0.01469
1.96655	0.14581	3.98640	0.09150
0.49624	1.0	1.14293	0.30611
0.15331	1.0	0.359450	0.50734
		0.114600	0.31735
<u>Fluorine S</u>		<u>Fluorine P</u>	
9994.79	0.00117	44.3555	0.01636
1506.03	0.00887	10.0820	0.10199
350.269	0.04240	2.9959	0.31063
104.053	0.14291	0.9383	0.48636
34.8432	0.35527	0.2733	0.34424
12.2164	0.46223		
4.36885	0.14063		
1.20775	1.0		
0.36340	1.0		

APPENDIX II

COORDINATES USED IN MOLECULAR ORBITAL AND  
EXPERIMENTAL CHARGE DISTRIBUTION CALCULATIONS

The coordinates are given in either atomic units or Ångstrom units (1 a.u. = 0.529167 Å) depending on whether the calculation was ab initio or CNDO. (The input for the ab initio molecular orbital programs is in atomic units while that for the CNDO/2 program is in Ångstrom units.)

Coordinates used for Minimal Slater Basis Set Calculations

<u>Molecule</u>	<u>Z-Coordinates (a.u.)</u>				
HCCH	0.0	2.00200	4.28300	6.28500	
HCN	0.0	2.00914	4.19248		
FCN	0.0	2.38109	4.58265		
CO	0.0	2.13203			
OCO	0.0	2.191747	4.383494		
OCCCO	0.0	2.24882	4.66772	7.08662	9.33544
SCS	0.0	2.93480	5.86960		
OCS	0.0	2.19212	5.14015		
NN	0.0	2.07420			
NNO	0.0	2.132767	4.376955		

Coordinates used for ab initio Calculations on Halomethanes

<u>Molecule</u>	<u>Atom</u>	<u>X</u>	<u>Y</u>	<u>Z</u>	(a.u.)
CH <sub>4</sub>	H	1.6818060	0.0	1.1839167	
	H	-1.6818060	0.0	1.1839167	
	H	0.0	1.6818060	-1.1839167	
	H	0.0	-1.6818060	-1.1839167	
	C	0.0	0.0	0.0	
CH <sub>3</sub> F	H	-1.9420180	0.0	-0.6865450	
	H	0.9710090	1.6818850	-0.6865450	
	H	0.9710090	-1.6818850	-0.6865450	
	C	0.0	0.0	0.0	
	F	0.0	0.0	2.5190450	
CH <sub>2</sub> F <sub>2</sub>	H	1.6818060	0.0	1.1893167	
	H	-1.6818060	0.0	1.1893167	
	C	0.0	0.0	0.0	
	F	0.0	2.0567408	-1.4544580	
	F	0.0	-2.0567408	-1.4544580	
CHF <sub>3</sub>	H	0.0	0.0	2.0598410	
	C	0.0	0.0	0.0	
	F	-2.3745640	0.0	-0.8408770	
	F	1.1872820	2.0564330	-0.8408770	
	F	1.1872820	-2.0564330	-0.8408770	
CF <sub>4</sub>	C	0.0	0.0	0.0	
	F	2.0567408	0.0	1.4544580	
	F	-2.0567408	0.0	1.4544580	
	F	0.0	2.0567408	-1.4544580	
	F	0.0	-2.0567408	-1.4544580	
CH <sub>3</sub> Cl	H	-1.9420130	0.0	-0.6865450	
	H	0.9710090	1.6818850	-0.6865450	
	H	0.9710090	-1.6818850	-0.6865450	
	C	0.0	0.0	0.0	
	Cl	0.0	0.0	3.3656670	
CH <sub>2</sub> Cl <sub>2</sub>	H	1.6818060	0.0	1.1893167	
	H	-1.6818060	0.0	1.1893167	
	C	0.0	0.0	0.0	
	Cl	0.0	2.7485721	-1.9424948	
	Cl	0.0	-2.7485721	-1.9424948	

Coordinates for IBMOL5 Calculations on Fluorobenzene  
and Toluene

	<u>X</u>	<u>Y</u>	<u>Z</u> (a.u.)
Ring carbon atoms			
C1	0.0	2.639998	
C2	2.286235	1.319999	
C3	2.286235	-1.319999	
C4	0.0	-2.639998	
C5	-2.286235	-1.319999	
C6	-2.286235	1.319999	
Hydrogen atoms			
H2	4.061100	2.343306	
H3	4.061100	-2.343306	
H4	0.0	-4.688501	
H5	-4.061100	-2.343306	
H6	-4.061100	2.343306	
Fluorine atom			
F1	0.0	5.155272	
Methyl group			
C7	0.0	5.512437	
H8	0.0	6.200878	-1.947400
H9	-1.684240	6.200878	0.973795
H10	1.684240	6.200878	0.973795

Coordinates for Fluoro- and Chloro- Benzenes

<u>ATOM</u>	<u>X</u>	<u>Y</u> (Ångstroms)
C1	0.0	1.3970
C2	1.2098	0.6985
C3	1.2098	-0.6985
C4	0.0	-1.3970
C5	-1.2098	-0.6985
C6	-1.2098	0.6985
H1	0.0	2.4810
H2	2.1490	1.2400
H3	2.1490	-1.2400
H4	0.0	-2.4810
H5	-2.1490	-1.2400
H6	-2.1490	1.2400
F1	0.0	2.7280
F2	2.3628	1.3635
F3	2.3628	-1.3635
F4	0.0	-2.7280
F5	-2.3628	-1.3635
F6	-2.3628	1.3635
C11	0.0	3.0970
C12	2.6818	1.5485
C13	2.6818	-1.5485
C14	0.0	-3.0970
C15	-2.6818	-1.5485
C16	-2.6818	1.5485

Coordinates for

Dodecafluorotricyclo [5,2,2,0<sup>2,6</sup>]undeca-2,5,8 triene

<u>ATOM</u>	<u>X</u>	<u>Y</u>	<u>Z</u> (Ångstroms)
C	0.0	0.0	0.0
C	1.54000	0.0	0.0
C	1.95408	1.27442	0.0
C	0.77000	2.24357	0.0
C	-0.41408	1.27442	0.0
F	3.22931	1.65215	0.0
F	-1.68931	1.65215	0.0
C	2.11689	-1.42786	0.0
C	-0.57689	-1.42786	0.0
F	3.44689	-1.42786	0.0
F	-1.90689	-1.42786	0.0
C	1.53850	-2.00687	1.30453
C	0.00149	-2.00687	1.30453
F	1.95273	-3.26169	1.45533
F	1.95273	-1.27692	2.33627
F	-0.41273	-1.27692	2.33627
F	-0.41273	-3.26169	1.45533
C	1.47859	-1.88817	-1.32373
C	0.06141	-1.88817	-1.32373
F	2.25117	-2.24374	-2.34627
F	-0.71117	-2.24374	-2.34627
F	0.77000	3.01012	1.08574
F	0.77000	3.01012	-1.08574

Coordinates for

Tetradecafluorotricyclo [6,2,2,0<sup>2</sup>,7] dodeca 2,6,9 triene

<u>ATOM</u>	<u>X</u>	<u>Y</u>	<u>Z</u> (Ångstroms)
C	0.0	0.0	0.0
C	1.54000	0.0	0.0
C	2.25009	1.13638	0.0
C	1.54377	2.50485	0.0
C	-0.71009	1.13638	0.0
C	-0.00377	2.50485	0.0
F	3.58009	1.13638	0.0
F	-2.04009	1.13638	0.0
F	1.89718	3.18687	-1.08575
F	1.89718	3.18687	1.08575
F	-0.35718	3.18687	1.08575
F	-0.35718	3.18687	-1.08575
C	2.11689	-1.42786	0.0
C	-0.57689	-1.42786	0.0
F	3.44689	-1.42786	0.0
F	-1.90689	-1.42786	0.0
C	0.00149	-2.00687	1.30453
C	1.53850	-2.00687	1.30453
F	1.95273	-3.26169	1.45533
F	1.95273	-1.27692	2.33627
F	-0.41273	-1.27692	2.33627
F	-0.41273	-3.26167	1.45534
C	1.47858	-1.88817	-1.32374
C	0.06141	-1.88817	-1.32374
F	2.25117	-2.24374	-2.34627
F	-0.71117	-2.24374	-2.34627

Coordinates for Perfluoroindene and its 2- and 3- Hydro  
Substituted Compounds

<u>ATOM</u>	<u>X</u>	<u>Y</u>	<u>Z</u> (Ångstroms)
C	0.0	0.0	0.0
CC	1.3970	0.0	0.0
CC	2.0955	1.2098	0.0
CC	1.3970	2.4197	0.0
CC	0.0	2.4197	0.0
CC	-0.6985	1.2098	0.0
CC	-2.1570	0.8190	0.0
CC	-2.3435	-0.5079	0.0
CC	-0.9864	-1.1699	0.0
FF	2.0635	-1.1540	0.0
FF	3.4285	1.2098	0.0
FF	2.0635	3.5741	0.0
FF	-0.6665	3.5741	0.0
3F	-3.1554	1.7023	0.0
2F	-3.5205	-1.1338	0.0
F	-0.8625	-1.9294	-1.0884
F	-0.8625	-1.9294	1.0884
2H	-3.2970	-1.0150	0.0
3H	-2.9660	1.5350	0.0

Coordinates for Model Compound No. 1. C<sub>10</sub>F<sub>16</sub>

<u>ATOM</u>	<u>X</u>	<u>Y</u>	<u>Z</u> (Angstroms)
C	0.56750	0.0	0.0
C	1.52866	1.27672	0.0
C	2.98388	0.77280	0.0
C	1.52866	-1.27672	0.0
C	2.98388	-0.77280	0.0
F	1.29870	2.00409	-1.08947
F	1.29870	2.00409	1.08947
F	3.59465	1.22985	-1.08947
F	3.59465	1.22985	1.08947
F	3.59465	-1.22985	-1.08947
F	1.29870	-2.00409	-1.08947
F	1.29870	-2.00409	1.08947

From the symmetry properties of this molecule the remainder of the coordinates are the same as above except that X is replaced by -X

Coordinates for Model Compound No. 2 C<sub>10</sub>F<sub>16</sub>

<u>ATOM</u>	<u>X</u>	<u>Y</u>	<u>Z</u> (Ångstroms)
C	0.73300	0.0	0.0
C	1.65980	1.22990	0.0
C	3.09509	0.67174	0.0
C	2.94748	-0.86117	0.0
C	1.43206	-1.13520	0.0
F	3.53185	-1.35244	1.08906
F	3.53185	-1.35244	-1.08906
F	1.41823	1.95411	1.08906
F	1.41823	1.95411	-1.08906
F	3.72654	1.10082	1.08906
F	3.72654	1.10082	-1.08906
F	0.98263	-2.38696	0.0
C	-0.73300	0.0	0.0
C	-1.65980	-1.22990	0.0
C	-3.09509	0.67174	0.0
C	2.94748	0.86117	0.0
C	-1.43206	1.13520	0.0
F	-3.53185	1.35244	1.08906
F	-3.53185	1.35244	-1.08906
F	-1.41822	-1.95411	1.08906
F	-1.41822	-1.95411	-1.08906
F	-3.72654	-1.10082	1.08906
F	-3.72654	-1.10082	-1.08906
F	-0.98263	2.38696	0.0

Coordinates for C<sub>12</sub>F<sub>18</sub> Isomer I

<u>ATOM</u>	<u>X</u>	<u>Y</u>	<u>Z</u> (Ångstroms)
C	0.66500	0.0	0.0
C	0.77242	1.53625	0.0
C	-0.66500	0.0	0.0
C	-0.77242	1.53625	0.0
F	1.29363	2.09329	-1.08947
F	1.29363	2.09329	1.08947
F	-1.29363	2.09329	1.08947
F	-1.29363	2.09329	-1.08947
C	1.71527	-1.12629	0.0
C	2.56724	-2.03991	1.78407
C	2.93767	-0.84045	0.89206
C	1.34486	-2.32577	0.89206
F	2.02551	-1.45897	-1.24979
F	0.17830	-2.19334	1.51695
F	1.39559	-3.49872	0.26716
F	2.25700	-1.70722	3.03386
F	3.47429	-3.01261	1.78407
F	4.10423	-0.97288	0.26716
F	2.88694	0.33251	1.51696
C	-1.71527	-1.12629	0.0
C	-2.56724	-2.03991	-1.78417
C	-2.93767	-0.84045	-0.89206
C	-1.34486	-2.32577	-0.89206
F	-2.02551	-1.45897	1.24979
F	-0.17830	-2.19333	-1.51695
F	-1.39559	-3.49872	-0.26716
F	-2.25700	-1.70722	-3.03386
F	-3.47429	-3.01261	-1.78407
F	-4.10423	-0.97288	-0.26716
F	-2.88694	0.33251	-1.51696

Coordinates for C<sub>12</sub>F<sub>18</sub> Isomer IV

<u>ATOM</u>	<u>X</u>	<u>Y</u>	<u>Z</u> (Angstroms)
C	0.66500	0.0	0.0
C	0.77242	1.53625	0.0
C	-0.66500	0.0	0.0
C	-0.77242	1.53625	0.0
F	1.29363	2.09329	-1.08947
F	1.29363	2.09329	1.08947
F	-1.29363	2.09329	1.08947
F	-1.29363	2.09329	-1.08947
C	1.71528	-1.12629	0.0
C	1.26246	-3.35659	0.0
C	1.48887	-2.19144	1.08894
C	1.48887	-2.19144	-1.08894
C	3.13285	-0.52456	0.0
F	0.42320	-1.96493	-1.85180
F	2.55453	-2.41796	-1.85180
F	0.03819	-3.77626	0.0
F	2.16952	-4.22929	0.0
F	2.55453	-2.41796	1.85180
F	0.42320	-1.96493	1.85180
C	4.77564	-1.19769	1.26150
C	3.65339	-0.15234	1.40075
C	4.25511	-1.56992	-0.13925
F	5.11473	-1.31101	-1.12054
F	3.81703	-2.82190	-0.23680
F	2.79377	-0.41125	2.38204
F	4.09147	1.09965	1.49830
F	4.70221	-2.18891	2.14523
F	5.99991	-0.67802	1.26150
F	3.20628	0.46666	-0.88374
F	-1.57206	-0.97270	0.0

APPENDIX III

COMPUTER PROGRAMS USED FOR THE  
ANALYSIS OF ESCA DATA

The programs described and listed in this appendix are those which have been written specifically for the analysis of ESCA data as well as other standard programs such as the linear least squares regression program. Since some of the programs employ the same subroutines the first section of the appendix gives a brief description of the program and , in general , only a listing of the main program. The second section of the appendix gives a listing of the subroutines in alphabetical order. Where a program requires input of atomic coordinates the format of this has been made the same as that required for the CNDO program used in this work and is also the same as the format of the punched card output from the geometry program.

1) NEWPOT

This program was written primarily to calculate the intra-molecular Madelung-type potential at an atom i.e. the  $\sum_{j \neq i} \frac{q_j}{r_{ij}}$  term in the charge potential model<sup>17</sup>,

$$E = E^0 + kq_i + \sum_{j \neq i} \frac{q_j}{r_{ij}}$$

Values of k may also be used as input when the theoretical shift,  $E - E^0$ , is required. The input and output are both flexible. The coordinate input may be in either A or a.u. and is in the same format as that required for the program CNINDO<sup>148</sup> i.e. (I4,3(3X,F12.7)) where the I4 format is used for input of the atomic number. The electron population on the atoms may be input as (i) the valence electron population (ii) the total electron population (iii) the charge on the atom (iv) the individual orbital populations contributing to the total population on the atom or (v) if the program is to be used for the calculation of inter-atomic distances and/or the nuclear repulsion energy only, no electron population data need be input. The output includes a listing of the coordinates in both Angstrom units and atomic units. Also, if required, an inter-atomic distance matrix may be printed in Angstrom units, atomic units or both. The program may thus be used not only for the calculation of the intra-molecular Madelung potentials and theoretical shifts but also for the calculation of inter nuclear distances and nuclear repulsion energies. Subroutine MATPRT is used for printing matrices.

```

1      C
2      C          ESCA MADFLUNG POTENTIAL PROGRAM      D.B.ACAMS
3      C
4      IMPLICIT REAL*8(A-H,C-Z)
5      DATA END,UNIT1,UNIT2/'END',0.52914700,27.210700/
6      DIMENSION X(50),Y(50),Z(50),AUX(50),AUY(50),AUZ(50),AKAY(50)
7      DIMENSION NZ(50),R(50,50),CHAR(50),NORR(50)
8      WRITE(6,501)
9      1000 READ (5,100) TEST,(X(I),I=1,77)
10     1001 WRITE(6,501) TEST,(X(I),I=1,77)
11     IF(TEST.EQ.END) CALL EXIT
12     C
13     C INPUT IN A.U. INPUT1=1 , OTHERWISE IN ANGSTROMS
14     C DISTANCE OUTPUT IPRINT1=0 NO PRINT OUT IN ANGSTROMS
15     C IPRINT2=0 NO PRINT OUT IN A.U.
16     READ (5,101) NATOMS,INPUT1,IPRINT1,IPRINT2
17     IF(INPUT1.NE.1) GO TO 1010
18     C
19     C INPUT IN ATOMIC UNITS AND CONVERSION TO ANGSTROMS
20     C
21     1020 WRITE(6,502)
22     DO 1021 I = 1,NATOMS
23     READ (5,110) NZ(I),AUX(I),AUY(I),AUZ(I)
24     X(I) = AUX(I) * UNIT1
25     Y(I) = AUY(I) * UNIT1
26     Z(I) = AUZ(I) * UNIT1
27     1021 CONTINUE
28     GO TO 1030
29     C
30     C INPUT IN ANGSTROMS AND CONVERSION TO A.U.
31     C
32     1010 WRITE(6,503)
33     DO 1011 I=1,NATOMS
34     READ (5,110) NZ(I),X(I),Y(I),Z(I)
35     AUX(I) = X(I) / UNIT1
36     AUY(I) = Y(I) / UNIT1
37     AUZ(I) = Z(I) / UNIT1
38     1011 CONTINUE
39     C
40     C IF COP = 0 DOES NOT REQUIRE K VALUES AND DOES NOT CALCULATE SHIFT
41     C NCHOP=1 VALENCE E POPLN. , 2,TOTAL POPLN. 3, CHRGES
42     C 4,ORBITAL POPULATIONS, 5,NO DATA
43     C 4,ORBITAL POPULATIONS , 5,NO DATA-CALCULATES INTER ATOMIC DISTE
44     C
45     1030 READ (5,111) KOP,NCHOP,NUC
46     IF(KOP.EQ.0) GO TO 1050
47     READ (5,120) (AKAY(I),I=1,NATOMS)
48     1050 CONTINUE
49     GO TO (1060,1060,1060,1070,1130),NCHOP
50     1060 READ(5,120) (CHAR(I),I=1,NATOMS)
51     GO TO (1080,1090,1100),NCHOP
52     1080 DO 1081 I=1,NATOMS
53     IF(NZ(I).GE.11) CHAR(I) = CHAR(I) + 1.001
54     IF(NZ(I).LE.10.AND.NZ(I).GT.2) CHAR(I) = CHAR(I) + 2.000
55     1081 CONTINUE
56     GO TO 1090
57     1070 READ (5,122) (NORR(I),I=1,NATOMS)
58     DO 1071 J=1,NATOMS
59     NO = NORR(J)
60     READ (5,120) (R(I,1),I=1,NO)
61     TEMP = 0.0
62     DO 1072 I=1,NO
63     TEMP = TEMP + R(I,1)
64     1072 CONTINUE
65     CHAR(J) = TEMP
66     1071 CONTINUE
67     C
68     C CALCULATE CHARGES FROM TOTAL POPULATION
69     C
70     1090 DO 1091 I=1,NATOMS
71     TEMP = NZ(I)
72     CHAR(I) = TEMP - CHAR(I)
73     1091 CONTINUE
74     1100 IF(KOP.EQ.0) GO TO 1110
75     C

```

```

76 C WRITE COORDINATES ETC.
77 C
78 1120 WRITE(6,510)
79 WRITE(6,515)
80 WRITE(6,525) ((I,NZ(I),X(I),Y(I),Z(I),CHAR(I),AKAY(I)),I=1,NATOMS)
81 WRITE(6,511)
82 WRITE(6,515)
83 WRITE(6,525) ((I,NZ(I),AUX(I),AUY(I),AUZ(I),CHAR(I),AKAY(I)),I=1,
84 NATOMS)
85 GO TO 2000
86 1110 WRITE(6,510)
87 WRITE(6,514)
88 WRITE(6,525) ((I,NZ(I),X(I),Y(I),Z(I),CHAR(I)),I=1,NATOMS)
89 WRITE(6,511)
90 WRITE(6,515)
91 WRITE(6,525) ((I,NZ(I),AUX(I),AUY(I),AUZ(I),CHAR(I)),I=1,NATOMS)
92 GO TO 2000
93 1130 WRITE(6,510)
94 WRITE(6,517)
95 WRITE(6,527) ((I,NZ(I),X(I),Y(I),Z(I)),I=1,NATOMS)
96 WRITE(6,511)
97 WRITE(6,517)
98 WRITE(6,527) ((I,NZ(I),AUX(I),AUY(I),AUZ(I)),I=1,NATOMS)
99
100 C
101 C CALCULATION OF INTER ATOMIC DISTANCES IN ANGSTROMS
102 C
103 2000 DO 2001 I=1,NATOMS
104 DO 2002 J=1,NATOMS
105 R(I,J) = DSQRT((X(I)-X(J))**2+(Y(I)-Y(J))**2+(Z(I)-Z(J))**2)
106 2002 CONTINUE
107 2001 CONTINUE
108 IF(IPRNT1.EQ.0) GO TO 2020
109 WRITE(6,530)
110 CALL MATPRT(R,NATOMS,NATOMS,50,10,C)
111 2020 DO 2021 I=1,NATOMS
112 DO 2022 J=1,NATOMS
113 R(I,J) = R(I,J) / UNIT1
114 2022 CONTINUE
115 2021 CONTINUE
116 IF(IPRNT2.EQ.0) GO TO 2040
117 WRITE(6,531)
118 CALL MATPRT(R,NATOMS,NATOMS,50,10,C)
119 2040 IF(NUC.EQ.0) GO TO 22050
120 ENUC = 0.0
121 DO 22401 I=1,NATOMS
122 DO 22402 J=1,NATOMS
123 IF(I.EQ.J) GO TO 22402
124 TEMP = NZ(I) * NZ(J)
125 ENUC = ENUC + TEMP / R(I,J)
126 22402 CONTINUE
127 22401 CONTINUE
128 ENUC = ENUC / 2.00
129 WRITE(6,130) ENUC
130 130 FORMAT(/20X,'NUCLEAR REPULSION ENERGY(A.U.) =',F22.12/)
131 22050 CONTINUE
132 IF(NCHOP.EQ.5) GO TO 1000
133 DO 2041 I=1,NATOMS
134 X(I) = C.C.
135 2041 CONTINUE
136 C
137 C CALCULATION OF MADELUNG POTENTIALS
138 DO 2042 I=1,NATOMS
139 DO 2043 J=1,NATOMS
140 IF(I.EQ.J) GO TO 2043
141 X(I) = X(I) + CHAR(J) / R(I,J)
142 2043 CONTINUE
143 2042 CONTINUE
144 C
145 C CONVERSION OF POTENTIALS TO EV
146 C
147 DO 2044 I=1,NATOMS
148 Y(I) = X(I) * UNIT2
149 2044 CONTINUE
150 IF(KOP.FQ.0) GO TO 3050
151 C

```

```

151 C      CALCULATE PREDICTED SHIFT IN EV
152 C
153 DO 3001 I=1,NATOMS
154 Z(I) = AKAY(I) *CHAR(I) + Y(I)
155 3001 CONTINUE
156 WRITE(6,540)
157 WRITE(6,541) ((I,AZ(I),CHAR(I),Y(I),X(I),Z(I)),I=1,NATOMS)
158 GO TO 4000
159 3050 WRITE(4,550)
160 WRITE(5,551) ((I,AZ(I),CHAR(I),Y(I),X(I)),I=1,NATOMS)
161 4000 TEMP = 0.0
162 DO 4001 I=1,NATOMS
163 TEMP = TEMP + CHAR(I)
164 4001 CONTINUE
165 WRITE(6,560)TEMP
166 WRITE(5,561)
167 GO TO 1000
168 500 FORMAT('I',20X,'**** PADELUNG POTENTIAL AND INTER ATOMIC DISTANCE
169 PROGRAM ****')
170 501 FORMAT('C',20X,A3,77A1'///)
171 502 FORMAT(' ',20X,'COORDINATE INPUT WAS IN ATOMIC UNITS'///)
172 503 FORMAT(' ',20X,'COORDINATE INPUT WAS IN ANGSTROMS'///)
173 510 FORMAT(' ',20X,'**** COORDINATES IN ANGSTROMS ****')
174 511 FORMAT('///',20X,'**** COORDINATES IN ATOMIC UNITS ****')
175 515 FORMAT('//5X,'CENTRE ATOMIC NO.',10X,'X',11X,'Y',11X,'Z',11X,'Q',
176 111X,'K'///)
177 516 FORMAT('//5X,'CENTRE ATOMIC NO.',10X,'X',11X,'Y',11X,'Z',11X,'C'//
178 1)
179 517 FORMAT('//5X,'CENTRE ATOMIC NO.',10X,'X',11X,'Y',11X,'Z'///)
180 525 FORMAT(' ',5X,I4,6X,I4,6X,5F12.6)
181 526 FORMAT(' ',5X,I4,6X,I4,6X,4F12.6)
182 527 FORMAT(' ',5X,I4,6X,I4,6X,3F12.6)
183 530 FORMAT('I',20X,'**** INTER ATOMIC DISTANCES IN ANGSTROMS ****')
184 531 FORMAT('I',20X,'**** INTER ATOMIC DISTANCES IN ATOMIC UNITS ****'//
185 1/)
186 540 FORMAT('I',5X,'CENTRE ATOMIC NO.',6X,'CHARGE',6X,'POTENTIAL(EV)
187 1POTENTIAL(AU)',5X,'SHIFT(EV)'///)
188 541 FORMAT(' ',5X,I4,4X,I4,10X,F10.4,5X,F10.4,5X,F10.4,5X,F10.4)
189 550 FORMAT('I',5X,'CENTRE ATOMIC NO.',6X,'CHARGE',6X,'POTENTIAL(EV)
190 1POTENTIAL(AU)'///)
191 551 FORMAT(' ',5X,I4,4X,I4,10X,F10.4,5X,F10.4,5X,F10.4)
192 560 FORMAT('//20X,'TOTAL CHARGE =',F12.6)
193 100 FORMAT(A3,77A1)
194 101 FORMAT(4I4)
195 110 FORMAT(I4,3(3X,F12.7))
196 111 FORMAT(3I4)
197 120 FORMAT(9F10.0)
198 122 FORMAT(20I4)
199 541 FORMAT('I')
200 END

```

## ii) CHARGES

This program is used to set up a series of simultaneous equations which may be solved to yield the experimental charge distribution within a molecule (cf. Chapter IV.3). The input required for each atom is the  $k$ -value in eV/unit charge, its experimental shift in core electron binding energy ( $E-E^0$ ) in eV, and its coordinates in Angstrom units. (The coordinate input is consistent with the format used in the CNDO/2 program) The output from the program CHARGES is in a format which may be used as direct input to the standard IBM program SOLN<sup>202</sup> for the solution of simultaneous equations and this is achieved by storing the relevant output from the program in a scratch file on disc and using this as input to the program SOLN in the following job step. The program CHARGES also prints a listing of the input data for each molecule (i.e. title, atomic number, coordinates,  $k$  and  $E-E^0$  values) together with a numbering system for the atoms, which is also the numbering system for the atomic charges produced by the program SOLN. The printing of the input matrix by the program SOLN was suppressed for production runs of the program. The subroutines used by SOLN are MATIN, MXOUT, SIMQ, and LOC<sup>202</sup>.

```

1      C
2      C      ESCA CHARGES PROGRAM      D.B. ADAMS
3      C
4      DIMENSION A(50,50),DIAG(50),X(50),Y(50),Z(50),K(50),P(50),TLE(2,1)
5      NINE = 9
6      50  READ(5,100) IT,NUM,NC
7      IF(IT.EQ.95) GO TO 300
8      READ(5,120) TLE
9      WRITE(6,121) TLE
10     READ(5,101) (DIAG(I),I=1,NC)
11     READ(5,101) (B(I),I=1,NC)
12     WRITE(5,122)
13     DO 200 I=1,NC
14     READ(5,172) K(I),X(I),Y(I),Z(I)
15     WRITE(5,123) I,K(I),X(I),Y(I),Z(I),DIAG(I),B(I)
16     200 CONTINUE
17     DO 202 I=1,NC
18     DO 201 J=1,NC
19     IF(I.EQ.J) GO TO 201
20     A(I,J)=50*(X(I)-X(J))**2+(Y(I)-Y(J))**2+(Z(I)-Z(J))**2)
21     A(I,J)= 14.309/A(I,J)
22     201 CONTINUE
23     202 CONTINUE
24     DO 203 I=1,NC
25     A(I,I) = DIAG(I)
26     203 CONTINUE
27     WRITE(7,150) NUM,NC,NC
28     DO 250 I=1,NC
29     WRITE(7,151) (A(I,J),J=1,NC)
30     250 CONTINUE
31     WRITE(7,152) NINE
32     WRITE(7,151) (B(I),I=1,NC)
33     GO TO 50
34     300 WRITE(7,153) NINE,NINE
35     100 FORMAT(12,3I4)
36     120 FORMAT(20A4)
37     121 FORMAT('1',20A4/)//)
38     101 FORMAT(7F10,2)
39     122 FORMAT('0',10X,'*****COORDINATES*****//')
40     102 FORMAT(14,3(3X,F12,8))
41     123 FORMAT(' ',2I4,5(3X,F12,8))
42     150 FORMAT(2X,3I4)
43     151 FORMAT(7F10,6)
44     152 FORMAT(11)
45     153 FORMAT(78X,11/78X,11)
46     STOP
47     END
48
49
50
51
52
53     DIMENSION A(2500),B(50)
54     10 FORMAT('1',' SOLUTION OF SIMULTANEOUS EQUATIONS')
55     11 FORMAT('0',' DIMENSIONED AREA TOO SMALL FOR INPUT MATRIX',I4)
56     12 FORMAT('0',' EXECUTION TERMINATED')
57     13 FORMAT('0',' ROW AND COLUMN DIMENSIONS NOT EQUAL FOR MATRIX',I4)
58     14 FORMAT('0',' INCORRECT NUMBER OF DATA CARDS FOR MATRIX',I4)
59     15 FORMAT('0',' GO ON TO NEXT CASE')
60     16 FORMAT('0',' STRUCTURE CODE IS NOT ZERO FOR MATRIX',I4)
61     17 FORMAT('1',' ORIGINAL B VECTOR',//)
62     18 FORMAT('1',' SOLUTION VALUES',//)
63     19 FORMAT('0',' MATRIX IS SINGULAR')
64     20 FORMAT(7F10,2)
65     21 FORMAT(13,10X,E15,6)
66     22 FORMAT('0',' END OF CASE')
67     WRITE(6,10)
68     25 CALL MATN(ICOD,A,2500,N,M,MS,(ER)
69     IF(N) 30,95,30
70     30 IF(IEP-1) 45,35,40
71     35 WRITE(6,11) ICOD
72     GO TO 90
73     40 WRITE(6,14) ICOD
74     GO TO 95
75     45 IF(N-M) 50,55,50

```

```
76      50 WRITE(6,13) ICCD
77      GO TO 30
78      55 IF(MS) 60,65,60
79      60 WRITE(6,16) ICCD
80      GO TO 30
81      65 CALL PYGOUT(ICCD,A,M,M,MS,60,120,2)
82      READ(5,21)(P(I),I=1,N)
83      WRITE(5,17)
84      DO 70 I=1,N
85      70 WRITE(5,21) I,P(I)
86      CALL SIMQ(A,B,N,KS)
87      IF(KS-1) 80,75,80
88      75 WRITE(5,19)
89      WRITE(5,15)
90      GO TO 25
91      80 WRITE(5,19)
92      DO 85 I=1,N
93      85 WRITE(5,21) I,P(I)
94      WRITE(5,22)
95      GO TO 25
96      90 READ(5,21) (R(I),I=1,N)
97      WRITE(5,15)
98      GO TO 25
99      95 WRITE(6,12)
100     RETURN
101     END
```

iii) ATCH

This program is used to calculate experimental charge distributions from ESCA data and is more versatile than the charges program described previously. The input format of the coordinates is again consistent with the programs CNINDO and NEWPOT and may be in either Angstroms or atomic units. The input of the  $k$  and  $(E-E^0)$  values is facilitated by use of NAMELIST input instead of the more rigid input format of the other programs. This program also has the facility to declare that two or more atoms have the same charge and impose the condition that the sum of the charges is zero for a molecule. There is also a facility to fix the charge on an atom to any desired value. (However these latter two facilities have not been employed in any of the work reported in this thesis.) The matrix of coefficients for the set of simultaneous equations may be printed if required, and the final output includes a listing of the charges on each atom and the constraint, if any, placed on the charge. The sum of the experimental charges is also printed. The program uses the subroutines MATPRT, SIMQ, and ARRAY<sup>202</sup>.

```

1 C
2 C          ESCA CHARGES PROGRAM          ATCM          C.B.ACAMS
3 C
4 REAL X(50),Y(50),Z(50),SHIFT(50),CONST(50),TITLE(50),R(50,50),
5 I      CNSTR(50),FXCHAR(50),S(2500)
6 INTEGER ATNO(50),NVAL(50),NEQ(50),PRINT(5),UNIT
7 EQUIVALENCE(F(1),S(1))
8 DATA BLANK, FIXED, EQUIV, FND/ ' ', 'FIXD', 'EQU', 'END' /
9 NAMELIST /INPUT/ SHIFT,CONST,PRINT
10 READ (5,10)(TITLE(I),I=1,20)
11 IF(TITLE(1).EQ.END) CALL EXIT
12 WRITE(5,11)
13 WRITE(5,115) (TITLE(I),I=1,20)
14 C READ NUMBER OF ATOMS, TOTAL MOLECULAR CHARGE AND INPUT UNITS
15 C 0 FOR AU. 1 FOR ANGSTROMS
16 READ (5,15) NATOMS,NOLCH,UNIT
17 C READ ATOMIC NUMBERS AND COORDINATES
18 READ (5,20) (ATNO(I),X(I),Y(I),Z(I)),I=1,NATOMS)
19 C SET MATRIX PRINT OPTIONS TO ZERO
20 DO 1010 I=1,5
21 PRINT(I) = 0
22 1010 CONTINUE
23 C READ SHIFTS, K-VALUES AND PRINT OPTIONS - NAMELIST INPUT
24 READ(5,INPUT)
25 C IF COORDINATES IN ANGSTROMS PRINT AND CONVERT TO AU.
26 IF(UNIT.NE.1) GO TO 1020
27 WRITE(5,125)
28 DO 1015 I=1,NATOMS
29 WRITE(5,126) I,ATNO(I),X(I),Y(I),Z(I)
30 X(I) = X(I) / 0.529167
31 Y(I) = Y(I) / 0.529167
32 Z(I) = Z(I) / 0.529167
33 1015 CONTINUE
34 1020 CONTINUE
35 C WRITE COORDINATES, K-VALUES AND SHIFTS
36 WRITE (6,130)
37 WRITE (6,131)((I,ATNO(I),X(I),Y(I),Z(I),SHIFT(I),CONST(I)),I=1,NAT
38 OMS)
39 C CALCULATE 1/R FROM INTERNUCLEAR DISTANCES AND CONVERT TO EV
40 M = 1
41 N = NATOMS - 1
42 DO 1030 I=1,N
43 M = M + 1
44 DO 1025 J=M,NATOMS
45 P(I,J) = SQRT((X(I)-X(J))**2 + (Y(I)-Y(J))**2 + (Z(I)-Z(J))**2)
46 IF(P(I,J).LT.1.0-4) P(I,J)=1.0-4
47 R(I,J) = 27.2107 / P(I,J)
48 P(J,I) = P(I,J)
49 1025 CONTINUE
50 1030 CONTINUE
51 C PLACE K-VALUES ON THE DIAGONAL
52 DO 1035 I=1,NATOMS
53 R(I,I) = CONST(I)
54 1035 CONTINUE
55 C PRINT THIS INITIAL MATRIX IF REQUIRED
56 IF(PRINT(1).EQ.0) GO TO 1040
57 WRITE(6,135)
58 CALL MATPRT(R,NATOMS,NATOMS,50,10,0)
59 1040 CONTINUE
60 C SET UP EQUATIONS FOR ATOMS WITH A GIVEN CHARGE
61 READ (5,15) NFIX
62 IF(NFIX.EQ.0) GO TO 1044
63 READ (5,15) (NVAL(I),I=1,NFIX)
64 READ (5,25)(FXCHAR(I),I=1,NFIX)
65 DO 1042 I=1,NFIX
66 K = NVAL(I)
67 SHIFT(K) = FXCHAR(I)
68 DO 1041 J=1,NATOMS
69 R(K,J) = 0.0
70 1041 CONTINUE
71 R(K,K) = 1.0
72 1042 CONTINUE
73 1044 CONTINUE
74 C READ SET OF ATOMS ASSIGNED EQUAL CHARGE
75 READ (5,15) NI

```

```

76 C READ (5,15) NI
77 IF(NI.EQ.0) GO TO 1040
78 READ (5,15) (NEQ(I),I=1,NI)
79 C SET VALUE OF SHIFT FOR THESE TO 0 AND MOLCH FOR THE LAST EQUATION
80 DO 1045 I=1,NI
81 K = NEQ(I)
82 SHIFT(K) = 0.0
83 1045 CONTINUE
84 K = NEQ(NI)
85 SHIFT(K) = MOLCH
86 C SET COEFFICIENTS TO ZERO EXCEPT FOR LAST EQUATION
87 NIT = NI - 1
88 DO 1050 I=1,NIT
89 K = NEQ(I)
90 DO 1049 J=1,NATOMS
91 R(K,J) = 0.0
92 1049 CONTINUE
93 1050 CONTINUE
94 C SET UP EQUATIONS FOR DIFFERENCE OF CHARGES ON TWO ATOMS
95 DO 1055 I = 1,NIT
96 K = NEQ(I)
97 J = NEQ(I+1)
98 R(K,K) = 1.0
99 R(K,J) = -1.0
100 1055 CONTINUE
101 C SET UP EQUATION FOR SUM OF CHARGES
102 K = NEQ(NI)
103 DO 1060 J=1,NATOMS
104 R(K,J) = 1.0
105 1060 CONTINUE
106 C WRITE FINAL FORM OF MATRIX IF REQUIRED
107 IF(PRINT(2).EQ.0) GO TO 1065
108 WRITE(6,140)
109 CALL MATPRF(R,NATOMS,NATOMS,50,10,0)
110 1065 CONTINUE
111 C WRITE FINAL SHIFT VECTOR IF REQUIRED
112 IF(PRINT(3).EQ.0) GO TO 1075
113 WRITE (6,145)
114 WRITE (6,150) (SHIFT(I),I=1,NATOMS)
115 1075 CONTINUE
116 CALL ARRAY(2,NATOMS,NATOMS,50,50,S,R)
117 CALL SING(S,SHIFT,NATOMS,KS)
118 IF(KS.EQ.1) GO TO 1115
119 C SUM CHARGES
120 SUM = 0.0
121 DO 1080 I=1,NATOMS
122 SUM = SUM + SHIFT(I)
123 1080 CONTINUE
124 C SET CNSTR TO BLANK, FIXED OR EQUIV DEPENDING ON CONSTRAINT PLACED ON
125 DO 1085 I=1,NATOMS
126 CNSTR(I) = BLANK
127 1085 CONTINUE
128 IF(NFIX.EQ.0) GO TO 1091
129 DO 1090 I=1,NFIX
130 K = NVAL(I)
131 CNSTR(K) = FIXED
132 1090 CONTINUE
133 1091 CONTINUE
134 IF(NI.EQ.0) GO TO 1096
135 DO 1095 I=1,NI
136 K = NEQ(I)
137 CNSTR(K) = EQUIV
138 1095 CONTINUE
139 1096 CONTINUE
140 WRITE(6,155)
141 WRITE(6,160) ((I,ATNO(I),SHIFT(I),CNSTR(I)),I=1,NATOMS)
142 WRITE(6,165) SUM
143 GO TO 1000
144 1115 WRITE(6,170)
145 GO TO 1000
146 10 FORMAT(20A4)
147 15 FORMAT(20I4)
148 20 FORMAT(14,F15.7,F15.7,F15.7)
149 25 FORMAT(9E10,G)
150 110 FORMAT('1',20X,'***** CALCULATION OF ATOMIC CHARGES FROM ESCA CHE

```

```
151          IMICAL SHIFTS ****)
152          115 FORMAT(' ',10X,2'A4)
153          125 FORMAT('//1'X,'COORDINATES IN ANGSTROM UNITS'//5X,'ATOM  ATOMIC NO.
154          ' ',4X,'X',15X,'Y',15X,'Z'//)
155          126 FORMAT(5X,14,4X,14,3F15.6)
156          130 FORMAT('//1'X,'COORDINATES IN ATOMIC UNITS'//5X,'ATOM  ATOMIC NO.',
157          ' ',4X,'X',15X,'Y',15X,'Z',10X,'SHIFT  K'//)
158          131 FORMAT(5X,14,4X,14,3F15.6,3X,3F9.4,1X,3F9.4)
159          135 FORMAT('//1'X,'INITIAL MATRIX OF COEFFICIENTS'//)
160          140 FORMAT('//1'X,'FINAL MATRIX OF COEFFICIENTS'//)
161          145 FORMAT('//1'X,'FINAL SHIFT VECTOR'//)
162          150 FORMAT(12X,F10.4)
163          155 FORMAT(' ',5X,'ATOM  ATOMIC NO.  CHARGE'//)
164          160 FORMAT(' ',5X,14,15,4X,F10.5,2X,A4)
165          165 FORMAT('//5X,'SUM OF CALCULATED CHARGES=',F9.5)
166          170 FORMAT('//5X'MATRIX SINGULAR CONTINUE WITH NEXT CALCULATION')
167          END
```

iv) GEOM 1

This program is used to calculate the coordinates of atoms in a molecule using bond angles and distances. Punched card output of the coordinates in a format consistent with coordinate input format of the programs CNINDO, NEWPOT, CHARGES, and ATCH is obtained. The input data required is clearly set out in the comment cards in the program listing. Subroutine MATPRT is used for printing inter-nuclear distance matrices.

```

1 C FORTRAN IV PROGRAM GEOM1 (INPUT, OUTPUT, PUNCH, TAPE 5=INPUT,
2 C I TAPE 6=OUTPUT, TAPE 7=PUNCH)
3 C GEOM1 CALCULATES THE COORDINATES IN 3-DIMENSIONAL MOLECULES, GIVEN
4 C THE BOND LENGTHS, BOND ANGLES AND DIBEDRAL ANGLES
5 C THE CARD OUTPUT FROM GEOM1 CAN BE USED DIRECTLY AS INPUT TO INDO
6 C PROGRAMMED BY M.J.C. FFWAR AND REVISED BY H.C. BAIRD-U. OF TEXAS
7 C ***** INPUT DATA FOR EACH MOLECULE *****
8 C FIRST CARD HAS MOLECULE CHARGE IN COLS. 1-2, AND HAS THE MOLECULE
9 C NAME IN COLS. 3-34
10 C SECOND CARD. NOAT 12
11 C IZAT(1) 12
12 C IZAT(2) 12
13 C IZAT(3) 12
14 C KWIK 11
15 C R12 F7.4
16 C R23 F7.4
17 C THETA F14.7
18 C EACH SUCCESSIVE CARD. NA 12
19 C NR 12
20 C NC 12
21 C ND 12
22 C IZAT(ND) 12
23 C ILAZY 11
24 C RCC F7.4
25 C THRCO F14.7
26 C PHARCO F14.7
27 C A CARD WITH 99 IN COLS. 1-2 MUST BE ADDED AT THE END OF
28 C THE ENTIRE DECK OF MOLECULES TO TERMINATE THE PROGRAM
29 C CARDS FOR ATOMS WITH IZAT=99 ARE NOT PUNCHED
30 C
31 C DIMENSION X(100), Y(100), Z(100), R(100,100), IZAT(100), NAME(18)
32 C WRITE(7, 987)
33 C 980 FORMAT(4H )
34 C 45 READ(5, 980) ICHG, (NAME(I), I=1, 18)
35 C 990 FORMAT(12, 18A4)
36 C IF(ICHG.EQ.99) GO TO 99
37 C WRITE(6, 950) (NAME(I), I=1, 18), ICHG
38 C 950 FORMAT(11H1, 18A4, 7HCHARGE=, I3)
39 C WRITE(7, 981) ICHG, (NAME(I), I=1, 18)
40 C 981 FORMAT(12, 8X, 18A4)
41 C READ(5, 991) NCAT, (IZAT(I), I=1, 3), KWIK, R12, R23, THETA
42 C 991 FORMAT(4I2, 1I, 2F7.4, F14.7)
43 C WRITE(6, 952) R12, R23, THETA
44 C WRITE(6, 951) NOAT, (IZAT(I), I=1, 3), KWIK
45 C 951 FORMAT (8HNOAT = 12, 14H IZAT(1) = 12, 14H IZAT(2) = 12,
46 C 114H IZAT(3) = 12, 11H KWIK = 11)
47 C 952 FORMAT (7H R12 = F7.4, 10H R23 = F7.4, 12H THETA = E14.7)
48 C
49 C NOAT IS THE NUMBER OF ATOMS. IZAT(I) IS THE ATOMIC NUMBER OF ATOM
50 C NUMBER I. KWIK ALLOWS AUTOMATIC CALCULATION OF COORDINATES OF
51 C ATOMS 1, 2, 3 IN SIMPLE CASES, KWIK = 0, TETRAHEDRAL, KWIK = 1,
52 C ANGLE 120 DEGREES, KWIK = 2, ANGLE SUPPLIED AS DATAUM.
53 C R12, R23 ARE BOND LENGTHS. THETA IS THE 123 BOND ANGLE.
54 C
55 C IF (KWIK - 1) 1, 2, 3
56 C 1 CCOS=-1./3.
57 C SSIN=(2./3.)=SQRT(2.)
58 C GO TO 4
59 C 2 CCOS=-.5
60 C SSIN=.5*SQRT(3.)
61 C GO TO 4
62 C 3 THETA=THETA*3.1415926536/180.
63 C CCOS=COS(THETA)
64 C SSIN=SIN(THETA)
65 C 4 DO 5 I=1,3
66 C X(I)=0.0
67 C Y(I)=0.0
68 C 51 Z(I)=0.0
69 C X(2)=R12
70 C X(3)=R12-R23*CCOS
71 C Y(3)=R23*SSIN
72 C DO 5 I = 4, NOAT
73 C 5 X(I) = 10000.0
74 C WRITE(5, 953)
75 C 953 FORMAT (8RH0 NA NB NC ND IZAT(ND) ILAZY RCC

```

```

76      1          THRCO          PHARCO/)
77      DO 52 I=4,NQAT
78      C
79      C      ATOMS NA, NB, NC, HAVE KNOWN COORDINATES AND ARE NOT COLLINEAR.
80      C      IZAT(ND) IS THE ATOMIC NUMBER OF ATOM ND. THRCO IS THE BCD BOND
81      C      ANGLE IN DEGREES AND PHARCO THE DIHEDRAL ANGLE OF CD RELATIVE TO
82      C      AB, MEASURED CLOCKWISE ALONG THE DIRECTION B TO C. ILAZY ALLOWS
83      C      AUTOMATIC CALCULATION OF ANGLES IN NORMAL TETRAHEDRAL AND PLANAR
84      C      SYSTEMS. ILAZY = 0, 1, 2, 3, 4, 5 TETRAHEDRAL WITH DIHEDRAL
85      C      ANGLES OF RESPECTIVELY 0, 60, 120, 180, 240, 310 DEGREES.
86      C      ILAZY = 6, 7 PLANAR CIS, TRANS RESPECTIVELY. ILAZY = 8, ATOMS
87      C      B, C, D COLLINEAR. ILAZY = 9, ANGLES FROM DATA
88      C
89      READ(5,902)NA,NB,NC,NO,IZAT(ND),ILAZY,PCD,THRCO,PHARCO
90      902 FORMAT(5I2,11,F7.4,2F1-.7)
91      C
92      C      CHECK THAT COORDINATES OF ATOMS NA, NB, NC HAVE BEEN CALCULATED
93      C
94      7 IF (X(NA) + X(NB) + X(NC) - 7070.0) 8, 50, 50
95      8 WRITE(6,954)NA,NB,NC,IZAT(ND),ILAZY,PCD,THRCO,PHARCO
96      954 FORMAT (3X,I2,3X,I2,3X,I2,3X,I2,6X,I2,10X,11,7X,F7.4,6X,E14.7,4X,
97      1E14.7)
98      IF (ILAZY - 8) 79, 70, 79
99      70 RBC=SQRT((X(NC)-X(NB))**2+(Y(NC)-Y(NB))**2+(Z(NC)-Z(NB))**2)
100     X(ND) = X(NC) + (X(NC) - X(NB))*PCD/RBC
101     Y(ND) = Y(NC) + (Y(NC) - Y(NB))*PCD/RBC
102     Z(ND) = Z(NC) + (Z(NC) - Z(NB))*PCD/RBC
103     GO TO 52
104     C
105     C      MOVE ATOM C TO ORIGIN
106     C
107     79 XA = X(NA) - X(NC)
108     YA = Y(NA) - Y(NC)
109     ZA = Z(NA) - Z(NC)
110     XB = X(NB) - X(NC)
111     YB = Y(NB) - Y(NC)
112     ZB = Z(NB) - Z(NC)
113     C
114     C      ROTATE ABOUT Z-AXIS TO MAKE YB = 0, XB +VE. IF XYB TOO SMALL,
115     C      ROTATE FIRST 90 DEGREES ABOUT Y AXIS
116     C
117     XYB=SQRT(XB**2+YB**2)
118     K = 1
119     IF (XYB - 0.1) 9, 10, 10
120     9 K = 0
121     XPA = ZA
122     ZPA = -XA
123     XA = XPA
124     ZA = ZPA
125     XPB = ZB
126     ZPB = -XB
127     XB = XPB
128     ZB = ZPB
129     XYB=SQRT(XB**2+YB**2)
130     10 COSTH = XE/XYB
131     SINTH = YB/XYB
132     XPA = XA*COSTH + YA*SINTH
133     YPA = YA*COSTH - XA*SINTH
134     C
135     C      ROTATE ABOUT Y AXIS TO MAKE ZB VANISH
136     C
137     11 RBC=SQRT(XB**2+YB**2+ZB**2)
138     SINPH = ZB/RBC
139     COSPH=SQRT(1.-SINPH**2)
140     XQA = XPA*COSPH + ZA*SINPH
141     ZQA = ZA*CCSPH - XPA*SINPH
142     C
143     C      ROTATE ABOUT X AXIS TO MAKE ZA = 0, YA +VE
144     C
145     12 YZA=SQRT(YPA**2+ZQA**2)
146     COSKH = YPA/YZA
147     SINKH = ZQA/YZA
148     C
149     C      COORDINATES A, (XQA,YZA,0), B, (RBC,0,0), C, (0,0,0), NONE -VE
150     C      COORDINATES OF D NOW CALCULATED IN NEW FRAME

```

```

151
152
153 IF (ILAZY - 1) 13, 14, 15
154   13 COSD = 1.0
155   SIND = 0
156   GO TO 21
157   14 COSD = 0.5
158   SIND=0.5*SQRT(3.)
159   GO TO 21
160   15 IF (ILAZY - 3) 16, 17, 18
161   16 COSD = -0.5
162   SIND=0.5*SQRT(3.)
163   GO TO 21
164   17 COSD = -1.0
165   SIND = 0
166   GO TO 21
167   18 IF (ILAZY - 5) 19, 20, 22
168   19 COSD = -0.5
169   SIND=-0.5*SQRT(3.)
170   GO TO 21
171   20 COSD = 0.5
172   SIND=-0.5*SQRT(3.)
173   21 COSA = -1.0/3.0
174   SINA=(2./3.)*SQRT(2.)
175   GO TO 29
176   22 IF (ILAZY - 7) 23, 24, 26
177   23 COSD = 1.0
178   SIND = 0
179   GO TO 25
180   24 COSD = -1.0
181   SIND = 0
182   25 COSA = -0.5
183   SINA=0.5*SQRT(3.)
184   GO TO 29
185   26 IF (ILAZY - 9) 27, 28, 28
186   27 CONTINUE
187   GO TO 29
188   28 THBCD=THBCD*3.1415926536/180.
189   PHABCD=PHABCD*3.1415926536/180.
190   SINA=SIN(THBCD)
191   COSA=COS(THBCD)
192   SIND=SIN(PHABCD)
193   COSD=COS(PHABCD)
194   29 CONTINUE
195   XD = PCD*CCSA
196   YD = PCD*SINA*COSD
197   ZD = PCD*SINA*SIND
198
199 C
200 C
201 C
202 C
203 C
204 C
205 C
206 C
207 C
208 C
209 C
210 C
211 C
212 C
213 C
214 C
215 C
216 C
217 C
218 C
219 C
220 C
221 C
222 C
223 C
224 C
225 C
30 YPD = YD*COSKH - ZD*SINKH
31 ZPD = ZD*COSKH + YD*SINKH
32 XPD = XD*CCSPH - ZPD*SINPH
33 ZQD = ZPD*CCSPH + XD*SINPH
34 XQD = XPD*CCSTH - YPD*SINTH
35 YQD = YPD*CCSTH + XPD*SINTH
36 IF (K - 1) 31, 32, 31
37 31 XRD = -ZQD
38 ZRD = XQD
39 XQD = XRD
40 ZQD = ZRD
41 32 X(ND) = XQD + X(ND)
42 Y(ND) = YQD + Y(ND)
43 Z(ND) = ZQD + Z(ND)
44 52 CONTINUE
45 WRITE(6,950) (NAME(I),I=1,18), ICMG
46 WRITE(6,955)
47 955 FORMAT (78HEND OF ATOM X-COORDINATE Y-COORDINAT
48 1E Z-COORDINATE/)
49 DO 41 I=1,NCAT
50 WRITE(6,956) I, X(I), Y(I), Z(I)
51 956 FORMAT(1H ,5X,12,15X,F10.7,11X,F10.7,11X,F10.7)
52 IF (IZAT(I).EQ.99) GO TO 41
53 WRITE(7,982) IZAT(I), X(I), Y(I), Z(I)
54 982 FORMAT(14,3(3X,F12.7))
55 41 CONTINUE

```

```
226      WRITE(7,980)
227      DO 88 I=1,NCAT
228      DO 88 J=1,NCAT
229      88 R(I,J)=SQRT((X(I)-X(J))**2+(Y(I)-Y(J))**2+(Z(I)-Z(J))**2)
230      WRITE(5,950)(NAME(I),I=1,19),ICMG
231      WRITE(5,957)
232      957 FORMAT(1H0,21HINTERATOMIC DISTANCES,/)
233      CALL MATPRT(9,NCAT,NCAT,100,1000)
234      GO TO 45
235      50 WRITE(6,958)
236      958 FORMAT(1H0,3EHCCCCPS.CF 1 REFERENCE ATOM UNAVAILABLE)
237      99 WRITE(7,983)
238      983 FORMAT(2H99)
239      END
```

v) LEAST SQUARES

This standard linear least squares regression program was used for the calculation of the correlations between (a) charges on an atom the Madelung potential-corrected binding energies to obtain values of  $k$  and  $E^0$  (cf. figure 4.1) and (b) experimental and CNDO charges (cf. Chapter IV).

```

1      C      SIMPLE REGRESSION BY LEAST SQUARES
2      C
3      INTEGER F,N,R
4      DOUBLE PRECISION X(200,2),Y(2,2),S(1,2),Z(2,2),R,SSR,RSQ,A,E,
5      FTEST,H=AM(2),SD(2),DSQRT
6      READ(5,70)F
7      DO 99 I=1,F
8      READ(5,100)F,N
9      IF(F.EQ.1)GOTO 1
10     IF(F.EQ.2)GOTO 2
11     DO 10 K=1,N
12     READ(5,101)(X(K,L),L=1,2)
13     10 CONTINUE
14     GOTO 3
15     DO 11 L=1,2
16     READ(5,101)(X(K,L),K=1,N)
17     11 CONTINUE
18     DO 4 J=1,2
19     DO 4 K=1,2
20     Y(J,K)=0
21     4 CONTINUE
22     DO 5 L=1,2
23     DO 6 M=1,2
24     DO 6 K=1,N
25     Y(L,M)=Y(L,M)+(X(K,L)*X(K,M))
26     6 CONTINUE
27     5 CONTINUE
28     DO 9 L=1,2
29     S(1,L)=0
30     9 CONTINUE
31     DO 7 K=1,N
32     S(1,L)=S(1,L)+X(K,L)
33     7 CONTINUE
34     DO 12 L=1,2
35     DO 12 M=1,2
36     Z(L,M)=0
37     Z(L,M)=Y(L,M)-(S(1,L)*S(1,M)/N)
38     12 CONTINUE
39     WRITE(6,112)
40     DO 50 L=1,2
41     MEAN(L)=S(1,L)/N
42     SD(L)=0.0
43     DO 51 K=1,N
44     SD(L)=SD(L)+(X(K,L)-MEAN(L))**2
45     51 CONTINUE
46     SD(L)=DSQRT(SC(L)/N)
47     WRITE(6,105)L,S(1,L),MEAN(L),SD(L)
48     50 CONTINUE
49     B=Z(1,2)/Z(2,2)
50     SSR=Z(1,2)+B
51     RSQ=SSR/Z(1,1)
52     A=(S(1,1)-(B*S(1,2)))/N
53     E=DSQRT((1.0/Z(2,2))*((Z(1,1)-SSR)/(N-2)))
54     WRITE(6,102)SSR,RSQ
55     IF(B.GT.0)GOTO 55
56     WRITE(6,103)A,B,E
57     GOTO 56
58     55 WRITE(6,106)A,B,E
59     FTEST=SSR/((Z(1,1)-SSR)/(N-2))
60     WRITE(6,104)FTEST
61     98 CONTINUE
62     99 FORMAT(I2)
63     100 FORMAT(I1,I3)
64     101 FORMAT(10(F8.3))
65     102 FORMAT(////IX,'SUM OF SQUARES DUE TO THE REGRESSION=',F12.4,
66     2//IX,'R SQUARED=',F5.4)
67     103 FORMAT(//IX,'Y=',F11.4,IX,F9.4,'X',/15X,'( ',F9.4,' )')
68     104 FORMAT(//IX,'F-VALUE=',F8.3)
69     105 FORMAT(//IX,12,2X,F13.3,F13.3,3X,F13.3)
70     106 FORMAT(//IX,'Y=',F11.4,'+',F9.4,'X',/15X,'( ',F9.4,' )')
71     112 FORMAT(//5X,'SUMS OF DATA',5X,'MEANS',3X,'STD.DEVIATIONS')
72     STOP
73     END

```

vi) ESCA KINETIC ENERGY DATA PROGRAM

This program, although not actually used in the analysis of ESCA data, is used to produce a listing of kinetic energies of photoelectrons for any given X-ray energy in a convenient and easily legible form. Where relevant, the spin-orbit splitting is also printed. The input required is the name and energy of the X-rays and for each element the atomic number, title, the principal quantum numbers of the shells to be considered and the binding energies. The two short subroutines called by the program, KINET and PRINT, are listed directly after the main program since they form an integral part of the program and are not used by any of the other programs.

1  
2  
3  
4  
5  
6  
7  
8  
9  
10  
11  
12  
13  
14  
15  
16  
17  
18  
19  
20  
21  
22  
23  
24  
25  
26  
27  
28  
29  
30  
31  
32  
33  
34  
35  
36  
37  
38  
39  
40  
41  
42  
43  
44  
45  
46  
47  
48  
49  
50  
51  
52  
53  
54  
55  
56  
57  
58  
59  
60  
61  
62  
63  
64  
65  
66  
67  
68  
69  
70  
71  
72  
73  
74  
75

```
C
C      ESCA KINETIC ENERGY DATA PROGRAM
C
DIMENSION XRAY1(3),XRAY2(3),ELMNT(6)
INTEGER SHELL
INTEGER ATNO
COMMON/FRED/BE(7),EMG(7),EAL(7),SPLIT(3)
READ (5,100) XRAY1,XRAY2
READ (5,105) EN1,EN2
1070 READ (5,110) ATNO,ELMNT
IF(ATNO.EQ.9999) GO TO 2000
WRITE(6,200) ELMNT,ATNO
WRITE(6,202) XRAY1,EN1
WRITE(6,202) XRAY2,EN2
WRITE(6,205)
WRITE(6,210) XRAY1,XRAY2
1100 READ (5,115) SHELL
GO TO (1010,1020,1030,1040,1050,1060,1070), SHELL
1010 READ (5,125) BE(1)
CALL KINET(1,EN1,EN2)
CALL PRINT(1,1)
GO TO 1100
1020 READ (5,105) (BE(I),I=1,3)
SPLIT(1) = BE(2) - BE(3)
CALL KINET(3,EN1,EN2)
CALL PRINT(3,2)
GO TO 1100
1030 READ (5,105) (BE(I),I=1,5)
SPLIT(1) = BE(2) - BE(3)
SPLIT(2) = BE(4) - BE(5)
CALL KINET(5,EN1,EN2)
CALL PRINT(5,5)
GO TO 1100
1040 READ (5,105) (BE(I),I=1,7)
SPLIT(1) = BE(2) - BE(3)
SPLIT(2) = BE(4) - BE(5)
SPLIT(3) = BE(6) - BE(7)
CALL KINET(7,EN1,EN2)
CALL PRINT(7,10)
GO TO 1100
1050 READ (5,105) (BE(I),I=1,5)
SPLIT(1) = BE(2) - BE(3)
SPLIT(2) = BE(4) - BE(5)
CALL KINET(5,EN1,EN2)
CALL PRINT(5,17)
GO TO 1100
1060 READ (5,105) (BE(I),I=1,5)
SPLIT(1) = BE(2) - BE(3)
SPLIT(2) = BE(4) - BE(5)
CALL KINET(5,EN1,EN2)
CALL PRINT(5,22)
GO TO 1100
2000 WRITE(6,1)
1 FORMAT('1')
200 FORMAT('1'////////25Y,'*****',6A4,'*****',9X,'ATOMIC NO.',I4////)
205 FORMAT(' ',5X,'LEVEL BINDING ENERGY',7X,'KINETIC ENERGY',10X,'SPLI
IN-ORBIT SPLITTING')
210 FORMAT(' ',29X,3A4,1X,3A4)
202 FORMAT(' ',15X,'ENERGY OF ',3A4,' XRAYS = ',F10.1,' EV//)
100 FORMAT(3A4,3A4)
105 FORMAT(8F10.0)
110 FORMAT(I4,6A4)
115 FORMAT(I1)
CALL EXIT
END

SUBROUTINE KINET(N,EN1,EN2)
COMMON/FRED/BE(7),EMG(7),EAL(7),SPLIT(3)
DO 10 I=1,N
EMG(I) = EN1 - BE(I)
EAL(I) = EN2 - BE(I)
IF(EMG(I).LT.0.0) EMG(I) = 0.0
```

```

76     IF(EAL(I).LT.0.0) EAL(I) = 0.0
77     IF(BE(I).EQ.0.0) BE(I)=0.0
78     IF(RE(I).EQ.0.0) EAL(I)=0.0
79     10 CONTINUE
80     RETURN
81     END
82
83
84
85
86     SUBROUTINE PRINT(N,J)
87     DOUBLE PRECISION L(24)
88     DATA L(1)/'1S'/
89     DATA L(2),L(3),L(4)/'2S','2P1/2','2P3/2'/
90     DATA L(5),L(6),L(7),L(8),L(9)/'3S','3P1/2','3P3/2','3D3/2','3D5/2'
91     1/
92     DATA L(10),L(11),L(12),L(13),L(14),L(15),L(16)/'4S','4F1/2','4P3/2
93     1','4D3/2','4D5/2','4F5/2','4F7/2'/
94     DATA L(17),L(18),L(19),L(20),L(21)/'5S','5P1/2','5P3/2','5D3/2','5
95     1D5/2'/
96     DATA L(22),L(23),L(24),L(25),L(26)/'6S','6P1/2','6P3/2','6D3/2','6
97     1D5/2'/
98     COMMON/FRED/RE(7),EMG(7),EAL(7),SPLIT(3)
99     K=1
100    DO 10 I=1,6
101    IF(I.EQ.3.OR.I.EQ.5.OR.I.EQ.7) GO TO 20
102    WRITE(5,215) L(J+I-1),BE(I),EMG(I),EAL(I)
103    GO TO 10
104    20 WRITE(5,215) L(J+I-1),BE(I),EMG(I),EAL(I),SPLIT(K)
105    K=K+1
106    10 CONTINUE
107    WRITE(6,1)
108    1 FORMAT('0')
109    215 FORMAT(' ',5X,A6,F11.1,8X,F8.1,5X,F8.1,13X,F5.1)
110    RETURN
111    END

```

**SUBROUTINES EMPLOYED IN PROGRAMS**

```

1      SUBROUTINE ARRAY (MODE,I,J,N,M,S,D)
2      DIMENSION S(I),D(I)
3      NI = N - I
4      C   TEST TYPE OF CONVERSION
5      IF(MODE-1) 100,100,120
6      C   CONVERT FROM SINGLE TO DOUBLE DIMENSION
7      100 IJ = I * J + 1
8          NM = N * J + 1
9          DO 110 K=1,J
10         NM = NM - NI
11         DO 110 L=1,I
12             IJ = IJ - 1
13             NM = NM - 1
14         110 D(NM) = S(IJ)
15         GO TO 140
16      C   CONVERT FROM DOUBLE TO SINGLE DIMENSION
17      120 IJ = 0
18          NM = 0
19          DO 130 K=1,J
20             DO 125 L=1,I
21                 IJ = IJ + 1
22                 NM = NM + 1
23             125 S(IJ) = D(NM)
24             130 NM = NM + NI
25         140 RETURN
26         END

```

```

27
28
29
30
31      SUBROUTINE LCC(I,J,IP,N,M,MS)
32      IX=I
33      JX=J
34      IF(MS-1) 17,20,30
35      10 IRX=N-(JX-1)+IX
36      GO TO 36
37      20 IF(IX-JX) 22,24,24
38      22 IPX=IX+(JX+JX-JX)/2
39      GO TO 36
40      24 IRX=JX+(IX+IX-IX)/2
41      GO TO 36
42      30 IRX=0
43      IF(IX-JX) 36,32,36
44      32 IRX=IX
45      36 IR=IRX
46      RETURN
47      END

```

```

48
49
50
51
52      SUBROUTINE MATIN(ICODE, A,ISIZE,IROW,ICOL,IS,IER)
53      DIMENSION A(I)
54      DIMENSION CARD(8)
55      1 FORMAT(7F10.0)
56      2 FORMAT(16,2I4,I2)
57      IDC = 7
58      IER = 0
59      READ (5,2) ICODE,IROW,ICOL,IS
60      CALL LCC(IROW,ICOL,ICNT,IROW,ICOL,IS)
61      IF(ISIZE-ICNT) 6,7,7
62      6 IER = 1
63      7 IF(ICNT) 38,38,8
64      8 ICOLT = ICOL
65      IROCP = 1
66      C   COMPUTE NO. OF CARDS IN THIS ROW
67      11 IRCDS = (ICOLT-1)/IDC+1
68      IF(IS-1) 15,15,12
69      12 IRCDS = 1
70      C   SET UP LOOP FOR NO. OF CARDS IN ROW
71      15 DO 31 K=1,IRCDS
72          READ(5,1) (CARD(I),I=1,IDC)
73      C   SKIP THRO' CARDS IF INPUT AREA TOO SMALL
74      IF(IER) 16,16,31
75      16 L=0

```

```

76 C COMPUTE COLUMN NO. FOR FIRST FIELD IN CURRENT CARD
77 JS=(K-1)*IDC+ICOL-ICOLT+1
78 JF=JS+IDC-1
79 IF((IS-1) 19,19,17
80 17 JE=JS
81 C SET UP LOOP FOR DATA ELEMENTS WITHIN CARD
82 19 DO 30 J=JS,JE
83 IF((J-ICOL) 20,20,31
84 20 CALL LCC(IPDCP,J,IJ,IPROW,ICOL,IS)
85 L=L+1
86 30 A(IJ)=CARD(I)
87 31 CONTINUE
88 IPDCP=IPDCP+1
89 IF((IPROW-IPDCP) 33,35,35
90 35 IF((IS-1) 37,36,37
91 36 ICOLT=ICOLT-1
92 37 GO TO 11
93 30 PFAO(5,1) CARD(I)
94 IF(CARD(I)-9.29) 39,40,39
95 39 IEP = 2
96 40 RETURN
97 END
98
99

```

```

100
101
102 SUPROUTINE MATPRT(A,N,M,MA,NC,II)
103 DIMENSION A(MA,MA)
104 C MATPRT PRINTS MATRICES** FROM KLOPMANS PROGRAM SCF
105 KK=0
106 NCM1=NC-1
107 J=0
108 L=1
109 IF(II-1) 13,13,14
110 14 L=II-10
111 II=0
112 KK=5
113 13 DO 5 IZ=L,M,NC
114 NIF=IZ+NCM1
115 IF(NIF.GT.M)NIF=M
116 J=J+N-II*(IZ-1)
117 IF(J-52)6,7,7
118 7 I=0
119 J=C
120 GOTO 8
121 6 I=1
122 8 CONTINUE
123 IF(I+KK-1)2,3,18
124 1 FORMAT(1H1)
125 2 WRITE(6,1)
126 3 WRITE(6,4)(K,K=IZ,NIF)
127 18 IJ=2*(NIF-IZ+1)+1
128 4 FORMAT(1HG,7IC110)
129 IF(II)9,9,10
130 10 DO 11 P=IZ,N
131 JJ=IR
132 IF(JJ.GT.NIF)JJ=NIF
133 11 WRITE(6,100)IR,(A(IR,IC),IC=IZ,JJ)
134 GOTO 5
135 9 DO 12 IP=1,N
136 12 WRITE(6,100)IR,(A(IR,IC),IC=IZ,NIF)
137 100 FORMAT(1H 12.2X,10F10.4)
138 5 CONTINUE
139 RETURN
140 END
141
142
143
144
145

```

```

146 SUBROUTINE MXOUT(ICODE,A,N,M,MS,LINS,IPOS,ISP)
147 DIMENSION A(1),R(8)
148 1 FORMAT(1H1,5X,7HMATRIX ,15,6X,13,5H PROWS,6X,13,8H COLUMNS,
149 18X,13HSTORAGE MODE ,11,8X,5HPAGE ,12,7)
150 2 FORMAT(12X,8HCOLUMN ,7(3X,13,10X))

```

```

151      3 FORMAT(1H 1
152      4 FORMAT(1H ,7X,4HP0W ,I3,7(F16.6))
153      5 FORMAT(1H0,7X,4HROW ,I3,7(F16.6))
154      J=1
155      C   WRITE HEADING
156          NEND = IPCS/IA - 1
157          LEND = (LINS/ISP) - 2
158          IPAGE = I
159      10  LSTRT = 1
160      20  WRITE(6,1) ICODE,N,M,MS,IPAGE
161          JNT = J + NEND - 1
162          IPAGE = IPAGE + 1
163      31  IF(JNT-M) 33,33,32
164      32  JNT = M
165      33  CONTINUE
166          WRITE(6,2) (JCUP,JCUP=J,JNT)
167          IF(ISP-1) 35,35,40
168      35  WRITE(6,3)
169      40  LEND=LSTRT+LEND-1
170          DO 80 L=LSTRT,LEND
171      C   FORM OUTPUT FOR LINE
172          DO 55 K=1,NEND
173          KK = K
174          JT = J+K-1
175          CALL LOC(L,JT,IJNT,N,M,MS)
176          R(K) = 0.0
177          IF(IJNT) 50,50,45
178      45  R(K) = A(IJNT)
179      50  CONTINUE
180      C   CHECK IF LAST COLUMN. IF YES GO TO 60
181          IF(JT-M) 55,60,60
182      55  CONTINUE
183      C   END OF LINE, NOW WRITE
184      60  IF(ISP-1) 65,65,70
185      65  WRITE(6,4) L,(B(JW),JW=1,KK)
186          GO TO 75
187      70  WRITE(6,5) L,(B(JW),JW=1,KK)
188      C   IF END OF ROWS, GO CHECK COLUMNS
189      75  IF(N-L) 85,85,80
190      80  CONTINUE
191      C   END OF PAGE, NOW CHECK FOR MORE OUTPUT
192          LSTRT = LSTRT+LEND
193          GO TO 20
194      C   END OF COLUMNS, THEN RETURN
195      85  IF(JT-M) 90,95,95
196      90  J = JT + 1
197          GO TO 10
198      95  RETURN
199      END
200
201
202
203
204      SUBROUTINE SIMQ(A,R,N,KS)
205      DIMENSION A(1),R(1)
206      TOL=0.0
207      KS=0
208      JJ=-N
209      DO 65 J=1,N
210          JY=J+1
211          JJ=JJ+N+1
212          BIGA=0
213          IT=JJ-J
214          DO 30 I=J,N
215              IJ=IT+I
216              IF(ABS(BIGA)-ABS(A(IJ))) 20,30,30
217      20  BIGA=A(IJ)
218          IMAX=I
219      30  CONTINUE
220          IF(ABS(BIGA)-TOL) 35,35,40
221      35  KS=I
222          RETURN
223      40  IL=J+N*(J-2)
224          IT=IMAX-J
225          DO 50 K=J,N

```

```

226      I1=I1+N
227      I2=I1+IT
228      SAVE=A(I1)
229      A(I1)=A(I2)
230      A(I2)=SAVE
231      50 A(I1)=A(I1)/RIGA
232      SAVE=B(IMAX)
233      B(IMAX)=B(J)
234      B(J)=SAVE/RIGA
235      IF(J-1) 55,70,55
236      55 IQS=N*(J-1)
237      DO 55 IX=JY,N
238      IXJ=IQS+IX
239      IT=J-IX
240      DO 60 JX=JY,N
241      IXJX=N*(JX-1)+IX
242      JJX=IXJX+IT
243      60 A(IXJX)=A(IXJX)-(A(IXJ)*A(JJX))
244      65 B(IX)=B(IX)-(B(J)*A(IXJ))
245      70 NY=N-1
246      IT=N*I.
247      DO 80 J=1,NY
248      IA=I-T-J
249      IB=N-J
250      IC=N
251      DO 80 K=1,J
252      B(IB)=B(IB)-A(IA)*B(IC)
253      IA=IA-N
254      80 IC=IC-1
255      RETURN
256      END

```

## REFERENCES

1. K. Siegbahn, C. Nordling, A. Fahlman, R. Nordberg, K. Hamrin, J. Hedman, G. Johansson, T. Bergmark, S.E. Karlsson, I. Lidgren and B. Lindberg, ESCA 'Atomic, Molecular and Solid State Structure Studied by Means of Electron Spectroscopy'. Almquist and Wiksells, Upsala, 1967.
2. H. Robinson and W.F. Rawlinson, Phil. Mag. 1914, 28, 277.
3. H. Robinson, Proc. Roy. Soc. A. 1923, 104, 455.
4. H. Robinson, Phil. Mag. 1925, 50, 241.
5. M. de Broglie, C.R. 1921, 172, 274.
6. J.A. Van den Akker and E.C. Watson, Phys. Rev. 1931, 37, 1631.
7. M. Ference Jr. Phys. Rev. 1937, 51, 720.
8. A. Bazin, Zhurnal Eksperimentalnoi i Teoreticheskoi Fiziki, 1944, 14, 23.
9. R.G. Steinhardt Jr., F.A.D. Granados and G.I. Post, Anal. Chem. 1955, 27, 1046.
10. K. Siegbahn and K. Edvarson, Nucl. Phys. 1956, 1, 137.
11. K. Siegbahn, 'Alpha-, Beta and Gamma-Ray Spectroscopy', Chapter III (Ed. K. Siegbahn) North Holland Publ. Co., Amsterdam 1965.
12. D. Pines, 'Elementary Excitations in Solids', W.A. Benjamin, Inc. New York 1963.
13. C. Nordling, E. Sokolowski and K. Siegbahn, Arkiv. Fysik, 1958, 13, 483.
14. S. Hagstrom, C. Nordling and K. Siegbahn, Z. Physik 1964, 178, 439.
15. O.Z. Stelling, Physik 1928, 50, 566.
16. A.M. Lindh 'Handbuck der Experimentalphysik' Bd 24. Teil 4, ed. W. Wiess and F. Harnes, Leipzig 1930.

17. K. Siegbahn, C. Nordling, G. Johansson, J. Hedman, P.F. Heden, K. Hamrin, U. Gelius, T. Bergmark, L.O. Werme, R. Manne and Y. Baer, 'ESCA Applied to Free Molecules', North Holland 1969.
18. D.W. Turner, C. Baker, A.D. Baker and C.R. Brundle 'Molecular Photoelectron Spectroscopy', John Wiley and Sons Ltd. 1970.
19. C.R. Brundle, M.B. Robin and G.R. Jones, J. Chem. Phys. 1970, 52, 3383.
20. T.A. Carlson and R.M. White, Faraday Discussions No. 54, 1972.
21. K. Siegbahn, 'Electron Spectroscopy' (Ed. D.A. Shirley) p.15. North Holland 1972.
22. M.O. Krause, Chem. Phys. Lett. 1971, 10, 65.
23. J.S. Levinger, Phys. Rev. 1953, 90, 11.
24. M.O. Krause, T.A. Carlson and R.D. Dismukes, Phys. Rev. 1968, 170, 37.
25. L.J. Aarons, M.F. Guest and I.H. Hillier, J. Chem. Soc. Faraday Trans II, 1972, 11, 1866.
26. U. Gelius, C.J. Allan, D.A. Allison, H. Siegbahn and K. Siegbahn Chem. Phys. Lett. 1971, 11, 224.
27. D.S. Urch, Quart. Rev. 1971, 25, 343.
28. A. Faessler, Angew. Chem. (Internat Ed.) 1972, 11, 34.
29. K. Siegbahn, Third International Conference on Atomic Physics, University of Colorado; August 1972.
30. P. Auger, J. Phys. Radium, 1925, 6, 205.
31. P. Auger, Compt. Rend. 1925, 180, 65.

32. J.J. Lander, *Phys. Rev.* 1953, 91, 1382.
33. C.C. Chang, *Surface Sci.* 1971, 25, 53.
34. D. Coster and R. de L. Kronig, *Physica* 1935, 2, 13.
35. E.H.S. Burhop, 'The Auger Effect and Other Radiationless Transitions', Cambridge University Press, 1952.
36. J.A. Bearden, *Rev. Mod. Phys.* 1967, 39, 78.
37. K. Siegbahn, D. Hammond, H. Fellner-Feldegg and E.F. Barnett, *Science* 1972, 176, 254.
38. U. Gelius and K. Siegbahn, *Faraday Discussion No. 54*, 1972.
39. E.M. Purcell, *Phys. Rev.* 1938, 54, 818.
40. J.C. Helmer and N.H. Weichert, *Appl. Phys. Lett.* 1968, 13, 268.
41. C.R. Brundle, *Appl. Spectrosc.* 1971, 25, 8.
42. E. Sokolowski, *Arkiv Fysik*, 1959, 15, 1.
43. C. Nordling, *Arkiv Fysik* 1959, 15, 397.
44. W.L. Jolly and D.N. Hendrickson, *J. Amer. Chem. Soc.* 1970, 92, 1863.
45. C.S. Fadley, S.B.M. Hagstrom, M.P. Klein and D.A. Shirley, *J. Chem. Phys.* 1968, 48, 3779.
46. M.A. Butler, G.K. Wertheim, D.L. Rouseau and S. Hufner, *Chem. Phys. Lett.* 1972, 13, 473.
47. D.N. Hendrickson, J.M. Hollander and W.L. Jolly, *Inorg. Chem.* 1969, 8, 2642.
48. D.A. Huchital and R.T. McKeon, *Appl. Phys. Lett.* 1972, 20, 158.
49. D.T. Clark, D. Kilcast, D.B. Adams and W.K.R. Musgrave, *J. Electron Spectrosc.* 1972/73, 1, 227.
50. J.M. Hollander and W.L. Jolly, *Acc. Chem. Res.* 1970, 3, 193.

51. W.L. Jolly, J. Amer. Chem. Soc. 1970, 92, 3260.
52. R.E. Watson and A.J. Freeman, Hyperfine Interactions (Ed. A.J. Freeman and R.B. Frankel) 1967, Academic Press, New York.
53. C.S. Fadley, D.A. Shirley, A.J. Freeman, P.S. Bagus and J.V. Mallow, Phys. Rev. Lett. 1969, 23, 1397.
54. J.H. van Vleck, Phys. Rev. Lett. 1934, 45, 405.
55. C.S. Fadley, Electron Spectroscopy (Ed. D.A. Shirley) p.781, North Holland 1972.
56. D.W. Davis and D.A. Shirley, J. Chem. Phys. 1972, 56, 669.
57. J.C. Carver, C.A. Thomas, L.C. Cain and G.K. Schweitzer, Electron Spectroscopy (Ed. D.A. Shirley) p.803, North Holland, 1972.
58. T. Novakov and J.M. Hollander, Phys. Rev. Lett. 1968, 21, 1133.
59. T. Novakov and J.M. Hollander, Bull. Amer. Phys. Soc. 1969, 14, 524.
60. G.K. Wertheim, Mossbauer Effect: Principles and applications, Academic Press, 1964.
61. T. Novakov, Ref 26 of C.S. Fadley, 'Electrons Spectroscopy (Ed. D.A. Shirley) p.781, North Holland 1972. 8
62. R.P. Gupta and S.K. Sen, Phys. Rev. Lett. 1972, 28, 1311.
63. G.K. Wertheim and A. Rosencwaig, Phys. Rev. Lett. 1971, 26, 1179.
64. J.M. Thomas, I. Adams and M. Barber, Solid State Commun. 1971, 9, 1571.
65. J. Utriainen, M. Linkoaho, E. Rautavouri, T. Aberg, and G. Graeffe, Z. Naturforsch 1968, 23A, 1178.
66. L.G. Parrat, Rev. Mod. Phys. 1959, 31, 616.

67. R.W. Shaw and T.D. Thomas, Phys. Rev. Lett. 1972, 29, 689.
68. R.M. Friedman, J. Hudis and M.L. Perlman, Phys. Rev. Lett. 1972, 29, 692.
69. M. Klasson, J. Hedman, A. Berndtsson, R. Nilsson, C. Nordling and P. Mel'nick. Phys. Scr. 1972, 5, 93.
70. J.C. Tracy, NATO Summer School, Ghent 1972.
71. D.T. Clark and D. Kilcast, J. Chem. Soc. B, 1971, 2243.
72. D.T. Clark, D. Kilcast, D.B. Adams and W.K.R. Musgrave, J. Electron Spectrosc. 1972/3, 1, 227.
73. D.M. Hercules, Anal. Chem. 1972, 44, 106R.
74. D.T. Clark, D. Briggs and D.B. Adams, J. Chem. Soc. Dalton, 1973, 19.
75. M. Barber, P. Swift, D. Cunningham and M.J. Frazer, Chem. Comm. 1970, 1338.
76. I. Adams, J.M. Thomas, G.M. Bancroft, K.D. Butler, and M. Barber, Chem. Comm. 1972, 751.
- 77a. R.E. Block, J. Magn. Resonance 1971, 5, 155.
- 77b. D. Zeroka, Chem. Phys. Lett. 1972, 14, 471.
- 77c. D.T. Clark and D. Kilcast, J. Chem. Soc. A, 1971, 3286.
78. J.S. Brinen and A. Melera, J. Phys. Chem. 1972, 76, 2525.
79. D.A. Whan, M. Barber and P. Swift, Chem. Comm. 1972, 198.
80. K.C. Tripathi and D.T. Clark, Nature (Phys Sci) 1973, 241, 163.
81. T.A. Carlson and G.E. McGuire, J. Electron Spectrosc. 1972, 1, 161.
82. L.D. Hullet, T.A. Carlson, B.R. Fish and J.L. Durham, Determination Air Qual. Proc. ACS Symp. 1971 (Pub. 1972) p.179.

83. M.M. Millard, Anal. Chem. 1972, 44, 828.
84. M.M. Millard and A.E. Pavlath, Text. Res. J. 1972, 42, 460.
85. D.T. Clark and D. Kilcast, J. Chem. Soc. B, 1971, 2243.
86. D.T. Clark, R.D. Chambers, D. Kilcast and W.K.R. Musgrave,  
J. Chem. Soc. Faraday II, 1972, 2, 309.
87. D.W. Davis, D.A. Shirley and T.D. Thomas, J. Amer. Chem. Soc.  
1972, 94, 6565.
88. G.A. Olah, G.D. Mateescue, L.A. Wilson and M.H. Gross, J.  
Amer. Chem. Soc. 1970, 92, 7231.
89. G.A. Olah, G.D. Mateescue and J.L. Riemenschneider, J. Amer.  
Chem. Soc. 1972, 94, 2529.
90. G.D. Mateescue, J.L. Riemenschneider, J.J. Svobada and  
G.A. Olah, J. Amer. Chem. Soc. 1972, 94, 7191.
91. D.T. Clark, W.J. Feast, M. Foster and D. Kilcast, Nature  
(Phys. Sci.) 1972, 236, 107.
92. D.T. Clark, D. Kilcast, W.J. Feast and W.K.R. Musgrave,  
J. Polymer Sci. part A-1, 1972, 10, 1637.
93. D.T. Clark, D. Kilcast and D.B. Adams, Faraday Discussions  
of the Chem. Soc. 1972, No. 54.
94. S.J. Brinen and J.E. McClure Anal. Lett. 1972, 5, 737.
95. W.E. Swartz and D.M. Hercules, Anal. Chem. 1971, 43, 1774.
96. T.W. Huntress and L. Wilson, Earth Planet Sci. Lett. 1972,  
15, 59.
97. A.P. Vinogradov, V.I. Nefedov, V.S. Uruaov and N.M. Zhavoronkov,  
Dokl. Acad. Nauk SSSR, 1971, 201, 957.
98. M.P. Klein and L.N. Kramer, Impr. Plant Protein, Nucl. Tech.  
Proc. Symp. 1970, 243, IAEA Vienna Austria.

99. M. Barber and D.T. Clark, Chem. Comm. 1970, 23.
100. M. Barber and D.T. Clark, Chem. Comm. 1970, 24.
101. L.D. Hulet and T.A. Carlson, Clin. Chem. 1970, 16, 677.
- 102.a H. Eyring, J. Walter and G.E. Kimball, 'Quantum Chemistry',  
John Wiley and Sons Inc. 1944.
- 102.b J.N. Murrell, S.F.A. Kettle and J.M. Tedder, 'Valence Theory',  
John Wiley and Sons Inc., 1965.
103. T.D. Thomas, J. Chem. Phys. 1970, 52, 1373.
- 104.a D.R. Hartree, Proc. Camb. Phil. Soc. 1928, 24, 89.
- b D.R. Hartree, Proc. Camb. Phil. Soc. 1928, 24, 111.
- c D.R. Hartree, Proc. Camb. Phil. Soc. 1928, 24, 426.
105. V. Fock, Z. Physik, 1930, 126, 61.
106. J.C. Slater, Phys. Rev. 1930, 35, 210.
107. D.R. Hartree, 'The Calculation of Atomic Structures', John  
Wiley and Sons, New York, 1957.
108. C.C.J. Roothaan, Rev. Mod. Phys., 1951, 23, 69.
109. J.C. Slater, Phys. Rev. 1930, 36, 57.
110. S.F. Boys, Proc. Roy. Soc. (London) 1950, A200, 542.
111. I. Shavitt, Methods in Computation Physics 1963, 2, 1.
112. S. Husinaga, J. Chem. Phys. 1965, 42, 1293.
113. H. Preuss, Z. Naturforsch, 1956, 11, 823.
114. J.L. Whitten, J. Chem. Phys. 1966, 44, 395.
115. A.A. Frost, J. Chem. Phys. 1967, 47, 3707.
116. J.C. Slater, Phys. Rev. 1930, 36, 57.
117. E. Clementi and D.L. Raimondi, J. Chem. Phys., 1963, 38, 2686.
118. E. Clementi, D.L. Raimondi and W.P. Reinhardt, J. Chem. Phys.  
1967, 47, 1300.

119. J.A. Pople and D.L. Beveridge, 'Approximate Molecular Orbital Theory', McGraw-Hill, New York 1970.
120. J.M. Foster and S.F. Boys, Rev. Mod. Phys. 1960, 32, 303.
121. W.J. Hehre, R.F. Stewart and J.A. Pople, J. Chem. Phys., 1969, 51, 2657.
122. R. Ditchfield, W.J. Hehre and J.A. Pople, J. Chem. Phys., 1971, 54, 724.
123. E. Clementi, J. Chem. Phys., 1964, 40, 1944.
124. E. Clementi, R. Matcha and A. Veillard, J. Chem. Phys., 1967, 47, 1865.
125. S. Huzinaga and C. Arnau, J. Chem. Phys., 1970, 53, 451.
126. P.S. Bagus and L.T. Gibert, reported in Argonne National Laboratory Report 7271 (Jan. 1968).
127. E. Clementi, 'Tables of Atomic Wave Functions' a supplement to I.B.M. J. Res. Develop., 1965, 9, 2.
128. C.J.J. Roothaan, Rev. Mod. Phys., 1960, 32, 179.
129. E. Clementi and R. Davis, J. Comput. Phys., 1967, 2, 223.
130. T.H. Dunning, J. Chem. Phys., 1970, 53, 2823.
131. R.K. Nesbet, Rev. Mod. Phys., 1960, 32, 272.
132. R.K. Nesbet, J. Chem. Phys., 1964, 40, 3619.
133. R.S. Mulliken, J. Chem. Phys., 1955, 23, 1833, 1841, 2338, 2343.
134. A.C. Wahl, J. Chem. Phys., 1964, 41, 2600.
135. L.C. Snyder and H. Basch., J. Amer. Chem. Soc., 1969, 91, 2189.
136. R. Ditchfield, W.J. Hehre, J.A. Pople and L. Radom, Chem. Phys. Lett., 1970, 5, 13.

137. W.J. Hehre, R. Ditchfield, L. Radom and J.A. Pople, *J. Amer. Chem. Soc.*, 1970, 92, 4796.
138. E.A. Hylleras, *Z. Physik*, 1929, 54, 347.
139. C.C.J. Roothaan and A.W. Weiss, *Rev. Mod. Phys.*, 1960, 32, 194.
140. W. Kolos and C.C.J. Roothaan, *Rev. Mod. Phys.*, 1960, 32, 205.
141. E.A. Hylleras, *Z. Physik*, 1928, 48, 469.
142. E. Clementi, *J. Chem. Phys.*, 1967, 46, 284.
143. J.A. Pople, D.P. Santry and G.A. Segal, *J. Chem. Phys.*, 1965, 43, S129.
144. J.A. Pople and G.A. Segal, *J. Chem. Phys.*, 1965, 43, S136.
145. J.A. Pople and G.A. Segal, *J. Chem. Phys.*, 1966, 44, 3289.
146. C.C.J. Roothaan, *J. Chem. Phys.*, 1951, 19, 1445.
147. D.P. Santry and G.A. Segal, *J. Chem. Phys.*, 1967, 47, 158.
148. J.A. Pople and D.L. Beveridge 'Approximate Molecular Orbital Theory', McGraw-Hill 1970 (Appendix A).
149. W.L. Jolly, 'Electron Spectroscopy', Ed. D.A. Shirley p.629, and references therein, North-Holland 1972.
150. D.C. Frost, F.G. Herring, C.A. McDowell and I.S. Woolsey, *Chem. Phys. Lett.*, 1972, 13, 391.
151. C.S. Fadley, S.B.M. Hagstrom, M.P. Klein and D.A. Shirley, *J. Chem. Phys.*, 1968, 48, 3779.
152. D.T. Clark, NATO Summer School, Ghent 1972.
153. T.A. Koopmans, *Physica*, 1933, 1, 104.
154. H. Hartman and E. Clementi, *Phys. Rev. A.*, 1964, 133, 1295.
155. C.W. Scherr, J.N. Silverman and F.A. Matsen, *Phys. Rev.*, 1962, 127, 830.

156. E. Clementi, Chem. Rev., 1968, 68, 341.
157. E. Clementi and H. Popkie, J. Amer. Chem. Soc., 1972, 94, 4057.
158. P.S. Bagus, Phys. Rev. A., 1965, 139, 619.
159. H. Basch and L.C. Snyder, Chem. Phys. Lett., 1969, 3, 333.
160. D.W. Davis, J.M. Hollander, D.A. Shirley, and T.D. Thomas, J. Chem. Phys., 1970, 52, 3295.
161. T.K. Ha and L.C. Allen, Internat. J. Quantum Chem., 1967, 15, 199.
162. C.R. Brundle, M. Robin and H. Basch, J. Chem. Phys., 1970, 53, 2196.
163. M.F. Chiu, M.F. Guest and V.R. Saunders, ATMOL2 user notice 5, Atlas Computer Laboratory, March 1973.
164. M.E. Schwartz, Chem. Phys. Lett., 1970, 5, 50.
165. U. Gelius and K. Siegbahn, Faraday Discussion of the Chem. Soc. No. 54, 1972, 257.
166. L.C. Snyder, J. Chem. Phys., 1971, 55, 95.
167. P.S. Bagus and H.F. Schaefer, J. Chem. Phys., 1972, 56, 224.
168. P.S. Bagus and H.F. Schaefer, J. Chem. Phys., 1971, 55, 1474.
169. T.A. Carlson, M.O. Krause and W.E. Moddeman, J. de Physique, 1971, 32, C4-76.
170. J.N. Murrell and B.J. Ralston, J. Chem. Soc. Faraday II, 1972, 68, 1393.
171. M.E. Schwartz, Chem. Phys. Lett., 1970, 6, 631.
172. H. Basch, Chem. Phys. Lett., 1970, 6, 337.
173. D.A. Shirley, Chem. Phys. Lett., 1972, 15, 325.

174. C. Edmiston and K. Ruedenberg, *Rev. Mod. Phys.*, 1963, 35, 457.
175. M.E. Schwartz, *Chem. Phys. Lett.*, 1970, 7, 78.
176. M.E. Schwartz and J.D. Switalski, *J. Amer. Chem. Soc.*, 1972, 94, 6298.
177. M.E. Schwartz, *J. Amer. Chem. Soc.*, 1972, 94, 6899.
178. D.W. Davis and D.A. Shirley, *Chem. Phys. Lett.*, 1972, 15, 185.
179. T.D. Thomas, *J. Amer. Chem. Soc.*, 1970, 92, 4184.
180. D.W. Davis, D.A. Shirley and T.D. Thomas, *J. Chem. Phys.*, 1972, 56, 671.
181. N.C. Baird and M.J.S. Dewar, *J. Chem. Phys.*, 1969, 50, 1275.
182. N.C. Baird, M.J.S. Dewar and R. Sustmann, *J. Chem. Phys.*, 1969, 50, 1275.
183. *Tables of Interatomic Distances*, Ed. L.E. Sutton, Chemical Society Special Publication Nos. 11, (1958) and 18, (1965).
184. C.J. Allen, U. Gelius, D.A. Allison, G. Johansson, H. Siegbahn and K. Siegbahn, *J. Electron. Spectrosc.*, 1972/3, 1, 131.
185. J.R. Sabin and H. Kim, *J. Chem. Phys.*, 1971, 56, 2195.
186. A. Veillard, *Theor. Chim. Acta*, 1968, 12, 405.
187. E. Clementi and J. Mehl, 'IBM system/360 IBMOL5 Program, Quantum Mechanical Concepts and Algorithms', IBM research laboratory, San Jose, June 1971.
188. V.R. Saunders, *ATMOL2*, Atlas Computer Laboratory 1972.
189. R.F. Stewart, *J. Chem. Phys.*, 1969, 50, 2485.
190. C.E. Moore, 'Atomic Energy Levels', Washington Nat. Bureau of Standards, Circ. 467, 1949.
191. Y.S. Khodeyev, H. Siegbahn, K. Hamrin and K. Siegbahn, *Chem. Phys. Lett.*, 1973, 19, 16.

192. 'Handbook of Chemistry and Physics'. Ed. R.C. Weaste Publ. The Chemical Rubber Co., 50<sup>th</sup> Edition 1969-70.
193. J.B. Mann, 'Atomic Structure calculations II. Hartree-Fock Wavefunctions and Radial Expectation Values: Hydrogen to Lawrencium', Report of the Los Alamos Scientific Laboratory of the University of California, 1968.
194. G. Burns, J. Chem. Phys., 1964, 41, 1521.
195. R.D. Brown and M.L. Heffernan, Trans. Faraday Soc., 1958, 54, 757.
196. D.M. Hercules, Anal. Chem., 1970, 42, 20A.
197. A. Fahlman, K. Hamrin, K. Hedman, R. Nordberg, C. Nordling and K. Siegbahn, Nature, 1966, 210, 4.
198. J.M. Hollander, D.N. Hendrickson and W.L. Jolly, J. Chem. Phys., 1968, 49, 3315.
199. L. Pauling, 'The Nature of the Chemical Bond' 3rd. Edition (New York 1960).
200. F.O. Ellison and L.L. Larcom, Chem. Phys. Lett., 1971, 10, 580.
201. W.L. Jolly, Faraday Discussion of the Chem. Soc. No 54, 1972.
202. I.B.M. System/360 Scientific Subroutine Package (FORTRAN).
203. W.J. Feast and W.E. Preston, Tetrahedron, 1972, 28, 2805.
204. D.T. Clark, Chem. Soc. Specialist Report, Organic Compounds of Sulphur, Selenium and Tellurium, 1970, 1, 1.
205. D.T. Clark, D. Kilcast, D.B. Adams and W.K.R. Musgrave, unpublished data.
206. G.D. Stuckey, D.A. Mathews, J. Hedman, M. Klasson, and C. Nordling, J. Amer. Chem. Soc. 1972, 94, 8009.

207. cf. 'The Polyatom System', B.T. Sutcliffe, Department of Chemistry, University of York.
208. A.D. McLean, Proceedings of the Conference on Potential Energy Surfaces in Chemistry 1970, p.87. Ed. W.A. Lester, Publ. IBM Research Lab. San Jose, California 1971.
209. M.F. Chiu, M.F. Guest and V.R. Saunders, ATMOL2, User Notice 12, Atlas Computer Laboratory, June 1973.
210. C.J.J. Roothaan, Rev. Mod. Phys., 1960, 32, 179.
211. J.A. Pople and R.K. Nesbet, J. Chem. Phys., 1954, 22, 571.
212. P.S. Bagus, B. Liu and H.F. Schaefer, Phys. Rev. A., 1970, 2, 555.
213. A.J. Freeman and R.E. Watson, 'Magnetism' Ed. G.T. Rado and H. Suhl (Academic Press, New York, 1965).
214. P.S. Bagus and B. Liu, Phys. Rev., 1966, 148, 79.
215. J.C. Tatlow, Endeavour, 1963, 22, 89.
216. J. Burdon, Tetrahedron, 1965, 21, 3373.
217. J. Burdon, D. Harrison and R. Stephens, Tetrahedron, 1965, 21, 927.
218. J. Burdon, B.L. Kane, and J.C. Tatlow, J. Chem. Soc. (C), 1971, 1601.
219. D.T. Clark, J.N. Murrell and J.M. Tedder, J. Chem. Soc., 1963, 1250.
220. D.J. Burton and R.L. Johnson, J. Amer. Chem. Soc., 1964, 86, 5361.
221. D.B. Adams, D.T. Clark, W.J. Feast, D. Kilcast, W.K.R. Musgrave and W.E. Preston, Nature (Phys. Sci), 1972, 239, 47.
222. W.E. Preston, Ph.D. Thesis, University of Durham 1972.
223. R.L. Pruett, C.T. Bahner and H.A. Smith, J. Amer. Chem. Soc., 1952, 74, 1638.
224. M.J.R. Fraticelli, Ph.D. Thesis, Cornell University, 1965; Diss. Abs., 1965, 26, 3045.

225. R.D. Chambers, M.Y. Gribble and E. Marper, J. Chem. Soc.,  
Perkin I, in press.

